

4
5/16/88 JS (D)

DE# 0462-6

SANDIA REPORT

SAND88-0458 • UC-236

Unlimited Release

Printed April 1988

Liquid Metal Thermal Electric Converter Bench Test Module

L. L. Lukens, C. E. Andraka, J. B. Moreno

Prepared by
Sandia National Laboratories
Albuquerque, New Mexico 87185 and Livermore, California 94550
for the United States Department of Energy
under Contract DE-AC04-76DP00789

DO NOT MICROFILM
COVER

DISTRIBUTION OF THIS DOCUMENT IS UNLIMITED

DISCLAIMER

This report was prepared as an account of work sponsored by an agency of the United States Government. Neither the United States Government nor any agency Thereof, nor any of their employees, makes any warranty, express or implied, or assumes any legal liability or responsibility for the accuracy, completeness, or usefulness of any information, apparatus, product, or process disclosed, or represents that its use would not infringe privately owned rights. Reference herein to any specific commercial product, process, or service by trade name, trademark, manufacturer, or otherwise does not necessarily constitute or imply its endorsement, recommendation, or favoring by the United States Government or any agency thereof. The views and opinions of authors expressed herein do not necessarily state or reflect those of the United States Government or any agency thereof.

DISCLAIMER

Portions of this document may be illegible in electronic image products. Images are produced from the best available original document.

Issued by Sandia National Laboratories, operated for the United States Department of Energy by Sandia Corporation.

NOTICE: This report was prepared as an account of work sponsored by an agency of the United States Government. Neither the United States Government nor any agency thereof, nor any of their employees, nor any of their contractors, subcontractors, or their employees, makes any warranty, express or implied, or assumes any legal liability or responsibility for the accuracy, completeness, or usefulness of any information, apparatus, product, or process disclosed, or represents that its use would not infringe privately owned rights. Reference herein to any specific commercial product, process, or service by trade name, trademark, manufacturer, or otherwise, does not necessarily constitute or imply its endorsement, recommendation, or favoring by the United States Government, any agency thereof or any of their contractors or subcontractors. The views and opinions expressed herein do not necessarily state or reflect those of the United States Government, any agency thereof or any of their contractors or subcontractors.

Printed in the United States of America
Available from
National Technical Information Service
U.S. Department of Commerce
5285 Port Royal Road
Springfield, VA 22161

NTIS price codes
Printed copy: A14
Microfiche copy: A01

DO NOT MICROFILM
COVER

DISCLAIMER

This report was prepared as an account of work sponsored by an agency of the United States Government. Neither the United States Government nor any agency thereof, nor any of their employees, makes any warranty, express or implied, or assumes any legal liability or responsibility for the accuracy, completeness, or usefulness of any information, apparatus, product, or process disclosed, or represents that its use would not infringe privately owned rights. Reference herein to any specific commercial product, process, or service by trade name, trademark, manufacturer, or otherwise does not necessarily constitute or imply its endorsement, recommendation, or favoring by the United States Government or any agency thereof. The views and opinions of authors expressed herein do not necessarily state or reflect those of the United States Government or any agency thereof.

SAND88-0458

LIQUID METAL THERMAL ELECTRIC CONVERTER BENCH TEST MODULE

Laurance L. Lukens SAND--88-0458
Charles E. Andraka DE88 009857
James B. Moreno

Environmental Sensing Device Division
Sandia National Laboratories
Albuquerque, New Mexico, 87185

Abstract

This report describes the design, fabrication, and test of a Liquid Metal Thermal Electric Converter Bench Test Module. The work presented in this document was conducted as a part of Heat Engine Task of the U. S. Department of Energy's (DOE) Solar Thermal Technology Program. The objective of the this task is the development and evaluation of heat engine technologies applicable to distributed receiver systems, in particular, dish electric systems.

MASTER

Acknowledgments

The authors are indebted to J. P. Abbin for his continued support and encouragement and for many fruitful conversations. They also wish to acknowledge the support and encouragement of J. A. Leonard. The early motivating activities of W. E. Boyd and a number of productive discussions with R. B. Diver should also be mentioned. All of the afore-mentioned are with Sandia National Laboratories, Albuquerque (SNLA).

Others at SNLA who deserve recognition are W. B. Vine, E. D. Brandon and G. M. Boruff (welding), M. J. Cieslak (welding metallurgy), R. M. Curlee, R. L. Chavez and J. J. Sarkis (brazing), F. M. Hosking (brazing metallurgy), M. K. Neilsen (stress analysis), R. E. Beauchamp (ceramic fracture analysis), W. F. Hammetter (solid electrolyte synthesis), and J. I. Martinez (electrolyte synthesis contracts). The authors are also grateful to D. Engi and F. M. Delnick for equipment loans.

Finally, the authors wish to express their appreciation to T. K. Hunt (Ford Motor Company) for his unselfish encouragement of their efforts and for several useful technical exchanges.

TABLE OF CONTENTS

Introduction.....	1
LMTEC Concept.....	1
LMTEC Application to Dish Electric Systems.....	2
LMTEC BTM Objectives.....	3
LMTEC BTM Design.....	3
LMTEC BTM Operation.....	3
LMTEC BTM Postmortem.....	4
LMTEC BTM Future Work.....	5
References.....	10
Figures	
1. Liquid Metal Thermal Electric Converter Cycle Schematic.....	6
2. Liquid Metal Thermal Electric Converter Application To Dish Electric Systems.....	7
3. Liquid Metal Thermal Electric Converter Bench Test Module Schematic.....	8
4. Liquid Metal Thermal Electric Converter Bench Test Module.....	9
Appendices	
A. Bench Test Module Design.....	11
B. Internal Electrode.....	33
C. Internal Bus And Current Distribution Network.....	43
D. Ceramic To Metal Seal.....	63
E. Electromagnetic Pump.....	131
F. Data Acquisition And Control System.....	139
G. Bench Test Module Bakeout.....	201
H. Bench Test Module Operation.....	211
J. LMTEC Performance Model.....	251
K. Bench Test Module Postmortem.....	263
L. Safe Handling Of Sodium.....	287

Liquid Metal Thermal Electric Converter Bench Test Module

Introduction

The work presented in this document was conducted as a part of the U. S. Department of Energy's (DOE) Solar Thermal Technology Program. Sandia National Laboratories, Albuquerque (SNLA) has been actively engaged in the Heat Engine Task of the DOE's Solar Thermal Technology Program since October of 1984. The objective of this task is the development and evaluation of heat engine technologies applicable to distributed receiver dish electric systems. A preliminary heat engine technology assessment, [1], identified the Liquid Metal Thermal Electric Converter (LMTEC) concept as having the potential to meet the DOE's Solar Thermal Technology Program long term cost and performance goals with further engineering development. LMTEC work at SNLA has concentrated on three major areas; the conceptual design of a 25 kWe unit for mounting at the focus of a parabolic dish type solar collector, analytical modeling of the LMTEC to better understand its limitations and advantages, and the design, construction, and test of a single cell bench test module. A report on the LMTEC program at SNLA was presented at the 22nd IECEC, [2].

LMTEC Concept

The LMTEC is a thermodynamic heat engine which converts heat directly to electricity, [3]. A schematic of the LMTEC cycle is shown in Figure 1. Liquid metal ionizes in the high temperature zone and the ions are forced isothermally through Beta" alumina, an ion conducting solid electrolyte, by the pressure differential between the high temperature and low temperature zones of the engine. The electrons from the ionization process are driven through an external circuit where they are made to do useful work. The electrons are rejoined with the metal ions in a porous electrode on the other side of the Beta" alumina. Metal vapor flows from the porous electrode to the low temperature zone where it is condensed to liquid form. The liquid metal is then pumped by an electromagnetic pump to the high temperature zone completing the cycle. The LMTEC concept is appealing because of its basic mechanical and electrical simplicity. The only moving part in the LMTEC is the liquid metal working fluid. The ideal thermodynamic efficiency of the LMTEC cycle closely approaches that of a Carnot cycle operating between the same temperature limits, [3]. The actual efficiency of the LMTEC cycle will also depend on thermal and electrical losses and

on nonideal electrode behavior. Results from numerical simulations that take these factors into account have been presented in reference 2, for the working fluids sodium, potassium, and mercury. An important conclusion of that work was that mercury and potassium may offer significant operational and efficiency advantages over sodium. Based on this conclusion, work on the development of a mercury conductive analog of sodium Beta" alumina was initiated and the preliminary results have been encouraging, [4].

LMTEC Application to Dish Electric Applications

A conceptual design for a 25 kWe LMTEC mounted at the focus of a parabolic dish is illustrated in Figure 2. This illustration shows the basic LMTEC elements described in the preceding section. In this design the Beta" alumina solid electrolyte is shown as closed end tubes, a commercially available form. Many tubes electrically connected in series are necessary because of the low voltage high current character of individual cells. The design shown in Figure 2, uses a refluxing boiler developed at SNLA. The refluxing boiler separates the high temperature high pressure side of the Beta" alumina tube from the liquid metal in the boiler. Heat and mass transport to the tube are by vapor flow from the liquid metal. About one fourth of the vapor transported metal ionizes and moves through the tube wall. The remainder of the metal condenses providing heat and drips back to the boiler. This feature allows the series connection of multiple tubes in the hot area of the engine without electrical shorting through the liquid metal. The design also features a unique configuration of the Beta" alumina tubes with the high temperature high pressure working fluid on the outside of the tubes so the structural loads in the tubes are kept compressive. The porous electrode is on the inside surface of the Beta" alumina tubes. Electrons reach the internal porous electrode through an internal bus and current distribution system, which also allows metal vapor flow through the tube to the low temperature zone. This feature allows alternate working fluids with higher working pressure ratios across the Beta" alumina (such as mercury or potassium) to be used because of the compressive structural loading on the Beta" alumina tube. The tube configuration also increases the reliability of the tubes when sodium is used as the working fluid because of the more favorable structural loading on the Beta" alumina tube. The design also features a remote condenser. The remote condenser prevents the hot low pressure side of the Beta" alumina tubes (the porous electrode) from directly viewing the cool condenser surface and substantially reduces the radiative heat transfer losses.

LMTEC BTM Objectives

The primary objective of the Bench Test Module (BTM) was to evaluate critical elements of the 25 kWe conceptual design. These included the internal porous electrode, current distribution network, and current bus configuration which was developed at SNLA. Another objective of the BTM was to evaluate the performance of a remote condenser. In addition, the design and fabrication of the bench test module provided experience with ceramic to metal joints and the sodium compatibility of materials.

LMTEC BTM Design

A schematic of the LMTEC BTM shown in Figure 3. This design contains all of the elements necessary to meet the objectives outlined in the preceding section. Details of the BTM design, the internal electrode, the internal bus and current distribution network, the ceramic to metal seal, the electromagnetic pump, and the data acquisition and control system have been included in Appendices A-F.

LMTEC BTM Operation

The BTM was assembled and leak tested in March, 1987. A photograph of the BTM is shown in Figure 4. The BTM was vacuum baked by heating the high temperature zone (boiler) to 800 C, while actively pumping with the vacuum system. Vacuum testing of the BTM indicated an acceptable leak rate of 1.4×10^{-9} cc/sec. A more detailed account of the vacuum testing is included in Appendix G. Sodium was transferred to the BTM sodium return loop between the electromagnetic (EM) pump and the low temperature zone (condenser) in a canister. On March 26, 1987 the BTM was heated to 150 C, and the sodium melted. A level sensing standpipe was used to monitor melting and pumping. The EM pump started promptly and performed very well as expected. Sodium was pumped into the boiler under nearly isothermal conditions at 150 C. The boiler temperature was increased to 800 C over a five hour period. Voltage and current data were taken periodically. During the initial operation of the BTM the boiler was maintained at a temperature of 800 C, and the condenser was maintained at a temperature of 200 C. The maximum open circuit voltage recorded during this period was approximately 0.9 volts. The LMTEC performance models had predicted an open circuit voltage of 1.2 volts. The maximum power output was approximately 1.8 Watts, at the electrode. The performance model had predicted a maximum power of about 45 watts. Approximately six hours after the boiler was initially

filled, a rapid and unexpected decline in boiler pressure was observed. At the same time the main heater failed. These events ended the operation of the BTM. Several positive accomplishments were made during the operation of the BTM. The remote condenser, the containment vessel, and the computer control and data acquisition system functioned as designed. The safe operation of a system with sodium at 800 C, was demonstrated. A more detailed account of the operation of the BTM and the data accumulated is included in Appendix H.

LMTEC BTM Postmortem

An extensive postmortem of the BTM was conducted. The primary goals of the postmortem were to explain the much lower than expected maximum power and the unexpected loss of boiler pressure which ended the operation of the BTM. A detailed account of the observations and conclusions from the postmortem analysis is included in Appendix K.

A detailed analytical model was used to identify three conditions which could have limited the power output to the level obtained: a very high sodium vapor flow resistance through the tube, a very impermeable electrode, or the presence of significant noncondensable gas in the condenser. A more detailed account of the computer model is included in Appendix J. Experimental evidence and analysis indicated the the most likely factor was electrode permeability. A method to assess electrode permeability was developed and tested. The results indicated that the chemical vapor deposited (CVD) tungsten electrode used in the BTM was approximately 1000 times less permeable than a nominal electrode, and limited the power output of the BTM.

The sudden loss of boiler pressure in the BTM was caused by the failure of the Beta" alumina tube. The Beta" alumina to stainless steel joint was still intact. The tube from the BTM was carefully examined to determine possible causes for its failure. The tube showed an extensive network of cracks which originated from the inside surface. It is believed that the major cause of the tube failure is a mechanism that has been observed by the sodium-sulfur battery community. They have observed that when liquid sodium is present on the sodium exit side of the ceramic (the interface between the internal porous electrode and the Beta" alumina in the BTM) with an ionic current flow greater than about one ampere per square centimeter, damage to the Beta" alumina will occur rapidly, [5]. In the BTM, liquid would not ordinarily be present on the exit side of the ceramic, but with the low permeability

of the electrode there is a flow induced pressure at the electrode electrolyte interface which could have exceeded the saturation pressure. Another possible failure mechanism for the tube is gold contamination, which was found in the sodium and in crystal form on the exit side of the tube. The gold contamination was the result of inadvertently using a gold based braze alloy to seal penetrating thermocouples into the BTM boiler. The theory behind this mechanism is that gold was ionically conducted through the alumina and formed crystals of NaAu_2 in flaw sites, causing a pressure build up and crack growth. The possibility of gold ionic transport is controversial. It is believed that the actual breach of the tube was caused by thermal shock when the main heater failed, and that the tube was already in a weakened condition caused by one or both of the mechanisms discussed above.

LMTEC BTM Future Work

A primary objective of future BTM work will be to develop an internal electrode with adequate permeability and electrical conductivity. Our analysis and experiments indicate that a nominal 20-Watt BTM would be possible utilizing a sputter coated molybdenum electrode 0.5 microns thick with current distribution contacts along lines 1-mm apart. An important first step has been the recent demonstration at SNLA of post cathode direct current magnetron sputter coating of molybdenum on the inside surface of a one inch diameter Beta" alumina tube, [6]. A preliminary evaluation of the coating has been completed and is the basis for the above projection. Additional work is in progress to improve coating uniformity and to develop the current distribution network. This work is proceeding at a very low level because of a severe reduction in funding for the Solar Thermal Technology Program at SNLA. This reduction has resulted in a focusing of efforts on a smaller number of solar specific tasks, to the exclusion of the LMTEC and several other projects. Assuming that an adequate electrode is developed, a second version of the BTM is planned which will feature a refluxing boiler. The refluxing boiler is an important untested concept judged necessary for electrical series connection of cells in a practical device, as was more fully explained in a preceding section.

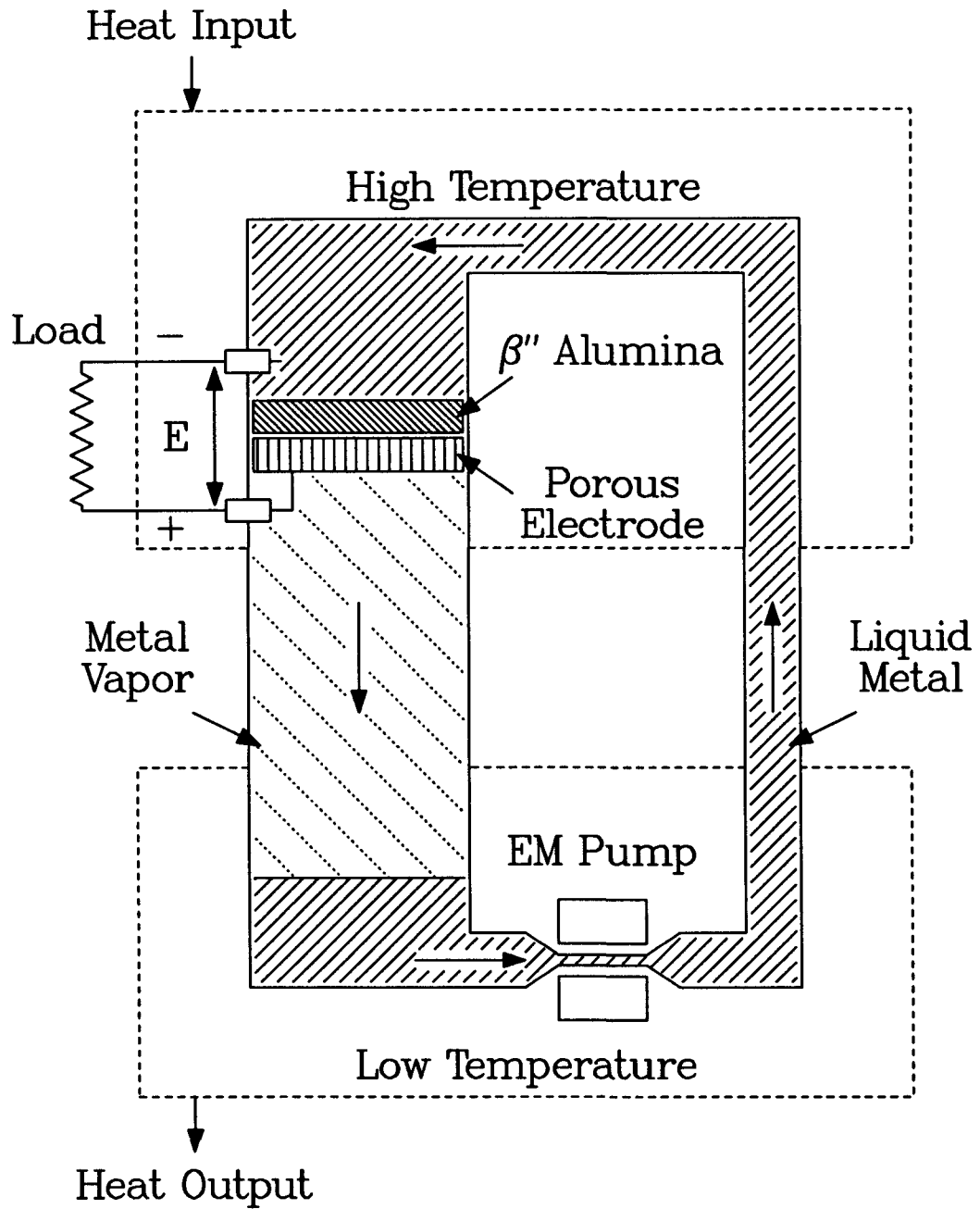


Figure 1. Liquid Metal Thermal Electric Converter Cycle Schematic.

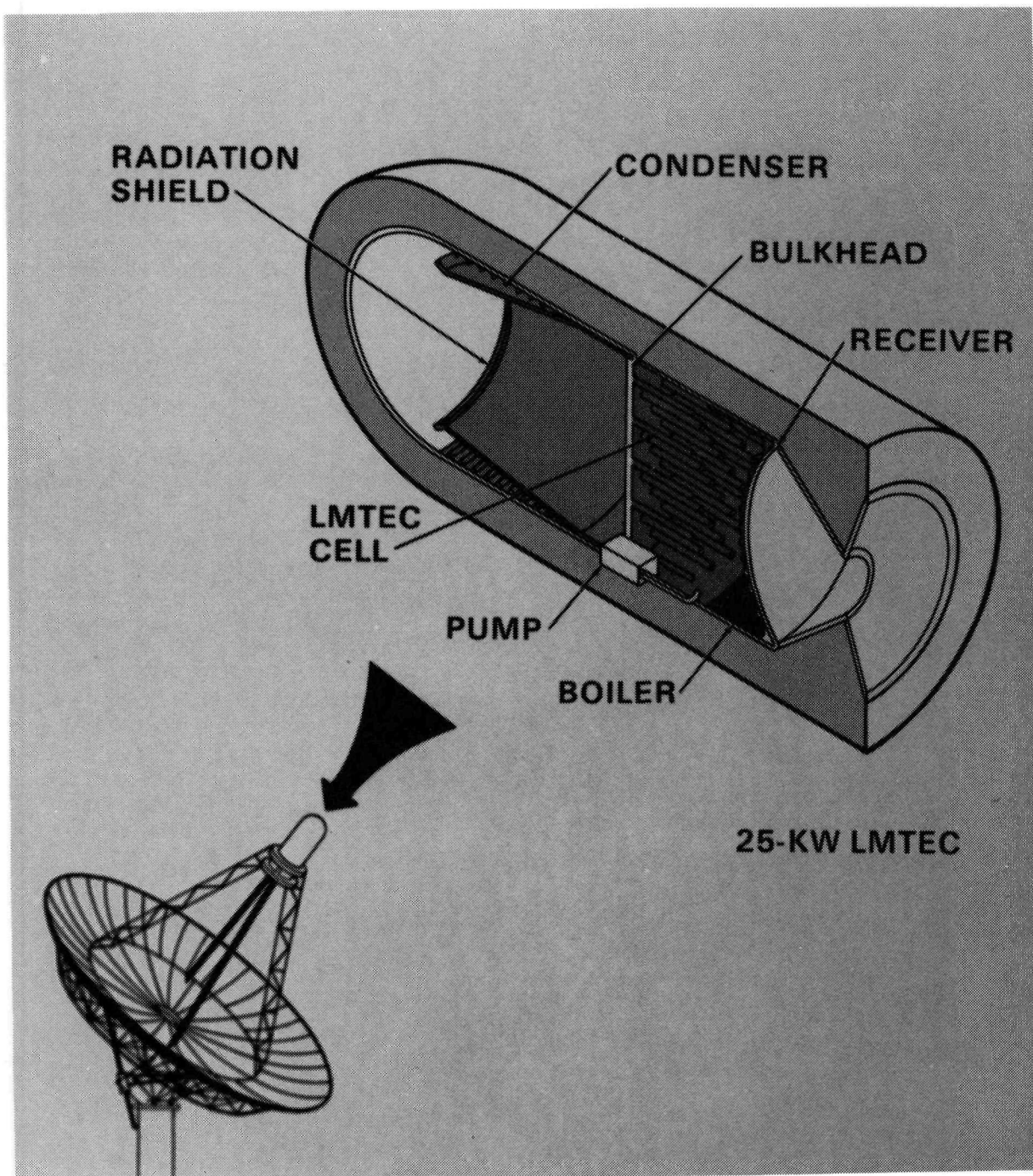


Figure 2. Liquid Metal Thermal Electric Converter Application To Dish Electric Systems.

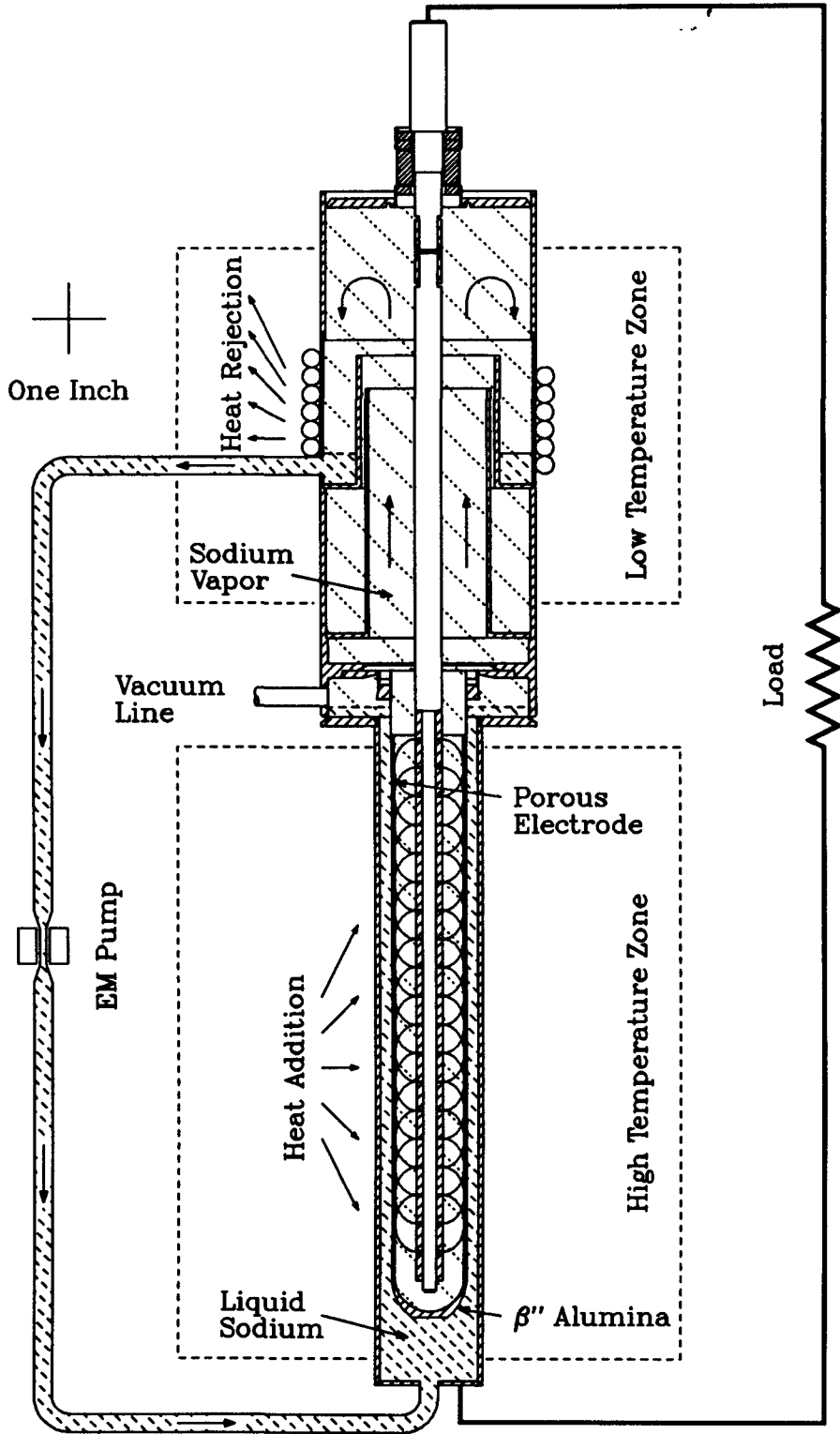


Figure 3. Liquid Metal Thermal Electric Converter Bench Test Module Schematic.

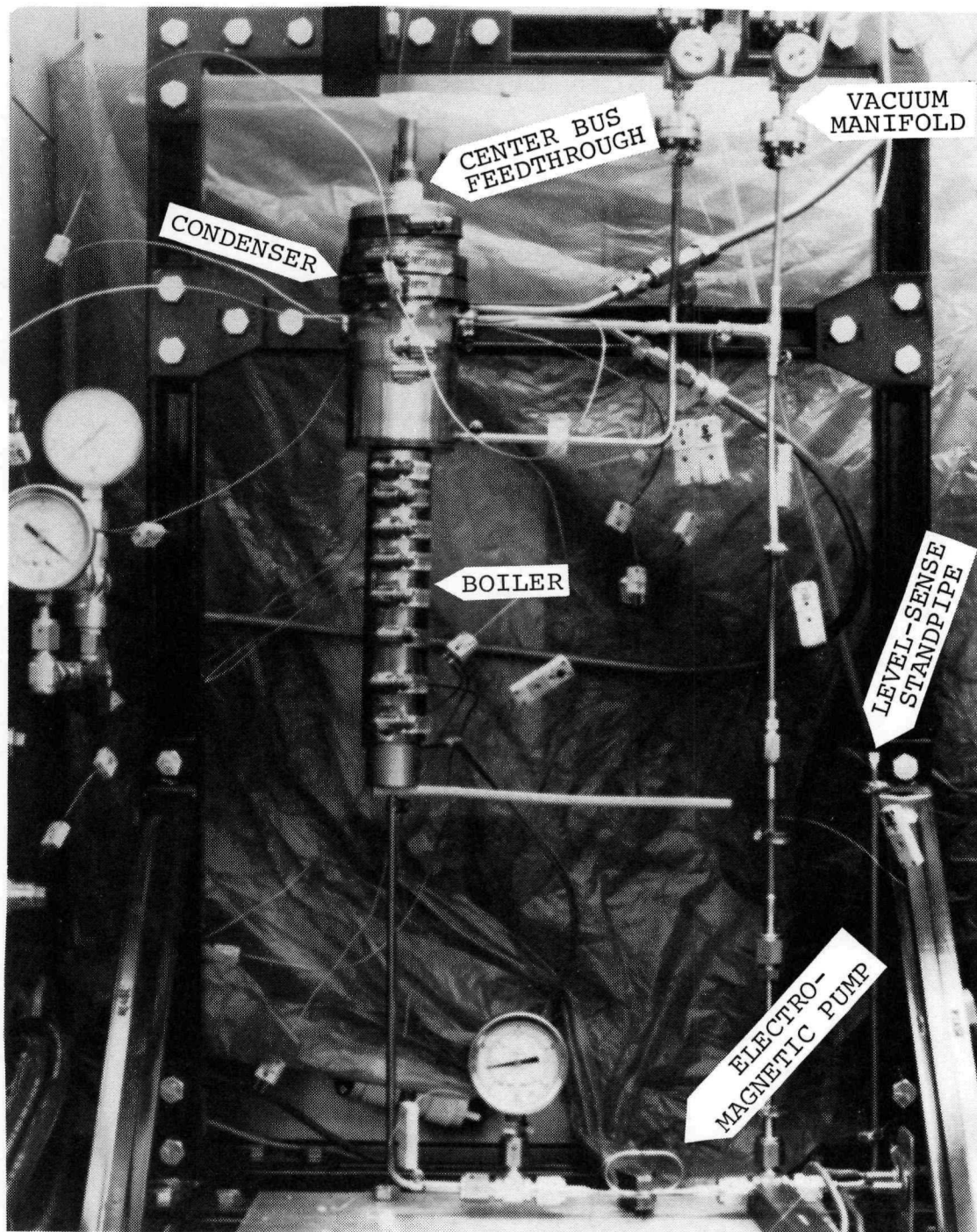


Figure 4. Liquid Metal Thermal Electric Converter Bench Test Module.

References

1. L. L. Lukens, "Dish Electric Systems Heat Engine Assessment," SAND85-0522, Sandia National Laboratories, Albuquerque, NM, June 1985.
2. L. L. Lukens, C. E. Andraka, J. B. Moreno, J. P. Abbin, "Liquid Metal Thermal Electric Converter," SAND86-2823C, Sandia National Laboratories, Albuquerque, NM. Presented at 22nd Intersociety Energy Conversion Engineering Conference, August 10-14, 1987, Philadelphia, PA.
3. N. Weber, "A Thermoelectric Device Based on Beta-Alumina Solid Electrolyte," *Energy Conversion* 14, 1 (1974).
4. W. F. Hammetter, G. C. Farrington, and E. E. Hellstrom, "Progress Toward A Mercury Heat Engine: Synthesis of a Mercury Electrolyte," Paper No. 879384. Presented at the 22nd Intersociety Energy Conversion Engineering Conference, August 10-14, 1987, Philadelphia, PA.
5. T. K. Hunt and N. Weber, "Research and Development Program on a Sodium Heat Engine, Final Report," Ford Motor Company, October 1982.
6. C. R. Peeples, R. E. Cuthrell, D. M. Mattox, "Post Cathode Magnetron Sputter Deposition Inside a Small Diameter Closed End Tube," submitted to the *Journal of Vacuum Science and Technology*.

APPENDIX A
BENCH TEST MODULE DESIGN

Blank Page

Bench Test Module Design

The purpose of this Appendix is to outline the considerations that were applied to:

1. The general design of the bench test module (BTM) - in particular the choice of components and the configuration.
2. The various choices of materials.
3. The selection of overall dimensions of the bench test module.
4. The detailed design of the condenser section.

The circumstances and constraints that governed the above decisions were:

1. The basic objective of developing and proving a number of innovative concepts motivated by the idea of adapting and demonstrating Ford Motor Company's Sodium Heat Engine for terrestrial solar applications.
2. The most basic of these new concepts were (a) using a refluxing boiler to facilitate series connection of many individual LMTEC cells, (b) placing the high-pressure zone outside of the ceramic solid electrolyte tube, with the electrode on the inside to put the tube in a more favorable stress state, (c) using a remote condenser, i.e. a cold section optically isolated from the hot section to reduce thermal radiation losses, (d) using an electrolyte tube of larger diameter (2.54 cm) than in previous efforts to reduce the number of parts in a multi-cell LMTEC, and (e) using alternative working fluids such as mercury rather than sodium in order to increase device efficiency and avoid operational problems such as fluid freezing. This last concept required the development of a new solid electrolyte that would be mercury-ion conductive. While that development was underway, two BTM's were to be built for operation with sodium and used to develop and prove the various concepts required to make a multi-cell mercury-based LMTEC. The first BTM (reported on here) was built primarily to prove the internal electrode and remote condenser concepts and the one-inch ceramic electrolyte to metal seal.

3. The beta" alumina tube size (nominally 2.5cm x 22cm). Developing a seal for this size tube would involve an extension of previous efforts.
4. The operating temperatures (up to 800°C at the boiler and 200-400°C at the condenser in a sodium-based system).
5. The use of elemental sodium throughout the BTM.
6. A host of operational requirements, including the limiting of thermal, electrical and flow losses, and the need for detailed temperature and voltage data from within the BTM.

Where possible the previous experiences of the Sodium Heat Engine development effort at Ford Motor Company were utilized. However, the bench test module differed in important respects from previous designs. In particular, the concept of locating the liquid-metal high-pressure region outside of the ceramic electrolyte tube was previously untried. This arrangement has the advantage of putting the electrolyte in compression rather than tension, an obvious advantage if the vapor pressure at operating temperature is very high. However it requires the development of an internal electrode - a permeable metallic electrode on the inside diameter of the tube - and a current collection scheme to efficiently distribute electrons over the electrode. Another important difference was the use of a remote condenser using features that should be adaptable to a multi-cell solarized LMTEC. This concept involves placing the condenser surfaces such that they are radiatively shielded from the hot surfaces associated with the boiler and the solid electrolyte.

An early decision was made to build the BTM with as many features of a practical solarized LMTEC as possible. This decision was intended to enable a realistic appraisal of LMTECs for terrestrial solar applications at as early a date as possible. Thus the BTM was conceived as a "recirculating test cell" (Ford's terminology) with high-temperature seals - as opposed to a "demountable test cell" with cooled o-ring seals and no provision for recirculating working fluid. The main elements of the BTM, shown in Figure A1, are:

1. The containment envelope, divided into a relatively high-pressure boiler section and a low-pressure condenser section.

2. The solid electrolyte tube, with permeable metallic electrode coating on its inside surface.
3. The radiation shields between the boiler and condenser.
4. The ceramic to metal seal assembly which, in conjunction with the solid electrolyte, forms the division between the boiler and condenser sections.
5. The central bus with current-collection and voltage-probe "spiders".
6. The high-temperature dielectric feedthroughs for the bus and voltage probes.

Materials recommendations and rationales were developed as a result of consultations as outlined in the memos included in this Appendix. The material used for the boiler and condenser envelope was type 316L stainless steel. This choice was based on availability of tubing and was within the range of recommendations. The use of low-carbon stainless steel was judged to be critical because of the well-known phenomenon of carbide precipitation in ordinary grades in high-temperature service. Joining was accomplished using tungsten-inert-gas welding, electron-beam welding, and hydrogen-atmosphere brazing with BNi-3 filler metal. The central bus was made from dispersion-strengthened copper, except that at the feedthru oxygen free high conductivity (OFHC) copper was used. The feedthroughs were commercially-available proprietary items. The bus, internal electrode and ceramic to metal seal are discussed in separate Appendices.

The overall BTM design was fixed to accommodate a 2.5 x 22 cm solid electrolyte tube mounted with the open end up. This approximates conditions expected for a single module of Sandia's multi-cell 25-kWe dish-electric conceptual design. The boiler diameter and length were chosen to minimize the required inventory of sodium, and to be consistent with commercial stainless-steel tubing dimensions.

The condenser section was sized to accommodate radiation shields and cooling coils. A number of criteria were to be satisfied:

1. Vapor-flow passage large enough so that flow-related pressure drop is not important compared to that occurring in the annulus between the bus and the electrolyte tube.

2. Cooled length of condenser section sufficient for easy extraction of 500 Watts using air cooling.
3. Cooled length separated from both the boiler and the guard-heated dielectric feedthroughs to limit thermal conduction from each to 50 Watts.
4. Outer diameter minimized to limit thermal losses.
5. Consideration given to the range of stainless-steel tubing sizes commercially available.

For both the boiler and condenser, the minimum wall thicknesses were determined in accordance with Section I of the ASME boiler code ("ASME Boiler and Pressure Vessel Code, Section I" published by the American Society of Mechanical Engineers, New York, 1979). It was assumed that the maximum service temperature would be 800°C for the entire envelope; this meant that the internal pressure would be sub-atmospheric at all times because the vapor pressure of sodium at 800°C is about 1/2 atmosphere. For conservative design purposes it was assumed that the differential pressure across the envelope wall was a full atmosphere at 800°C.

The condenser cooling scheme was designed with the objective of maintaining a uniform (10% of the Centigrade temperature) condenser-wall temperature at the maximum power point of the bench test module, for heat rejection temperatures of 200-400°C. The expected heat rejection rate at the maximum power point was estimated to be approximately 350 Watts. To promote uniform temperatures, the outside surface of the condenser section was covered with a layer of 0.007-inch-thick copper foil, and the cooling coils were configured as a double helix of copper tubing with coolant flowing in opposite directions for each adjacent pair of coils. Good thermal contact between the coils and the copper foil was established by mechanical clamping and soldering. Both analysis and experiments were used to establish the final design. Air was selected as the coolant, based on a desire for simplicity and on the availability of 100-psi house air.

A thermocouple-instrumented mockup of the condenser section was constructed to validate the design. An internal electric heater was used to simulate the actual heat rejection load. The mockup was tested without interruption over a four-day period to verify that the air supply was adequate to remove the anticipated thermal power, that the condenser temperature was sufficiently uniform, and that cooling efficiency did not deteriorate with time. All test objectives were met. Typical data are shown in Figure A2.

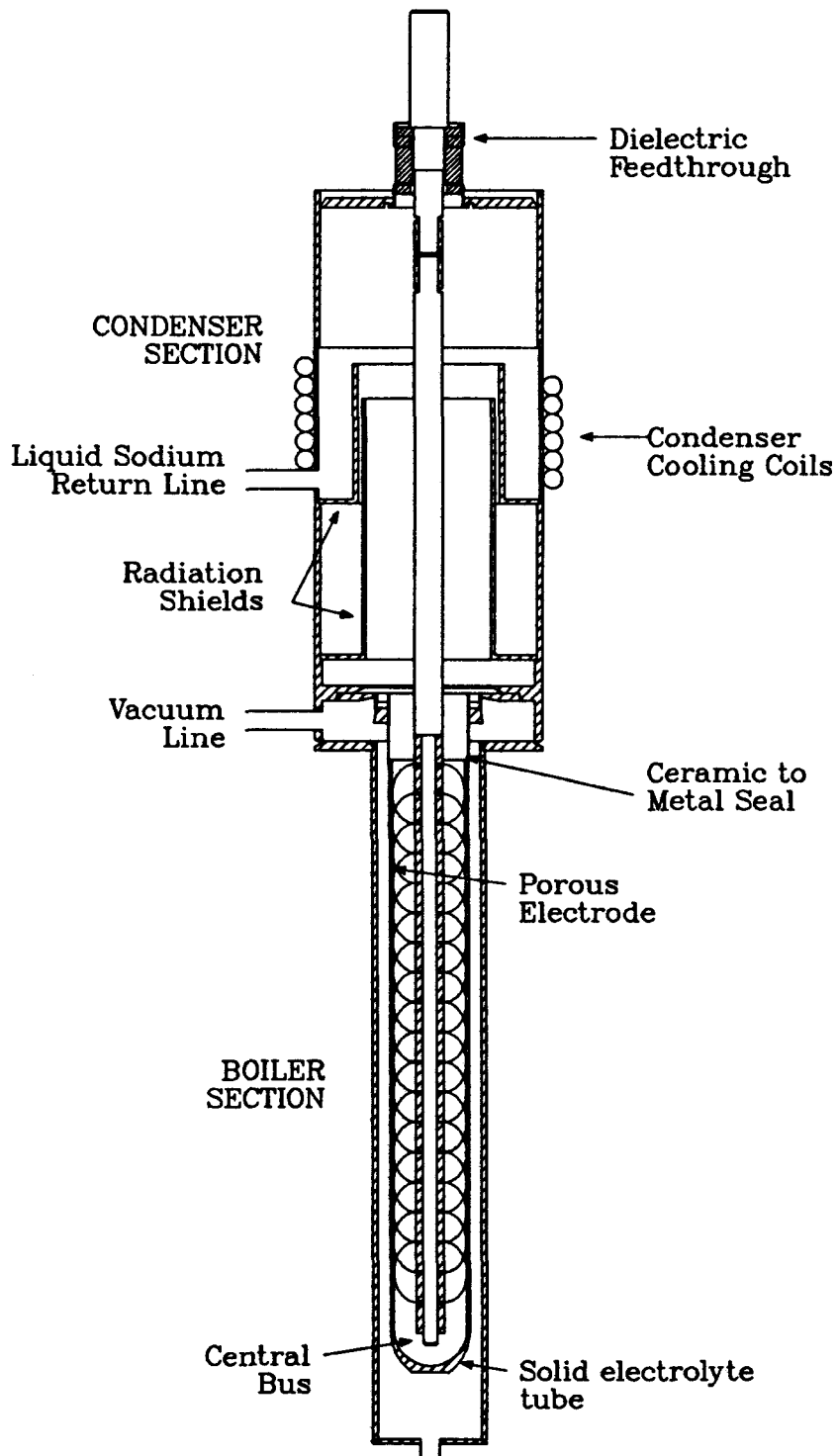


Figure A1. Bench Test Module Elements.

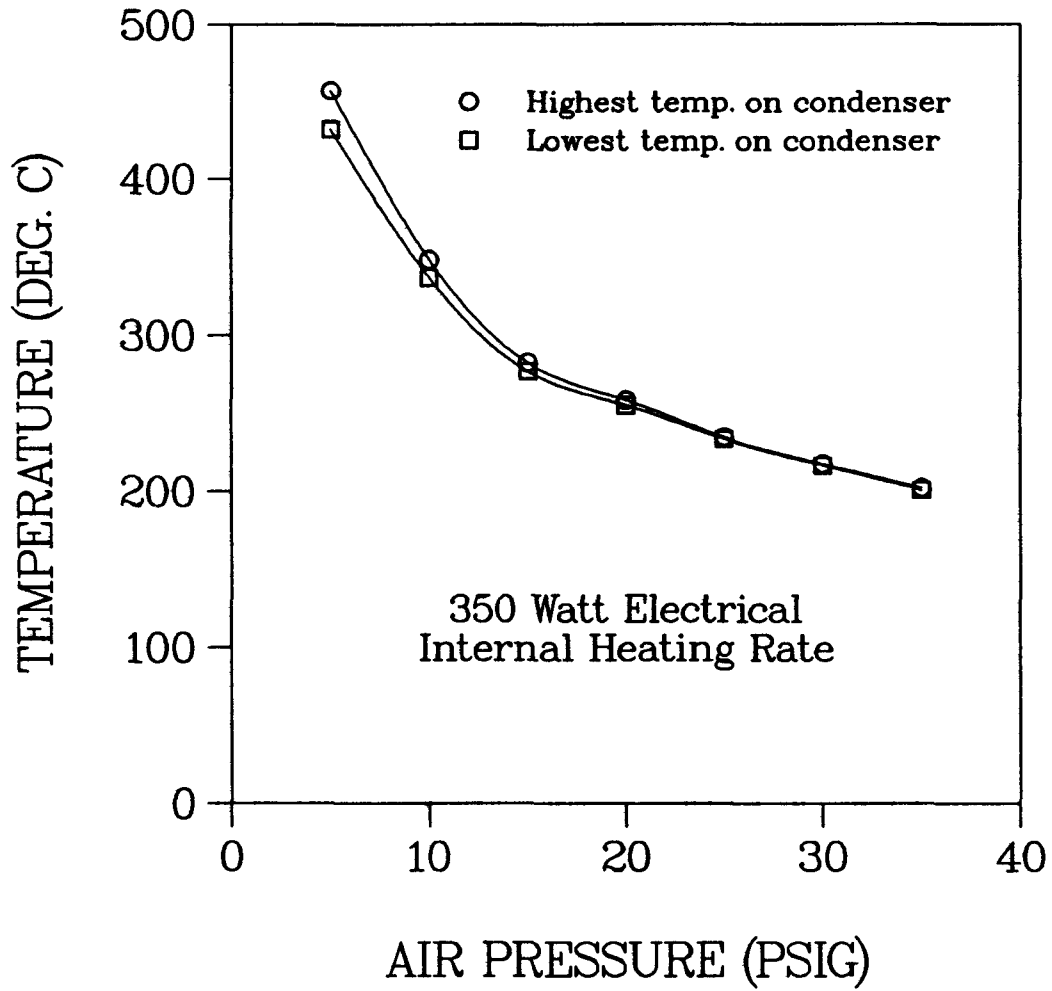


Figure A2. Condenser Mockup Test Results.

Date: October 22, 1985

Sandia National Laboratories

Albuquerque, New Mexico 87185

To: J.B. Moreno and L.L. Lukens, 2541

From: *J.J. Stephens* *M.J. Cieslak*
J.J. Stephens, 1832; M.J. Cieslak, 1833

Subject: Metals-Related Issues for the Liquid Metal Thermal Electric Converter (LMTEC)

We have received the memo from J.P. Abbin, 2541, dated October 11 requesting materials support for the LMTEC. It is our intention in this memo to address some of the metal-related issues for the Sodium based LMTEC.

I. Use of Copper and Copper Base Alloys for Current Collection Busbar

The major issues which need to be addressed for the metal used in the current collection busbar are:

- A. Electrical Resistivity at Temperature (800-900°C)
- B. Sodium Compatibility
- C. High Temperature Creep Strength

Ideally, we would like to specify a material with low electrical resistivity, no sodium compatibility worries, and good high temperature creep strength. Unfortunately, no material completely satisfies all 3 desired properties. Materials selection for the busbar must be based on trying to find a metal or alloy with the best combination of the desired properties.

We think that the dispersion strengthened copper base alloys (specifically: Glidcop Al-15 Low Oxygen Grade) promise to be the best candidate material, although sodium compatibility is definitely an issue with all copper base alloys.

A. Electrical Resistivity at Temperature (800-900°C)

To the best of our knowledge, pure metals always offer lower electrical resistivity (thus, higher electrical conductivity) than metallic alloys. Thus, in order to select a material to use for the busbar, the alloy should contain only those second phase additions necessary for high temperature strength, since this will cause only slight increases in the resistivity of the metallic matrix. If we examine the resistivity of pure metals as a function of temperature, only the metals Au, Ag, Cu, W and Mo bear examination. We rule out Au automatically as too expensive, and plot the resistivity of the four remaining metals as a function of temperature in

Figure 1. It is apparent that Cu is significantly less resistive than W or Mo, and only slightly more resistive than Ag in the range 800–900°C. Thus, Cu with a minimum amount of second phase additions for high temperature creep strength would be a reasonable choice. The Al₂O₃ dispersion strengthened copper alloys marketed by SCM metals appear to follow this scheme: with no intentional alloying addition to the Cu matrix, and ranges of 0.5–1.5 vol. % Al₂O₃ for high temperature strength. The room temperature resistivity of the Al-15 alloy is 1.09 times that of the International Annealed Copper Standard. The resistivity of Al-15 (measured by SCM) to 400°C is shown in Figure 2, which indicates that its resistivity is slightly larger than that of OFHC copper, but follows the same temperature dependence. Thus, in the temperature range 800–900°C, we would expect the resistivity of Al-15 to be about 10% greater than that of OFHC copper.

B. Sodium Compatibility

The major drawback in using a copper alloy in the busbar is that it will have to be protected from corrosion attack due to condensation of Sodium vapor. This is because the solubility of Cu in Na, as shown in Figure 3, is quite large at 800–900°C (1073–1173 K). The solubility of Cu in Na is on the order of 1000 wppm in this temperature range. This value is undoubtedly higher if the Na vapor contains a significant partial pressure of oxygen. Fortunately, there are materials which do have a low solubility in liquid Na, although again one must take great care to insure one has clean, oxygen free Na. As Figures 3 and 4 show, Mo, Ni and Fe all have low solubility in clean Na. We therefore recommend that the copper based busbar assembly be nickel plated to protect from liquid Na corrosion.

C. High Temperature Creep Strength

The major drawback in using OFHC copper as the busbar material for long term applications is its creep strength is very low at elevated temperatures. Copper melts at 1082°C, so that 900 and 1000°C correspond to 0.87 and 0.94 of the melting point. In Figures 5 and 6 we plot the expected steady state creep rate versus applied stress for pure copper at 900 and 1000°C. Note that at the lowest stresses the creep rate is close to linear (slope = 1.21 on log-log plot) and also depends on the grain size, while at high stresses power law dislocation creep is expected with a slope of 4.5. For the case of proof of concept experiments where the OFHC feedthrough is brazed at 1000°C for 15 minutes, it is reasonable to assume a grain size of 200–500 μm and an operating stress of 0.1 MPa. We can estimate the rupture life t_r by using the Monkman-Grant relation:

$$\dot{\epsilon}_{ss} t_r = \text{Constant}$$

see fig: 0.04 " per ft
I get 1000 hrs
@ 900 C

where the constant for copper is about 0.06. This implies that simply from a steady state creep point of view and neglecting creep/fatigue interactions arising from startup and shutdown that a rupture life of only about 1600 hrs can be expected at 1000°C. The effects of startup and shutdown will be minimized if the proof of concept device is heated up and cooled down slowly (eg, 4-5 hour heat up times). Clearly this implies that for the purposes of proof of concept experiments up to about 100-300 hrs. at temperature that OFHC copper will be sufficient, but devices for long term operation need a more creep resistant material.

The great advantage of a dispersion strengthened metal is that it can retain significant creep strength to large fractions of the melting point. SCM has measured the 100 hour creep strength of Al-15 at 871°C as 68.9 MPa, this would compare to a 100 hour creep strength of perhaps 1-2 MPa for OFHC copper. It will clearly be useful to measure the stress dependence of the strain rate for Al-15 in order to permit reasonable estimates of the 10^4 and 10^5 hr. rupture strength in the temperature regime 800-1000°C. In any event, there is no doubt that for the low design stresses expected in the busbar, dispersion strengthened copper alloys possess enough creep strength to permit their use for very long periods of time.

II. Container Materials and Welding

Fabrication of the LMTEC will require the application of hermetic welds. In considerations of hermeticity, the resistance of the metal to solidification cracking must be addressed. In general, austenitic stainless steels of the 304-L or 316-L type can be expected to be more forgiving than nickel base alloys such as Inconels 600 or 625, but all alloys should be considered weldable for the present application. To ameliorate the potential problems of weld metal hot cracking, filler wire can be used both to adjust weld metal chemistry to minimize cracking problems and to fill in areas of wide joint gaps.

In the 900°C temperature regime, the stainless steels and Inconel 600 all have tensile yield stresses of approximately 10 kpsi as compared to a tensile yield stress of approximately 30 kpsi for Inconel 625. Creep properties can be expected to show similar trends. The better mechanical properties of Inconel 625 are derived at some expense to the weldability. In addition, long time aging (>1000 hrs.) of Inconel 625 in the 800°C temperature range results in the precipitation of plates of Ni_3Cb which degrade the alloy's ductility. 304-L and 316-L stainless steel weld metal

are known to precipitate either sigma or chi phases upon exposure to temperatures in the 700°C temperature range. These phases also serve to reduce material ductility. Inconel 600 remains relatively inert when exposed to high temperatures.

For the proof of concept experiments, Inconel 625 is recommended as the container material because of its superior mechanical properties. Where necessary, matching filler metal should be used. It is highly recommended that subsequent to the proof of concept experiments that the unit be subjected to a full range of metallurgical analyses to determine the extent of material degradation during service. As a backup material, Inconel 600 is recommended. This alloy has very good thermal stability and improved weldability over Inconel 625, but poorer mechanical properties, as previously stated.

Distribution:

1830 M.J. Davis
1831 R.R. Sowell
1832 W.B. Jones
1833 J.L. Jellison
1833 F.J. Zanner
1833 F.M. Hosking
6227 J.A. Leonard
6226 J.I. Martinez
2541 J.P. Abbin
2541 C.E. Andraka
7473 T.P. Conlon
7471 D.M. Blankenship
7471 D.L. Stewart
1832 J.J. Stephens
1833 M.J. Cieslak
1832 file
1833 file

Resistivity of Pure Metals Vs. Temperature

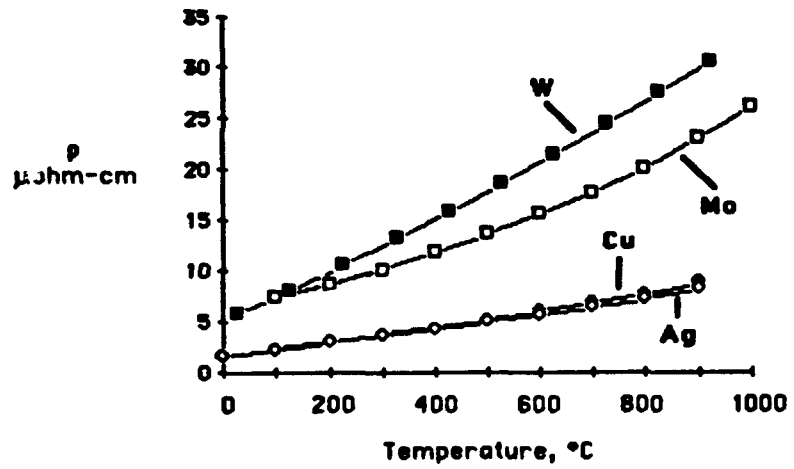


Fig. 1: Resistivity of pure W, Mo, Cu and Ag as a function of temperature. The resistivity of Cu is extremely close to that of Ag at elevated temperatures.

Resistivity Vs. Temp. - Copper Base Materials

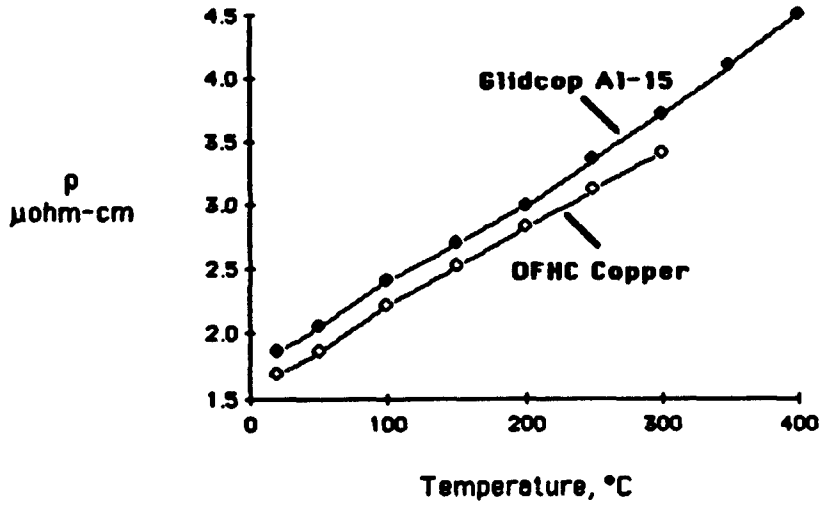


Fig. 2: Resistivity of Glidcop Al-15 compared to OFHC copper as a function of temperature. The net effect of Al_2O_3 dispersoids in Al-15 is to increase the resistivity by about 10%, but it follows the same temperature trend as OFHC copper.

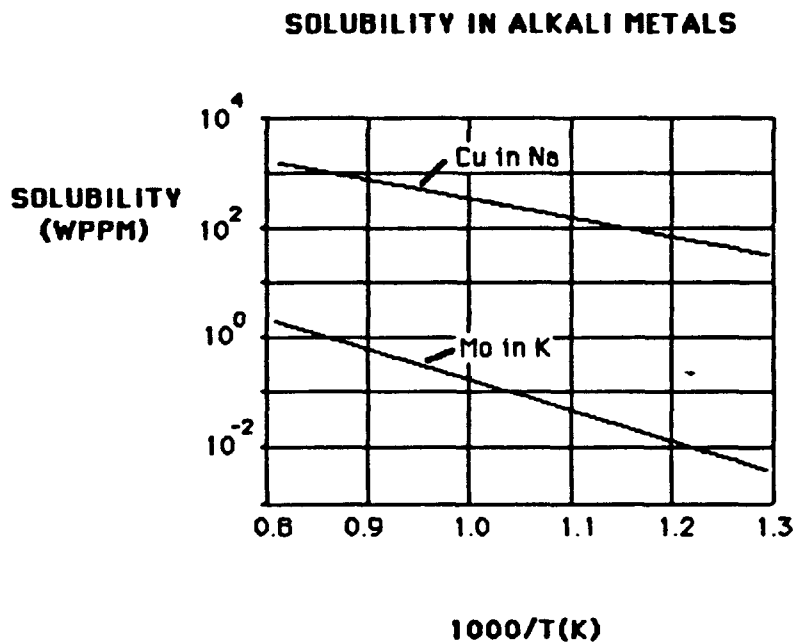


Fig. 3: Solubility of Cu in Na and of Mo in K as a function of inverse temperature. The solubility of Mo in Na would be expected to be similar to the solubility of Mo in K. Note that these values are for pure Na, Na with small amounts of dissolved oxygen should show much higher solubility at a given temperature.

SOLUBILITY OF IRON AND NICKEL IN SODIUM

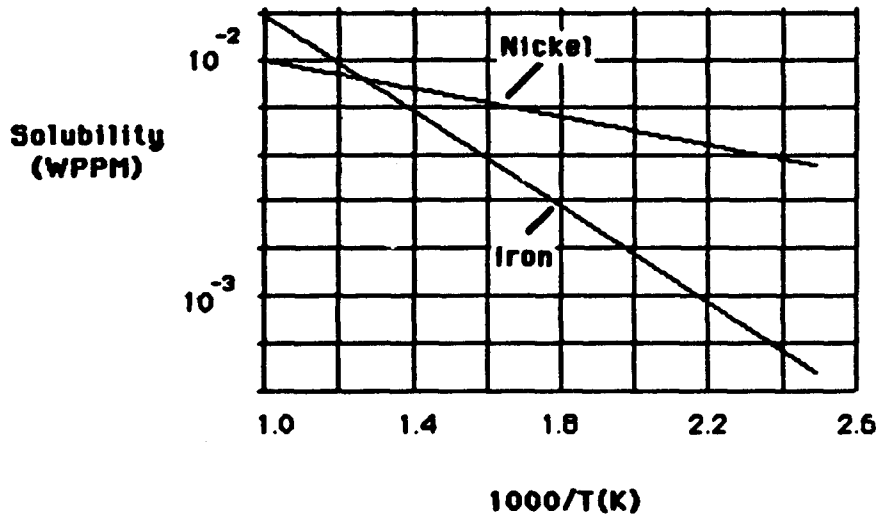
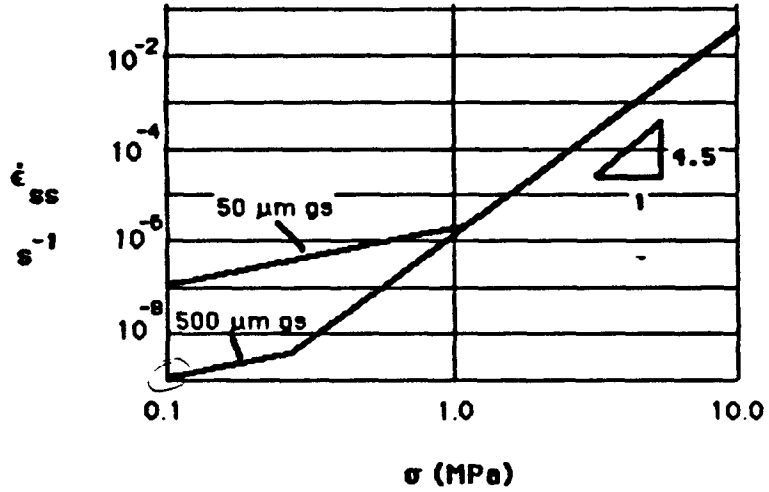


Fig. 4: Solubility of Ni and Fe in Na. Note that, as in Fig. 3, the solubility is expected to increase strongly if there is dissolved oxygen in the Na.

Creep of Copper - 900°C



$\frac{dx}{x} = 10^{-9} dt$
 $\ln x = 10^{-9} t$
 $\frac{x}{x_0} = e^{-10^{-9} t}$
 $\epsilon = -\left(1 - \frac{x}{x_0}\right) = -1 + e^{-10^{-9} t}$
 $= 3.6 \times 10^{-3} @ 1000 \text{ hrs}$
 (.04" in 1 ft)

Fig. 5: Steady state strain rate for copper as a function of applied stress at 900°C. At low stresses diffusional creep dominates and the strain rate depends on grain size. At higher stresses, power law dislocation creep dominates.

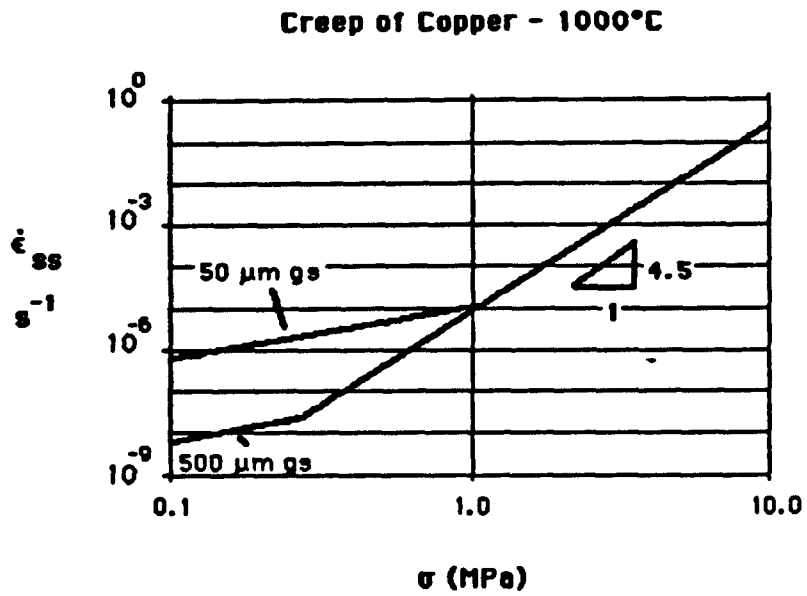


Fig. 6: Steady state strain rate for copper as a function of applied stress at 1000°C. At low stresses diffusional creep dominates and the strain rate depends on grain size. At higher stresses, power law dislocation creep dominates.

Sandia National Laboratories

Albuquerque, New Mexico 87185

date: October 25, 1985

to: Distribution



from: L. L. Lukens, 2541

subject: Liquid Metal Thermal Electric Converter (LMTEC) Materials Review Meeting

A materials and design review for the LMTEC Bench Test Module on October 23, 1985. This memo documents our understanding of the materials suggestions and warnings that came up during the meeting. Also included are some action items identified during the meeting.

Na LMTEC

Copper Buss

Copper creep strength looks adequate for 1000 hours or less at 900 C, whether OFHC or Glidcop. (Stephens)

The use of copper in the Na LMTEC is questionable from a long term Na compatibility point of view. Copper may be ok for 100 hours or less use if it is not in contact with liquid Na. (Lundberg, Zanner)

Operation of the LMTEC Bench Test Module may be the only good way to evaluate materials compatibility issues because of the complex interactions. (Lundberg, Zanner)

A molybdenum or nickel coating for the copper in the Na LMTEC should extend the working life to more than 1000 hours. A recommendation for coating type and thickness to protect the copper from Na will be made to 2541 by Cieslak and Stephens by 11/15/85. (Jones, Stephens, Zanner)

The effectiveness of using molybdenum "ink" for bonding the copper or molybdenum collector arms to the molybdenum porous electrode is not known. Experiments are planned to identify the feasibility of this bond. Curlee will review the planned experiments and report to 2541 on their current status by 10/31/85. (Curlee)

LMTEC Body

The materials acceptable for the major structural parts of the Na LMTEC Bench Test Module are 304L, 316L, IN600, or IN625. IN625 is the material of choice for long term use because of higher strength. (Cieslak, Jones, Lundberg)

Ed Martinez of the plating shops should be aware of surface treatments which would extend the life of 316L in a Na environment. (Zanner)

Beta'' Alumina

Brazing compounds for metal to Beta'' Alumina should be Ni base. Mike Hosking will contact Dale Blankenship and provide some brazing compound recommendations by 10/31/85. (Hosking, Curlee).

The compatibility of the glass seal developed by McCollister with Na is not known. Testing in the LMTEC Bench Test Module may be the best way to evaluate compatibility. Quinn will determine if a quick evaluation can be made with his facilities and when the evaluation could be made by 10/31/85. (McCollister, Quinn)

The chances of identifying a glass seal compatible with Na at 900 C are very low, and probably not worth the effort. (Lundberg)

Frank Gerstle's organization will initiate studies to identify the mechanical properties of Beta'' Alumina as a function of temperature in 11/85, and expects preliminary results on the thermoelastic properties in 01/85.. (Gerstle)

Na Working Fluid

Special procedures are needed to prepare and charge the LMTEC Bench Test Module with Na in order to assure purity of the Na. Zanner can help in the establishment of these procedures. (Hammetter, Zanner)

Hg LMTEC

The use of copper in the Hg LMTEC is probably not acceptable from Hg compatibility point of view. (Lundberg, Zanner)

High nickel alloys such as IN600, or IN625 are not acceptable materials for the major structural parts of the Hg LMTEC Bench Test Module. Materials used with Hg in the

past have been low alloy steels. There is not much information on the materials compatibility with Hg at temperatures over 500 C. 4130 steel has been used at temperatures up to 430 C. (Cieslak, Jones, Lundberg)

Distribution:

1831 R. R. Sowell
1832 W. B. Jones
1832 J. J. Stephens
1833 M. J. Cieslak
1833 F. M. Hosking
1833 J. L. Jellison
1833 F. J. Zanner
1841 L. J. Weirick
1845 F. P. Gerstle
1846 W. F. Hammetter
1846 R. K. Quinn
2525 J. Q. Searcy
2540 G. N. Beeler
2541 J. P. Abbin
2541 C. E. Andraka
2541 L. L. Lukens
2541 J. B. Moreno
6227 W. E. Boyd
6227 J. A. Leonard
6227 K. L. Linker
6227 J. I. Martinez
7471 D. M. Blankenship
7471 H. L. McCollister
7471 R. M. Curlee
7471 D. L. Stewart
7476 G. L. Cessac

Blank Page

APPENDIX B
INTERNAL ELECTRODE

Blank Page

Internal Electrode

The electrode used in the Bench Test Module was a one to two micron thick layer of tungsten applied by chemical vapor deposition (CVD). The electrode was applied by Ultramet, a California company. This appendix will outline the development of the tungsten electrode with Ultramet. A brief description of the process supplied by Ultramet is included at the end of this appendix. Several other processes for electrode application were explored in parallel with the effort at Ultramet. These methods included a molybdenum ink process, a molybdenum solution metallizing process, and a molybdenum oxide evaporation and hydrogen reduction process. These processes did not develop to a point suitable for use in the first Bench Test Module.

The initial contract with Ultramet for CVD application of a tungsten electrode on the inside surface of Beta" alumina tubes was placed in March, 1986. One of the tubes from this contract was sectioned and used to characterize the sheet resistance, thickness, and morphology of the coating. SEM analysis indicated that the tungsten coating was approximately 1 micron thick with a crude columnar structure. The sheet resistance of the tungsten coating was measured as .090 ohms/square. This is slightly less than twice as high as would be expected for 1 micron thickness of solid tungsten. The sheet resistance of a .001" thick piece of molybdenum foil was measured as a reference point and was as expected. An Auger analysis of the surface showed the presence of carbon, calcium, oxygen, sodium, aluminum, and silicon in addition to the tungsten. This analysis was repeated after sputtering several angstroms of the surface and showed the presence of carbon, oxygen, and aluminum in addition to the tungsten. These analyses were not qualitative.

An attempt to fabricate a seal assembly using a Beta" alumina tube from the first group of Ultramet applied electrodes was not successful. After 3 braze cycles the Beta" alumina to molybdenum seal still leaked. It was initially believed that the outgassing from the tungsten electrode contaminated the braze alloy and surfaces preventing a good seal. The tungsten electrode appeared to have disintegrated during the braze cycle which takes place in a vacuum furnace at a peak temperature of 1005 C. Evidence of outgassing from the inside of the tungsten metallized tube after the first and second braze cycles indicated that the disintegration of the tungsten electrode occurred during the first two braze cycles. The major difference in processing between this

attempt to fabricate the Beta" alumina to stainless steel seal assembly and the previous successful attempt was in the preparation of the Beta" alumina tube. In the previous attempt the Beta" alumina tube was air fired as the final step of the cleaning process. In this attempt the tube was not air fired because that operation would have destroyed the tungsten.

The unsuccessful attempt to braze a tungsten metallized Beta" alumina tube to a molybdenum sleeve created doubts as to the acceptability of the tubes. An experiment was conducted to determine whether the outgassing noted during the braze cycle is inherent in the tungsten coating or resulted from the cleaning process of the coated tube. A metallized Beta" alumina tube, as delivered from Ultramet, was exposed to the braze heating cycle in a vacuum furnace. A clean coupon of alpha alumina was placed near the mouth of the tube to intercept potential outgassing products. Examination of the alpha alumina coupon after the experiment indicated that the tungsten was outgassing. SEM and Auger analysis showed that the outgassing was primarily tungsten. In addition the tungsten coating blistered and lost adhesion over a major portion of the tube.

A potential explanation for the brazing problem was the outgassing of water during the braze cycle carrying off tungsten and separating the coating from the Beta" alumina with local pressure increases. If this was the case a long vacuum bake with a slow temperature increase might allow the water to escape without damaging the tungsten coating. An experiment was conducted to test this theory. A tube with a tungsten electrode applied was placed in a vacuum oven and after a 1-day pumpdown by the vacuum system, the temperature was ramped to 1050°C at a rate of 10°C per hour. After cooling down, the tube was examined, and the coating was found damaged in a similar fashion to the one that experienced a braze cycle. The surface flaked off and bubbled up in many places, and was rendered useless. A second experiment was conducted to determine the stability of the tungsten coating to the LMTEC's operating temperature, 800 C. This experiment indicated that the tungsten coating was stable at 800 C, and it was decided to attempt to apply the electrode to completed tube bulkhead assemblies.

A contract was placed with Ultramet to coat tube-bulkhead assemblies with tungsten for the Bench Test Module. Ultramet used the same process developed for the first tubes coated. Ultramet was unable to successfully apply the tungsten electrode to the tube bulkhead assemblies. The tungsten CVD

process was not yielding a uniform coating and the tube to bulkhead braze and the molybdenum sleeve were being damaged. The practice tube bulkhead assembly and two of the good tube bulkhead assemblies had their brazed seals destroyed in attempts to apply the tungsten electrode. An examination of the destroyed seals indicated that the damage was caused by a chemical attack of the titanium based braze alloy by the chemicals used in the tungsten CVD process.

The Beta" alumina tubes used in the tube bulkhead assemblies sent to Ultramet were stored, handled, and prepared for the braze and CVD processes more appropriately and carefully than the last tubes sent to Ultramet. It was considered possible that because of these changes in handling that the tungsten CVD coating on these tubes might be more stable than it was on the last group of tubes coated at Ultramet. A tungsten coated tube from one of the damaged tube bulkhead assemblies was separated from the bulkhead. The tube was then twice subjected to the pressure and temperature cycle required for the vacuum braze of the tube to the bulkhead. The tungsten electrode survived this cycle with no apparent damage. The tungsten electrode was also checked for adhesion and sheet resistance, both of which were good. A second tube from the damaged assemblies was subjected to this test and the results were again favorable.

The stability of the tungsten electrode to the vacuum braze cycle suggested that it might be possible to braze a tube with a tungsten electrode to a bulkhead assembly. A third tube with electrode from the damaged assemblies was separated from its bulkhead. A bulkhead from one of the earlier unsuccessful tube to bulkhead braze attempts was salvaged by cutting the moly sleeve to separate it from the tube. The tube was prepared for brazing to the bulkhead by subjecting it once to the pressure and temperature cycle which would be used for the braze. The braze of the tube to the bulkhead was considered successful. A slight leak was detected (10^{-5} cc/sec He) but it was believed to be a result of cracks in the tube resulting from the cutting process used to separate the tube from the damaged header.

The successful braze of the tungsten coated tube to a bulkhead suggested that properly handled and prepared tubes could have the tungsten electrode applied before they are brazed to the bulkhead assemblies. A group of tubes with documented handling histories were prepared for the CVD process and coated by Ultramet. Three Beta" alumina tubes with tungsten electrodes already applied were successfully brazed to a molybdenum and stainless steel bulkhead. One of these tubes was selected for use in the Bench Test Module.

ULTRAMET 12173 MONTAGUE STREET · PACOIMA, CALIFORNIA 91331
TELEPHONE (818) 899-0236
TELEX (910) 496-3490

TO: Sandia National Laboratories
FROM: Richard R. Babboni, Engineering Administrative Manager
Richard R. Babboni
RE: Process History, your PO#04-1441
DATE: 04/10/86

This document outlines the steps which were used in coating the inside of your Beta-Alumina tubes (dwg. s66306, issue B) with a 1-3 micron film of tungsten. Please note that the sealed container used for shipping the tubes had lost its 3 psig dry argon atmosphere by the time it had arrived at Ultramet. Also note that when the parts were removed from the container, some of the foam packing material was found inside the parts. To resolve this problem, Argon was blown through the parts before processing began. All handling of the parts was performed while wearing plastic gloves, and the parts were transported and stored in plastic bags with a desiccant. The following steps were used to process these parts:

1. The part was removed from the container, blown clean with argon, and placed in a plastic bag with a desiccant.
2. The part was weighed before processing.
3. The part was placed in the CVD apparatus, and the device was leak-checked for 10-15 minutes.
4. The system was back-flushed with Argon two times.
5. The part was heated slowly with H₂ flowing.
6. The temperature was stabilized between 550 and 600°C for 15-20 minutes before WF₆ was introduced.
7. WF₆ was run for 2-3 minutes with the temperature constant at 550-600°C.
8. The part was cooled in H₂, and back-flushed with Argon.
9. The part was removed from the holder and weighed again.
10. The part was sealed in a new plastic bag with a desiccant and returned to the shipping container.

ULTRAMET 12173 MONTAGUE STREET · PACOIMA, CALIFORNIA 91331
TELEPHONE (818) 899-0236
TELEX (910) 496-3490

This procedure was executed for five parts, because one part (#BCL-1261-07) was observed to have scratches on the internal surface, as well as some black marks on the bottom. This part was used as a test piece. The only parameter which varied for the parts was the net weight gain. Prior to processing these parts the acceptable weight gain for a film of 1-3 microns was calculated to be 0.3376 - 1.013g. All of the parts were in the acceptable range as indicated in Table I below.

TABLE I

<u>Part</u>	<u>Wt. Before</u>	<u>Wt. After</u>	<u>Wt. Gain</u>
BCL-1258-06	53.812g	54.370g	0.558g
BCL-1258-02	53.009g	53.610g	0.601g
BCL-1261-07	53.299g	53.689g	0.389g
BCL-1262-06	53.546g	54.027g	0.481g
BCL-1262-07	54.692g	55.340g	0.648g

PRESS FIRMLY — THE LAST COPY IS YOURS

★ U.S. GOVERNMENT PRINTING OFFICE 1985-579 727

SNLA ROUTING 3741-1, BLDG 839 3741-2, BLDG. T50 3715, BLDG. 840 SNLL ROUTING 8264, BLDG. 916

Sandia National Laboratories
PURCHASE REQUISITION

DATE 2/14/86	NUMBER 04-1441	CH NO 00	PAGE 1	PAGES 2
-----------------	-------------------	-------------	-----------	------------

SUGGESTED SOURCE Ultramet		GOVERNMENT PRIORITY <input type="checkbox"/> DOE 2 <input type="checkbox"/> DXE 2 <input checked="" type="checkbox"/> NONE	SHIP TO SANDIA NATIONAL LABORATORIES		SHIP VIA <input type="checkbox"/> Contractor Choice and Expense <input type="checkbox"/> Sandia Pick-up
12173 Montague St.		SECURITY CLASSIFICATION Material U	BLDG 894 <input type="checkbox"/> BLDG _____ 1515 EUBANK BLVD S.E. ALBUQUERQUE, NM 87123		FOB <input type="checkbox"/> DESTINATION <input type="checkbox"/> ORIGIN
Pacoima, California			BLDG 916, EAST AVE LIVERMORE, CA 94550		CONFIRMING ORDER <input type="checkbox"/> DO NOT DUPLICATE
Attn: Richard Kaplan		Information U	NO SHIPMENT <input type="checkbox"/> SEE BELOW <input checked="" type="checkbox"/>	AOA NO	TERMS
818 899-0236	ZIP 91331				

ITEM	QTY & UNIT	MATERIAL OR SERVICE DESCRIPTION	DRAWING NUMBER	INSR	PROP	EST UNIT PRICE	UNIT PR/TAX	EXTENSION
1		Metallization of ID of Beta-Alumina Tubes --		X	✓			
		Sandia will supply Ceramatec beta-alumina tubes per 566306 issue B the number of which will be negotiated. Ultramet will return at least 4 tubes metallized per the spec below, as well as all tubes used in process development.						
		Ultramet will coat the inside of the tubes with a film of tungsten 1-3 microns thick over the length of the tube, except about 1 cm at the open end of the tube shall remain clean. Metallization of the inside of the closed end is optional.						

0903707	346	0	2541	4000				043086
CASE/CCO.	SCL	ORG	ESC	\$ AMOUNT	ITEM	QTY.	FCST/SHIP DATES	

BRIEF DESCRIPTION METALLIZATION				DATE REQUIRED 3/31/86	SANDIA CONTRACTING REPRESENTATIVE			
DELIVER TO C. E. Andraka	ORG 2541	BLDG 807	ROOM 2008	E-NO 13972	Receiving Report Dist (SNLA)			
REQUESTER C. E. Andraka	ORG 2541	PHONE 4-8573	SPECIAL INFO <input type="checkbox"/> DEFENSE <input checked="" type="checkbox"/> NON DEFENSE <input type="checkbox"/> SHL PROPERTY/MATL FURNISHED <input type="checkbox"/> SHL PROPERTY ACQUISITION AUTHORIZED <input type="checkbox"/> COMPUTING EQUIPMENT			<input type="checkbox"/> NUCLEAR <input type="checkbox"/> PRECIOUS <input type="checkbox"/> RADIOACTIVE <input type="checkbox"/> EXPLOSIVE Q <input type="checkbox"/> OTHER HAZARD		
PURCHASE ANALYST <i>[Signature]</i>	PRELIMINARY OR REQUESTOR SUPERVISOR APPROVAL			PRICE JUSTIFICATION <input type="checkbox"/> COMPETITION <input type="checkbox"/> PUBLISHED <input type="checkbox"/> AOA/GSA <input type="checkbox"/> COMPARISON <input type="checkbox"/> JUDGEMENT			ACCTG CERT 2/22/86	
SPECIAL APPROVALS		TOTAL EST \$ \$4,000	COMMITMENT APPROVAL SIGNATURE <i>[Signature]</i>			NO ACCEPTABLE EQUIPMENT FOUND <input type="checkbox"/>		
BUYER 2/14	SUPPLIER	TERMS	BIDS REQUESTED	BIDS RECEIVED	C	A	CCD 3/20	FOR SHIP

APPENDIX C
INTERNAL BUS
AND
CURRENT DISTRIBUTION NETWORK

Blank Page

Internal Bus and Current Distribution Network

The purpose of the internal bus and current distribution network in the LMTEC Benchtest Module (LMTEC BTM) is to provide a path for electrons from the device's external positive terminal to its internal electrode.

The configuration used in the LMTEC BTM is illustrated in Figure C1. The primary elements of the configuration are a central bus (coaxial with the solid electrolyte tube), a spider assembly consisting of radial arms attached to the bus and making sliding contact with the electrode on the inside surface of the electrolyte tube, and a dielectric feedthru for the bus (not shown). The bus and distribution network were designed with a number of objectives in mind. These included:

1. Low electrical losses in the LMTEC electrode and between the electrode and the external positive terminal. The design-point assumption for voltage and specific current was 0.5 volts and 0.7 A/cm^2 at 800 C.
2. Acceptably-small blockage of the flow of sodium vapor exiting the electrode and moving axially between the center bus and the solid electrolyte tube wall.
3. Compliant connection between the bus and the electrode on the solid electrolyte, to accommodate differences in thermal expansion.
4. Provision for electrically isolated electrode-voltage probes at three axial locations.

The design was intended to demonstrate the feasibility of the internal bus and internal electrode concept without necessarily representing the optimum configuration or choices of material and joining methods.

The purpose of the electrode-voltage probes was to provide information on electrode-electrolyte interfacial pressure, which can be derived from the electrode voltage. In the event of poor LMTEC performance, the axial variation of the interfacial pressure can be used to discriminate between excessive pressure loss of the flow in the electrode-bus annulus and poor electrode permeability.

The bus was made out of alumina-dispersion-strengthened copper. This provided a low electrical resistance while at the same time minimizing creep and loss of strength problems at high temperature. The bus diameter was chosen to be 3/8 inch, resulting in very low electrical loss.

The dielectric feedthru was a proprietary design obtained from a commercial supplier. It was joined to the bus by a threaded turnbuckle.

A crucial part of the bus and distribution network is the connection between the bus and the electrode. Radial spring-type wiper arms in a spider shape clamped to the center bus were chosen after consideration of a number of different possibilities. The possibilities fell into two classes: those that relied on spring force for electrical contact with the electrode, and those that used a brazed joint to achieve electrical contact. The brazed joint was rejected for the initial LMTEC BTM because of concerns about resultant stresses in the solid electrolyte and anticipated difficulties in assembly. The clamping of the spiders to the bus was accomplished by making the bus a threaded rod, with the spiders interleaved with nuts on the rod. This arrangement is illustrated in Figure C1.

The concerns associated with the spring wiper approach included loss of spring force at 800 C, excessive contact resistance between the wipers and the electrode, and optimum configuration with respect to electrode blockage and to electrical dissipative losses in the electrode and the wipers. For the purposes of the test of the first LMTEC bench test module, a design capable of stable performance over 100 hours was deemed adequate.

The spring wiper configuration that was selected was based in part on the brief study summarized in the memo "LMTEC Electrode/Bus Loss Estimates" presented at the end of this section. Other considerations included ease of fabrication and assembly, and behavior during thermal cycling. In particular, it was determined that the configuration shown in Figure 1 (Case 2) of the above-referenced memo came closest to satisfying all criteria. However, it was found that during thermal cycling this configuration was not stable and radial-arm buckling would occur. The final choice was to use radial arms in the form of loops with both loop ends terminating on the center bus. It was also realized that fabrication and assembly would be greatly facilitated by making the arms from sheet stock rather than wire. Molybdenum was chosen for the material because of its good high-temperature electrical

conductivity and creep strength. Another interesting possibility that was considered was to use a low-strength material such as copper, held in place by ceramic springs. This concept was rejected after a brief study that is summarized in the memo "Ceramic springs for LMTEC" following this section. Figure C2, shows a pattern used for wire electric discharge machining of the molybdenum spiders.

The basic concept for the spring wiper radial-arm current collector was tested before a prototype electrode was available. A segment of the center bus that included two spiders was inserted into an open-ended beta" alumina tube lined with 0.001-inch thick molybdenum foil. This arrangement was instrumented for a four-wire measurement of contact resistance in an 800 C vacuum oven. The contact resistance was found to be essentially independent of time and temperature over the one-week duration of the test. This was interpreted as showing that the molybdenum arms would maintain adequate spring force during the LMTEC BTM test. The contact resistance was found to amount to approximately 30 milliohms which was judged to be acceptably low (results obtained during and after the operation of the BTM are at variance with this value, see appendix K).

The last objective that was set for the internal bus and current distribution network was to provide electrode-voltage probes at three axial locations. This was accomplished by modifying individual spiders at the three locations of interest. The modified spiders consisted of a single radial arm clamped to the central bus and contacting the electrode at one "point". The arm was electrically isolated from the bus by alumina washers. Nickel wires insulated with alumina tubing were fastened to each voltage probe. The other end of each wire was connected to small high-temperature electrical feedthroughs at the top of the benchtest module.

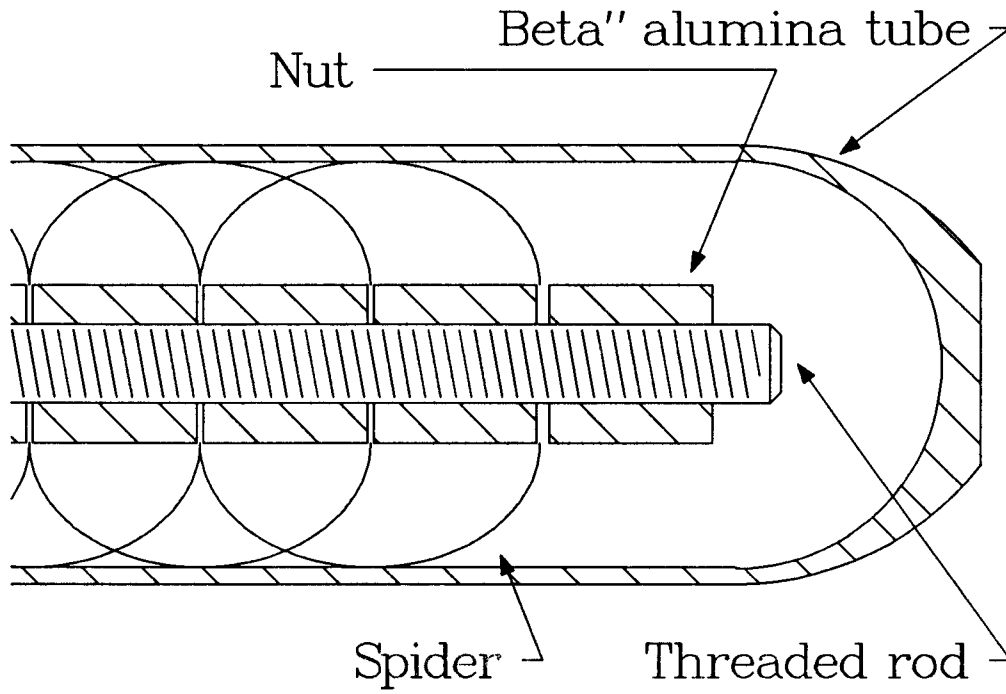


Figure C1. Internal Bus and Current Distribution Network.

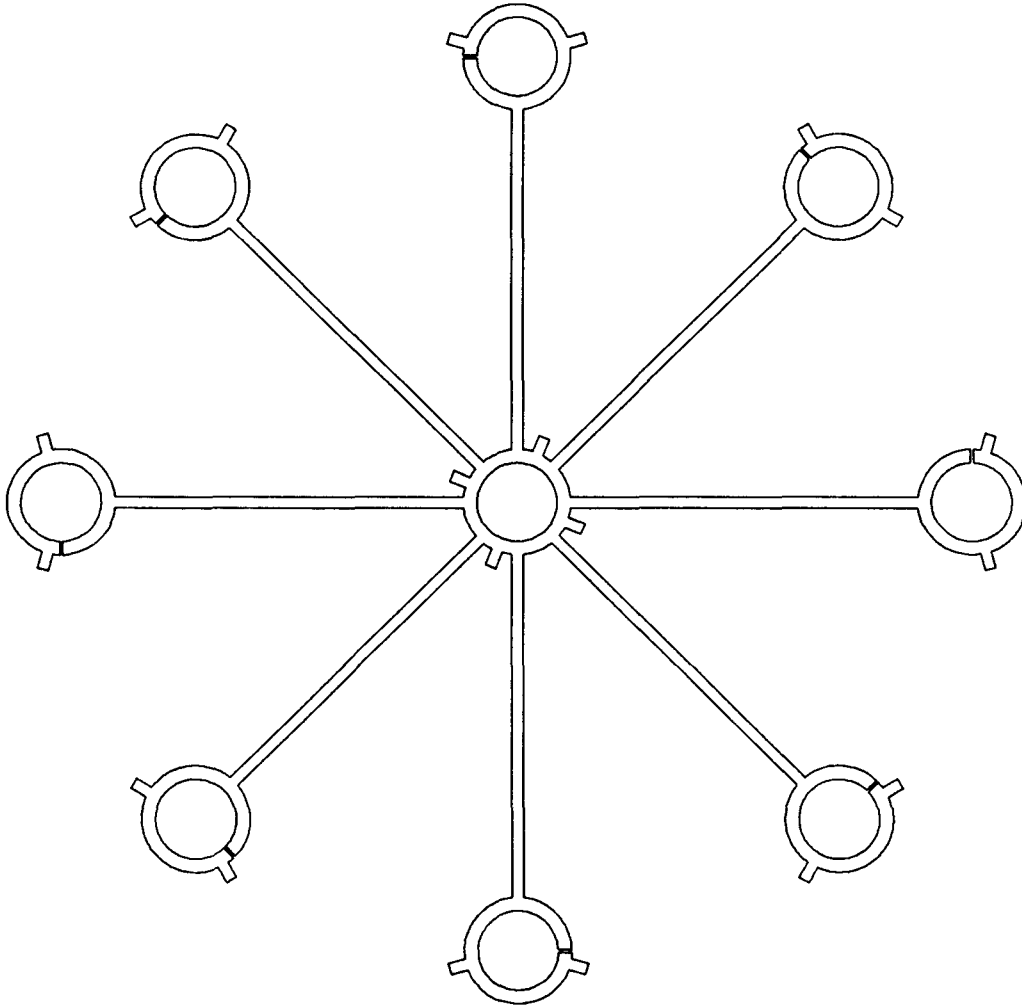


Figure C2. Spring-Wiper Radial Arm Pattern.

Sandia National Laboratories

Albuquerque New Mexico 87185

date August 23, 1985

to Distribution

from 
J. B. Moreno, 2541

subject LMTEC Electrode/Buss Loss Estimates

Estimates have been made of the electrical losses in three electrode/buss configurations. These estimates show that the losses can be considerable if care is not exercised in the choice of design parameters.

The three cases span the range of schemes currently being considered for the LMTEC testbed. The losses that were estimated are the sum of those occurring in the porous electrode and in the current collection wires between the electrode and the central copper buss bar. All three configurations have the following features in common:

1. One-micron-thick molybdenum electrode having a sheet resistance of 0.2 ohm/square, deposited on the one-inch i.d. of the BASE tube.
2. One-centimeter-diameter copper buss coaxial with the BASE tube.

The three cases differ in how current is gathered within the electrode and conducted to the copper buss. Each case is illustrated in Figure 1 and enumerated below:

1. For each $A\text{-cm}^2$ of electrode, a radial wire of diameter d conducts current from the electrode to the copper buss. The wire makes contact with the electrode through a relatively thick pad of conductor that obscures a fraction f of the area A .
2. For each electrode-area element $l\text{-cm}$ long and $w\text{-cm}$ wide, a radial wire of diameter d conducts current from the electrode to the copper buss. The wire makes contact with the electrode along a strip running the length l of the area element.

Distribution

-2-

3. A square mesh consisting of wires of diameter d and spacing w lines the BASE tube, in contact with the electrode at the corner of each square mesh element. These contacts are assumed to each cover d^2 electrode area. The mesh is brought up off the electrode and radially into the copper buss at two opposite azimuths.

Results are presented in Figures 2, 3 and 4, as percentage loss of generated power versus the design parameters. It is assumed that the LMTEC is operated at 0.7 amperes and 0.35 watts per square centimeter.

In Figure 2, results are shown for case 1. It is seen that the losses are objectionably high for practical values of electrode area per wire. The dominant loss is in the electrode film when the pad area is small. When the pad area is large, the dominant loss is obscuration of the electrode by the pad.

In Figure 3, results are shown for case 2. Severe constraints on wire size and electrode area per wire are evident. The loss in the film electrode is small for 1-cm wire spacing but increases sharply as spacing increases. The loss in the wire is a sensitive function of both wire diameter and contact length.

The results for case 3 are shown in Figure 4. Severe constraints on wire size and spacing are evident. With wire diameter/spacing-ratio fixed, the loss in the mesh dominates when spacing becomes small, because wire diameter also becomes small. When spacing becomes large, the loss in the electrode film dominates. As wire diameter/spacing-ratio increases, these losses decrease, but obscuration of the electrode increases.

JBM:2541:lh

Distribution:

2541 J. P. Abbin
2541 C. E. Andraka
2541 L. L. Lukens
6226 W. E. Boyd
6226 J. I. Martinez
7471 D. M. Blankenship

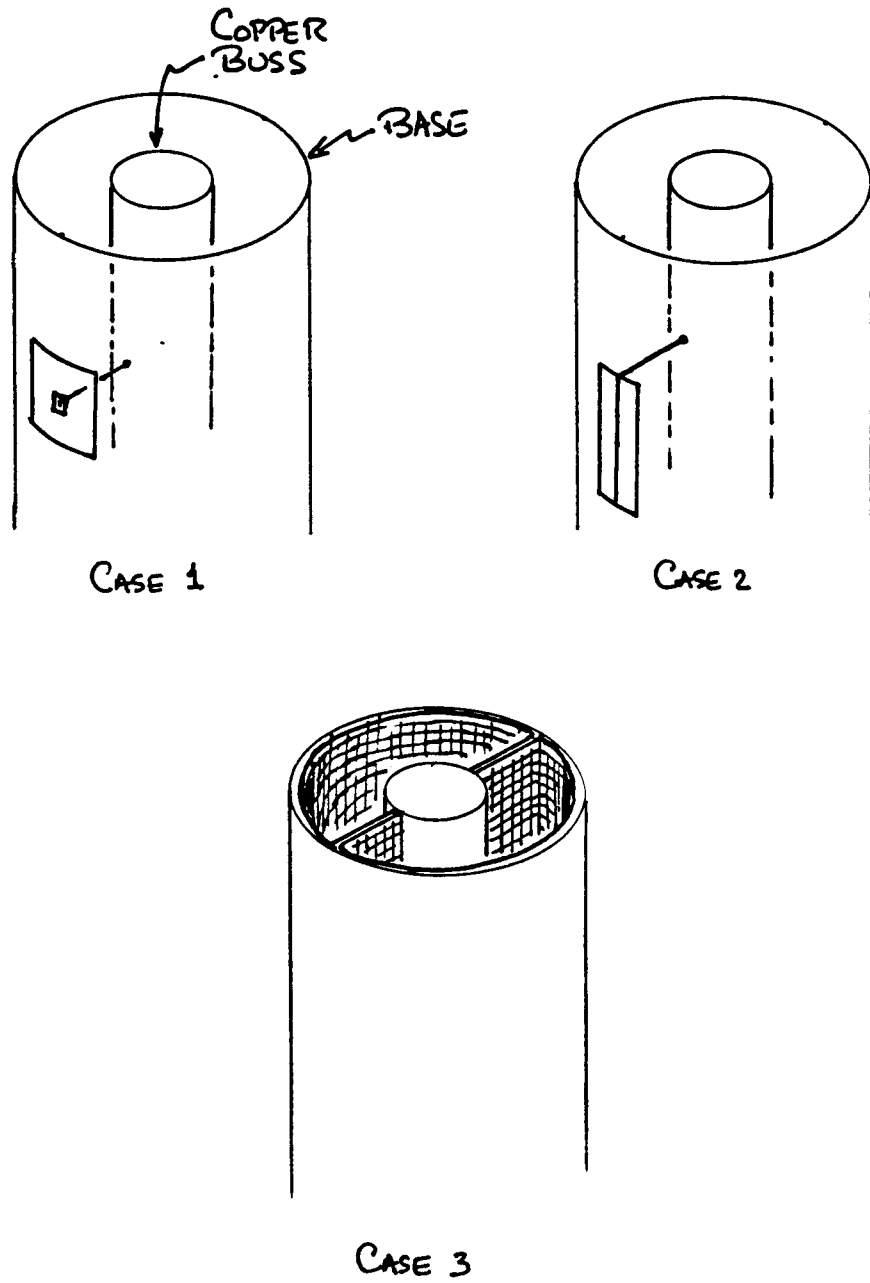


FIGURE 1. THREE CURRENT-COLLECTION SCHEMES CONSIDERED.

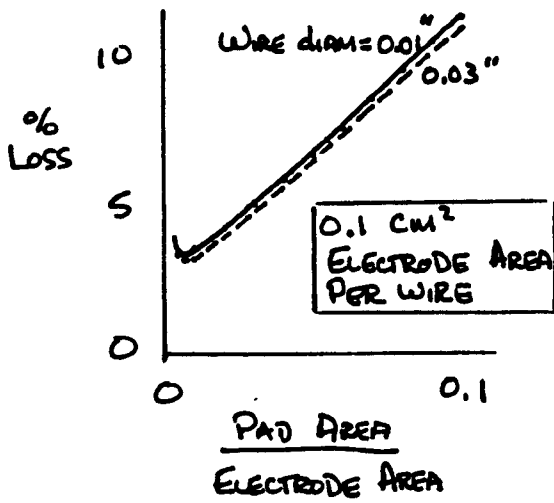
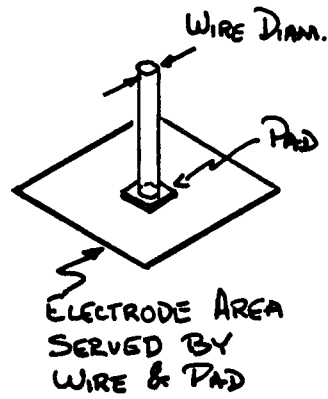
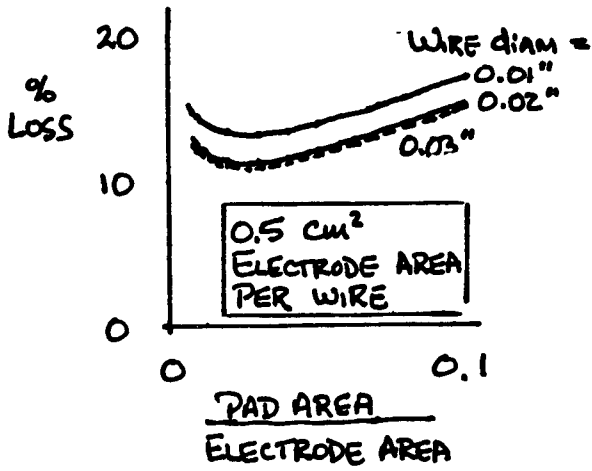


FIGURE 2 . RESULTS FOR CASE 1 .

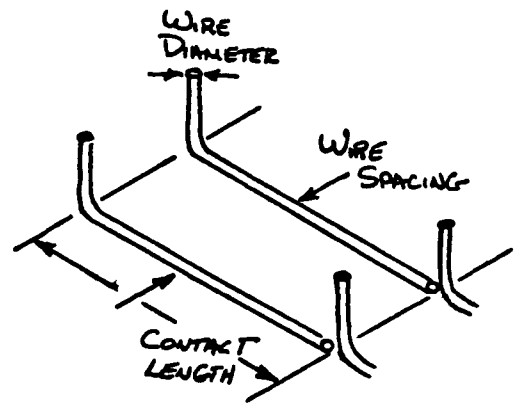
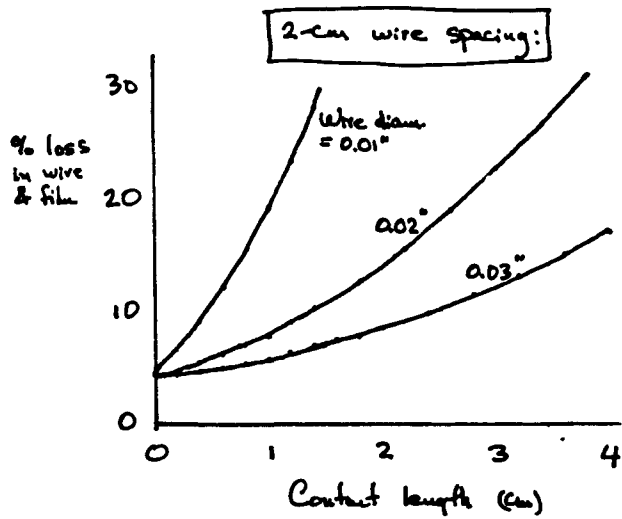
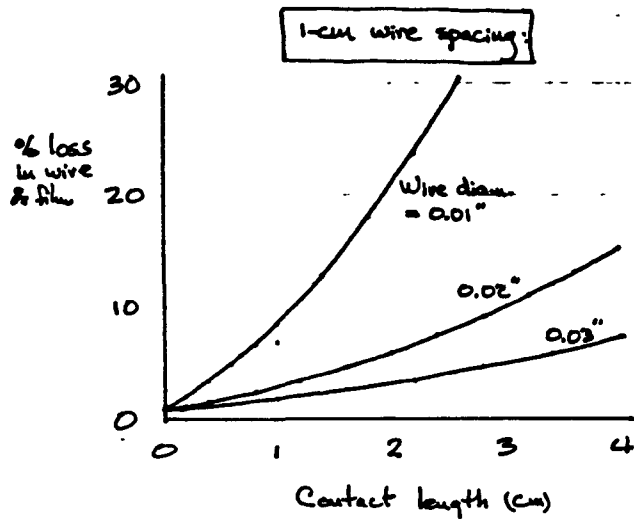


FIGURE 3. RESULTS FOR CASE 2.

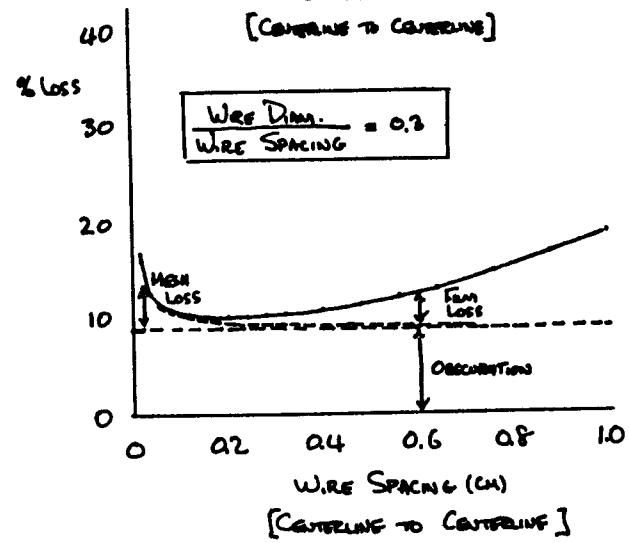
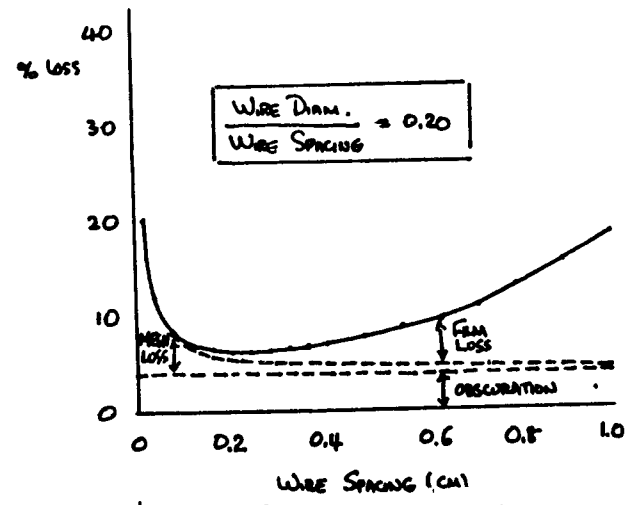
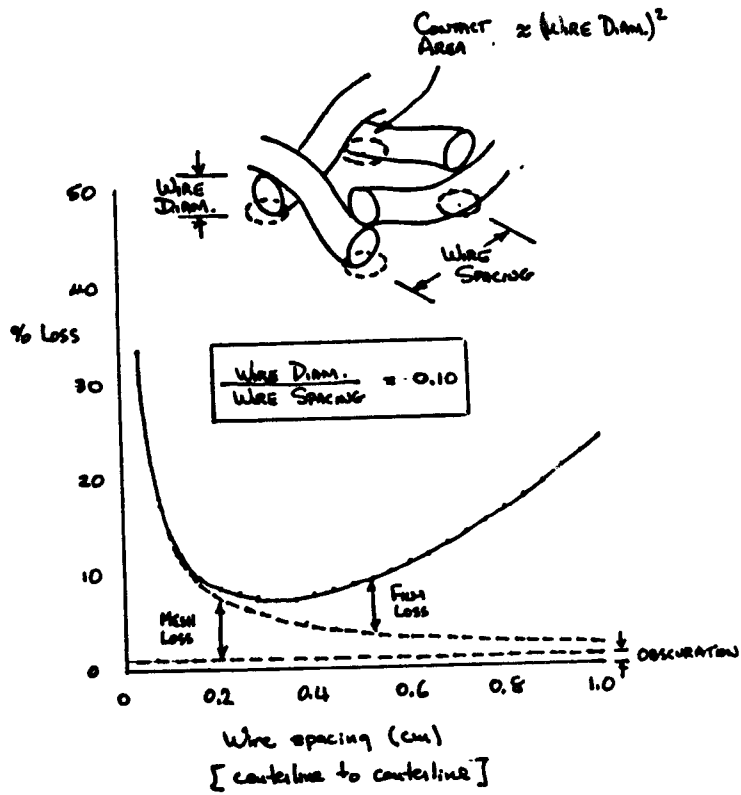


FIGURE 4. RESULTS FOR CASE 3.

Sandia National Laboratories

Albuquerque, New Mexico 87185

date: November 25, 1985

to: J. P. Abbin, 2541

from: C. E. Andraka, 2541

Charles E. Andraka

subject: Ceramic springs for LMTEC

A quick analysis was performed on the prospect of using ceramic springs to hold the internal electrode in place on the test cell LMTEC. Rough sizing and stress analysis was performed to see if such an approach is reasonable. Ring shaped springs as well as a ceramic "Christmas tree" bottle brush were considered.

The rings were assumed "C" shaped with a rectangular cross section. Based on data provided by Sarkis (7471), the tube inside diameter varied 0.012 tube to tube. Therefore, a 0.020 diameter change was specified to allow placement into the beta tube with some spring force remaining to hold the electrode in place.

The rings cannot hold their round shape when compressed, as this would require a constant moment around the ring, an impossible situation. Instead, two contact points were assumed (actually 3), one at the opening (2) and one opposite the ring opening at the center of the ring. When squeezed in this fashion, the ring did indeed fit into the tube and contact at these points.

The deflection was determined by the moment-area method (Marks Handbook) which agreed with Castigliano's Theorem. The stresses were analyzed with the curved beam formulae, also found in Marks and most basic deformables texts. Only bending moment stresses were considered, because the radius was expected to be much greater than the thickness, so other stresses would be negligible (Shigley). The analysis is attached.

The bottle brush was assumed to slant 60 degrees from straight out, a reasonable first guess at trading off the stress against the electrical losses. The end was displaced inward 0.020 perpendicular to the tube wall, subject to the same restrictions as above. The formulae for a cantilevered beam can be found in basic design texts (Shigley).

The results were tabulated by varying the thickness to calculate the stress based on the above assumptions. The strength of alumina in tension is 320 MPa (Ceramatec) and the modulus is 370 GPa. A safe stress was considered 50 MPa, which gives a thickness of about 5 mils for the rings and 1.4 mils for the brush. This is probably far too small to consider making from ceramic, and would apply a very small force to hold the electrode in place. (the force depends on the width of the ring, and the appropriate formula is included in the analysis)

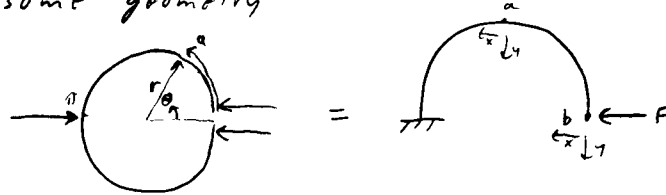
The use of alumina springs to hold a copper strip in place is an interesting idea because the alumina holds its spring properties at temperature. However, the extremely high modulus combined with the low tensile strength of alumina precludes its use. Other, lower modulus, high temperature materials will be considered, as well as possible geometry changes.

Copy to:
2541 C. E. Andraka
2541 L. L. Lukens
2541 J. B. Moreno

Rings

11/10/85

assume geometry:



by Moment-Area theory (Marks 8th ed, p5-46)

$$\begin{aligned} M &= FR \sin \theta & ds &= R d\theta \\ x &= R(1 - \cos \theta) & y &= R \sin \theta \end{aligned}$$

$$\Delta x = \int_{-a}^{\pi} \frac{M y ds}{EI} \quad \Delta y = \int_a^{\pi} \frac{M x ds}{EI}$$

$$\Delta x = \frac{FR^3}{EI} \left(\frac{1}{2} \theta - \frac{1}{4} \sin 2\theta \right) \Big|_0^{\pi} = \frac{FR^3}{EI} \left(\frac{\pi}{2} - \frac{a}{2} + \frac{1}{4} \sin 2a \right)$$

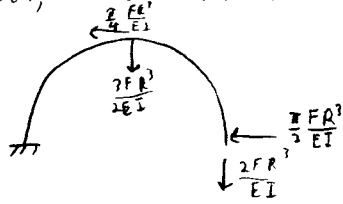
$$\begin{aligned} \Delta y &= \frac{FR^3}{EI} \int_a^{\pi} \sin \theta (1 - \cos \theta) d\theta \\ &= \frac{FR^3}{EI} \left(-\cos \theta - \frac{1}{2} \sin^2 \theta \right) \Big|_a^{\pi} = \frac{FR^3}{EI} \left(1 + \cos a + \frac{1}{2} \sin^2 a \right) \end{aligned}$$

at b): $\delta_x = \frac{\pi}{2} \frac{FR^3}{EI}$ $\delta_y = \frac{2}{EI} FR^3$

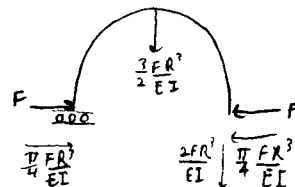
at a): $\delta_x = \frac{\pi}{4} \frac{FR^3}{EI}$ $\delta_y = \frac{3}{2} \frac{FR^3}{EI}$

This deflection (radial inward) is greater than δ_x at b (radial inward, diameter), so ring does touch in two places only

model, one end fixed:



actual:



Rings

11/20/85

Stress:

The largest tensile stress is at the outer fiber where the largest moment is.

from Marks,

$$\sigma = \frac{M}{AR} \left[1 + \frac{y}{Z(R+y)} \right] \quad ; \quad Z = -\frac{1}{A} \int \frac{y}{R+y} dA$$

$$= -1 + \frac{R}{b} \left(\ln \left(\frac{R+c}{R-c} \right) \right)$$

for rectangle cross section

$$M_{\max} = FR_0$$

$$R+c = R_0$$

$$R-c = R_0 - t$$

$$y = c \quad (\text{outer fiber})$$

$$A = bt$$

$$\sigma = \frac{F \left[r_0 - \frac{t}{2} - \frac{t}{2} \ln \left(\frac{r_0 + t}{r_0 - t} \right) \right]}{bt \left[r_0 - \frac{t}{2} - \frac{t}{2} \ln \left(\frac{r_0}{r_0 - t} \right) \right]}$$

At the open end, the minimum motion Δx needed is:

$$\Delta x = \frac{\pi}{2} \frac{FR^3}{EI} = 0.020'' \quad \text{on the diameter}$$

$$F = \frac{\Delta x E b t^3}{6 \pi R^3}$$

So,

$$\sigma_{\max} = \frac{\Delta x E t^2 \left(r_0 - \frac{t}{2} - \frac{t}{2} \ln \left(\frac{r_0}{r_0 - t} \right) \right)}{6 \pi \left(r_0 - \frac{t}{2} \right)^2 \left(r_0 - \frac{t}{2} - \frac{t}{2} \ln \left(\frac{r_0}{r_0 - t} \right) \right)}$$

$$\Delta x = 0.020$$

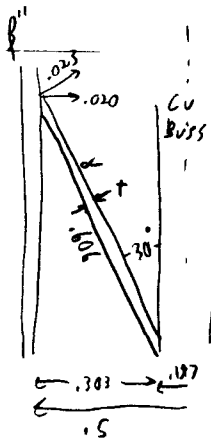
$$r_0 = 1.0$$

vary t to get σ_{\max}

Results for ring spring

```
RUN
enter deflection in inches? .020
enter thickness min,max,step in inches? 0.01,.1,.01
deflection = .02
t= .01      ma stress= 113.4578      MPa
t= .02      ma stress= 197.683      MPa
t= .03      ma stress= 302.9806      MPa
t= .04      ma stress= 414.8692      MPa
t= .05      ma stress= 531.1461      MPa
t= .06      ma stress= 652.7977      MPa
t= .07      ma stress= 790.8742      MPa
t= .08      ma stress= 914.6839      MPa
t= 8.999999E-02      ma stress= 1095.169      MPa
t= 9.999999E-02      ma stress= 1202.46      MPa
OK
```

```
10 E=3700001:1mpa
20 RO=.5:1in
30 INPUT "enter deflection in inches";DX
40 INPUT "enter thickness min,max,step in inches";TM,TX,DT
45 PRINT "deflection = ";DX
50 FOR T=TM TO TX STEP DT
60 SIG = DX*E*T^2*(RO-T/LOG(RO/(RO-T)))/(6*3.14159*(RO-T/2)^3*(RO-T/2-T/LOG(RO/(RO-T))))
70 PRINT "t= ";T;"      ma stress= ";SIG;"      MPa"
80 NEXT
```



Ceramic brush
H/22/85

- 1) $\Delta x = \frac{PL^3}{3EI}$
- 2) $M = PL$
- 3) $\sigma = \frac{Mc}{I} = \frac{PLt}{2I}$

solve 1:

$$P = \frac{3\Delta x EI}{L^3}$$

solve 3:

$$\sigma = \frac{3\Delta x E I L t}{L^3 I 2} = \frac{3 \Delta x E t}{2 L^2}$$

$$\text{or } t = \frac{2L^2 \sigma}{3 \Delta x E}$$

$$\begin{aligned} \sigma &= 50 \text{ MPa} \\ E &= 370000 \text{ MPa} \\ \Delta x &= 0.023 \text{ in} \end{aligned}$$

$$t = 3.917 \times 10^{-3} L^2$$

for $L = .606$,

$$t = 1.438 \times 10^{-3} \text{ in} = 1.4 \text{ mil}$$

for $t = 0.1 \text{ in}$,

$$L = 5.05 \text{ in}$$

APPENDIX D
CERAMIC TO METAL SEAL

Blank Page

Ceramic to Metal Seal

The BTM design required a high temperature hermetic joint between the Beta" alumina tube and the stainless steel bulkhead which separates the high temperature zone from the low temperature zone. A new joint configuration was designed and has been experimentally verified at SNLA for use in the LMTEC BTM. A schematic of SNLA's new joint configuration is shown in Figure D1. The molybdenum ring is brazed to the stainless steel plate on its outside diameter, and to a molybdenum sleeve on its inside diameter. A nickel based braze alloy is used for the molybdenum to molybdenum, and the molybdenum to stainless steel brazes. The molybdenum sleeve has a wall thickness ranging from .005 inch at the end brazed to the molybdenum ring to .001 inch at the opposite end. The thin end of the molybdenum sleeve is brazed to the Beta" alumina tube with a titanium based active metal braze alloy. The thin molybdenum sleeve minimizes stresses on the Beta" alumina tube. The relatively massive molybdenum ring matches the expansion of the thin sleeve and transmits the high strain to the stainless steel bulkhead. The stainless steel is relatively ductile and can survive many more thermal cycles than the thin molybdenum sleeve. This joint design is therefore tolerant of the large mismatch in thermal expansion between the Beta" alumina and commonly available materials used in construction of the rest of LMTEC and maintains the required hermetic seal for a practical engine.

Two memos on the analysis of the ceramic to metal seal are included in this appendix. A memo which documents the processes used to fabricate the assembly used in the BTM is also included in this appendix.

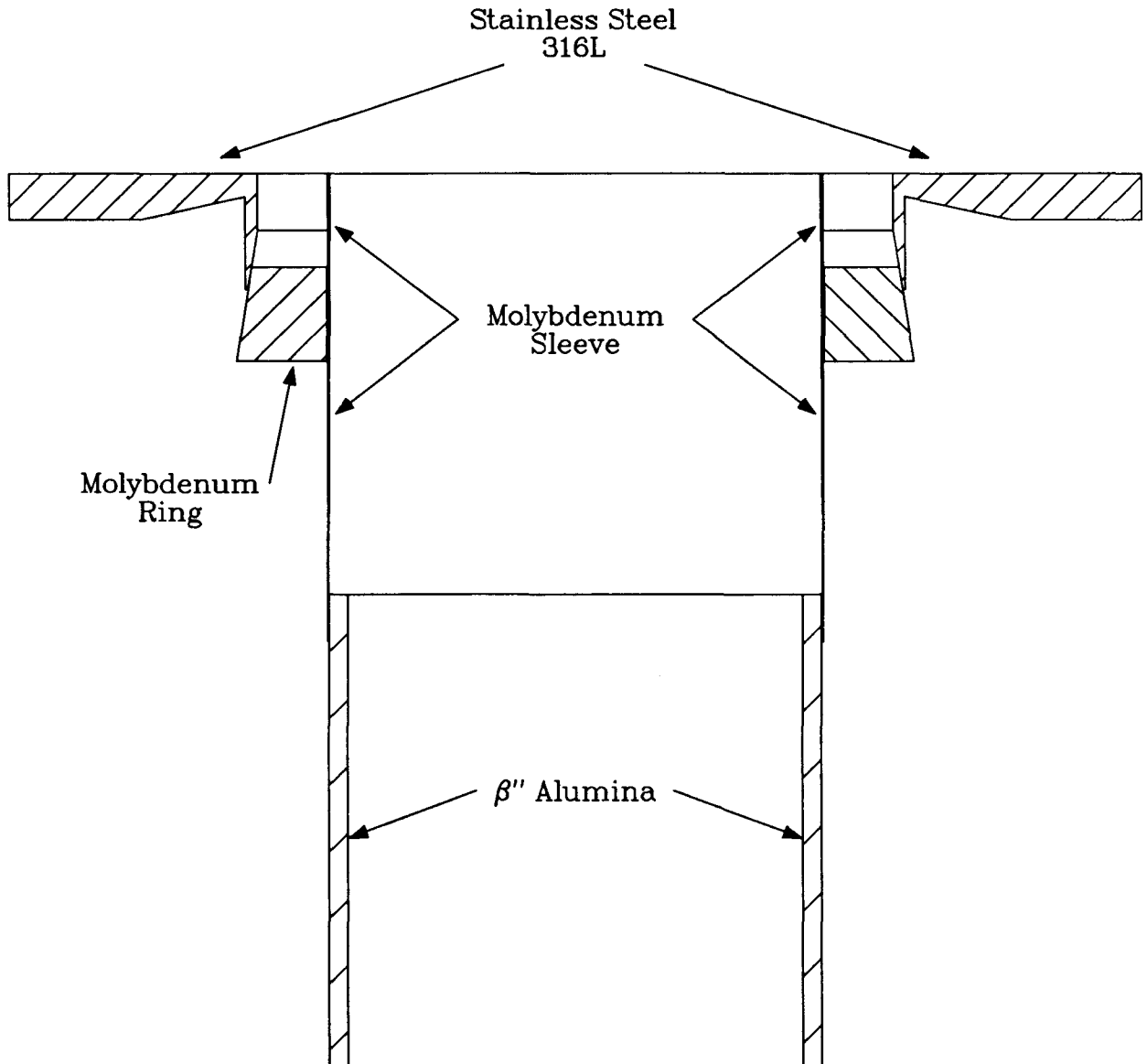


Figure D1. Liquid Metal Thermal Electric Converter Bench Test Module Beta" Alumina To Metal Joint.

Sandia National Laboratories

Albuquerque, New Mexico 87185

date: September 23, 1987

to: R. M. Curlee, 7471-2

from: *J. J. Sarkis*
J. J. Sarkis, 7471-2

R. L. Chavez
R. L. Chavez, 7471-2

subject: Assembly Procedure Beta'' Tube and Header Assembly

The purpose of this memo is to document fully the requirements necessary to successfully braze and leak test a Beta'' tube to header assembly.

The assembly requirements were developed by 7471-2 and 2541, with assistance from other outside organizations, for Larry Lukens of Division 2541.

Although it took us many months to develop the assembly process, we are still learning and refining this sequence as different coatings and parts are designed.

The first step to any successful vacuum furnace braze is to clean the parts. The cres header, moly back-up ring and moly sleeve were given a typical 3-step cleaning: 1,1,1 chloroethane electronic grade Sm (*) as a vapor degreaser; acetone rinse; topped off with 1 propanol rinse and heat lamp dry.

See Figure 1 for part numbers and braze material. No attempt is made at this time to show braze fixturing for this assembly or fixturing for He leak testing after brazing.

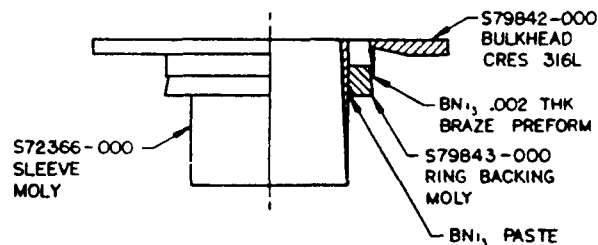


FIGURE 1 (HEADER ASSEMBLY REQUIREMENTS)

See Figure 2 for Vacuum braze cycle.

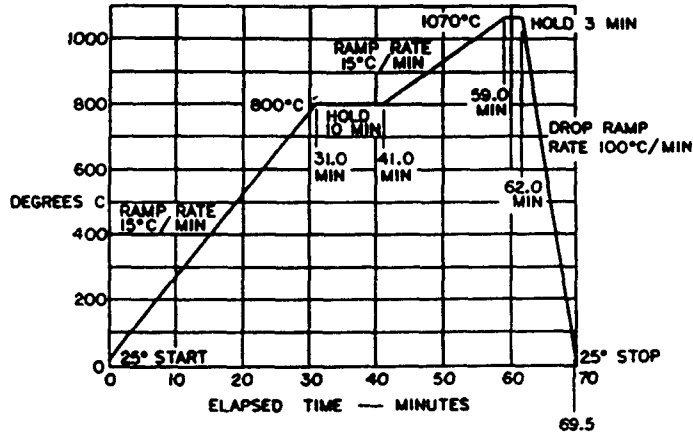


FIGURE 2 (HEADER BRAZE CYCLE)

The Beta'' tube that has been inspected and leak tested and stored in a partial pressure chamber by 2541 is brought to us for cleaning.

The cleaning of the Beta'' tube is identical to the typical three-step cleaning as the metal parts. We also air fire the tube to remove any moisture or surface contaminants.

Air firing is done in our ashing furnace. See Figure 3.

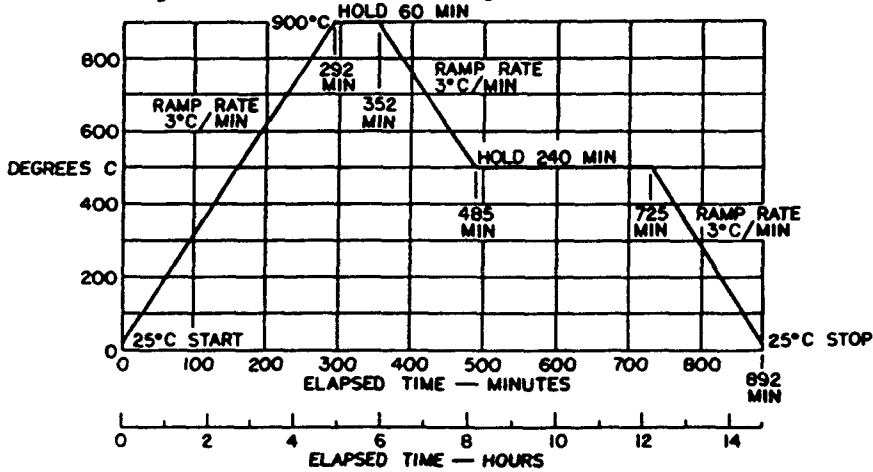


FIGURE 3 (ASHING CYCLE)

After air firing of the tube, the header assembly and Beta'' tube are assembled per Figure 4. Again, no attempt is made to show fixturing for this assembly at this time. Experience has shown us to try to achieve an overlap of .001 inch of Beta'' tube inside moly tube.

The amount of braze material to be used is approximately two times the gap vol between the sleeve ID and Beta'' tube OD and to expect to see voids after first run. We'll then rebraze with same braze material at 1.5 times gap volume. Also noteworthy, no stop-off is used.

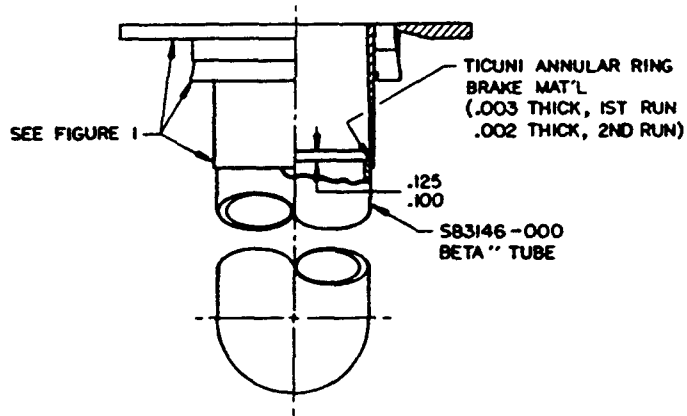


FIGURE 4 (HEADER AND TUBE ASSEMBLY)

The braze cycle for both runs is identical. See Figure 5.

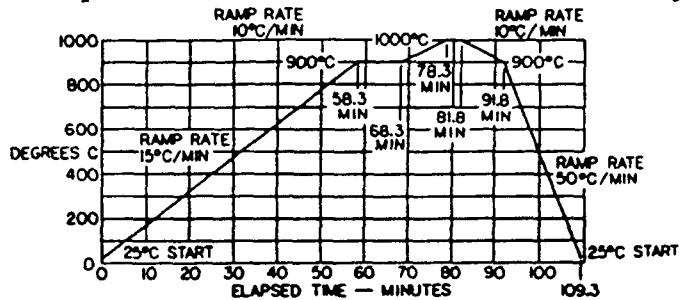


FIGURE 5 (HEADER AND TUBE ASSEMBLY BRAZE CYCLE)

R. M. Curlee, 7471-2

-4-

September 23, 1987

Figure 6 is sketch for braze fixture.

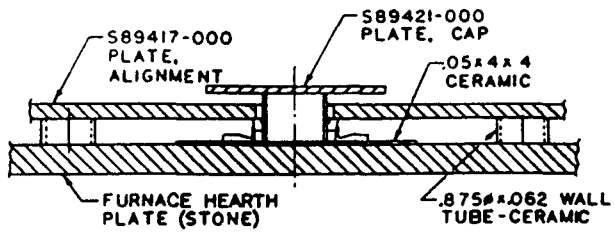


FIGURE 6 (HEADER ASSEMBLY FOR BRAZING)

Figure 7 is leak test for header assembly

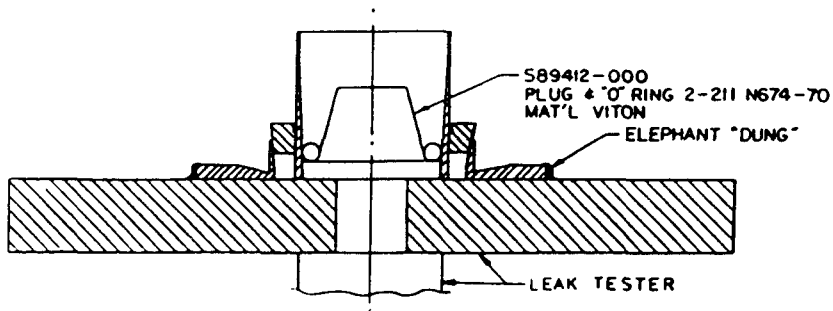


FIGURE 7 (HEADER ASSEMBLY LEAK TEST)

Figure 8 is fixture for tube and header assembly.

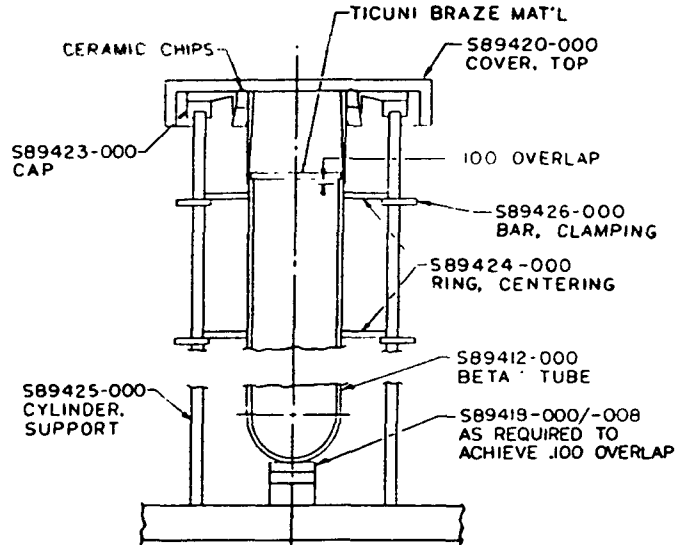


FIGURE 8 (HEADER & TUBE ASSEMBLY FIXTURE)

Figure 9 is leak test for final assembly.

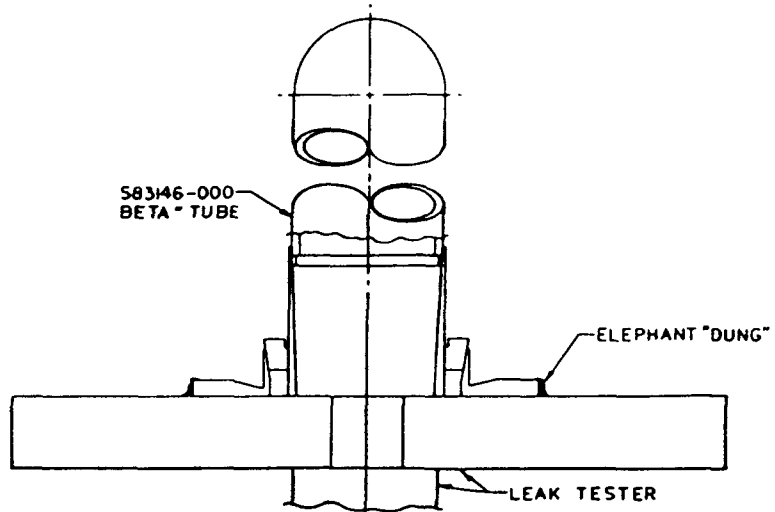


Figure 9 (HEADER AND TUBE ASSEMBLY LEAK TEST)

- 72--73-

Sandia National Laboratories

Albuquerque, New Mexico 87185

date March 23, 1987

to Distribution

Mike Tinker

from M. K. Neilsen, 1521

subject Stress Analysis of the LMTEC Beta Alumina Tube to Sleeve Joint

INTRODUCTION

A Liquid Metal Thermal Electrical Converter (LMTEC) is currently being developed. During manufacture of this device (Figure 1), a thin molybdenum sleeve was brazed to a beta alumina tube at 1100°C and then cooled to room temperature. In the original design, a 5 mil molybdenum sleeve was used and the alumina tube cracked as the joint was cooled to room temperature. In a second design, the molybdenum sleeve was tapered from 5 mils to 1 mil and the 1 mil section was brazed to the alumina tube. No failures were observed during manufacture of a prototype using the second design. Results from an initial series of analyses [2], indicated that a maximum tensile stress of 12,000 psi would be generated in the beta alumina tube as a result of the brazing process. Thus, the second design should survive the brazing process but is marginal since beta alumina has a tensile strength of only 15,000 psi. Results from the initial analyses also indicated that use of a tantalum sleeve in place of the molybdenum sleeve would significantly improve the design.

As requested, an additional series of analyses was completed to further investigate the effects of variations in the tube to sleeve joint design. Design changes that were investigated in this series of analyses included variations in braze material thickness, variations in sleeve material and geometric variations. Results from this investigation are presented in this memo.

EFFECTS OF VARIATIONS IN BRAZE MATERIAL THICKNESS

A series of analyses was completed to investigate the effects of variations of braze material thickness on the design. This series of analyses was completed using JAC [3] and the two-dimensional, axisymmetric finite element models shown in Figure 2. The top end of these models were not allowed to rotate or translate in the z-direction. This boundary condition was used to represent the effects of the rest of the beta alumina tube on the joint section. These two-dimensional models were assumed stress free at the braze temperature of 1100°C and then cooled to room temperature. The stresses generated by the temperature change were then investigated. Material properties used in

Distribution

-2-

March 23, 1987

this analyses are given in Table 1. All of the metals were assumed to be elastic perfectly plastic and the beta alumina was assumed to be elastic. Properties for the braze material were estimated to be similar to those for titanium since a large percentage of the braze material is titanium [4].

Results from this series of analyses are shown in Figures 3 to 11 and summarized in Figure 12. Results obtained using a 1 mil thick molybdenum sleeve are shown in Figures 3 to 7. Since the beta alumina tube has a higher thermal expansion coefficient than molybdenum, it tries to contract more than the molybdenum sleeve as the joint is cooled to room temperature and the tensile stress shown in Figure 3 is generated in the tube. Increasing the braze layer thickness from 1 mil to 4 mils (Figures 4 to 7) tends to reduce the tensile stress caused by the mismatch in thermal expansion between the molybdenum and the alumina. This occurs because the braze material has a higher thermal expansion coefficient than either the alumina or the molybdenum and increasing the thickness of the braze layer tends to reduce the effects of the mismatch in expansion between the alumina and the molybdenum. However, if the braze layer thickness is increased beyond 4 mils, tensile stress in the alumina near the ends of the joint tends to increase (Figure 7). At this point, enough braze material has been added so that the high expansion braze material in combination with the molybdenum sleeve try to contract more than the alumina. Note that the location and orientation of the maximum tensile stress in the alumina tube was significantly altered when the braze layer thickness was increased from 3 mils (Figure 5) to 5 mils (Figure 7).

Results obtained using a 1 mil thick tantalum sleeve are shown in Figures 8 to 11. The tensile stress distribution generated when no braze material is present was similar to the distribution obtained when a molybdenum sleeve with less than 4 mils of braze material was used. This occurs because the alumina tube has a slightly higher expansion coefficient than the tantalum sleeve and, therefore, tries to contract more than the tantalum sleeve as the joint is cooled to room temperature. Tensile stress in the alumina is minimized when a 0.5 mil thick braze layer is used with the tantalum sleeve. Recall that with a molybdenum sleeve, tensile stress in the alumina was minimized when a 4 mil thick braze layer was used. Since the mismatch in thermal expansion between the tantalum and alumina is much smaller than the mismatch between the molybdenum and alumina, the amount of braze material required to minimize the effects of this mismatch is much smaller when a tantalum sleeve is used (Figure 12). When a tantalum sleeve is used and the braze layer thickness is increased beyond 0.5 mils, the tantalum sleeve in combination with the braze material has a net expansion coefficient that is higher than the expansion coefficient for the alumina tube. Therefore, as the joint is cooled to room temperature the braze material and tantalum sleeve contract more than the beta alumina tube and generate a residual tensile stress near the

ends of the joint. The tensile stress generated in the alumina tube increases as more braze material is used.

The final analysis in this series was completed to determine what effect allowing the braze material to flow beyond the end of the joint would have on stress levels in the alumina. This analysis was completed using the axisymmetric finite element model in Figure 13. This model was exactly like the previous models except a section of braze material was included beyond the end of the joint. This analysis was completed using a 2 mil braze joint and a 1 mil molybdenum sleeve. A comparison of results from this analysis (Figure 14) with results from the previous analysis (Figure 4) indicated that allowing the braze material to flow beyond the end of the joint would have little effect on stresses in the alumina near the sleeve but would generate another area of high tensile stress in the alumina near the end of the braze material that had flowed up the tube.

EFFECTS OF USING A DISK IN PLACE OF A SLEEVE

A second series of analyses was completed to determine what effects using a disk in place of the sleeve would have on the stress generated in the alumina tube. This design change was attractive because it would significantly relax the tolerance requirements on the diameter and roundness of the ends of the ceramic tubes. The initial analysis in this series was completed using the axisymmetric finite element model shown in Figure 15. A 4 mil thick disk was used because this was the smallest size that was readily available. Results obtained using a 4 mil molybdenum disk and a 1 mil braze joint are shown in Figures 16 and 17. This analysis indicated that critical levels of tensile stress would be generated in the alumina tube if this design was used. Also by changing from a sleeve design to a disk design, critical levels of tensile stress in the hoop direction have been introduced. In the previous analyses of the sleeve design, the maximum tensile stress generated in the hoop direction was always significantly smaller than the maximum in-plane tensile stress.

Results obtained using a tantalum disk and a 1 mil braze joint are shown in Figures 18 and 19. Results from this analyses indicated that a maximum tensile stress of 5870 psi would be generated in the alumina when a 4 mil tantalum disk was brazed to the alumina tube. This result indicated that it may be possible to use a tantalum disk in the joint design. The next analysis was completed to further investigate this possibility.

The final analyses of the disk design were completed using the model in Figure 20. This model represents a large ring of tantalum that is welded to a tantalum disk that is subsequently brazed to the alumina tube. The first analysis was completed using a 10 mil thick tantalum

Distribution

-4-

March 23, 1987

disk and the second analysis was completed using a 4 mil thick tantalum disk. These thicknesses were used because tantalum sheet stock with these thicknesses was readily available. Results from the first analysis (Figures 21 and 22) indicated that a maximum tensile stress of 10,940 psi would be generated in the alumina tube if a 10 mil thick tantalum disk was used. Results from a second analysis (Figures 23 and 24) indicated that a maximum tensile stress of 7700 psi would be generated in the alumina tube if a 4 mil thick tantalum disk was used.

CONCLUSIONS

The following conclusions were made based on results from the above analyses:

1. Tensile stress in the beta alumina can be minimized by using a tantalum sleeve and a 0.5 mil thick braze layer.
2. If a molybdenum sleeve is used, tensile stress in the beta alumina can be minimized by using a braze layer thickness of approximately 4 mils.
3. The braze material should not be allowed to flow beyond the end of the sleeve joint because another area of high tensile stress will be generated in the alumina near the end of the braze layer flow, if this is allowed.
4. If a tantalum disk design is used, tensile stress in the beta alumina can be minimized by minimizing the thickness of the tantalum disk.

REFERENCES

1. Drawing provided by J. B. Moreno, 2541.
2. M. K. Neilsen, "Structural Analysis of Liquid Metal Thermal Electrical Converter," internal memorandum, Sandia National Laboratories, Albuquerque, New Mexico, October 1986.
3. J. H. Biffle, "JAC - A Two-dimensional Finite Element Computer Program for the Non-linear Quasistatic Response of Solids with the Conjugate Gradient Method," SAND81-0998, Sandia National Laboratories, Albuquerque, New Mexico, April 1984.
4. Communication with J. B. Moreno, 2541.

MKN:1521:tbh

Table 1. Material Properties

Material	Temperature (°C)	Young's Modulus (psi)	Poisson's Ratio	Yield Strength (psi)	Thermal Exp. Coefficient (/°C)
Beta Alumina	0	28.4E+06	0.20	-	7.6E-06
	1100	22.7E+06	0.20		
Molybdenum	0	46.0E+06	0.31	115.E+03	5.5E-06
	1100	30.0E+06	0.31	35.E+03	
Tantalum	0	27.0E+06	0.36	158.E+03	7.3E-06
	1100	10.0E+06	0.36	55.E+03	
BNI Braze (Titanium)	0	18.0E+06	0.30	110.E+03	9.0E-06
	1100	12.0E+06	0.30	55.E+03	



Sandia National Laboratories
Solar Energy

LMTEC
BENCH TEST
MODULE

Copper

Stainless Steel

Molybdenum

BASE

Sodium



1058603

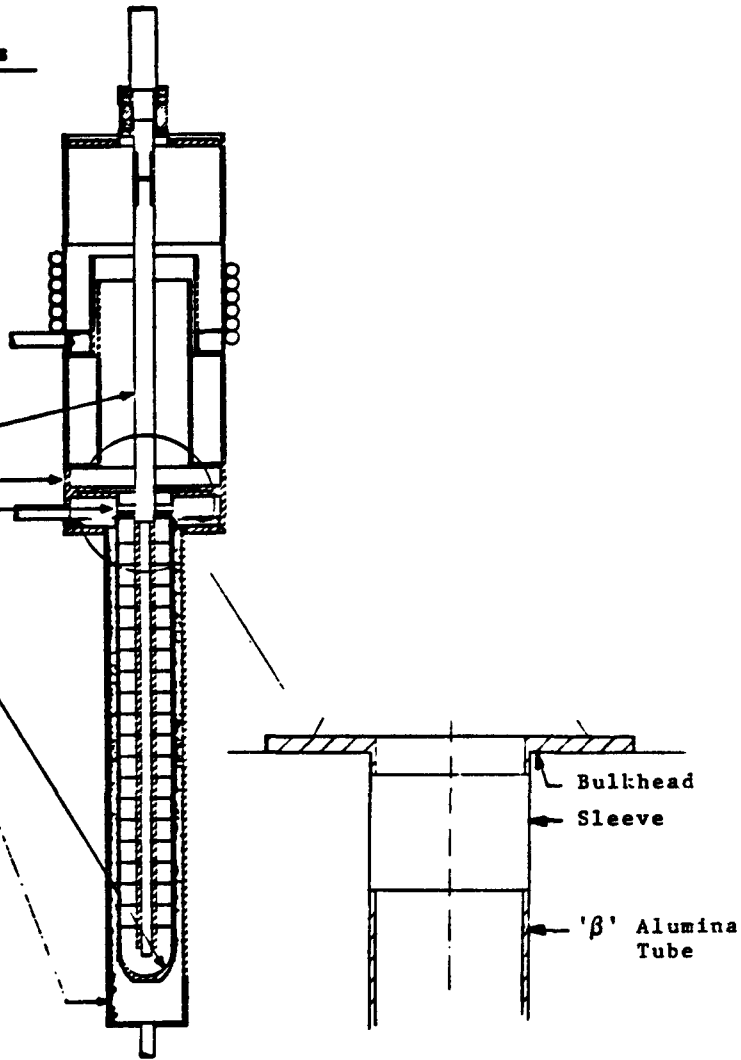


FIGURE 1. LMTEC Bench Test Module. [1]

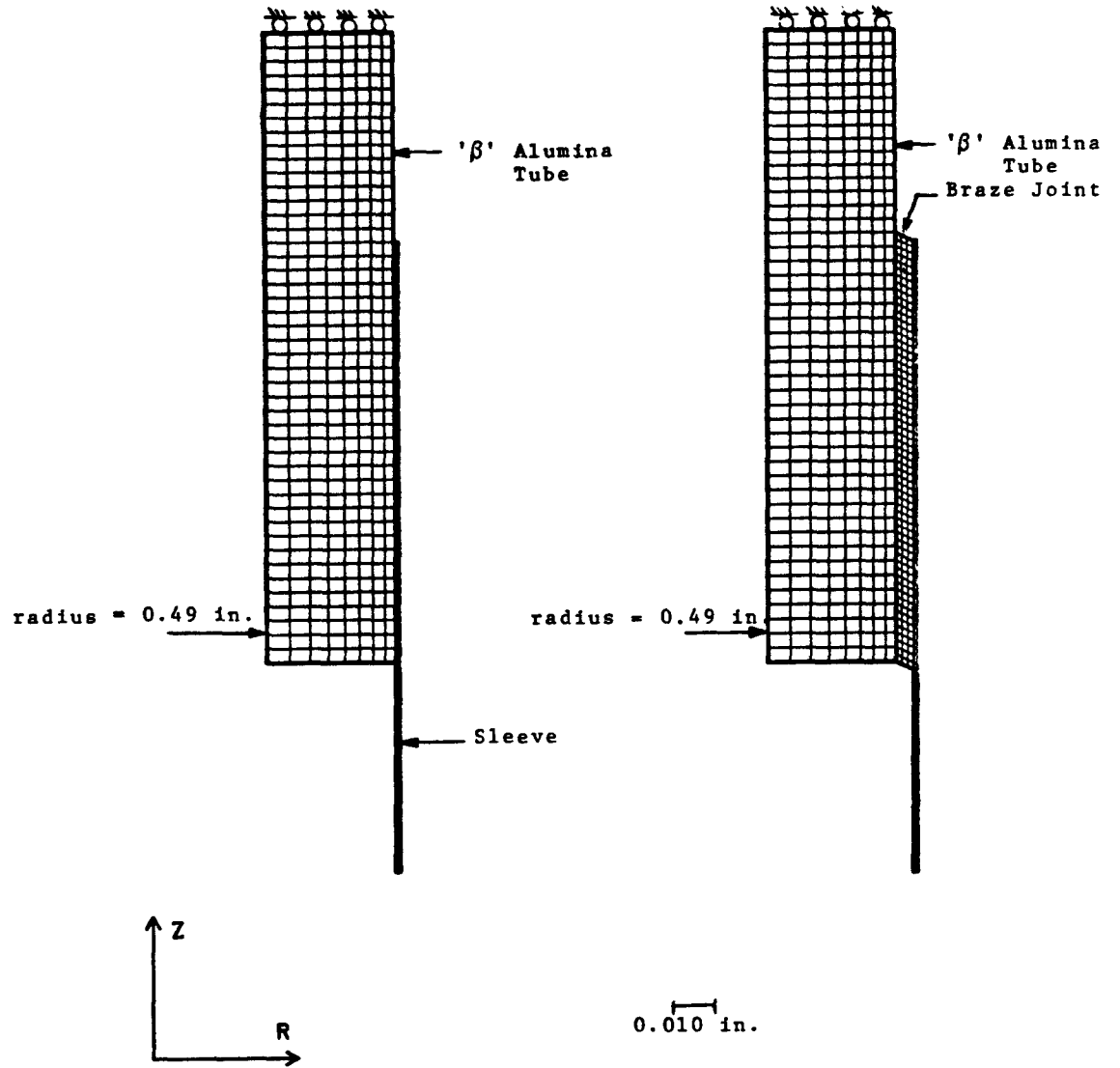


FIGURE 2. Axisymmetric Finite Element Models - Sleeve Design.

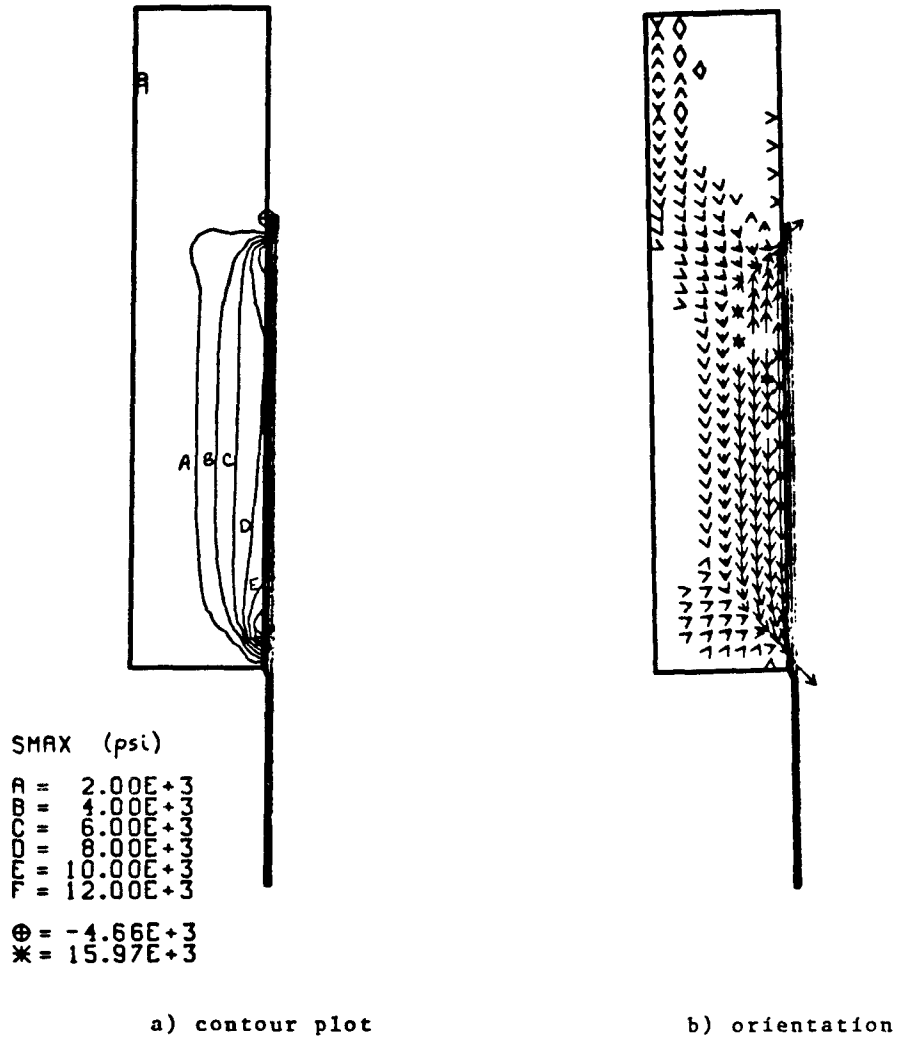


FIGURE 3. Maximum Tensile Stress in 'β' Alumina Tube -
1 mil Molybdenum Sleeve, 1 mil Braze Joint.

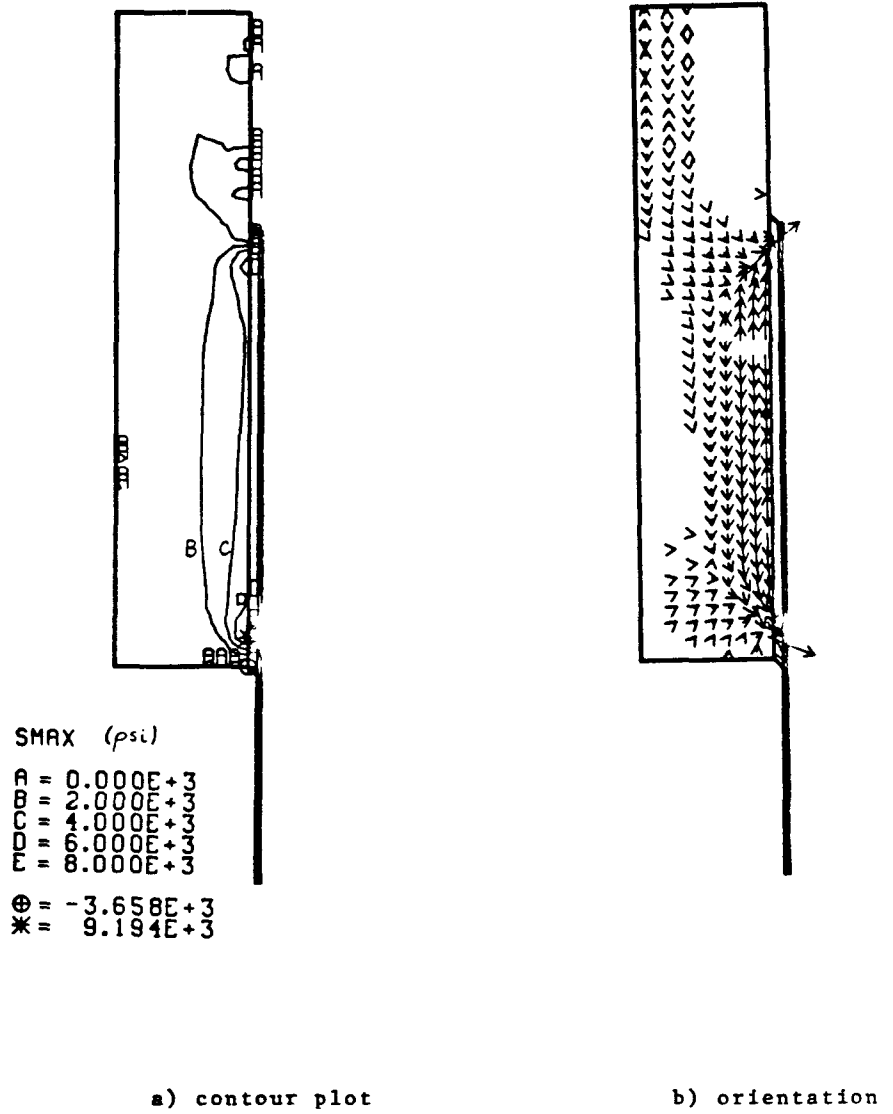


FIGURE 4. Maximum Tensile Stress in ' β ' Alumina Tube - 1 mil Molybdenum Sleeve, 2 mil Braze Joint.

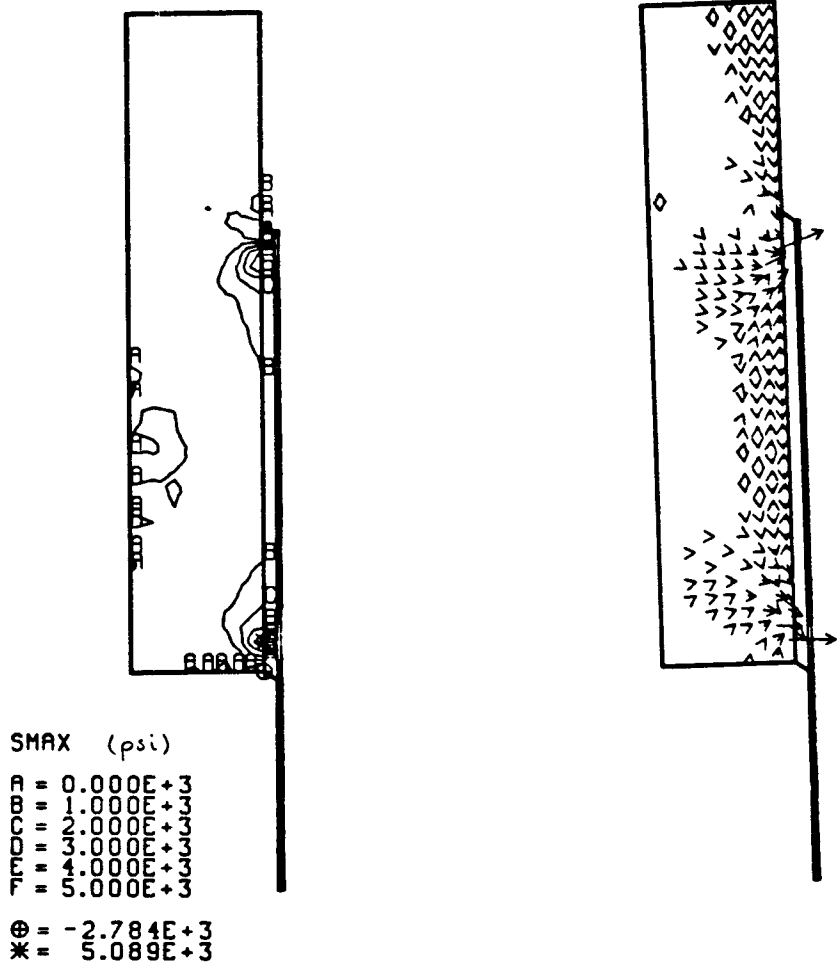


FIGURE 5. Maximum Tensile Stress in ' β ' Alumina Tube -
1 mil Molybdenum Sleeve, 3 mil Braze Joint.

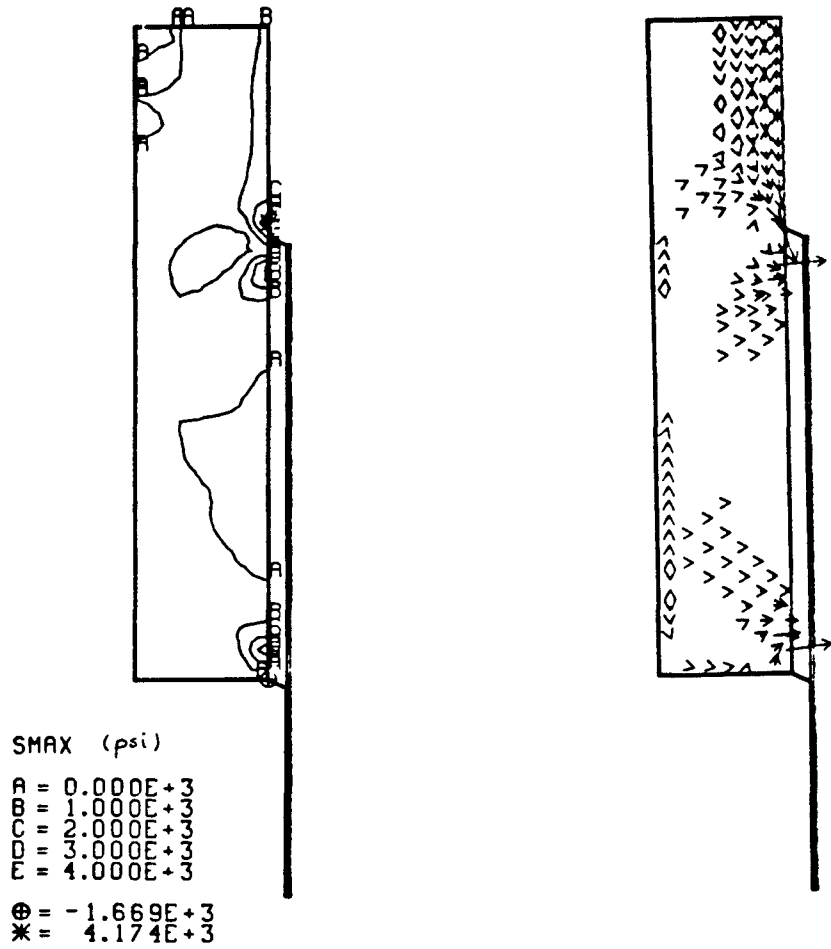


FIGURE 6. Maximum Tensile Stress in ' β ' Alumina Tube - 1 mil Molybdenum Sleeve, 4 mil Braze Joint.

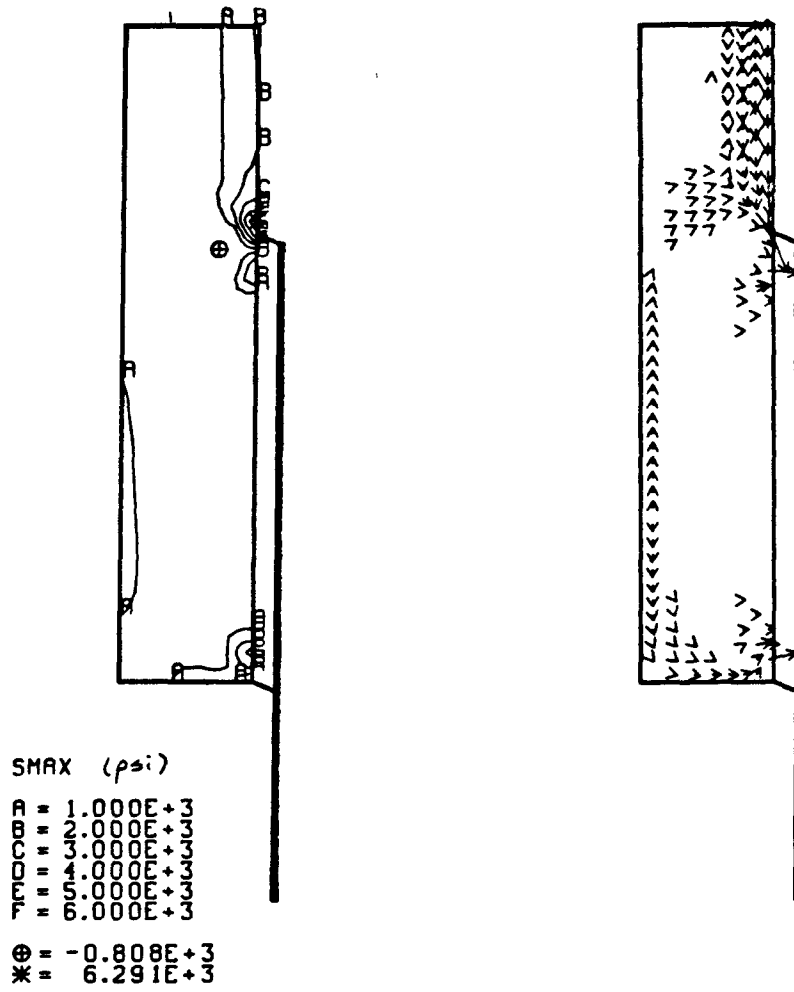


FIGURE 7. Maximum Tensile Stress in ' β ' Alumina Tube -
1 mil Molybdenum Sleeve, 5 mil Braze Joint.

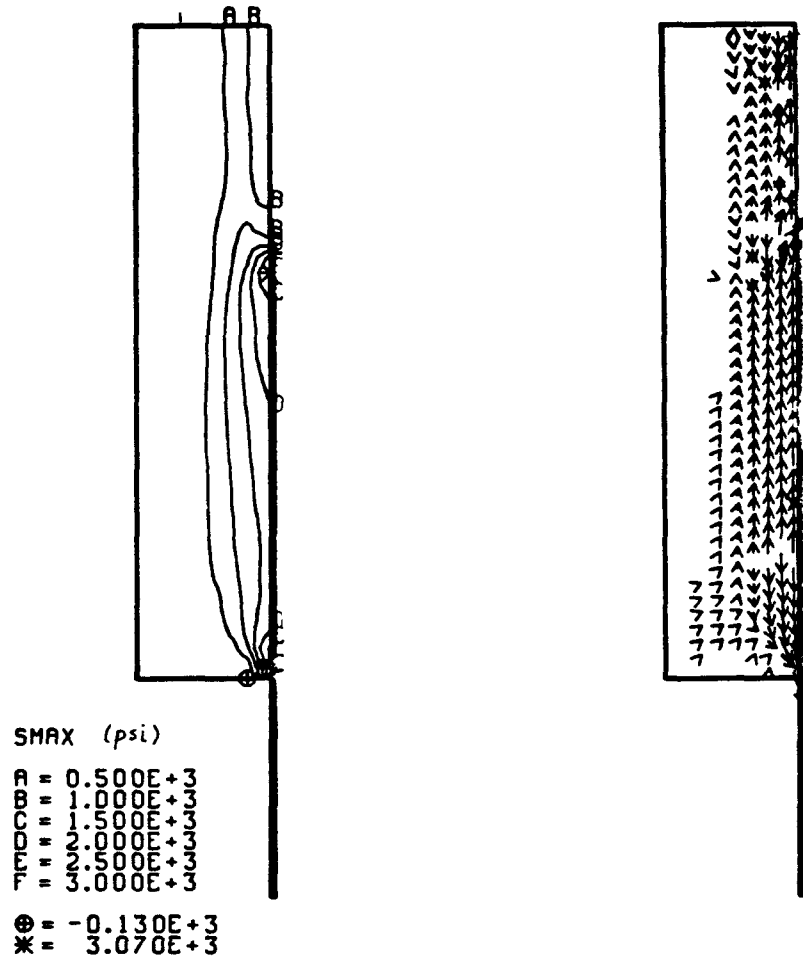


FIGURE 8. Maximum Tensile Stress in ' β ' Alumina Tube - 1 mil Tantalum Sleeve, No Braze Material.

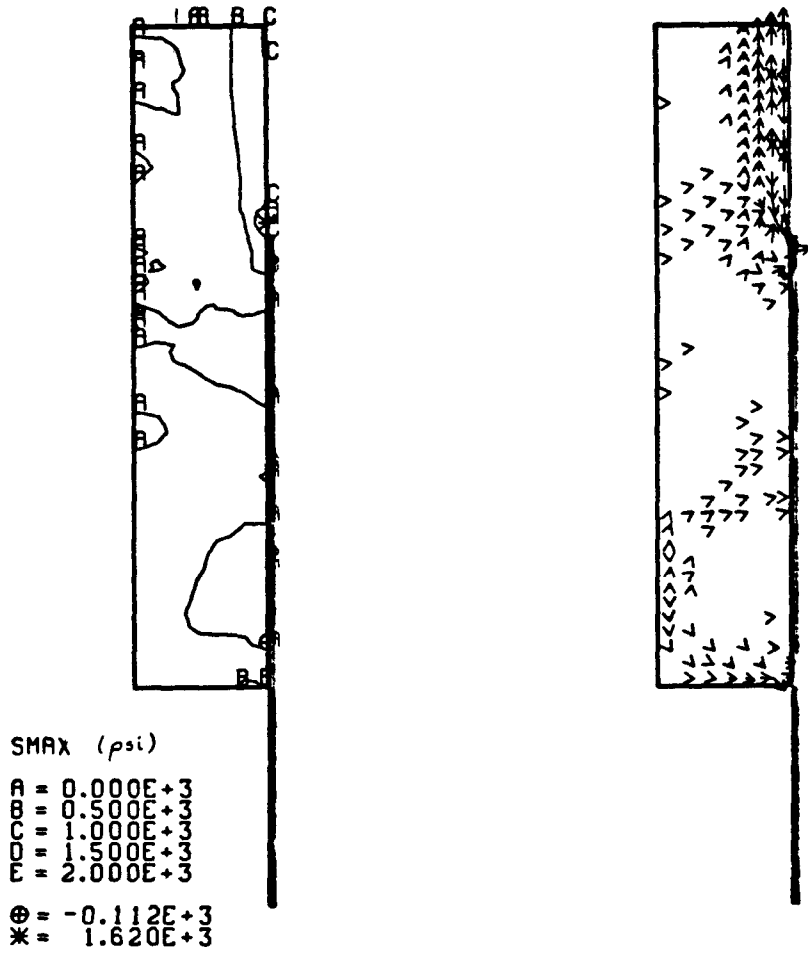


FIGURE 9. Maximum Tensile Stress in ' β ' Alumina Tube -
1 mil Tantalum Sleeve, 0.5 mil Braze Joint.

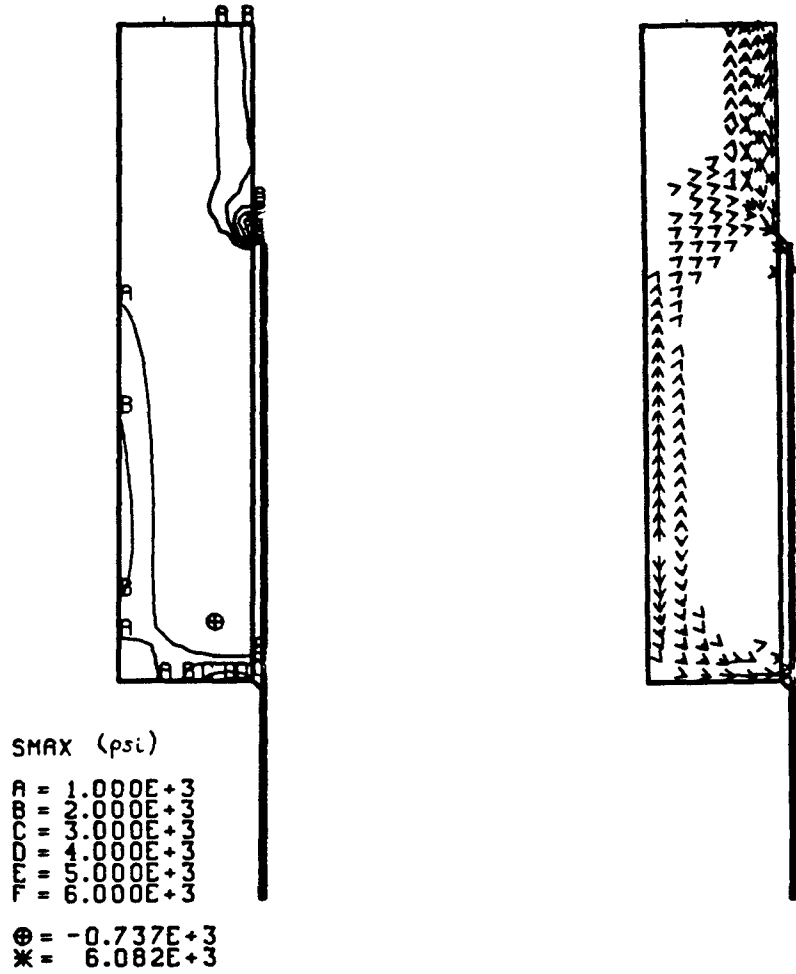


FIGURE 10. Maximum Tensile Stress in ' β ' Alumina Tube - 1 mil Tantalum Sleeve, 2 mil Braze Joint.

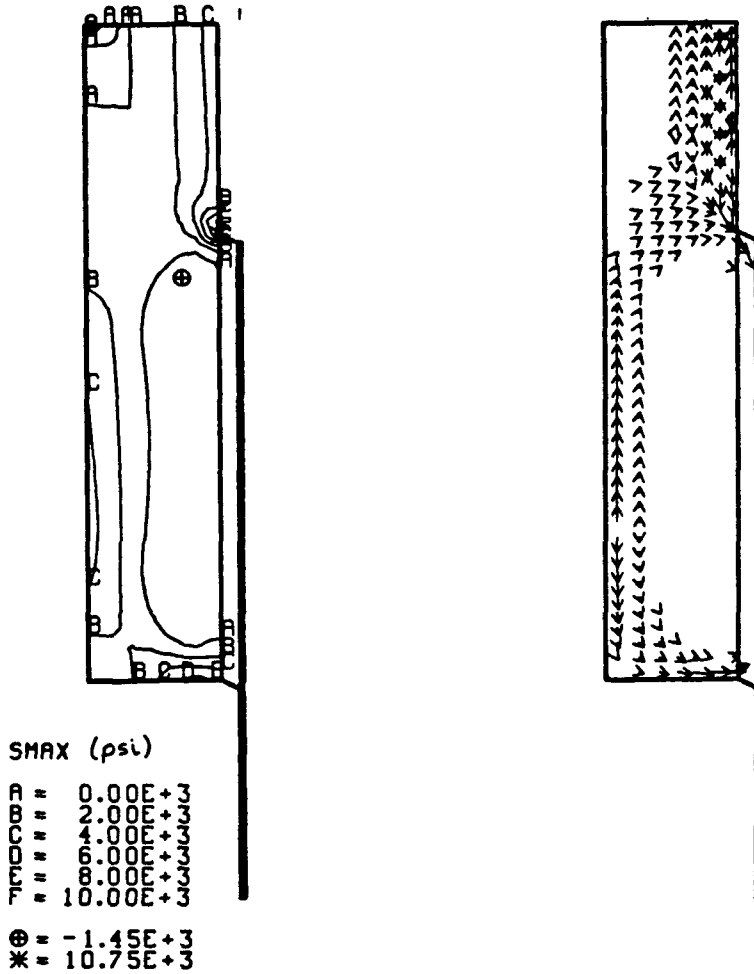


FIGURE 11. Maximum Tensile Stress in ' β ' Alumina Tube - 1 mil Tantalum Sleeve, 4 mil Braze Joint.

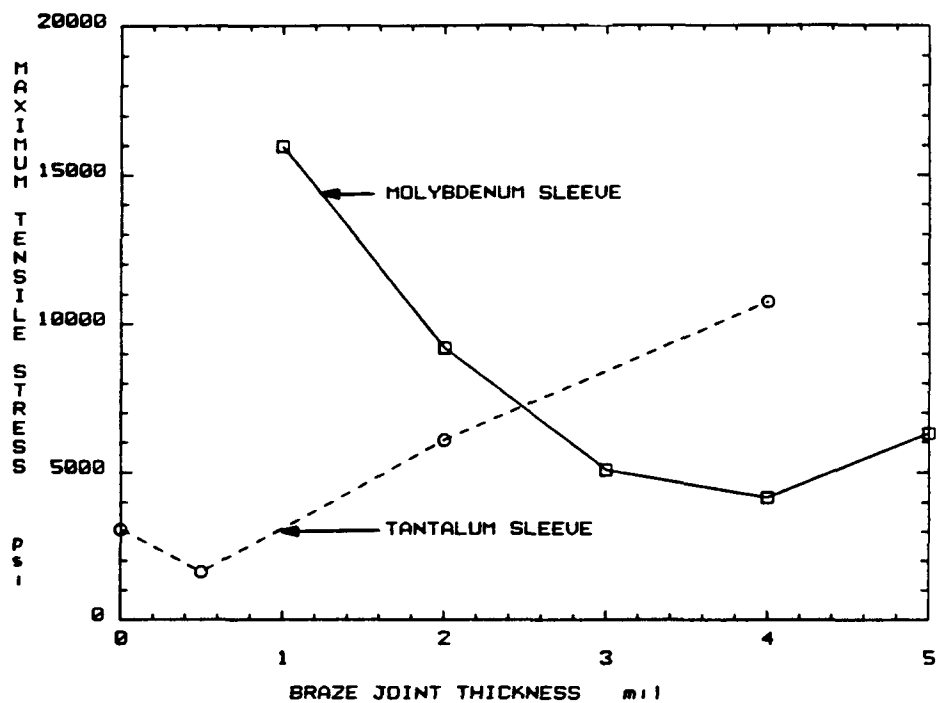


FIGURE 12. Maximum Tensile Stress in the ' β ' Alumina Tube as a Function of the Sleeve Material and the Braze Layer Thickness.

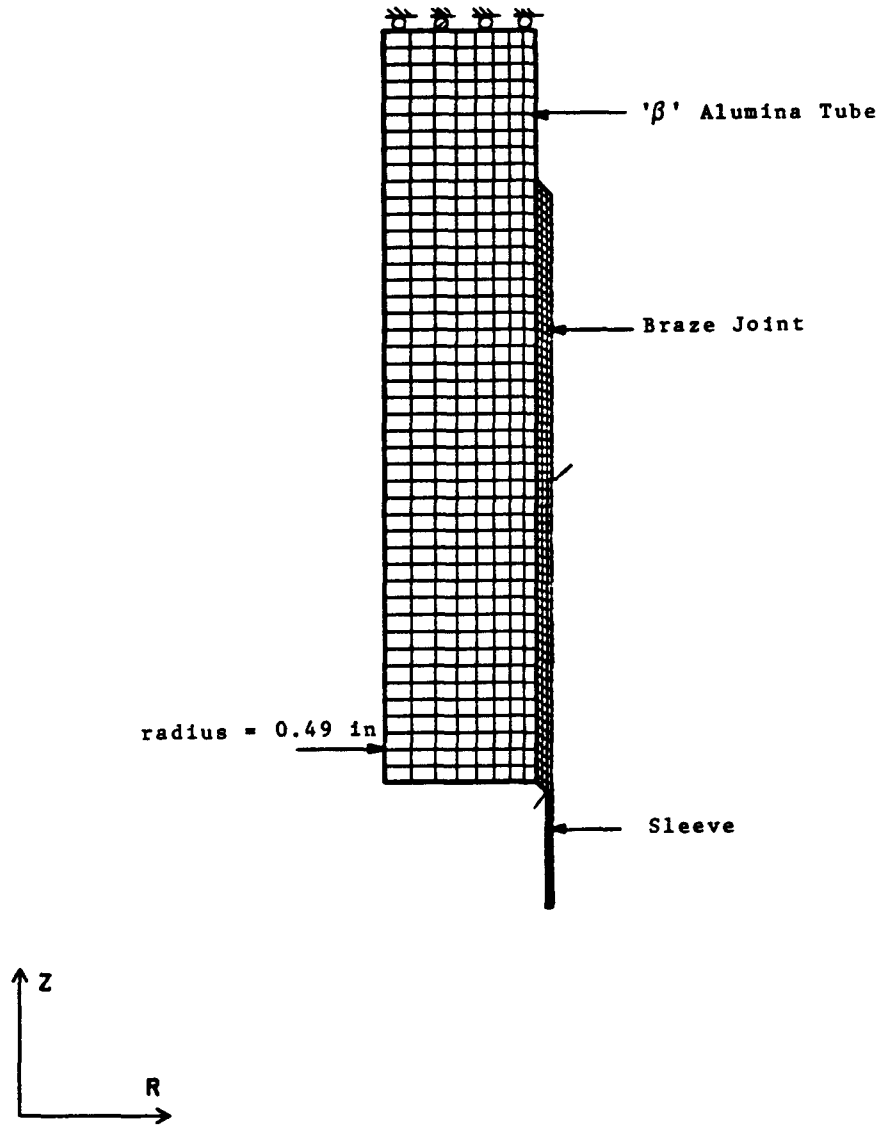
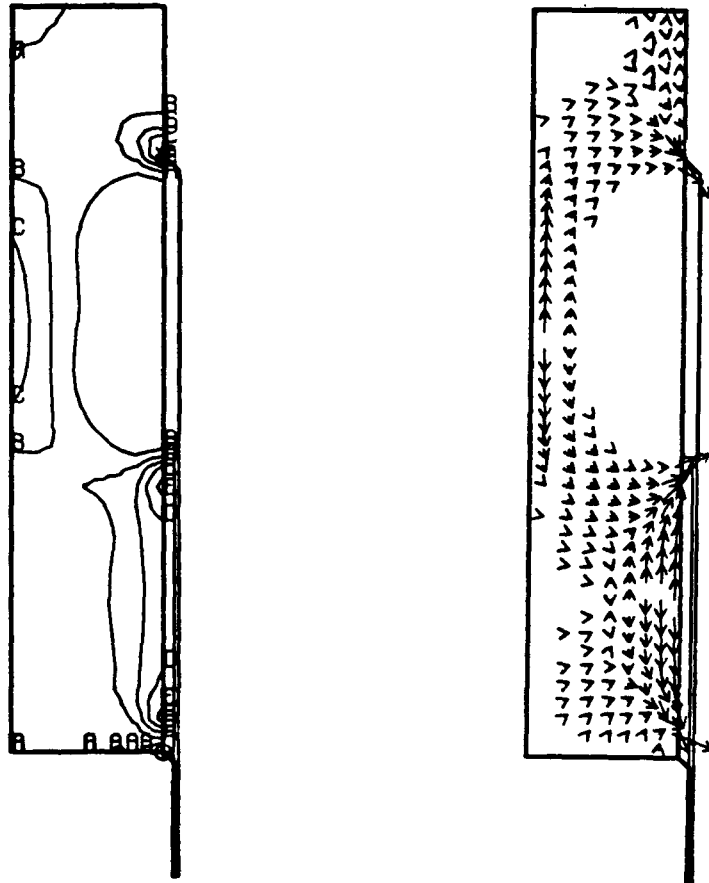


FIGURE 13. Axisymmetric Finite Element Model.



SMAX (psi)

A = 0.00E+3
B = 2.00E+3
C = 4.00E+3
D = 6.00E+3
E = 8.00E+3
F = 10.00E+3

⊕ = -3.819E+3
* = 9.285E+3

FIGURE 14. Maximum Tensile Stress in ' β ' Alumina Tube -
1 mil Molybdenum Sleeve, 2 mil Braze Joint.

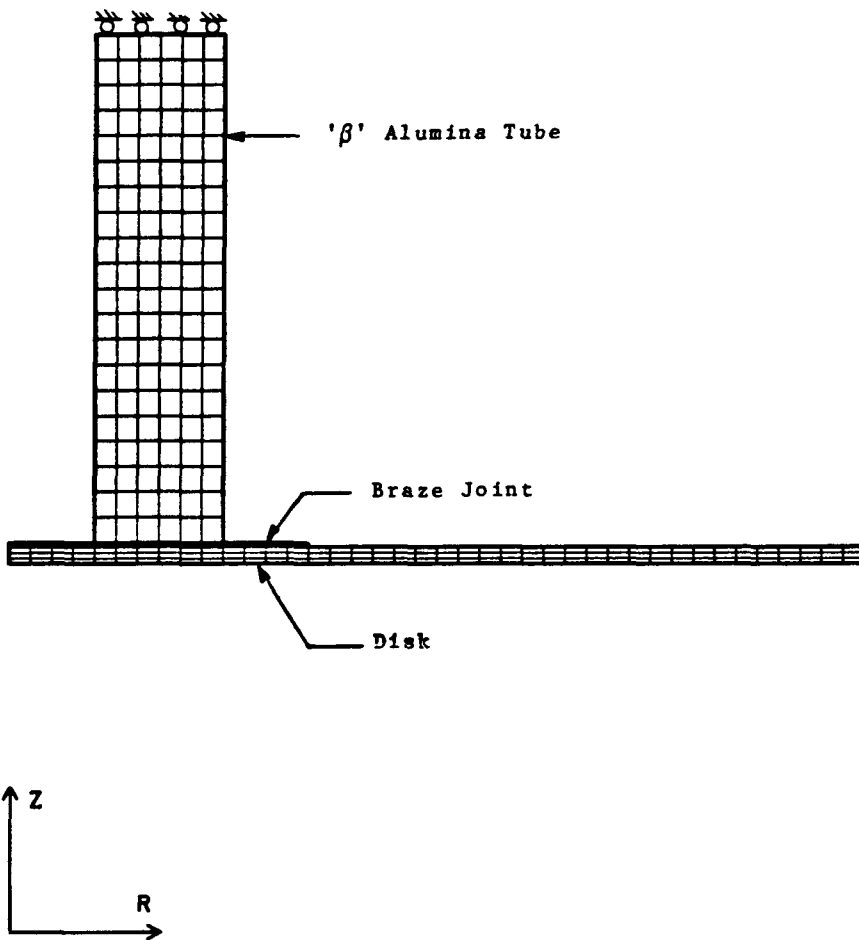
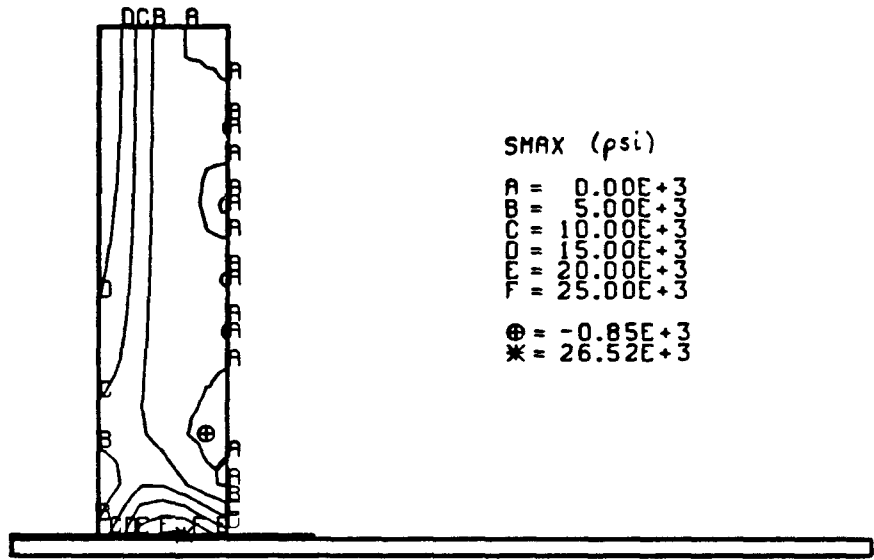
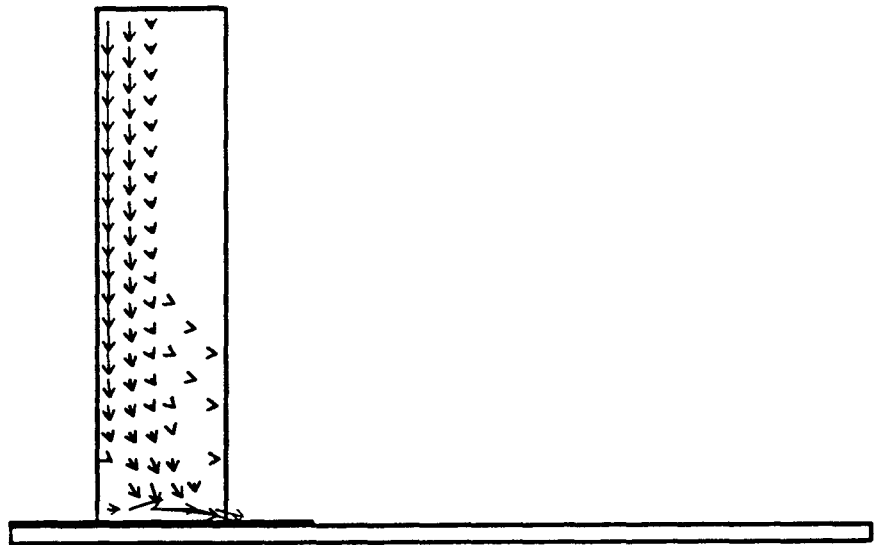


FIGURE 15. Axisymmetric Finite Element Model - Disk Design.



a) contour plot



b) orientation

FIGURE 16. Maximum In-plane Tensile Stress in ' β ' Alumina Tube - 4 mil Molybdenum Disk, 1 mil Braze Joint.

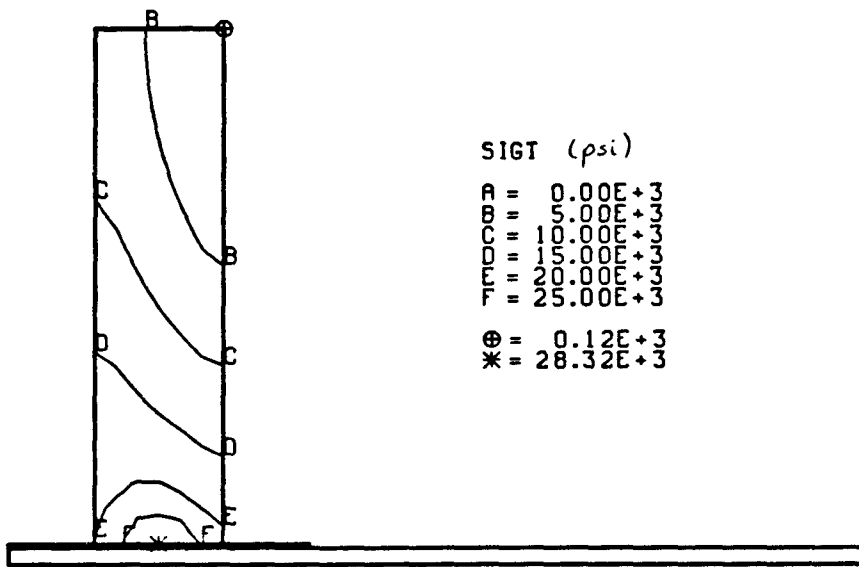
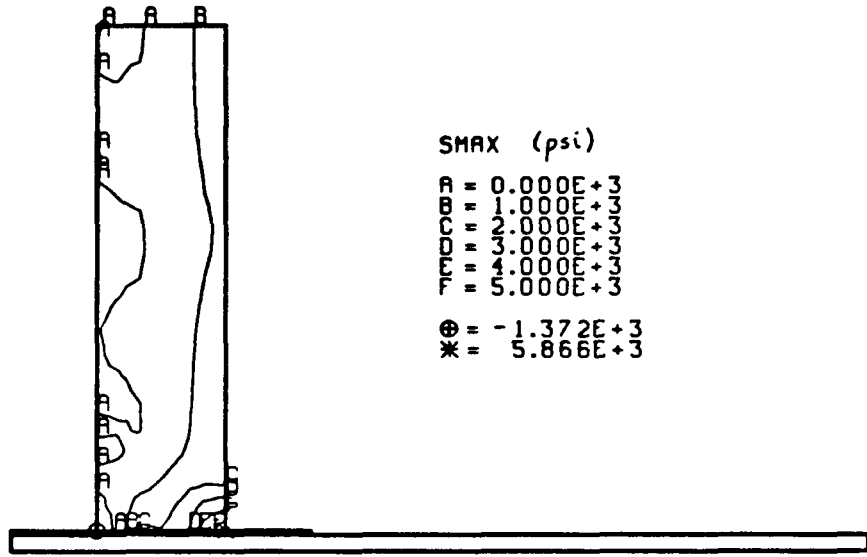
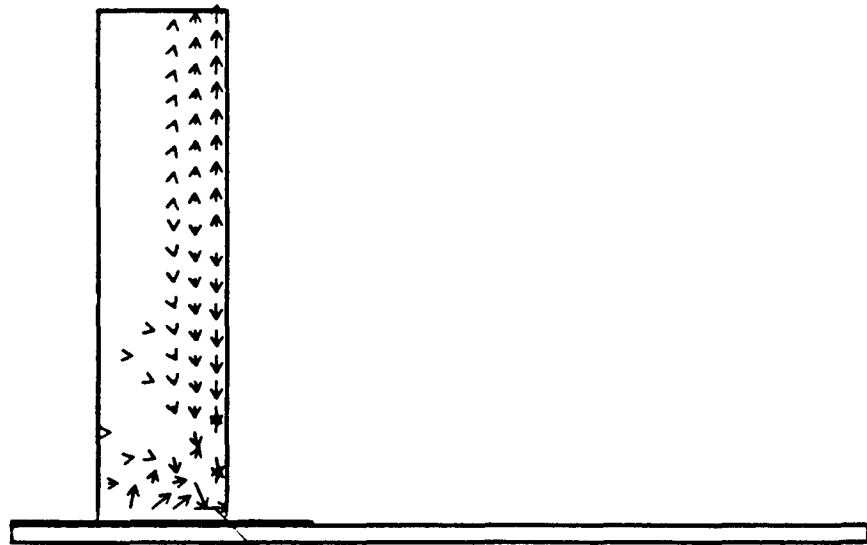


FIGURE 17. Circumferential Tensile Stress in ' β ' Alumina
4 mil Molybdenum Disk, 1 mil Braze Joint.



a) contour plot



b) orientation

FIGURE 18. Maximum In-plane Tensile Stress in ' β ' Alumina Tube - 4 mil Tantalum Disk, 1 mil Braze Joint.

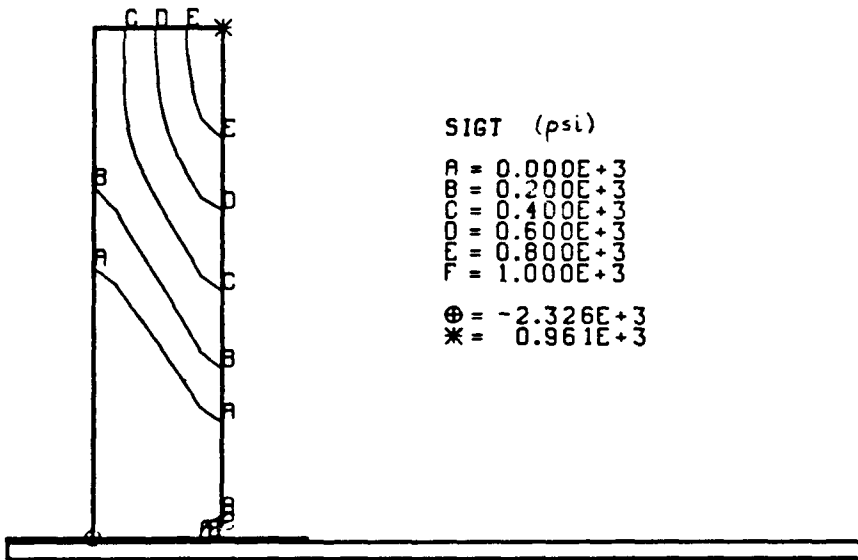


FIGURE 19. Circumferential Tensile Stress in ' β ' Alumina
4 mil Tantalum Disk, 1 mil Braze Joint.

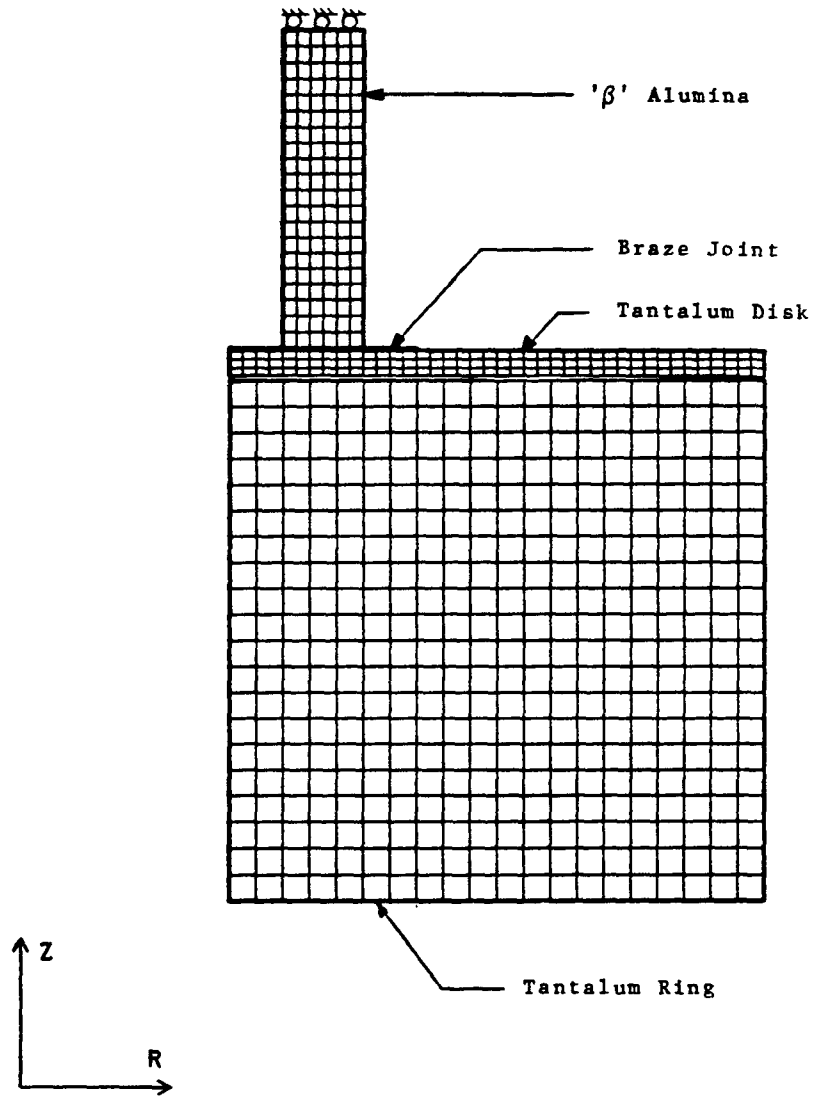
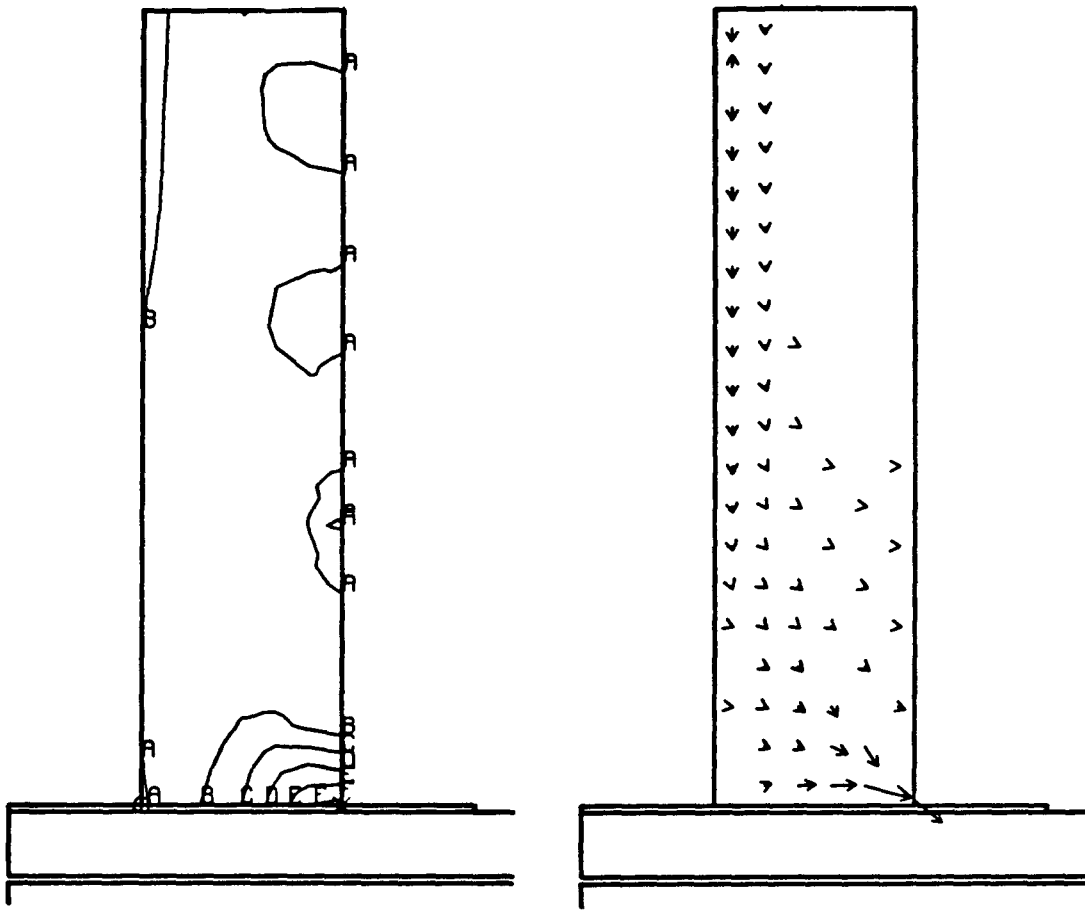


FIGURE 20. Axisymmetric Finite Element Model - Disk Design.



S MAX (psi)
A = 0.00E+3
B = 2.00E+3
C = 4.00E+3
D = 6.00E+3
E = 8.00E+3
F = 10.00E+3
G = -0.14E+3
H = 10.81E+3

FIGURE 21. Maximum In-plane Tensile Stress in ' β ' Alumina - 10 mil Tantalum Disk, 1 mil Braze Joint.

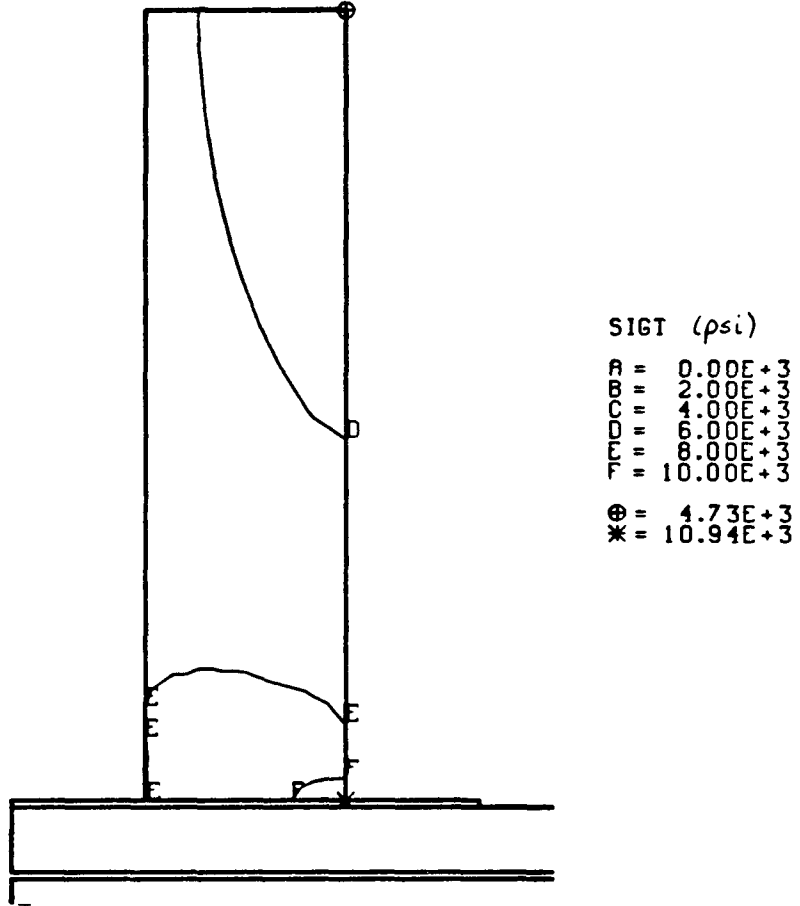
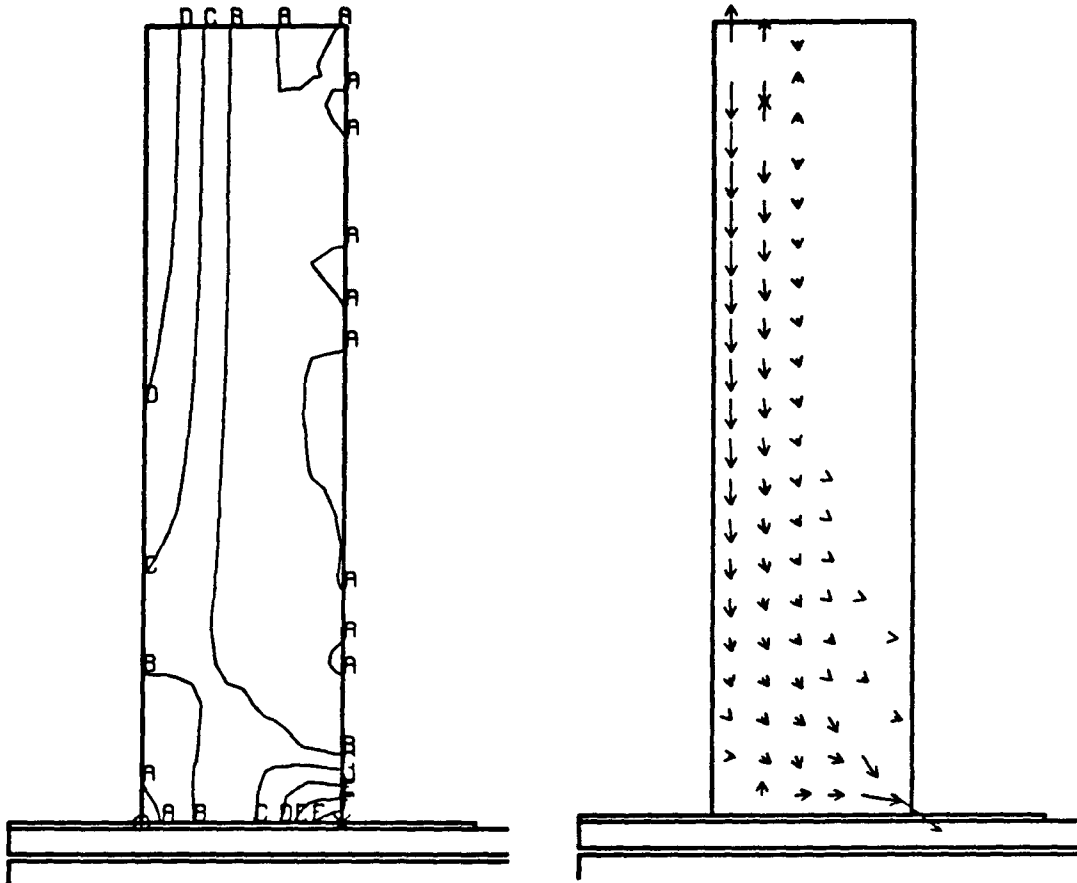


FIGURE 22. Circumferential Tensile Stress in ' β ' Alumina - 10 mil Tantalum Disk, 1 mil Braze Joint.



S_{MAX} (psi)

A = 0.000E+3
B = 1.000E+3
C = 2.000E+3
D = 3.000E+3
E = 4.000E+3
F = 5.000E+3

⊕ = -0.574E+3
* = 5.901E+3

FIGURE 23. Maximum In-plane Tensile Stress in ' β ' Alumina -
4 mil Tantalum Disk, 1 mil Braze Joint.

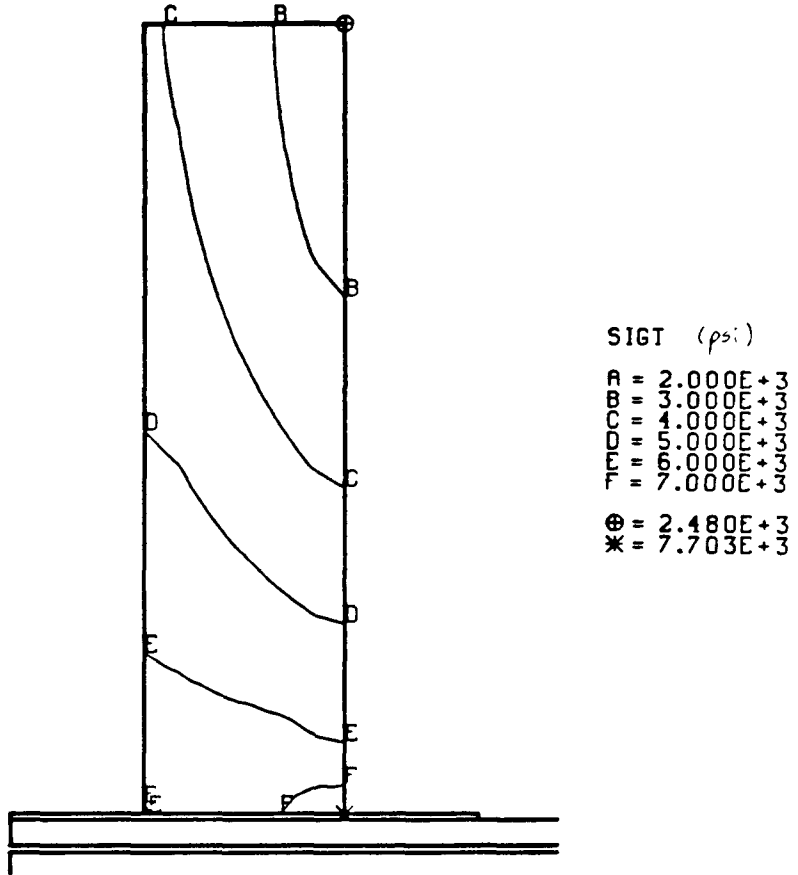


FIGURE 24. Circumferential Tensile Stress in ' β ' Alumina - 4 mil Tantalum Disk, 1 mil Braze Joint.

Sandia National Laboratories

Albuquerque, New Mexico 87185

date October 20, 1986

to Distribution

M. K. Neilsen

from M. K. Neilsen, 1521

subject Stress Analysis of Liquid Metal Thermal Electrical Converter

INTRODUCTION

A Liquid Metal Thermal Electrical Converter (LMTEC) is currently being developed. During manufacture of a bench test module (Figure 1, detail in Figure 2a), a thin molybdenum sleeve was brazed to a stainless steel bulkhead at 1100°C and then cooled to room temperature. This molybdenum sleeve buckled as it was cooling after the brazing operation. The primary reason for this failure was the mismatch in thermal expansion coefficients for molybdenum and 316L Stainless Steel. As the joint was cooled from 1100°C to room temperature, the 316L SS contracted more than the molybdenum and caused the thin molybdenum sleeve to buckle. Subsequent thermal cycles caused the molybdenum sleeve to crack.

A second design that would hopefully eliminate this failure mechanism was proposed by members of Division 2541. This design was like the original design except a molybdenum backup ring was brazed to the outside of the molybdenum sleeve as shown in Figure 2b. The purpose of this backup ring was to limit deformation of the molybdenum sleeve and thus prevent buckling of the sleeve. An initial analysis of this second design was completed by W. Gerstle, 1542 [2]. Results from this analysis indicated that the backup ring would prevent failure of the thin molybdenum sleeve. However, this analysis also indicated that a radial tensile stress of approximately 50,000 psi would have to be carried by the braze joint with this design.

In response to this initial analysis, some additional designs were proposed. The third design consisted of brazing a molybdenum ring to the inside surface of the 316L SS bulkhead as shown in Figure 2c. The fourth design (Figure 2d) was similar to the third design except the inside surface of the bulkhead and the outside surface of the molybdenum ring were tapered so that they could be fit together at room temperature. An additional series of analyses was completed to investigate the third and fourth designs. Results from this series of analyses are reported in this memo.

At the other end of this joint, the molybdenum sleeve was brazed to an alumina tube at 1100°C and then cooled to room temperature. In the original design (Figure 3) a 5 mil sleeve was used and the alumina tube

Distribution

-2-

October 20, 1986

cracked as the joint was cooled to room temperature. In the second design, the molybdenum sleeve was tapered from 5 mil to 1 mil and the 1 mil thick section was brazed to the alumina tube. This second design appears to work well. An additional series of analyses was completed to investigate the behavior of the molybdenum sleeve to beta alumina tube joint. Results from this additional series of analyses are also included in this memo.

ANALYSIS OF 316L SS BULKHEAD TO MOLYBDENUM SLEEVE JOINT

A finite element series of analyses was completed to investigate the behavior of the various 316L SS bulkhead to molybdenum backup ring joint designs. This series of analyses was completed using JAC [3] and the two-dimensional, axisymmetric finite element models shown in Figure 4. The finite element models were assumed stress free at the braze temperature of 1100°C and then cooled to room temperature. The stresses generated by this temperature change were then investigated. In all of these models the molybdenum backup ring was rigidly attached to the bulkhead. The effects of the braze material were not investigated. Material properties used in this and a later series of analyses are given in Table 1.

The analysis of Design II was completed using Model A. This analysis was similar to the analysis completed by W. Gerstle [2] except different boundary conditions were used. In this analysis, the steel bulkhead was not allowed to rotate along its upper surface as shown in Figure 4a. This boundary condition was used to model the effects of the 316L SS body on the bulkhead. Results from the analysis of Design II are shown in Figure 5. A contour plot of effective stress (Figure 5a) indicated that the extension from the bulkhead that is brazed to the molybdenum ring would yield when the joint was cooled and that only a very small section of the molybdenum ring would yield. Results from this analysis also indicated that a maximum radial tensile stress of 80,000 psi (Figure 5b) would have to be carried by the braze joint if this design was used. This indicates that the braze joint will probably fail if this design is used.

The next analysis was of Design III and was completed using Model B. This analysis was like the first analysis except the molybdenum backup ring was moved from the outside surface of the bulkhead extension to the inside surface. A plot of effective stress at room temperature (Figure 6a) indicated that the extension from the bulkhead that was brazed to the molybdenum ring would yield when the joint was cooled. A contour plot of radial stress (Figure 6b) indicated that a maximum radial stress of 40,000 psi would be generated across the braze joint with this design. This maximum radial stress is significantly smaller than the maximum radial stress generated with the first design but is still large enough to initiate failure of the braze joint.

The final analysis in this series was of Design IV and was completed using Model C. This analysis was like the previous analysis except for some geometric changes. Results from this analysis indicated that all of the stainless steel in the bulkhead extension would again yield when the joint was cooled to room temperature (Figure 7a). A contour plot of radial stress (Figure 7b) indicated that a maximum radial stress of only 3000 psi would be generated across the braze joint if Design IV was used. The braze joint has a much better chance of surviving if Design IV is used in place of any of the previously investigated designs. Parts have already been manufactured using Design IV and they work well.

Radial stress across the braze joint for all three designs as a function of distance from the bottom of the joint was plotted in Figure 8. A comparison of Design II with Design III indicated that the radial stress near the top of the braze joint would be significantly reduced if the molybdenum ring was placed on the inside of the stainless steel instead of on the outside. However, radial stress near the bottom of the joint was only slightly reduced by this design change. A comparison of Design IV with the other two designs indicated that the maximum radial tensile stress across the braze joint would be significantly lower if Design IV was used.

At this point, it may be beneficial to investigate why Design IV is better than the other two designs and why Designs II and III had nearly the same radial stress near the bottom end of the joint. First, consider concentric thin rings of molybdenum and 316L SS. Since, the 316L SS has a higher thermal expansion coefficient than molybdenum, it will want to contract more than the molybdenum as the joint is cooled to room temperature. If the 316L SS ring yields before the molybdenum ring then the maximum radial stress caused by differential radial thermal contraction (σ_r) would be given by

$$\sigma_r = \sigma_y \frac{t}{r}$$

where r is the radius of the joint, t is the thickness of the 316L SS ring and σ_y is the yield strength of the 316L SS. This equation predicts a radial tensile stress of 2160 psi if the 316L SS ring is on the inside of the molybdenum ring and a radial compressive stress of 2160 psi if the 316L SS ring is on the outside of the molybdenum ring. The finite element analyses of Designs II and III predicted maximum radial tensile stresses of 80,000 and 40,000 psi, respectively. This indicates that the above equation does not capture some behaviors that are significantly altering the stresses generated along the braze joint. Two effects that are not included in the above equation are, the effect of differential thermal contraction in the axial direction along the braze joint and the effect of the rest of the bulkhead on the stresses along the braze joint. Contraction of the rest of the bulkhead has a significant effect on radial stresses near the top of the braze joint. The differential thermal contraction in the axial direction causes the

Distribution

-4-

October 20, 1986

radial stress across the joint to be significantly higher near the ends of the joint. There are two possible reasons why Design IV is better than Design III: the bulkhead extension is thinner and the braze joint is shorter for Design IV. Both of these changes help to reduce the effects of differential axial contraction.

ANALYSIS OF MOLYBDENUM SLEEVE TO BETA ALUMINA TUBE JOINT

A second series of analyses was completed to investigate the behavior of the molybdenum sleeve to beta alumina tube joint. This series of analyses was completed using JAC [3] and the two-dimensional axisymmetric finite element models shown in Figure 9. These models represent only a small section of the braze joint near the end of the tube. The top end of the models were not allowed to rotate or translate in the z direction. This boundary condition was used to represent the effects of the rest of the body on this section of the braze joint. The finite element models were assumed stress free at the braze temperature of 1100°C and then cooled to room temperature. Stresses generated by this temperature change were then investigated. A layer of nickel was included in Models E and G between the molybdenum sleeve and the alumina tube to provide some indication about what effects inclusion of the braze material would have on the results. Material properties used in this and the previous series of analyses are given in Table 1.

The first analysis in this series was completed using Model D which had a 5 mil thick molybdenum sleeve and no braze material. The magnitude and orientation of the maximum tensile stress in the alumina is shown in Figures 10a and 10b. Since the maximum tensile stress exceeds the tensile strength of beta alumina (15,000 psi), cracking of the alumina tube in a direction perpendicular to the orientation of the maximum tensile stresses would be expected. A contour plot of effective stress in the molybdenum (Figure 10c) indicated that the molybdenum sleeve near the end of the tube would not yield when it was brazed to the tube and cooled to room temperature.

The second analysis was like the first except a 2 mil thick layer of nickel was placed between the molybdenum and the beta alumina. This analysis was completed to provide some information about what effects inclusion of a braze material layer could have on the results. The magnitude and orientation of the maximum tensile stress in the alumina is shown in Figures 11a and 11b. A comparison of these results with those obtained from the first analysis indicated that the location and magnitude of the maximum tensile stress would be affected by inclusion of the braze material layer in the analysis. Results from this analysis, however, indicated that the maximum tensile stress in the alumina would still exceed the tensile strength of beta alumina if a 5 mil thick molybdenum sleeve was used. A contour plot of effective stress in the molybdenum sleeve and the braze material (Figure 11c)

indicated that the relatively soft braze material layer would yield when the joint was cooled to room temperature.

The third analysis was like the second analysis except a tantalum sleeve was used in place of the molybdenum sleeve. Results from this analysis (Figure 12) indicated that the maximum tensile stress in the beta alumina tube could be reduced to 4650 psi by using a tantalum sleeve in place of a molybdenum sleeve. A comparison of the second analysis with this analysis indicated that the orientation and magnitude of the maximum tensile stress in the alumina was significantly affected by the change in sleeve material. A plot of effective stress in the tantalum and the braze material indicated that the braze material would yield when the joint was cooled to room temperature.

The fourth analysis was like the first analysis except a 1 mil thick molybdenum sleeve was used in place of the 5 mil thick molybdenum sleeve. Results from this analysis (Figure 13) indicated that tensile stress in the beta alumina could be reduced by using a 1 mil thick sleeve in place of a 5 mil thick sleeve but that the maximum tensile stress would still exceed the tensile strength of beta alumina. A plot of effective stress in the molybdenum sleeve (Figure 13c) indicated that the molybdenum located more than 10 mils from the free end of the joint would yield when the joint was cooled to room temperature.

The fifth and final analysis was like the fourth analysis except a 2 mil thick layer of nickel was included between the 1 mil thick molybdenum sleeve and the beta alumina tube. Results from this analysis (Figure 14) indicated that tensile stress in the beta alumina would be significantly affected by inclusion of the braze material in the analysis. A maximum tensile stress of 12,000 psi in the beta alumina was predicted by this analysis. This would indicate that this design may survive but is marginal. The contour plot of effective stress in the molybdenum sleeve and braze material indicated that all of the braze material and a significant portion of the molybdenum sleeve would yield when this joint was cooled to room temperature.

CONCLUSIONS

The following conclusions were made based on results from the above analyses:

1. Radial stress across the 316L SS bulkhead to molybdenum tube joint can be minimized by minimizing the thickness of the bulkhead extension near the joint and minimizing the length of the joint.
2. Tensile stress in the beta alumina can be minimized by minimizing the thickness of the molybdenum tube near the joint and minimizing the length of the joint.

Distribution

-6-

October 20, 1986

3. Use of a tantalum sleeve in place of the molybdenum sleeve would significantly reduce tensile stress in the alumina. This design change is recommended.
4. Inclusion of the braze material layer in the analyses tends to reduce the magnitude of tensile stress predicted. Deformation of the braze materials helps to isolate the beta alumina from the molybdenum. A more accurate analysis could be completed if accurate material properties for the braze material could be determined.
5. Experimental results have indicated that the Design IV molybdenum sleeve to 316L SS bulkhead joint worked satisfactorily. The analysis of this design indicated that this was not a singular result but is to be expected.
6. Experimental results have also indicated that use of a 1 mil thick molybdenum sleeve near the beta alumina to alumina sleeve joint worked satisfactorily. The analysis of this joint indicated that it should work but that it is marginal.

FUTURE WORK

The current design consists of using the Design IV molybdenum sleeve to 316L SS bulkhead joint and a 1 mil thick molybdenum sleeve near the alumina tube. This series of analyses has indicated that the molybdenum sleeve to alumina tube joint is marginal. A variety of design changes have been suggested during the course of this investigation. If further analyses are needed to evaluate these design changes, they will be completed when requested.

REFERENCES

1. Drawing provided by J. B. Moreno, 2541.
2. W. Gerstle, "Structural Analysis of LMTEC Stainless Steel-Molybdenum Joint," internal memorandum to J. B. Moreno, July 1986.
3. J. H. Biffle, "JAC - A Two-dimensional Finite Element Computer Program for the Non-linear Quasistatic Response of Solids with the Conjugate Gradient Method," SAND81-0998, April 1984.

MKN:1521:tbh

Table 1. Material Properties.

Material	Temperature (°C)	Young's Modulus (psi)	Poisson's Ratio	Yield Strength (psi)	Thermal Exp. Coefficient (/°C)
Beta Alumina	0	28.4E+06	0.20	-	7.6E-06
	1100	22.7E+06	0.20		
Molybdenum	0	46.0E+06	0.31	115.E+03	5.5E-06
	1100	30.0E+06	0.31	35.E+03	
Tantalum	0	27.0E+06	0.36	158.E+03	7.3E-06
	1100	10.0E+06	0.36	55.E+03	
316L SS	0	28.0E+06	0.30	45.E+03	20.0E-06
	1100	10.0E+06	0.30	5.E+03	
Nickel	0	30.0E+06	0.30	30.E+03	16.3E-06
	1100	30.0E+06	0.30	15.E+03	

Note: Hardening Modulus for all metals was assumed equal to zero.



Sandia National Laboratories
Solar Energy

LMTEC
BENCH TEST
MODULE

Copper

Stainless Steel

Molybdenum

BASE

Sodium



One inch

LD58603

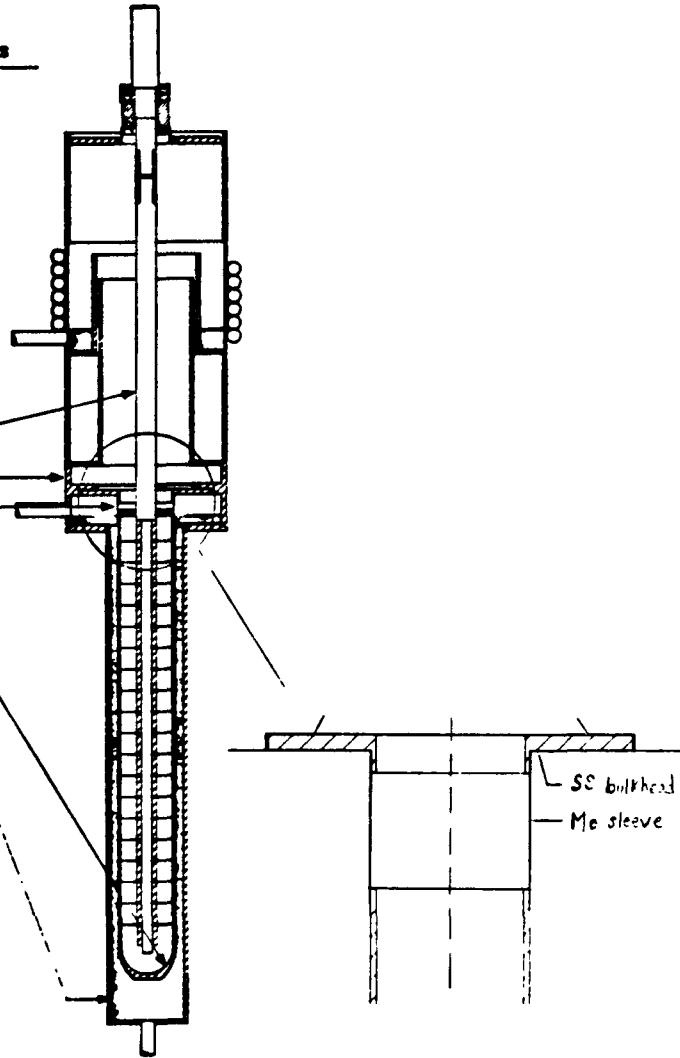
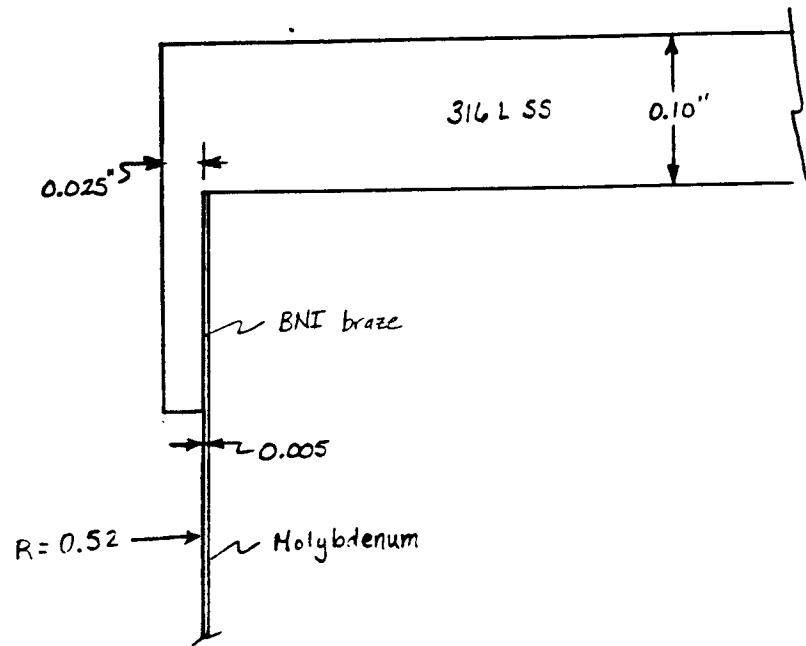
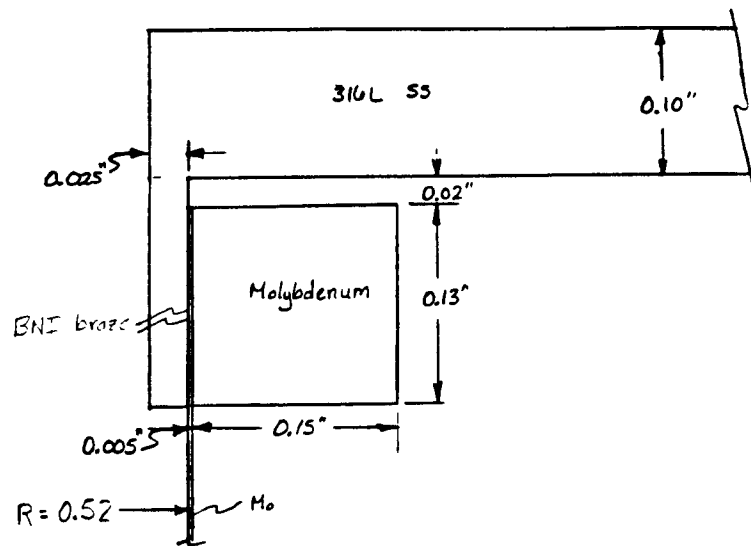


FIGURE 1. LMTEC Bench Test Module. [1]



a) Design I - Original



b) Design II

FIGURE 2. Molybdenum Sleeve to 316L SS Bulkhead Joint Designs.

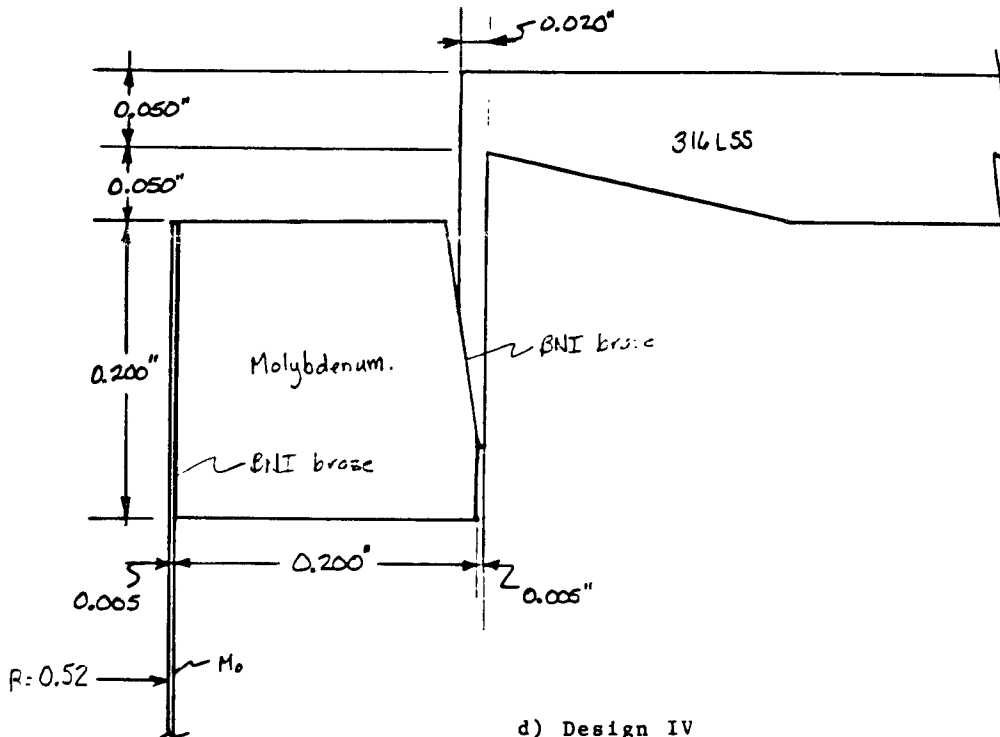
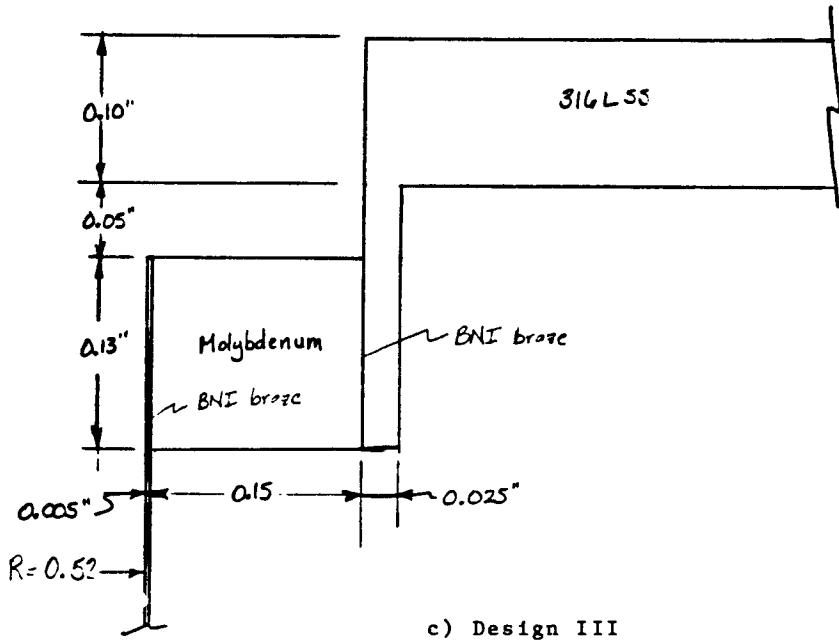


FIGURE 2. Molybdenum Sleeve to 316L SS Bulkhead Joint Designs.

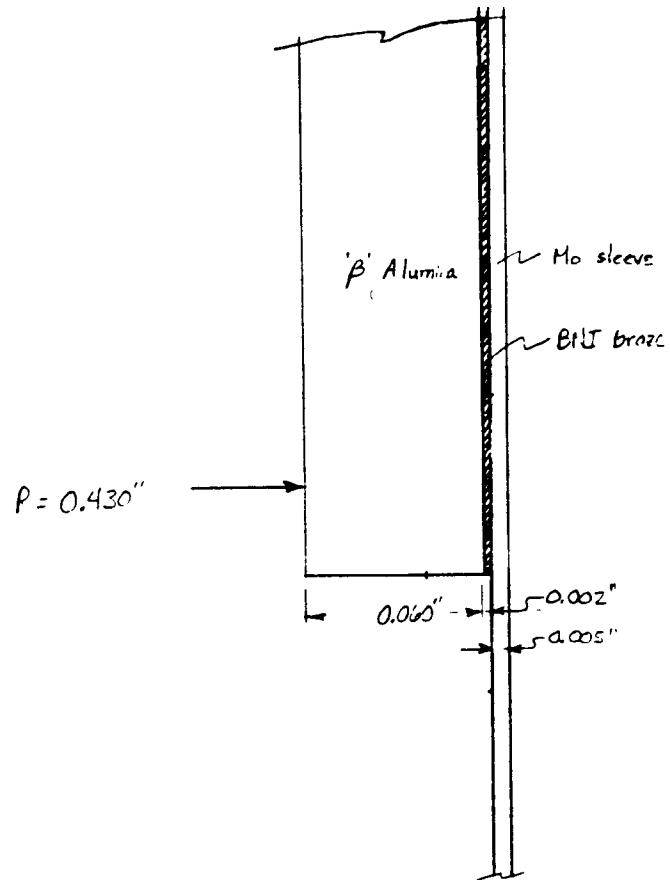
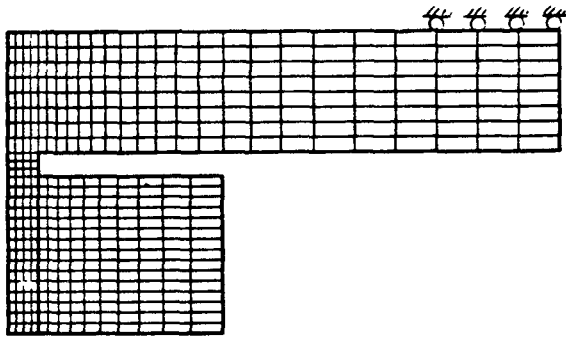
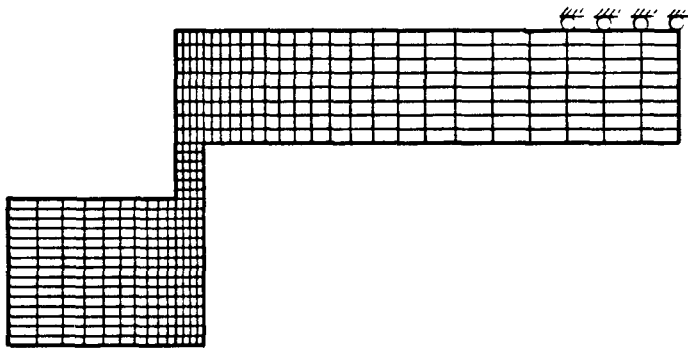


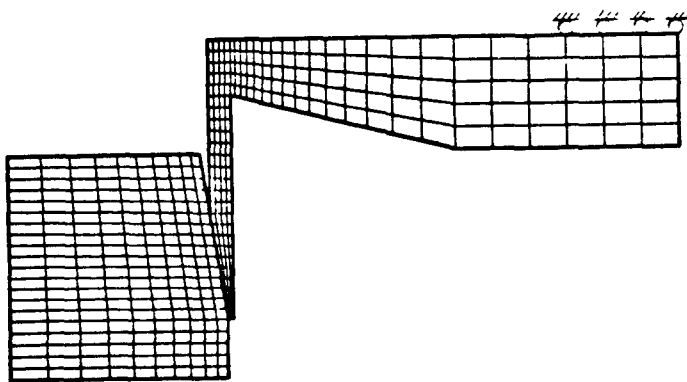
FIGURE 3. Molybdenum Sleeve to Beta Alumina Tube Joint Design.



a) Model A



b) Model B



c) Model C

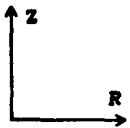
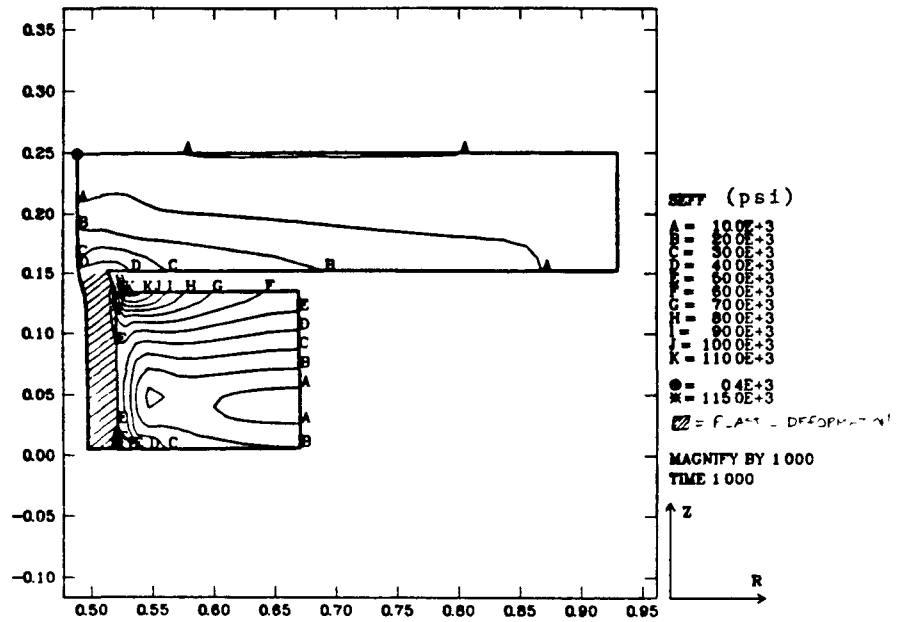
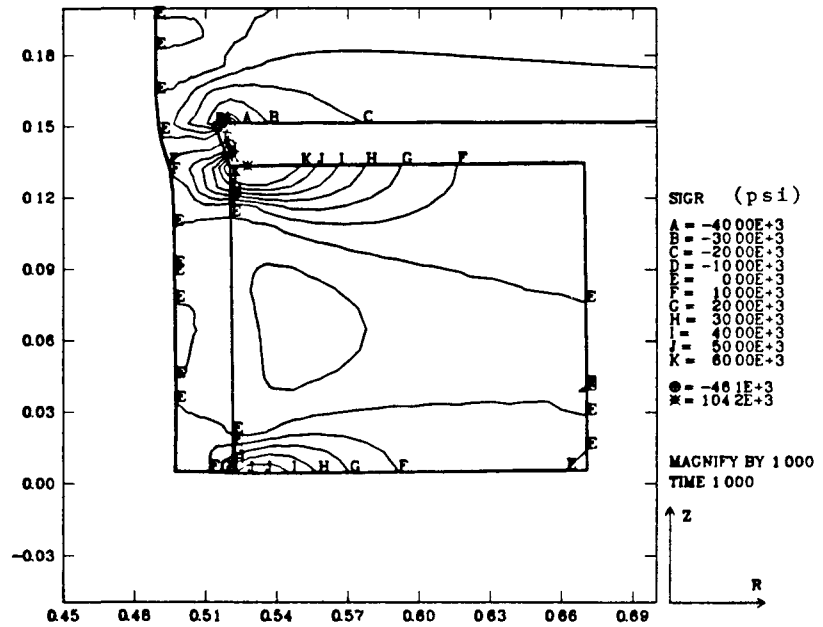


FIGURE 4. Axisymmetric Finite Element Models.

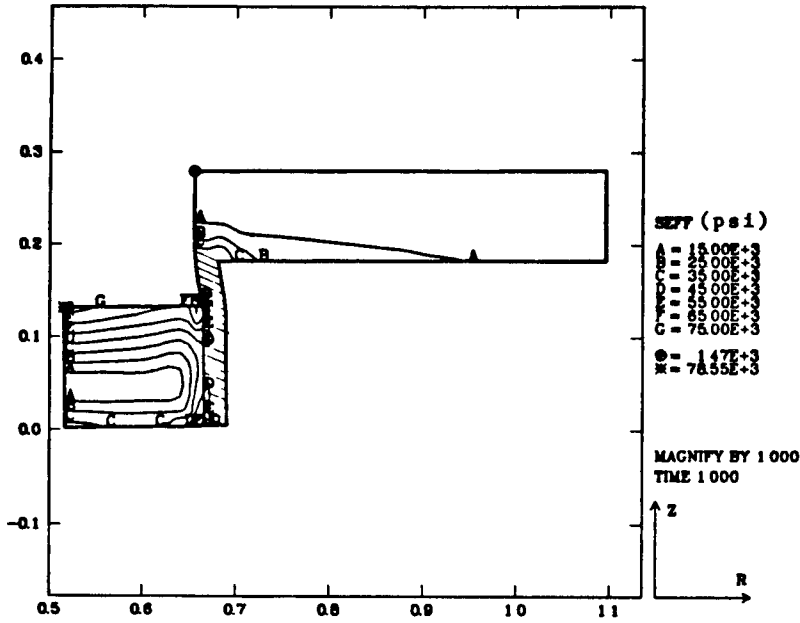


a) Contour plot of effective stress.

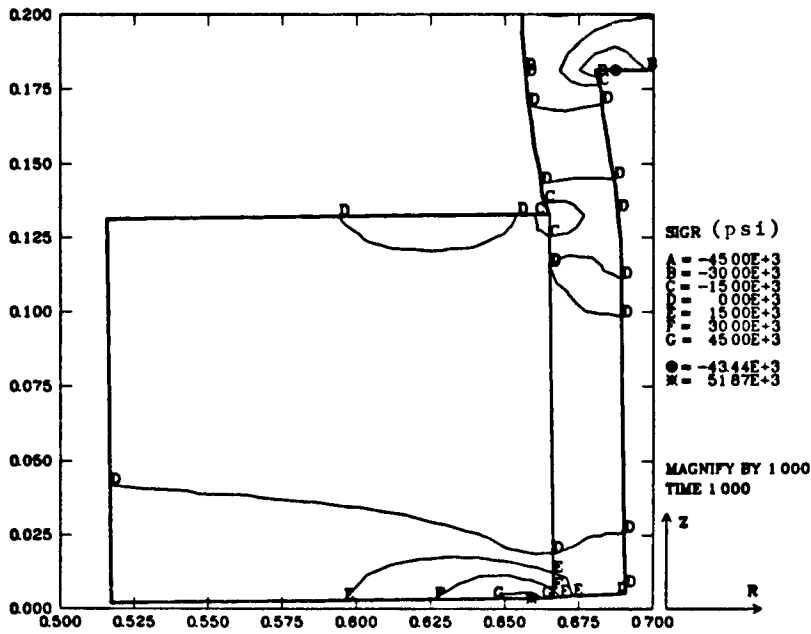


b) Contour plot of radial stress.

FIGURE 5. Results from Analysis of Design II.

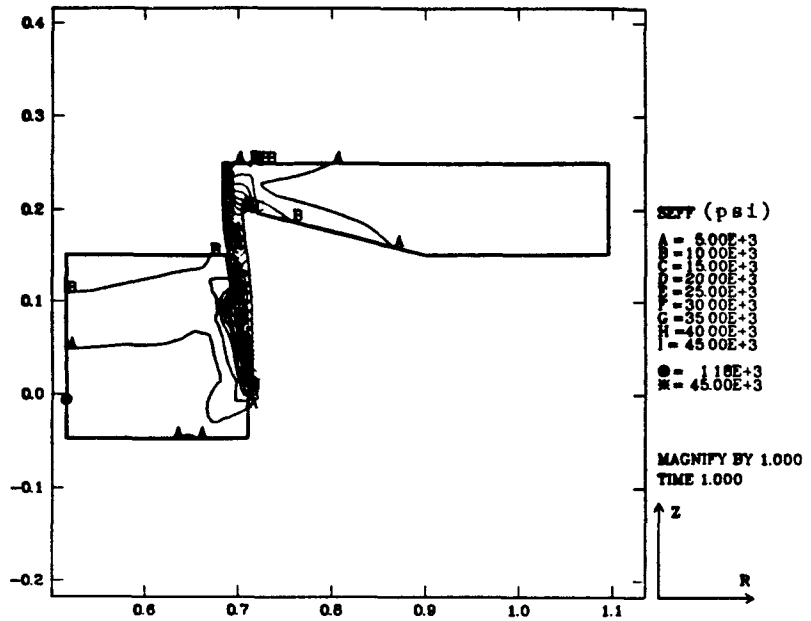


a) Contour plot of effective stress.

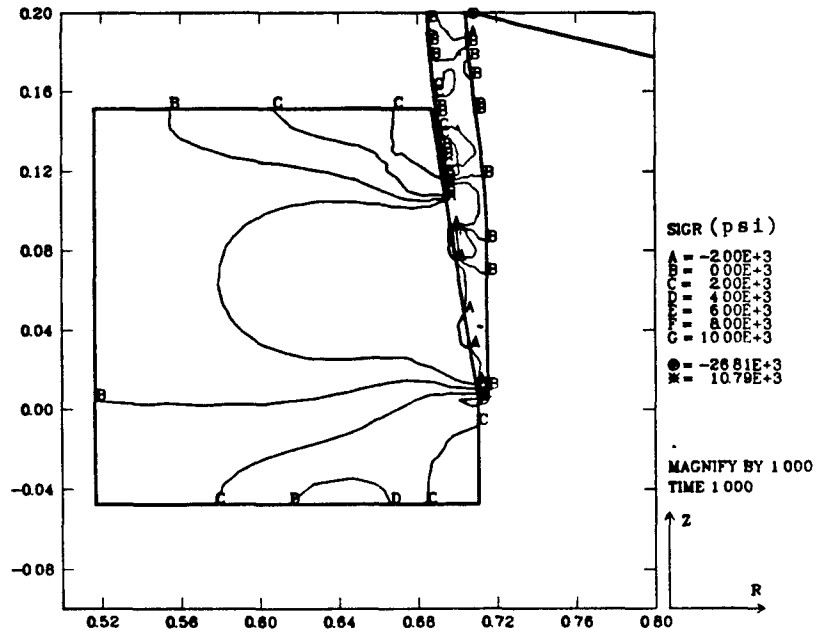


b) Contour plot of radial stress.

FIGURE 6. Results from Analysis of Design III.



a) Contour plot of effective stress.



b) Contour plot of radial stress.

FIGURE 7. Results from Analysis of Design IV.

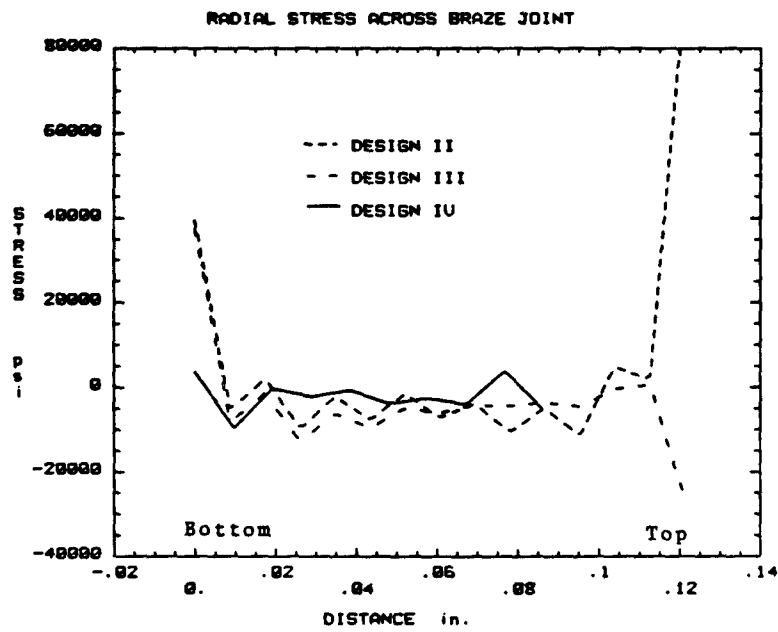


FIGURE 8. Radial Stress Across Braze Joint as a Function of Distance from the Bottom End.

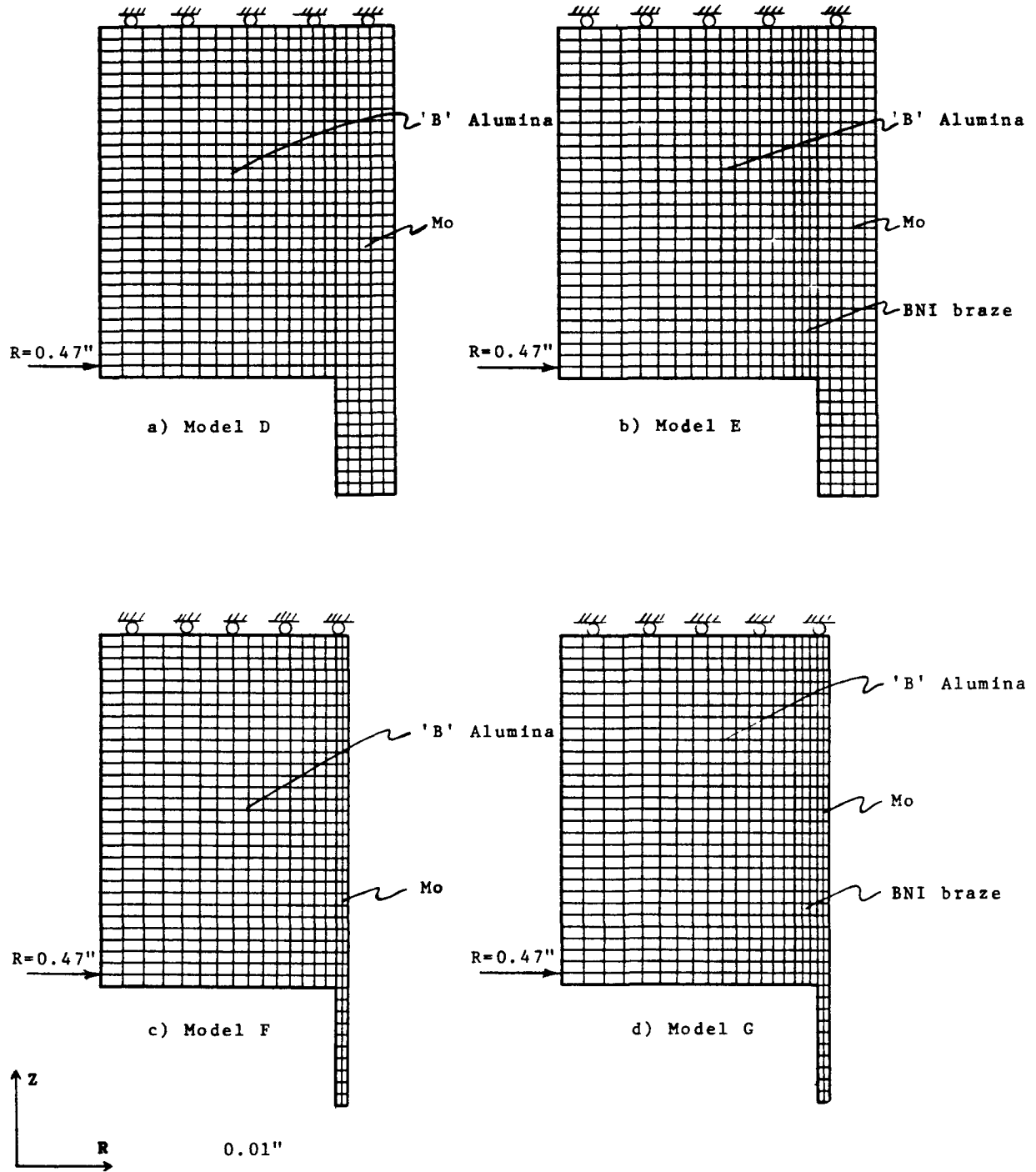
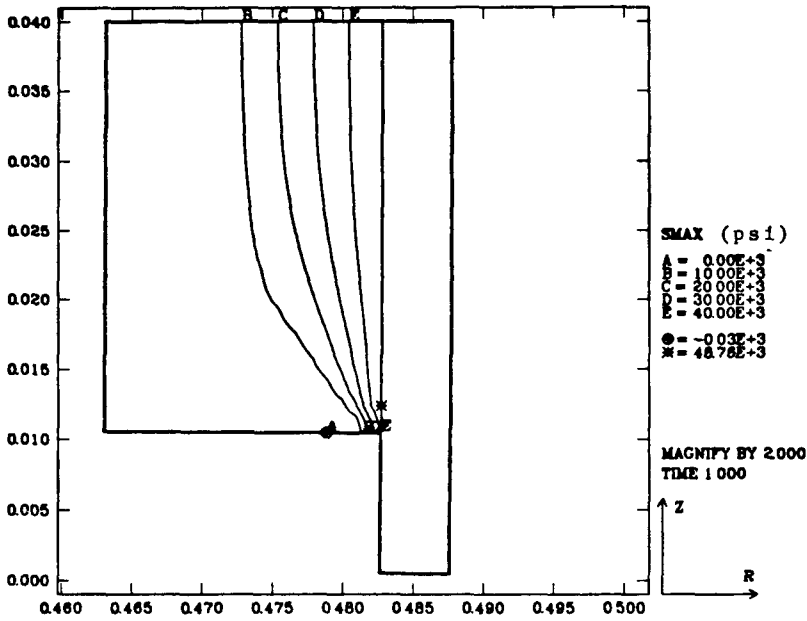
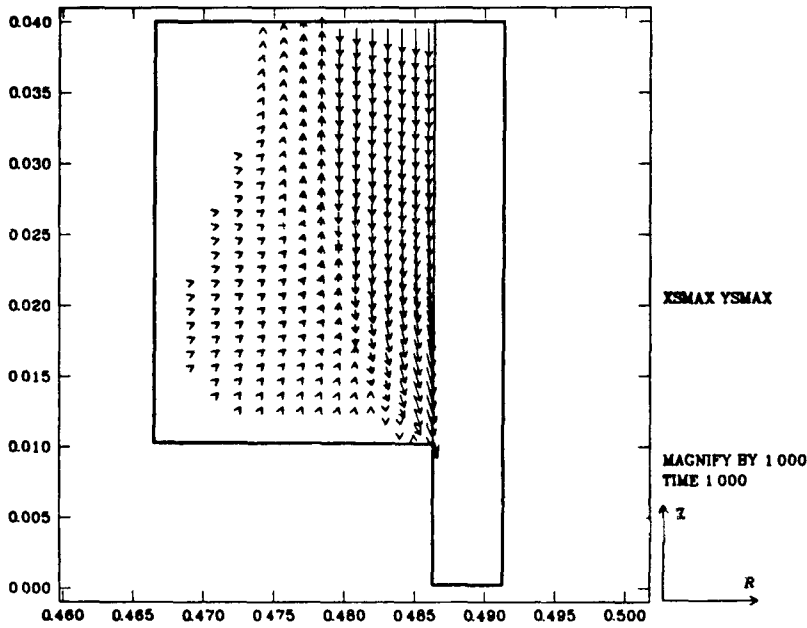


FIGURE 9. Axisymmetric, Finite Element Models.

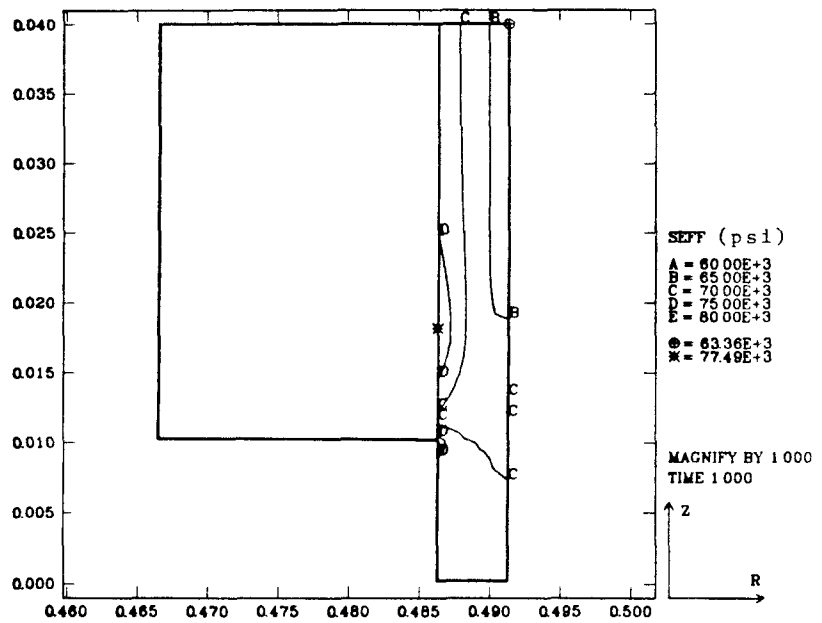


a) Maximum tensile stress in alumina tube.



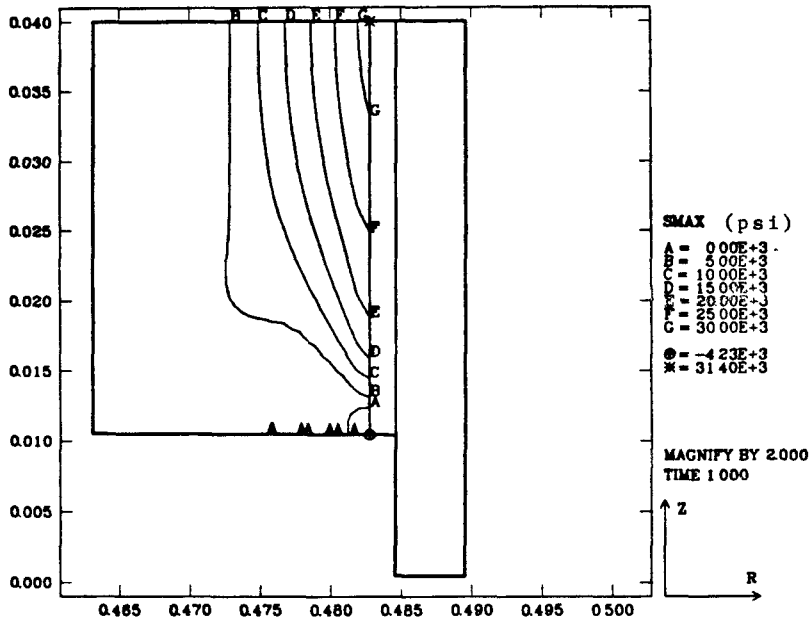
b) Maximum tensile stress orientation.

FIGURE 10. Results from Analysis of Molybdenum Sleeve to Alumina Tube Joint - 5 mil sleeve, No braze.

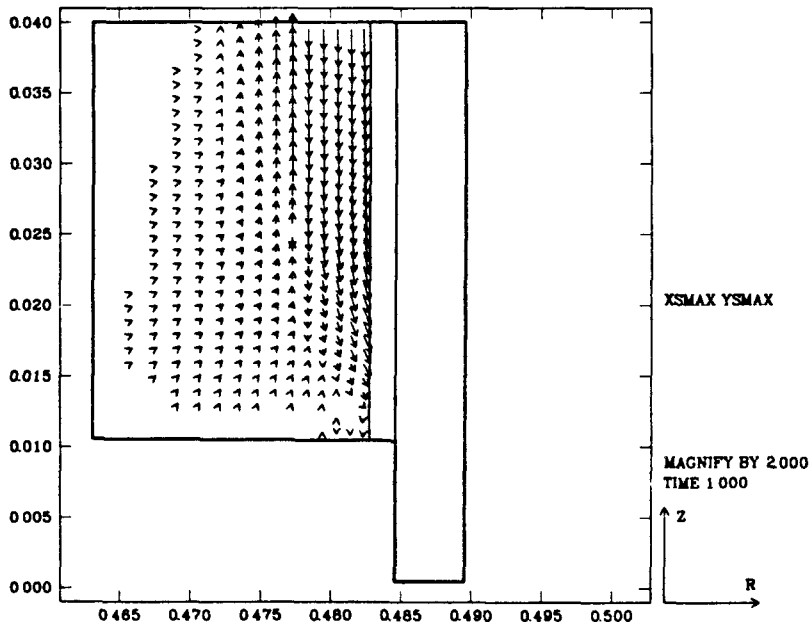


c) Effective stress in molybdenum sleeve.

FIGURE 10. Results from Analysis of Molybdenum Sleeve to Alumina Tube Joint - 5 mil sleeve, No braze.

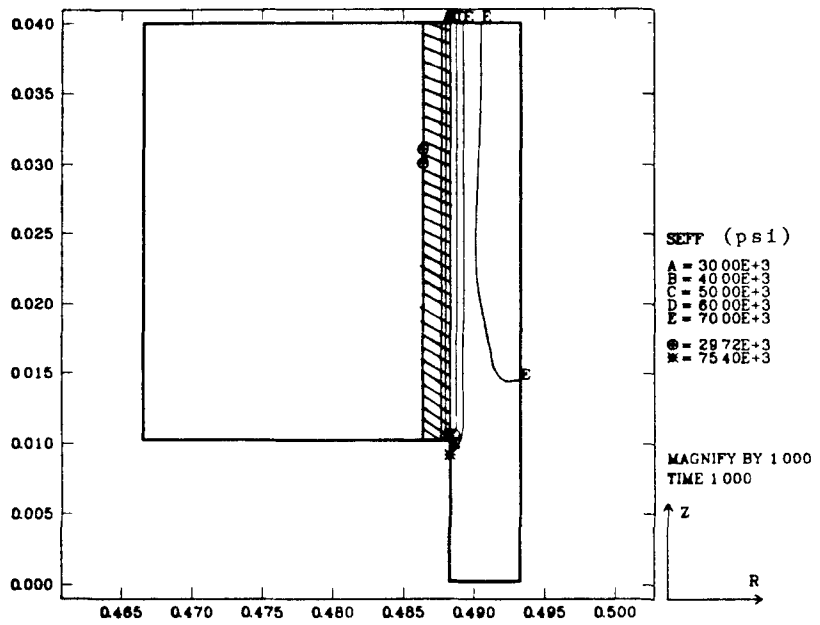


a) Maximum tensile stress in alumina tube.



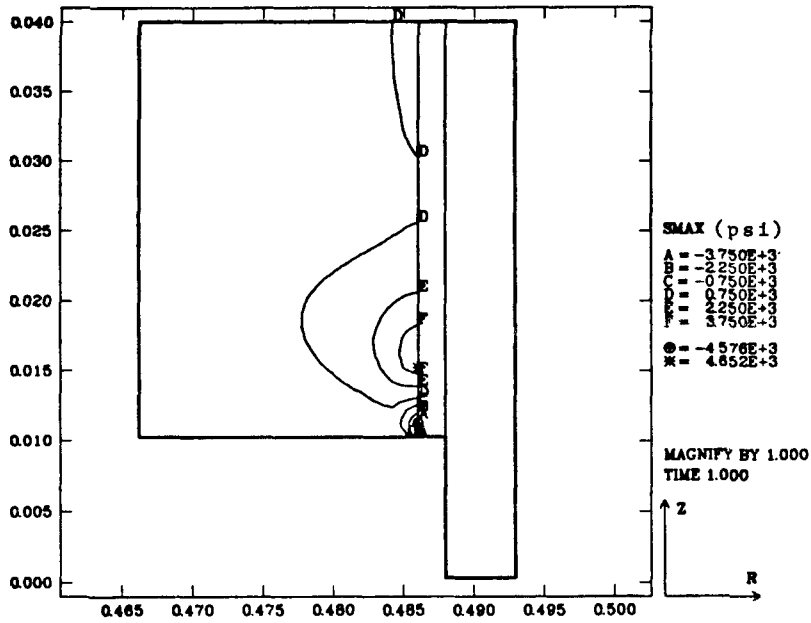
b) Maximum tensile stress orientation.

FIGURE 11. Results from Analysis of Molybdenum Sleeve to Alumina Tube Joint - 5 mil sleeve, 2 mil braze.

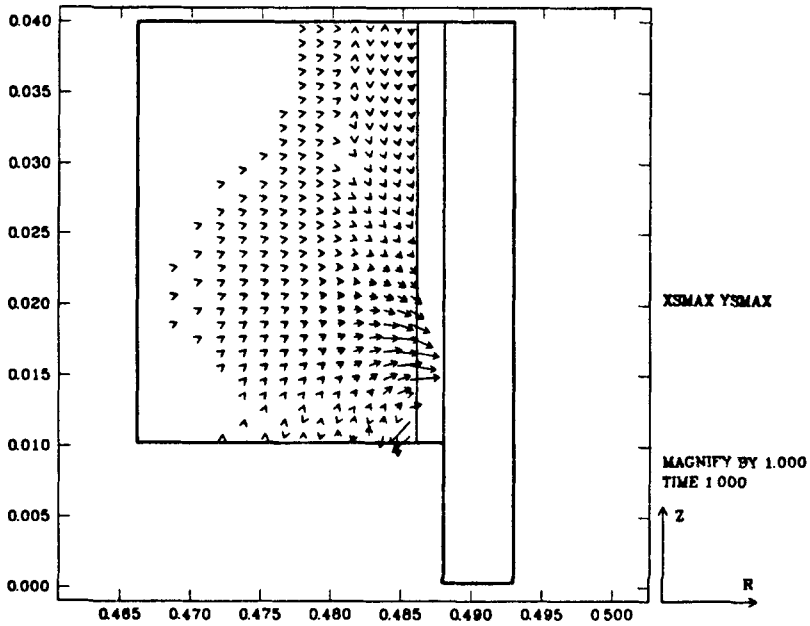


c) Effective stress in molybdenum sleeve and braze material.

FIGURE 11. Results from Analysis of Molybdenum sleeve to Alumina Tube Joint - 5 mil sleeve, 2 mil braze.

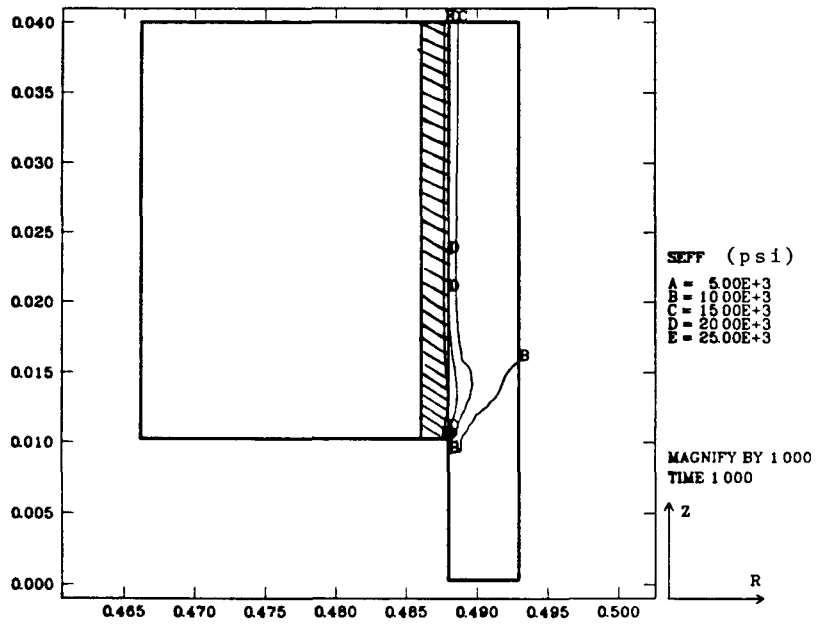


a) Maximum tensile stress in alumina.



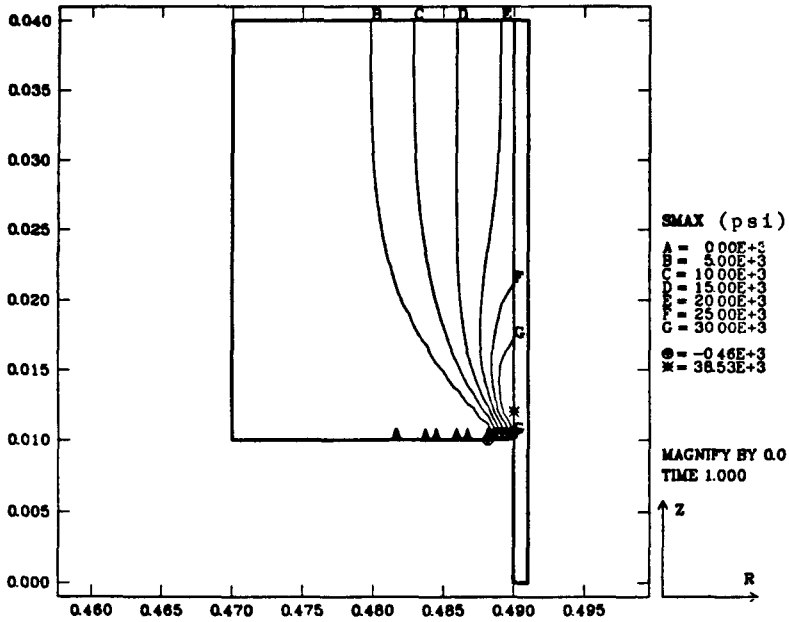
b) Maximum tensile stress orientation.

FIGURE 12. Results from Analysis of Tantalum Sleeve to Alumina Tube Joint - 5 mil sleeve, 2 mil braze.

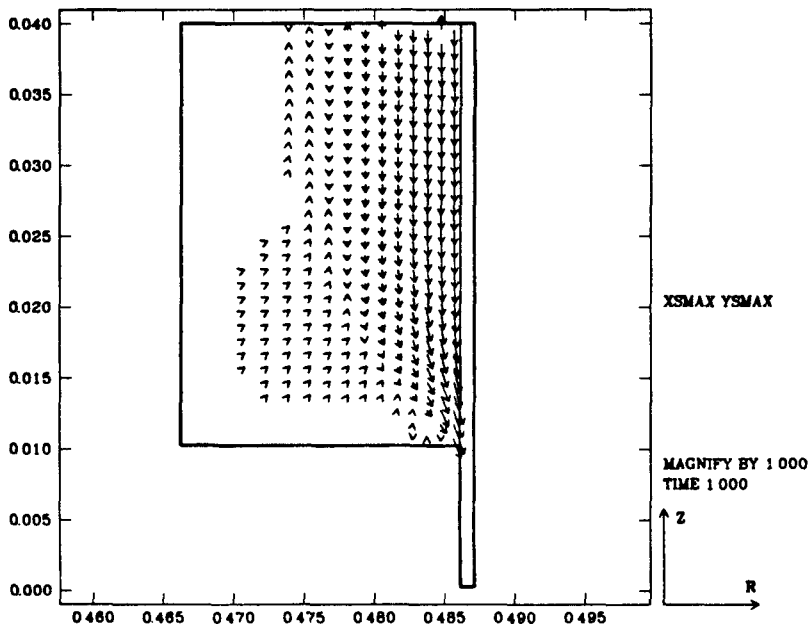


c) Effective stress in tantalum sleeve and braze material.

FIGURE 12. Results from Analysis of Tantalum Sleeve to Alumina Tube Joint - 5 mil sleeve, 2 mil braze.

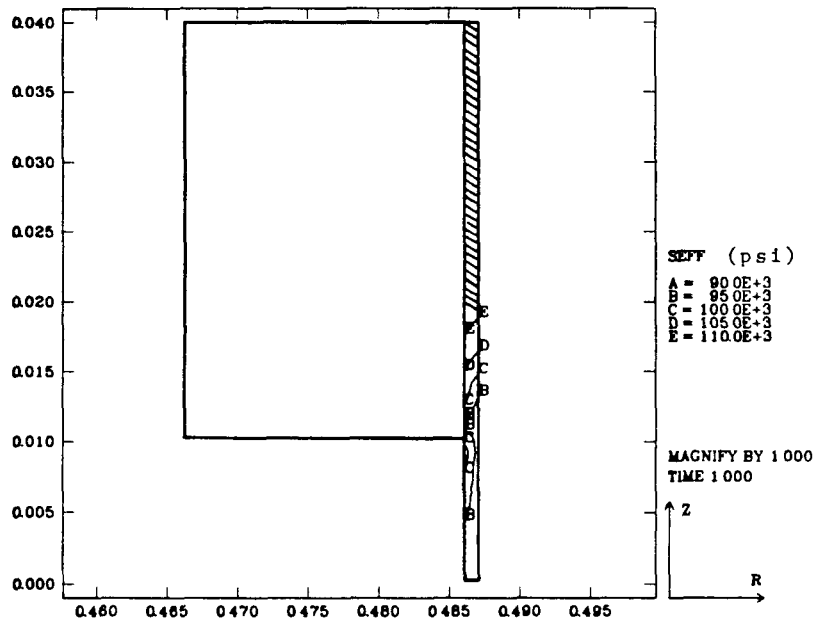


a) Maximum tensile stress in alumina tube.



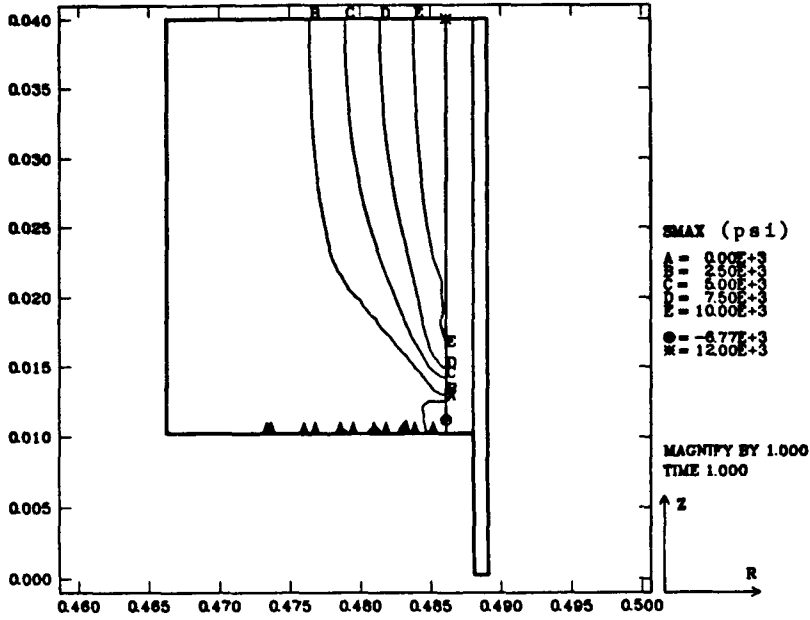
b) Maximum tensile stress orientation.

FIGURE 13. Results from Analysis of Molybdenum Sleeve to Alumina Tube Joint - 1 mil sleeve, No braze.

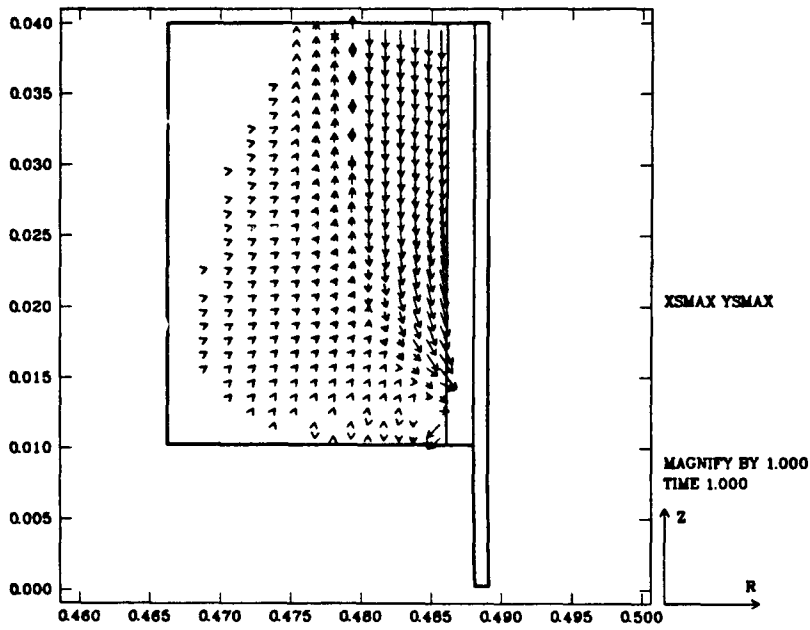


c) Effective stress in molybdenum sleeve.

FIGURE 13. Results from Analysis of Molybdenum Sleeve to Alumina Tube Joint - 1 mil sleeve, No braze.

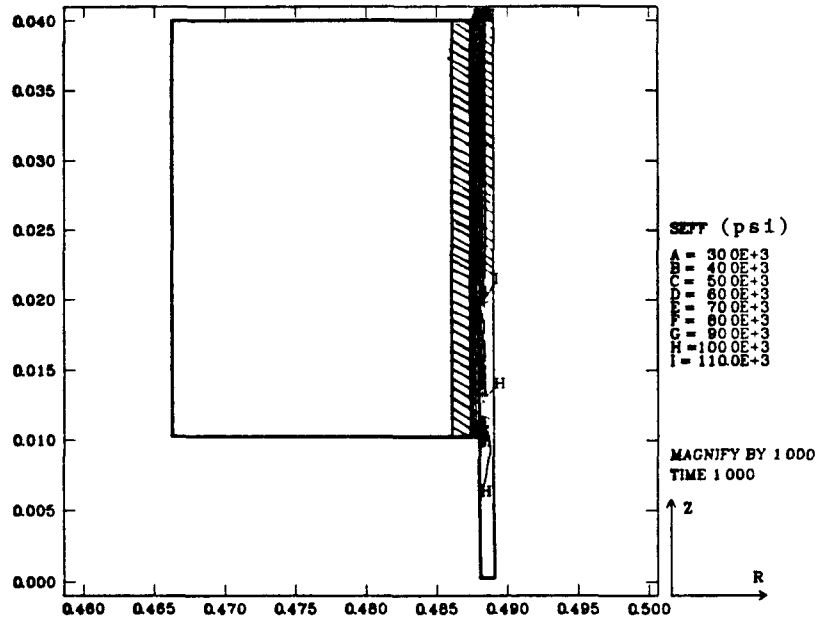


a) Maximum tensile stress in alumina tube.



b) Maximum tensile stress orientation.

FIGURE 14. Results from Analysis of Molybdenum Sleeve to Alumina Tube Joint - 1 mil sleeve, 2 mil braze.



c) Effective stress in molybdenum sleeve and braze material.

FIGURE 14. Results from Analysis of Molybdenum Sleeve to Alumina Tube Joint - 1 mil sleeve, 2 mil braze.

-130-/-131-

APPENDIX E
ELECTROMAGNETIC PUMP

Blank Page

Electromagnetic Pump

An electromagnetic pump was developed for the condenser-to-boiler return line of the LMTEC bench test module. The requirements were for a pump that could move 6cc/minute of liquid sodium, at temperatures of up to 400 C, from vacuum to at least one atmosphere pressure. The point of departure for the present design was a brief description of a direct-current permanent-magnet two-stage pump in a report by T. K. Hunt and N. Weber, "Research and Development on a Sodium Heat Engine", final report under U.S. Department of Energy Contract No. DE-AC02-79ER10347, October 1982.

In the present design, flattened thin-walled stainless steel tubing is used for the pump channel. At the flattened section, direct current is passed through the channel in the plane of the flattening and perpendicular to the tube axis. Magnetic-flux lines are passed through the channel perpendicular to the direction of the electrical current and the tube axis. The resulting electromagnetic force ($J \times B$) acts on the liquid metal within the channel.

In order to achieve the present design-pressure with reasonable electrical currents and magnetic fields, the height of the flattened channel must be on the order of 0.003-0.005 inches. But this channel height will not readily fill with liquid sodium because of surface tension. In order to achieve easy priming with a reasonable hydrostatic head, an inducer stage having a channel height on the order of 0.015 inches is necessary. Careful preparation of the inside surface of the pump is also necessary to minimize the fraction of electrical current initially shunted through the channel walls. The two stages can be linked electrically so as to use the same current source. They can also be arranged adjacent to one another in order to use the same magnet. In the present design the electrical and hydraulic connections are made by electron-beam welding. This technique results in a sturdy pump with good initial surface condition within the channels. The tubing that has been used is type 304 stainless steel, with 0.125-inch outside diameter and 0.012-inch wall thickness. A cobalt-samarium magnet with iron pole pieces was used to obtain 8800 Gauss in the pump channels. The completed pump is shown in Figure E1.

A number of two-stage pumps of the above design have been built and tested. All have performed as well or better than expected. In contrast to the experience of others (as in the aforementioned report) pump priming has always occurred very quickly - in minutes to tens of minutes.

A test loop was constructed and used to fully characterize the pump and to demonstrate its long-term stability. The loop is shown in Figure E2. Referring to the Figure and moving clockwise from the top, the loop consisted of a pressure-dropping valve, a vacuum pump-out tee, a droplet-rate observation port, a sodium canister, the em-pump, and a pressure gauge. Flow rate was estimated from the sodium droplet size and rate. The loop was heat traced and instrumented with a number of thermocouples. The temperatures were monitored and recorded by a system built around a small desk top computer. Safe operation of the loop was ensured by providing multiply-redundant automatic shutdown of the trace heating if a high-temperature limit was exceeded. A schematic of the loop with measured temperatures was displayed on the computer screen. A typical display is shown in Figure E3, with temperatures in degrees C. The pump test loop was operated for 140 hours with no degradation of pump performance. The pump characterization is presented in Figure E4.

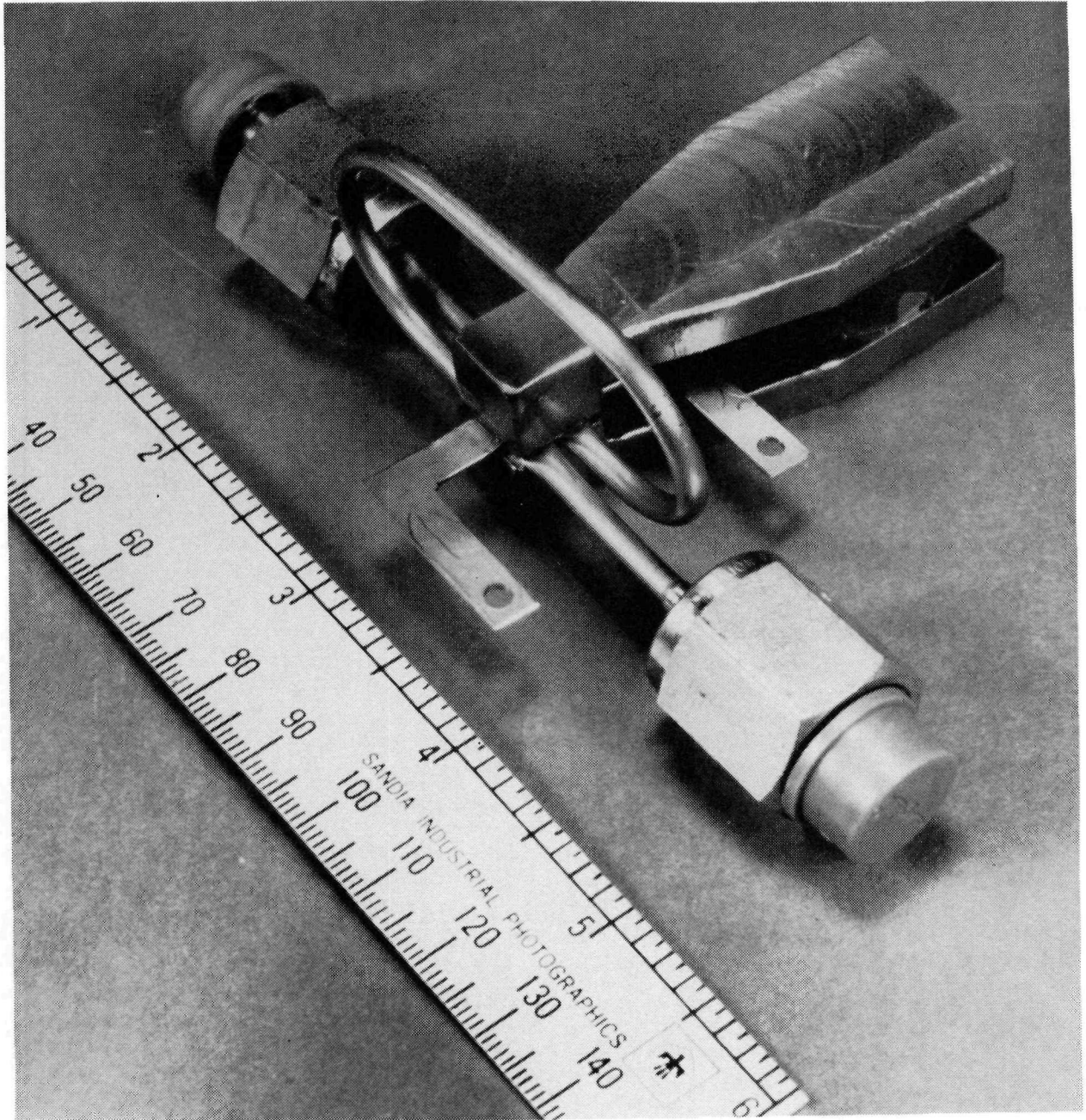


Figure E1. Electromagnetic Pump and Magnet Assembly.

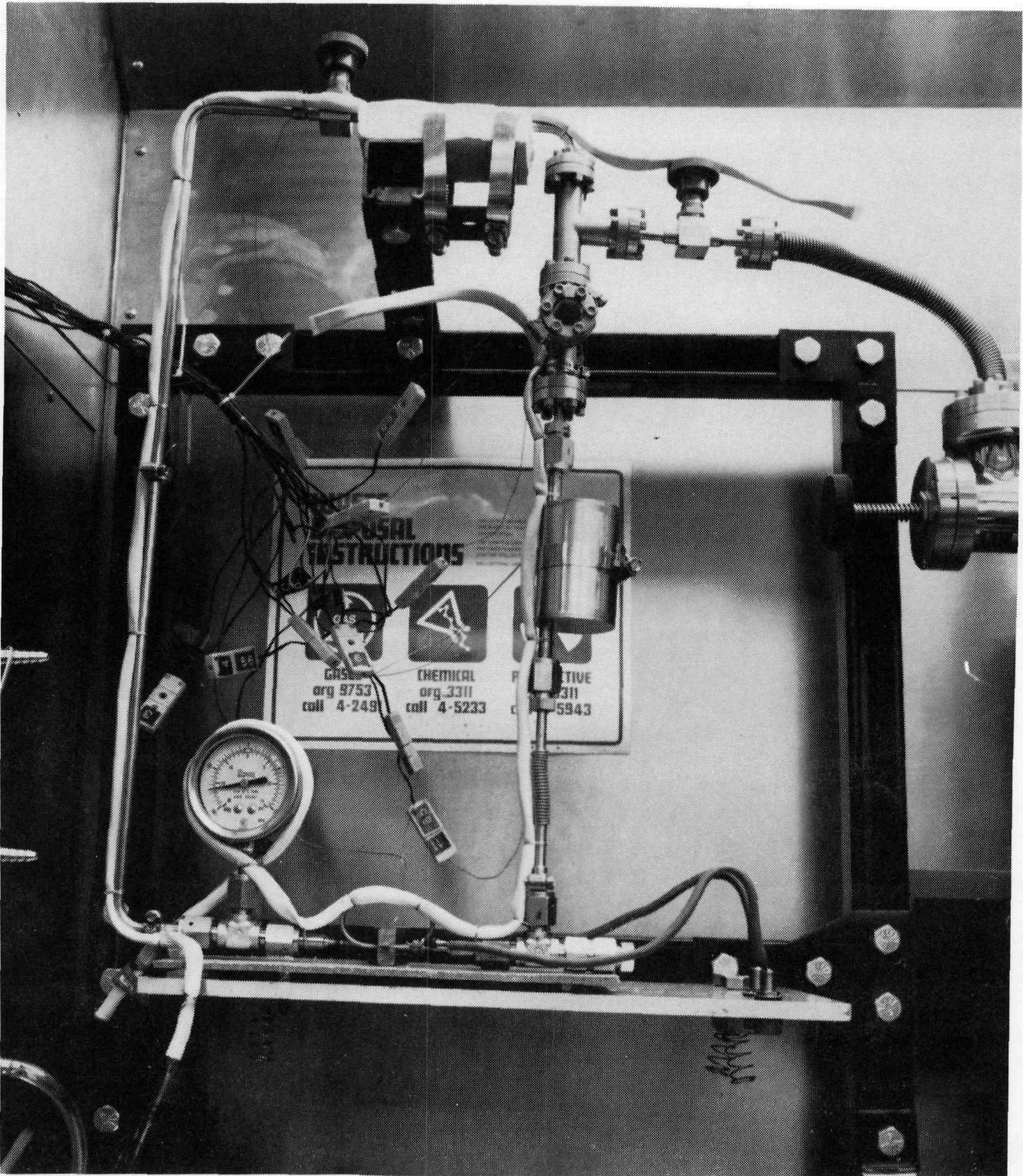


Figure E2. Electromagnetic Pump Test Loop.

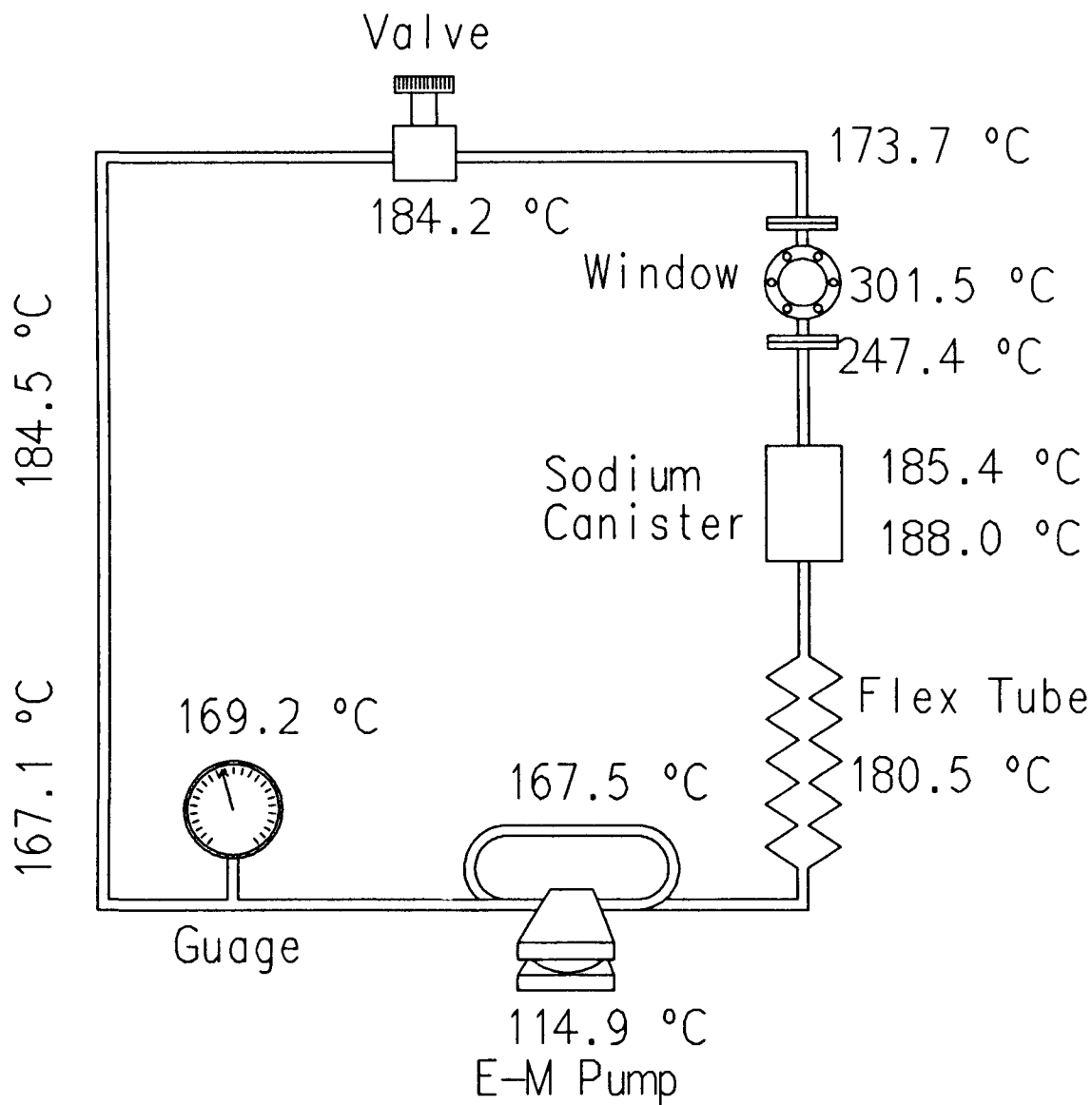


Figure E3. Electromagnetic Pump Test Loop Schematic and Operating Temperatures.

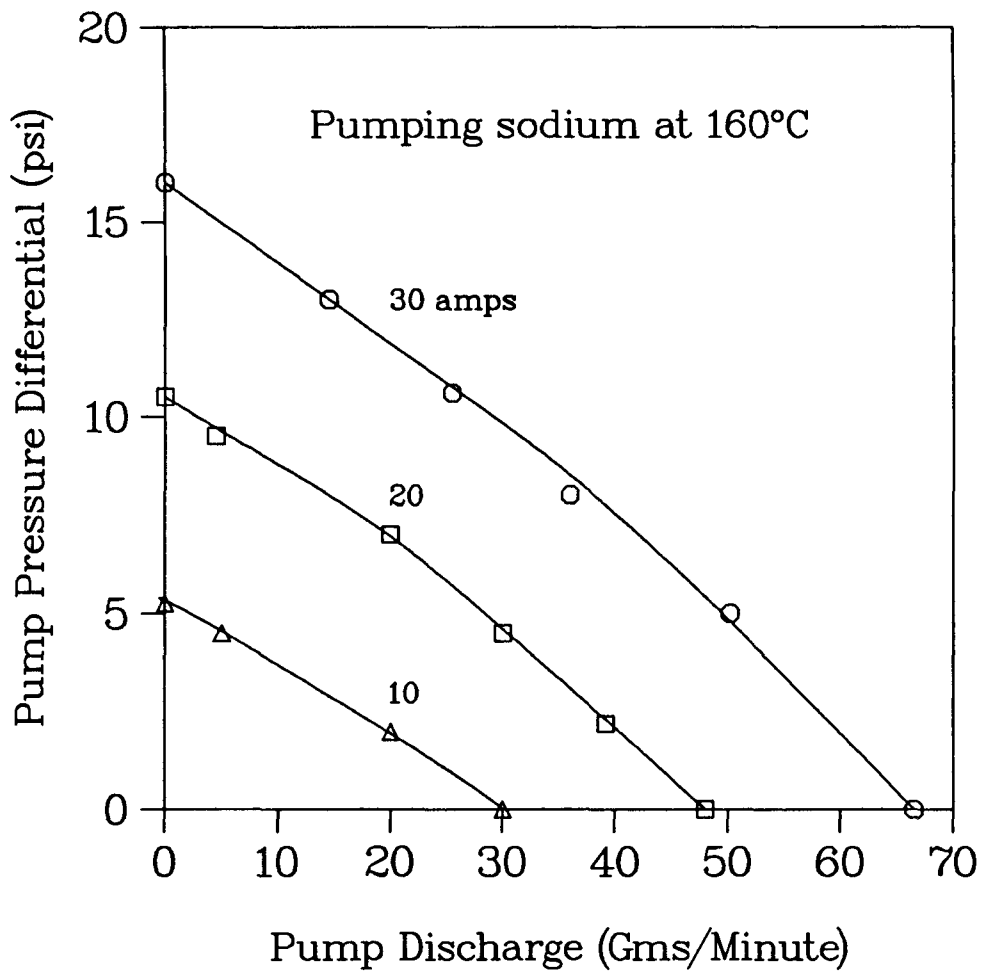


Figure E4. Electromagnetic Pump Performance Data.

APPENDIX F
DATA ACQUISITION AND CONTROL SYSTEM

Blank Page

Data Acquisition and Control System

F.1 Introduction

A computer operated data acquisition and control system has been implemented to permit un-attended safe operation of the LMTEC experiment. The computer monitors and controls temperatures throughout the system and performs data collection sequences to record complete voltage-current characteristic curves of the cell.

The LMTEC test was anticipated to last at least 100 hours in a steady state mode, in a populated area, so safe stand-alone operation was desirable. Many features of the data system are safety related, rather than data related. These features provide for automatic safe shutdown for any anticipated failure mode, and the system also notifies the project personnel in the case of a failure.

The data system records up to 36 thermocouples and 6 voltages on a regular basis. Most of the data is reduced in real time and displayed on the operators console, and is also stored on disk. The software is flexible to allow additional operator-initiated tests beyond the standard automated data collection. This could prove useful when un-anticipated results are seen in the data. The data can be sent to the VAX offline for further data manipulation, even during the test.

This appendix describes the system hardware and software capabilities separately, though in some cases it is difficult to separate the functions of the hardware and software.

F.2 System Hardware

A system block diagram of the data acquisition and control system is shown in Figure F1. The HP 9845 computer, voltmeter, scanner, and multiprogrammer are in a rack on loan from the downhole steam project. As much as possible, this instrumentation was used in its current condition without re-wiring. The temperature controllers, relays, and power supplies are housed in a second instrument rack. Most of the relays and controllers are part of the safe shutdown system. The LMTEC itself is located in a fume hood for additional safety in the case of a rupture.

An HP 9845 computer is the heart of the data system, and interfaces with the operator, safety equipment, control equipment, and data storage devices.

F.2.1 Control Hardware

The HP 9845 computer interfaces with an HP 6940B Multiprogrammer, which allows the computer to signal other devices with voltages, currents, resistances, and relay closures. The multiprogrammer is used to control non-HP-IB compatible equipment, including the Anavac residual gas analyzer, power supplies for the pump and load circuits, heater control relays, and the LMTEC open circuit relay.

A Eurotherm 821 temperature controller is used for the main heater. This microprocessor controlled PID controller can ramp the temperature at any rate, and then hold the temperature for up to 999 hours. Eight ramp and soak segments are possible in the internal program. The dynamic response of the controller is tuned to the thermal system of the LMTEC BTM. The 821 controller also has an RS-232 serial port, allowing communication with the HP 9845 computer. A Eurotherm 810 controller is used to control the temperature of the dielectric feedthru. This PID controller's setpoint is slaved to the actual boiler temperature measured by the 821 controller. Thus, the feedthru is held at the temperature of the boiler section, eliminating the large thermal loss through the copper buss.

Two Omega model 49 On-Off proportional temperature controllers are used to control the trace heaters on the sodium return loop. A variac controls the voltage to the heaters, essentially adding damping, so that the sensitivity of the dynamic thermal system can be reduced. The temperature around the loop is leveled by adjusting insulation thicknesses.

Figure F2, shows the LMTEC load circuit. The 300 amp power supply is connected in series with the LMTEC, a 200 milli-ohm resistor, and a relay. Open circuit voltages are measured with the relay open. Upon closure, and 0 volts at the power supply, current begins to flow through the circuit. As the power supply voltage is increased, effectively adding negative resistance to the circuit, the current through the circuit increases. The resistor is sized so that the maximum current desired from the BTM will be reached when the power supply reaches its maximum 7 volts (assuming LMTEC lives up to potential). This allows the lowest possible current when the power supply is at 0 volts (largest possible resistor).

The pump power supply is controlled by the HP 9845 computer. No feedback loop is presently used, as a pressure transducer for 400 C sodium is difficult to find. Instead, the pump

characteristic curve from the 100 hour test was used, and a Bourdon tube gauge is used for a visual check of the pressure. A voltage signal from the computer programs the power supply current. Another voltage signal switches a power relay to reverse the pump direction. In the future, a transducer will be incorporated to close the control loop.

The HP 9845 also controls the Anavac Residual Gas Analyzer. A voltage ramp is sent to the Anavac to scan the atomic mass, while output data is recorded, so the composition of the gas can be plotted. The computer also controls the safety overrides of the Anavac to prevent filament loss.

The HP 9845 computer switches a number of large power relays for heater control. These allow the computer to remove power from the heaters in the case of an emergency or manual shutdown.

F.2.2 Data Hardware

The HP 9845 computer is connected to an HP 3455A digital voltmeter and an HP 3495A scanner through the HP-IB buss to read voltages and resistances. Forty channels of the scanner are low voltage isothermal relays capable of switching type K thermocouples. A thermister is also contained in the terminal board for a reference junction temperature. The LMTEC BTM is fully instrumented with thermocouples, both in the hot zone and on the sodium return loop. Some thermocouples are connected both to the scanner and the controllers. This is possible because both instruments have high impedance inputs, so the readings are not affected.

Additional scanner channels are used in the resistance mode to check the position of the heater relays. This informs the computer of a hardware shutdown, and allows the computer to perform an orderly recovery and notify the operator. The scanner is also used to read the voltages along the length of the LMTEC buss (performance), the voltage of the standpipe (sodium level), and the voltage across the EM pump (pump power).

A standpipe is used to measure the height of sodium in the return loop. This simple device is a 1/8" vertical Stainless tube parallel to the return line. A current is passed through, and the voltage is measured end to end (4-wire resistance measurement). If the standpipe is full of sodium, the resistance, and therefore the voltage, is lower than an empty tube. This was used to determine when the EM pump is fully wetted and operational.

The computer also polls the Eurotherm controller to record heater power output, program status, setpoint, and measured temperature.

An internal clock allows the data to be tracked against real time.

F.2.3 Safety Hardware

Redundant safety devices are used throughout the system to ensure safe operation at all times. When possible, both hardware and software safety devices are used. The system not only looks for a failure of the LMTEC, but also checks for situations in which a failure would become more dangerous, such as a fume hood failure. All safety shutdowns require manual intervention and resetting before a re-start.

The primary safety concern is overtemperature, which leads to overpressure. During normal operation at 800 C, the sodium pressure is about 1/2 atmosphere, so a breach would cause air to leak in rather than sodium to leak out. Two Omega model 50 overtemperature controllers read the temperature of the boiler, and remove the heater (release a relay) if the temperature exceeds 850 C (881 C is 1 atmosphere of pressure). All controllers have upscale thermocouple break protection, so a thermocouple failure is seen as an overtemperature. Another overtemperature controller reads the feedthru temperature, and can shut the system down on overtemperature. The Eurotherm 821 (boiler) controller has an overtemperature alarm state, which also causes a hardware shutdown.

The HP 9845 computer checks each temperature around the entire sodium loop against predetermined tripout points. If the temperature reads too high, the thermocouple is checked for breakage. If it is not broken, the computer causes a software initiated system shutdown.

The main heater controller has a partial load failure sensor, which informs the computer of a main heater failure. The computer then performs an orderly shutdown. Also, a fume hood pressure sensor detects a fume hood failure (loss of vacuum) or a closed damper (high vacuum), either of which causes loss of fume hood operation. These failures also open a relay to the main heater and inform the computer for shutdown.

A computer failure also must cause a shutdown. A countdown hardware timer is set by the computer, and reset periodically. If the timer ever reaches 0, the computer is assumed hung, and a hardware shutdown is initiated. The computer also controls a relay for the main heater. Therefore, the program must specifically ask for power to be applied. This prevents an un-controlled re-start after a power outage.

Any failure mode listed above, in which the power is removed from the main heater, causes an automatic phone dialer to call three phone numbers and play a distress message 3 times each. The dialer is backed up by battery, so the calls are still made in the event of a power failure.

This hardware system was extensively tested, especially the safety aspects, before application to the LMTEC BTM. A dry vacuum furnace was used to simulate the LMTEC in some tests. The system was also used to control the 100 hour sodium EM-pump test, which was the first application to a sodium system outside the inert glovebox.

F.2.4 Miscellaneous Hardware

The vacuum system is a turnkey operation that will pump to high vacuum (10^{-11} atmospheres) with no oil backstreaming. The pump is a turbo-molecular pump with a 50 l/sec capacity. The pump controller and roughing pump are mounted with the turbo pump, and operation is by a single button. Piranni and Penning gauges measure the system pressure in different regimes, and the data is fed to the computer and also displayed on the instruments.

A frequency counter is available in the main computer rack, and will be used in future tests to measure the actual power used by LMTEC. Currently, the power reading from the Eurotherm 821 only provides the requested power, and only periodically. Since the power fluctuates significantly due to the control techniques, this number is unreliable. The frequency counter will allow the number of 60 cycle pulses sent to the heater to be compared to the 60 cycle line over a period of time. Since the controller is zero crossing fired, this ratio will be a measure of actual power used.

F.3 System Software

A simple flowchart of the system software is shown in Figure F3. The main program simply loops around while checking for failures, and records the current data at specified intervals. The remainder of the program can be called up by user initiated interrupts, listed in Table F1. The main loop is designed to handle normal operation of the BTM without intervention for up to 100 hours at a time. The user routines allow changes to the system characteristics and also allow detailed investigation of the BTM.

The program first sets up the variables, key operated interrupts, data files, and hardware. Then the safety diagnostic routine is run to be sure the hardware is ready for stand-alone operation. If this test is passed, the main loop begins, and user interaction is enabled.

F.3.1 Main Data Loop

A deadman's timer is set to allow enough time for a typical pass through the loop. Then the safety diagnostic scan is performed, and any problem causes an orderly shutdown. The data time pointers are checked, and the data is read and stored if the delay time has elapsed. The current data, whether stored or not, is always displayed in a graphics format on the console. Control then returns to the top of the main loop.

F.3.2 Safety Shutdown

The safety shutdown routine is called whenever a safety related problem is detected. This may be triggered by a hardware shutdown (relay tripout) or a software shutdown (data thermocouple reads high). The shutdown routine opens the load circuit and turns off the main heater and feedthru guard heater. The temperatures are monitored throughout the loop. When the sodium temperature falls to 300 C, the pump is reversed and the trace heaters are turned off, completing the shutdown. A Sonalert alarm also sounds, and the main heater shutdown causes a distress call to three phone numbers. If the failure involves an overtemperature in the return loop, the trace heaters as well as the main heaters are shut down immediately.

This shutdown routine performs a quick and safe shutdown, while avoiding possible further damage to the LMTEC due to back-flowing of hot sodium. The experimenters should be able to reach the lab before solidification of the sodium and diagnose and solve the problem.

F.3.3 User Interaction Routines

These routines, listed in Table F1, allow the flexibility needed in an experimental program such as LMTEC. While normal operation of the BTM is anticipated, providing for abnormal operation and investigations saves precious programming time during the operation of the cell. The user routines also allow close operator supervision during the startup cycle, when normal data is not recorded. During startup, user interaction is necessary while the thermal system is tuned, the cell is evacuated of outgassing elements, and other startup activities occur.

The flexibility of the LMTEC software allows it to be used as a subset to control experiments leading up to LMTEC. The same hardware and software was first used to control a simple vacuum furnace that simulated LMTEC operations. The furnace was also used for brazing and for tube bakeout and analysis. In addition, the same system was used to control the EM-pump 100 hour test, which was the first sodium system operated outside the inert atmosphere glove box.

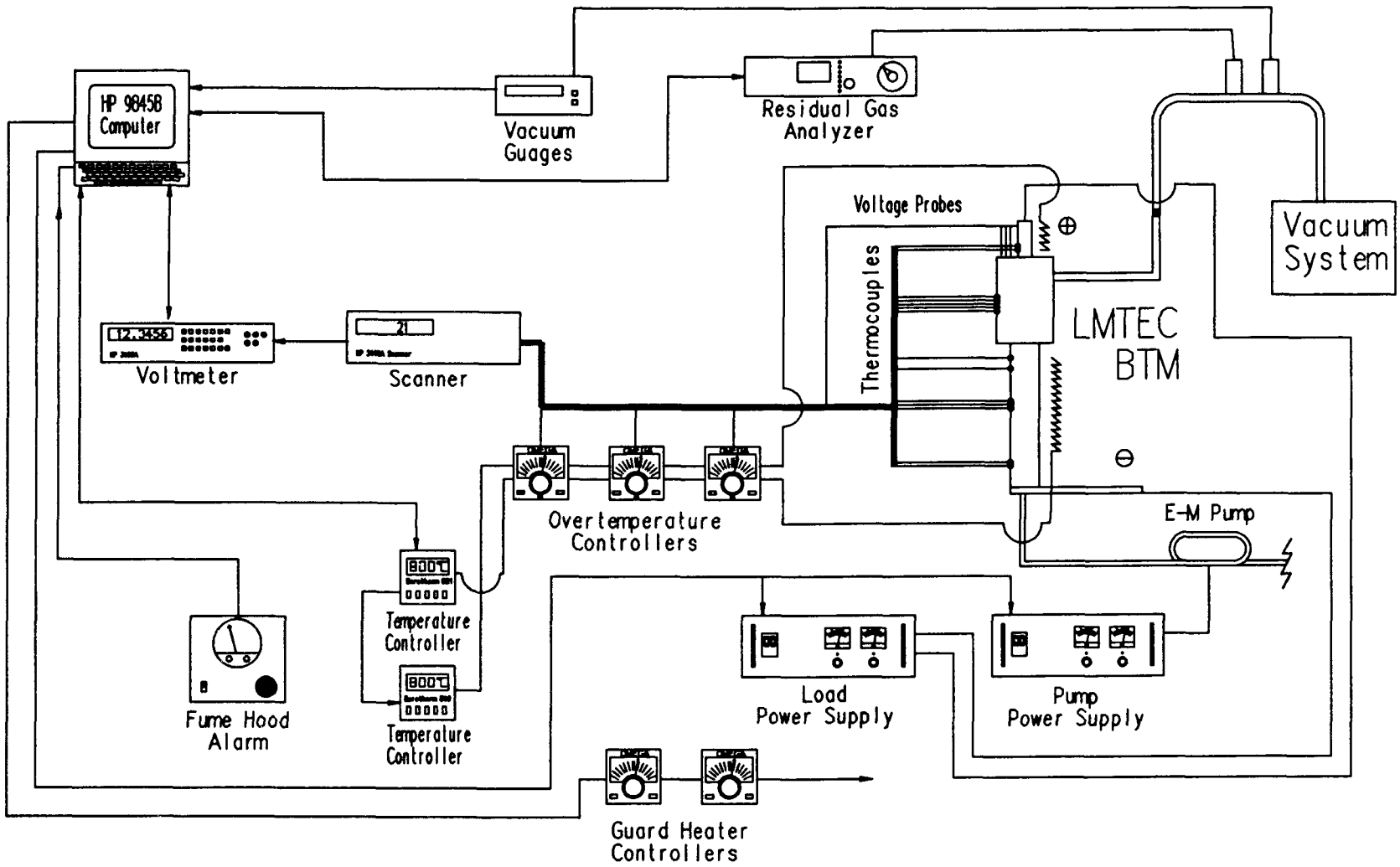
F.4 Results

The data system hardware and software performed as expected for the LMTEC BTM test as well as the component level tests prior to the BTM. Thorough debugging prior to operation allowed the operators to concentrate on the BTM itself rather than the control and data system.

Safe operation of a hot sodium system was demonstrated in a populated area. A power failure during the 100 hour pump test caused an orderly shutdown, and properly notified the operators at home. Operation of the LMTEC was safely terminated by the system after the computer sensed the heater failure of the main boiler.

For future LMTEC operation, a secondary data system is planned. An IBM PC will be used to collect data at a high rate, storing it on hard disk. This will allow a more detailed failure analysis should a failure occur. The present system, while adequate for normal operation and safety, does not record data often enough to determine failure sequences in all failure modes, so an improvement is necessary.

Figure F1. Block diagram of data acquisition and control system



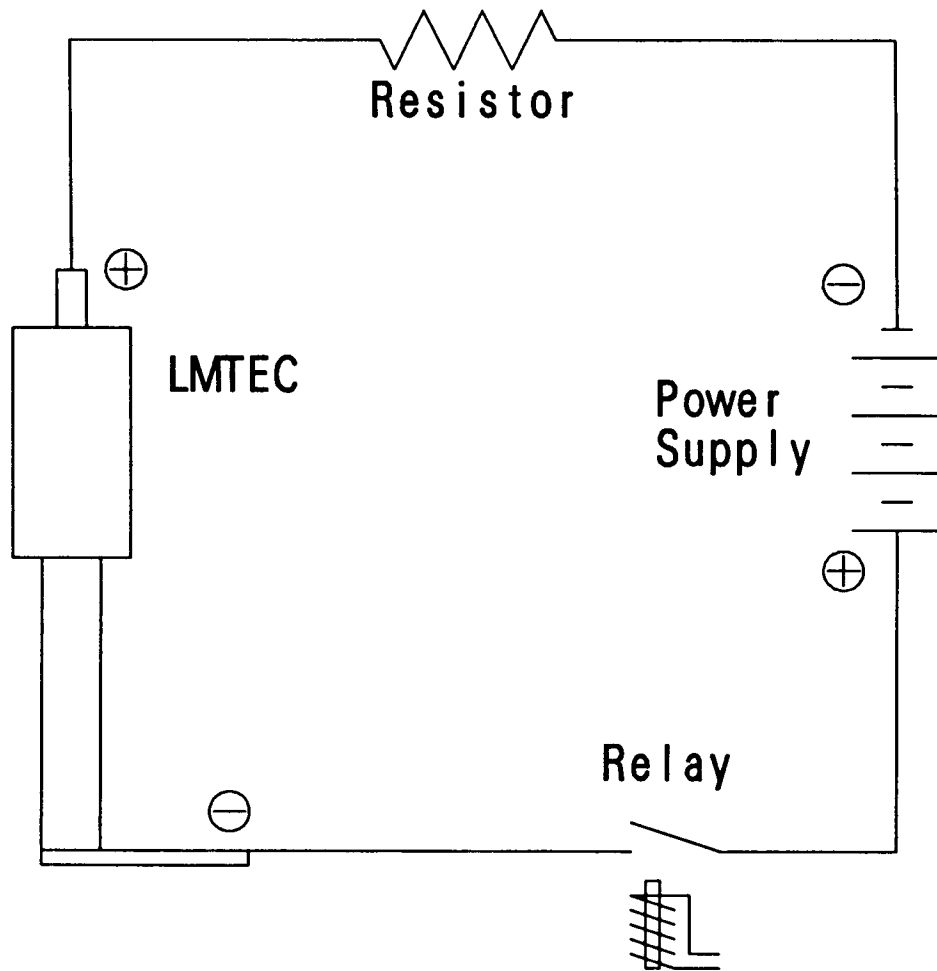


Figure F2. LMTEC load circuit schematic.

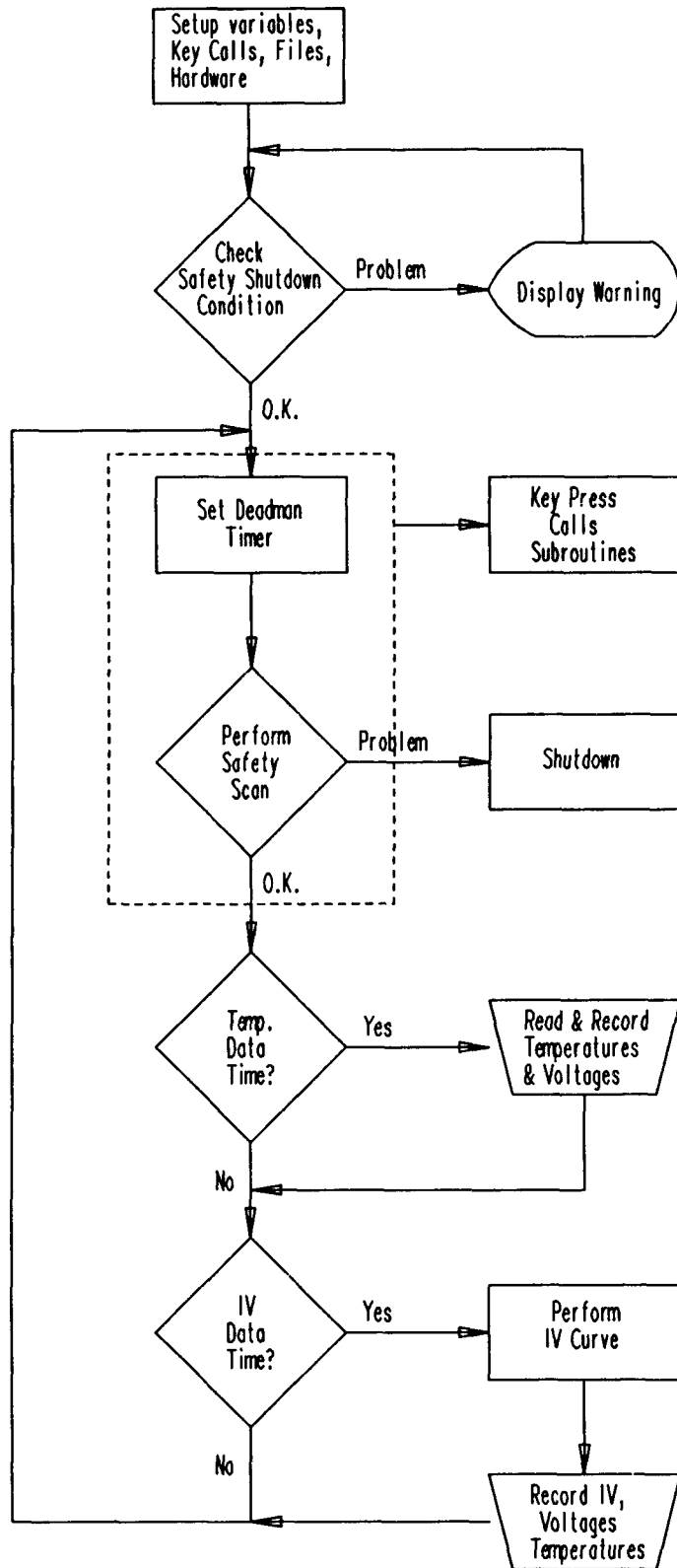


Figure F3. Data system flowchart.

Table F1.

Keypress Interrupt Subroutines

Key	Routine	Function
0.	Anavac	-Scan & plot anavac residual gas signature. -Hardcopy capability
1.	Hardcopy	-Trigger a screen data dump to printer.
2.	IV Parameters	-Menu to change IV curve parameters. -Display prior IV curve data.
3.	IV Curve	-Manually trigger & store IV curve.
4.	Print Parameters	-Hardcopy of current parameter values.
5.	Reverse EM Pump	-Reverse EM pump & update pointer.
6.	821 Communication	-Manually interface w/ 821 controller -Syntax checking -Change controller program or tuning parameters from the computer.
7.	Increment 821	-Step to next program segment of controller.
8.	Stop	-Initiate an orderly shutdown.
10.	Data Dump	-Data file maintenance menu. -Dump data to floppy, tape, or hard disk. -Initialize data files.
11.	Reset TC's	-Un-marks "broken" thermocouples after replacement.
12.	Change tripouts	-Change overtemperature values that cause a shutdown for each thermocouple.

Blank Page

F.5 Program Listing

```
10 ! Program name is LMTEC (03/10/87)
20 ! This program is the CONTROL/MONITOR program for the LMTEC system
30 ! *****
40 OPTION BASE 1
50 PRINTER IS 16
60 COM SHORT Tsnuz,Ntc,Nhtc,Tc,Tb,Btc(35),Mtc(35),Rlypo(5),Trecord,Vrecord
70 COM Atc$(35)[3],Ltc$(35)[18],Lrly$(5)[12],Relay$(5)[3],Lvolt$(6)[3]
80 COM SHORT Volt(6),St,Piv,Ivs,Hpower
90 COM Iiv,Itemp,INTEGER Gtc(35)
100 PRINT CHR$(12)
110 DIM Op(50)
120 Rheat=14.8 !RESISTANCE OF MAIN HEATER
130 Tsnuz1=60 !DELAY BEFORE DEAD COMPUTER ALARM
140 Tsnuz=999 !PREVENT ALARM BEFORE STARTUP FINISHED
150 Piv=999 !OUTPUT FOR 7-300 POWER SUPPLY
160 Ivs=10 !SPEED FOR IV CURVE
170 Mnto=0 !OLD MINUTE FOR TEMPERATURE DATA TRIP
180 Mnivo=0 !OLD MINUTE FOR IV-CURVE DATA TRIP
190 Itemp=10 !DATA INTERVAL FOR TEMPERATURES
200 Iiv=30 !DATA INTERVAL FOR IV CURVES
210 Mtrig=0 !Manual data triggre
220 Trig=0 !DATA TRIGGRE
230 Fb=0 !PUMP IS REVERSED
240 MAT Gtc=(1) !GOOD THERMOCOUPLES
250 FOR I=1 TO 10
260 Op(I)=0 !HEATER POWER
270 NEXT I
280 Iop=1 !POWER POINTER
290 ! *****
300 CALL Start
310 ! *****
320 OUTPUT 722;"F1R3M3A1HOT2T3"
330 ABORTIO 7
340 ON KEY #0 GOSUB KO !RUNS ANAVAC
350 ON KEY #1 GOSUB Sdump !TRIGGERS SCREEN DUMP
360 ON KEY #2 GOSUB K2 !IV PARAMETERS AND DISPLAY
370 ON KEY #4 GOSUB K4 !PRINT CHANGABLE PARAMETERS
380 ON KEY #3 GOSUB K3 !TAKE IV CURVE & STORE
390 ON KEY #5 GOSUB K5 !REVERSE EM PUMP
400 ON KEY #6 GOSUB K6 !TALK TO 821 MANUALLY
410 ON KEY #7 GOSUB K7 !INCREMENT PROGRAM SEGMENT
420 ON KEY #8 CALL Stop !SHUTDOWN EXPERIMENT!!!!
430 ON KEY #10 GOSUB K10 !DUMPS DATA TO FLOPPY
440 ON KEY #11 GOSUB K11 !RESETS BROKEN TC MARKERS
450 ON KEY #12 GOSUB K12 !CHANGE TRIPOUT VALUES
```

```
460 ! *****
470 PRINT PAGE
480 Check: ! ARE WE READY YET?
490 DISP "CHECK"
500 OUTPUT 723;"00140TK2500TK4500T"
510 Shtdn=0
520 GOSUB Diagno
530 IF Shtdn=0 THEN Mloop
540 GOSUB Warn
550 GOTO Check
560 ! *****
570 Mloop: ! MAIN LOOP STARTS HERE
580 ! *****
590 Tsnuz=Tsnuz1
600 PRINTER IS 16
610 DISP "MAIN LOOP"
620 CALL Timer(Tsnuz)
630 GOSUB Diagno
640 IF Shtdn=0 THEN 670
650 CALL Shutdown(Fb,Shtdn)
660 GOTO Check
670 DISP Trecord,Vrecord
680 GOSUB Dtrig
690 Trig=BINIOR(Mtrig,Trig)
700 Mtrig=0
710 IF (Trig=1) OR (Trig=3) THEN CALL Tdata
720 IF (Trig=2) OR (Trig=3) THEN CALL Ivdata
730 Trig=0
740 GOTO Mloop
750 ! *****
760 Diagno: ! DIAGNOSTIC ROUTINE LOOKS FOR TROUBLE
770 DISP "DIAGNOSTIC, Iop=";Iop
780 CALL Tcrd
790 CALL Rlyrd
800 CALL Voltrd
810 FOR Isd=1 TO 5
820 IF Rlypo(Isd)>0 THEN Shtdn=Isd
830 NEXT Isd
840 FOR I=1 TO Ntc
850 ! *****
860 Isd=Isd+1
870 NEXT I
880 IF Shtdn>0 THEN RETURN
890 Cs$=FNC821$("CS")
900 Sp$=FNC821$("SP")
920 IF Cs$[1,6]<>Co$[1,6] THEN CALL Csnew(Co$,Cs$)
921 FOR Jj=1 TO 2
925 Op$=FNC821$("OP")
930 Op(Iop)=VAL(Op$[3,8])
```

```
940 Iop=Iop MOD 50+1
941 NEXT Jj
950 Hpower=0
960 FOR I=1 TO 50
970 Hpower=Hpower+Op(I)
980 NEXT I
981 Hpower=Hpower/5
990 PRINT CHR$(128)
1000 CALL Draw(Mnto,Mnivo,Fb)
1010 IF Ndump=0 THEN RETURN
1020 Ndump=0
1030 CALL Dump(Mnto,Mnivo,Fb)
1040 RETURN
1050 ! *****
1060 Dtrig: ! CHECKS FOR DATA TIME
1070 ! *****
1080 Trig=0
1090 CALL Time(Time$)
1100 Mn=VAL(Time$[12,13])+VAL(Time$[9,10])*60+VAL(Time$[4,5])*24*60+
      VAL(Time$[1,2])*31*24*60-St
1110 IF INT(Mn/Itemp)=INT(Mnto/Itemp) THEN Ivd
1120 Mnto=Mn
1130 Trig=1
1140 Ivd: !
1150 IF INT(Mn/Iiv)=INT(Mnivo/Iiv) THEN RETURN
1160 Mnivo=Mn
1170 Trig=Trig+2
1180 RETURN
1190 ! *****
1200 Warn: ! WARNS OF SHUTDOWN PROBLEM ON STARTUP
1210 ! *****
1220 OUTPUT 723;"00140TK2000TK4000T"
1230 Isd=Shtdn
1240 PRINTER IS 16
1250 PRINT PAGE
1260 PRINT "SHUT-DOWN PROBLEM IDENTIFIED; REMEDY BEFORE CONTINUING"
1270 CALL Time(Time$)
1280 IMAGE "Date ",8A,9X,"Time",8A,9X
1290 PRINT USING 1280;Time$[1,8],Time$[9,16]
1300 IF Isd<6 THEN PRINT CHR$(129);Lrly$(Isd),"RELAY TRIPPED";CHR$(128)
1310 IF Isd>5 THEN PRINT CHR$(129);"TEMPERATURE HIGH AT ";Ltc$(Isd-6);CHR$(128)
1320 PRINT LIN(1)
1330 IMAGE 5(12A,4X)
1340 IMAGE 5(5D,11X)
1350 FOR I=1 TO Ntc STEP 5
1360 PRINT USING 1330;Ltc$(I),Ltc$(I+1),Ltc$(I+2),Ltc$(I+3),Ltc$(I+4)
1370 PRINT USING 1340;Btc(I),Btc(I+1),Btc(I+2),Btc(I+3),Btc(I+4)
1380 NEXT I
1390 Sw$=FNC821$("SW")
```

```
1400 Os$=FNC821$("OS")
1410 Cs$=FNC821$("CS")
1420 Sp$=FNC821$("SP")
1430 PRINT "821 STATUS:",Sw$,Os$,Cs$,Sp$
1440 Dum$=FNC821$("OS>0000")
1450 Dum$=FNC821$("SLO")
1460 CALL Timer(999)
1470 INPUT "HIT CONT WHEN PROBLEM IS RESOLVED",G$
1480 PRINT PAGE
1490 RETURN
1500 ! *****
1510 ! THIS SECTION CONTAINS KEY CALLS. KEYS DEFINED AS GOSUB ARE LOCAL.
1520 ! THUS, ROUTINE WILL NOT BE CALLED UNTIL CURRENT SEGMENT IS THE MAIN
1530 ! PROGRAM. THIS AVOIDS CONFLICTS OF RESOURCES
1540 ! *****
1550 Sdump:      ! TRIGGERS A SCREEN DUMP
1560 Ndump=1
1570 RETURN
1580 KO:      ! ANAVAC
1590 CALL Anavac
1600 RETURN
1610 K2:      ! IV PARAMETERS & DISPLAY
1620 CALL Ivp
1630 RETURN
1640 K3:      ! TRIGGER IV CURVE
1650 Mtrig=2
1660 RETURN
1670 K4:      ! PRINT PARAMETERS
1680 PRINTER IS 0
1690 PRINT LIN(3)
1700 PRINT "PARAMETERS: ",LIN(2)
1710 PRINT "TEMPERATURE DATA RECORD = ";Trecord
1720 PRINT "IV CURVE DATA RECORD = ";Vrecord
1730 PRINT "IV CURVE DURATION = ";Ivs
1740 PRINT "DATA INTERVALS = ";Iiv;" FOR IV; ";Itemp;" FOR TEMPS (MINUTES)"
1750 PRINT "LOAD SUPPLY STEADY POWER = ";Piv
1760 Fb$="REVERSED"
1770 IF Fb=1 THEN Fb$="FORWARD"
1780 PRINT "EM PUMP DIRECTION IS ";Fb$
1790 PRINT PAGE
1800 PRINTER IS 16
1810 RETURN
1820 K5:      ! REVERSE PUMP
1830 CALL Reverse(Fb)
1840 RETURN
1850 K6:      ! MANUAL 821 CONTROL
1860 CALL M821
1870 RETURN
1880 K7:      ! INCREMENT 821 PROGRAM SEGMENT
```

```
1890 CALL Cs
1900 RETURN
1910 K10: ! DUMP DATA TO FLOPPY
1920 CALL Ddump(0)
1930 RETURN
1940 K11: ! REPAIR TCS
1950 MAT Gtc=(1)
1960 RETURN
1970 K12: ! RESET TRIPOUT LEVELS
1980 CALL Nmtc
1990 RETURN
2000 ! *****
2010 ! *****
2020 END !END OF MAIN PROGRAM SEGMENT
2030 ! *****
2040 ! *****
```

```
2050 SUB Anavac
2060 ! Program name is ANAVAC (02/12/87)
2070 ! This program is the MONITOR/PLOT program for the ANAVAC system
2080 ! *****
2090 OPTION BASE 1
2100 COM SHORT Tsnuz
2110 CALL Timer(999)
2120 Printer=16
2130 PRINTER IS 16
2140 PRINT CHR$(12)
2150 DISP ""
2160 ! *****
2170 SHORT X(160),Y(160),Z(160)
2180 DIM Ppp(160)
2190 DIM Pp(160),Maxpp(11),Mass(11)
2200 ! *****
2210 Na=100
2220 Hc=0
2230 ! *****
2240 ON KEY #0,2 GOSUB Range !SETS ANAVAC RANGE
2250 ON KEY #1,2 GOSUB Hc !TRIGGERS HARDCOPY OF PLOT AND PEAKS
2260 ON KEY #3,2 GOSUB Trig !STARTS NEW SCAN
2270 ON KEY #8,2 GOSUB Aexit !EXITS SUBROUTINE
2280 GOSUB Range
2290 ! *****
2300 Loop: ! This section is the main loop
2310 ! *****
2320 OUTPUT 722;"F1R3M3A1HOT2T3"
2330 PRINTER IS 16
2340 CALL Time(Time$)
2350 IMAGE "Date ",8A,9X,"Time ",8A
2360 GOSUB Anavac
2370 GOSUB Aplot
2380 IF Hc=0 THEN Loop
2390 PRINTER IS 0
2400 PRINT LIN(2);"*****
*****";LIN(2)
2410 PRINT USING 2350;Time$[1,8],Time$[9,16]
2420 DUMP GRAPHICS
2430 FOR I=1 TO 10
2440 PRINT USING "8A,DD.D,14A,SD.DDE";"PEAK AT ";Mass(I)/2;" HAS VALUE OF";
Maxpp(I)
2450 NEXT I
2460 PRINT LIN(2);"*****
*****";LIN(2)
2470 PRINT PAGE
2480 PRINTER IS 16
2490 Hc=0
2500 GOTO Loop
```

```
2510 ! *****
2520 Range:          ! SETS ANAVAC RANGE
2530 ! *****
2540 Dum=FNTrip(0)
2550 INPUT "ENTER ANAVAC RANGE (ie. 1E-8)",Range
2560 Rc=0
2570 IF Range>1E-2 THEN 2600
2580 GOSUB Trig
2590 RETURN
2600 BEEP
2610 GOTO 2550
2620 ! *****
2630 Aexit:          ! LEAVES ANAVAC SUBROUTINE
2640 ! *****
2650 Dum=FNTrip(0)
2655 OUTPUT 723;"HKO"&VAL$(OCTAL(500*54/160))&"T"
2660 CALL Timer(Tsnuz)
2670 EXIT GRAPHICS
2680 SUBEXIT
2690 ! *****
2700 Hc:            ! TRIGGERS HARDCOPY
2710 ! *****
2720 Hc=1
2730 RETURN
2740 ! *****
2750 Trig:          ! TRIGGERS NEW SCAN
2760 ! *****
2770 Trig=1
2780 Dum=FNTrip(0)
2790 RETURN
2800 ! *****
2810 Anavac:        ! Scans thru anavac range & reads values
2820 ! *****
2830 Trig=0
2840 OUTPUT 722;"F1R3M3A1HOT2T3"
2850 Sc=500/160
2860 FIXED 0
2870 FOR I=1 TO Na
2880 IF Trig=1 THEN Anavac
2890 DISP I
2900 Lev=OCTAL(I*Sc)
2910 OUTPUT 723;"HKO"&VAL$(Lev)&"T"
2920 Dum=FNTrip(1)
2930 IF Dum=3 THEN GOTO Breach
2940 OUTPUT 709;"45E"
2950 OUTPUT 722;"F1R3M3A1HOT2T3"
2960 OUTPUT 722;"T3"
2970 ENTER 722;Pp(I)
2980 Pp(I)=Pp(I)*Range
```

```
2990 NEXT I
3000 FIXED 0
3010 OUTPUT 723;"HKO"&VAL$(OCTAL(500*54/160))&"T"
3020 OUTPUT 709;"C"
3030 FOR I=1 TO 10
3040 Mass(I)=0
3050 Maxpp(I)=-10
3060 NEXT I
3070 L1=0
3080 L2=0
3090 FOR I=1 TO Na
3100 IF L1>=L2 THEN GOTO Nopk
3110 IF Pp(I)>=L2 THEN GOTO Nopk
3120 Maxpp(11)=L2
3130 Mass(11)=I-1
3140 FOR J=10 TO 1 STEP -1
3150 IF Maxpp(J+1)<Maxpp(J) THEN GOTO Nomove
3160 Tempm=Mass(J)
3170 Tempm=Maxpp(J)
3180 Mass(J)=Mass(J+1)
3190 Maxpp(J)=Maxpp(J+1)
3200 Mass(J+1)=Tempm
3210 Maxpp(J+1)=Tempm
3220 Nomove: NEXT J
3230 Nopk: L1=L2
3240 L2=Pp(I)
3250 NEXT I
3260 Dum=FNTRIP(0)
3270 Mp=0
3280 Rc=0
3290 FOR I=1 TO 10
3300 IF Maxpp(I)>Mp THEN Mp=Maxpp(I)
3310 NEXT I
3320 IF Mp>10*Range THEN Rc=-1
3330 IF Mp<.9*Range THEN Rc=1
3340 RETURN
3350 Breach: Dum=FNTRIP(0)
3360 RETURN
3370 ! *****
3380 Aplot: ! BAKEPL: PLOTS BAKEOUT DATA--7/24/86
3390 ! *****
3400 FIXED 0
3410 PRINTER IS 16
3420 PRINT PAGE
3430 Ppmin=100
3440 FOR K=1 TO Na
3450 IF Pp(K)>.001 THEN Pp(K)=1.0E-12
3460 IF Pp(K)<Ppmin THEN Ppmin=Pp(K)
3470 NEXT K
```

```
3480 IF Ppmin>0 THEN 3520
3490 FOR K=1 TO Na
3500 Pp(K)=Pp(K)-Ppmin+1.0E-12
3510 NEXT K
3520 Zmax=0
3530 FOR I=1 TO Na
3540 Z(I)=Pp(I)
3550 IF Z(I)>Zmax THEN Zmax=Z(I)
3560 X(I)=I/2
3570 NEXT I
3580 FOR I=1 TO 10
3590 Ztest=10-I)
3600 IF Zmax>Ztest THEN 3620
3610 NEXT I
3620 Itest=I
3630 Ztesti=1/Ztest
3640 Zmax=INT(Zmax*Ztesti)+1
3650 FOR I=1 TO Na
3660 Z(I)=Z(I)*Ztesti
3670 NEXT I
3680 FIXED 0
3690 Xmax=Na/2
3700 Istart=1
3710 Istop=Na
3720 K=1
3730 ! *****
3740 GOSUB 3790 ! READ Y(*)
3750 GOSUB 3900 ! PLOT DATA
3760 ! *****
3770 RETURN
3780 !
3790 ! SR TO TRANSFORM # TO LABEL ***** END
3800 P$="RGA Spectrum"
3810 Q$="Specie Mass (AMU)"
3820 MAT Y=Z
3830 Units$="10(-"&VAL$(Itest)&") Torr"
3840 Ymax=Zmax
3850 X1=1 ! X-TICK SPACING
3860 X2=10 ! # MINOR TICKS PER MAJOR TICK
3870 Y1=.1 ! Y-TICK SPACING
3880 Y2=10 ! # MINOR TICKS PER MAJOR TICK
3890 RETURN
3900 ! SR TO PLOT DATA *****
3910 GCLEAR
3920 Plot: !
3930 Set_up: !
3940 PLOTTER IS 13,"GRAPHICS" ! MAKES THE CRT THE PLOTTER
3950 GRAPHICS ! ENABLES CRT
3960 LIMIT 0,180,0,145 ! mm UNITS FOR HARD CLIP AREA
```

```
3970 LOCATE 30,120,30,95
3980 CLIP 30,120,30,95 ! SOFT CLIP AREA
3990 FRAME ! BOX SOFT CLIP AREA
4000 CSIZE 4
4010 SCALE 0,Xmax,0,Ymax ! DEFINES 'USER DEFINED UNITS
4020 Start_plot: !
4030 AXES X1,Y1,0,0,X2,Y2,2 ! TICKS, AXES INTERCEPTS, TICKS, TICK SIZE
4040 LINE TYPE 1 ! SOLID LINE
4050 PLOT X(Istart),Y(Istart),-2
4060 FOR L=Istart+1 TO Istop
4070 PLOT X(L),Y(L),-1
4080 NEXT L
4090 UNCLIP
4100 CSIZE 4
4110 Ystp=Y1*Y2
4120 Xstp=X1*X2
4130 IF K>1 THEN Xstp=2*Xstp
4140 Ym15=Ymax/15
4150 Xm200=Xmax/200
4160 FIXED 0
4170 LORG 4
4180 FOR X_label=0 TO Xmax STEP Xstp
4190 MOVE X_label,-Ym15
4200 LABEL X_label
4210 NEXT X_label
4220 LORG 8
4230 FOR Y_label=0 TO Ymax STEP Ystp
4240 MOVE -Xm200,Y_label
4250 Y_lab=Y_label
4260 IF K=2 THEN Y_lab=-Ymax-Ymin+Y_label
4270 LABEL Y_lab
4280 NEXT Y_label
4290 SETGU
4300 CSIZE 6
4310 LORG 4
4320 MOVE 75,18
4330 LABEL Q$
4340 MOVE 75,10
4350 CSIZE 4
4360 CSIZE 6
4370 DEG
4380 LDIR 90
4390 LORG 4
4400 MOVE 14,65
4410 LABEL P$
4420 CSIZE 4
4430 MOVE 18,65
4440 LABEL Units$
4450 RETURN
4460 SUBEND
4470 ! *****
```

```
4480 ! *****
4490 SUB Beep
4500 Beep: ! BEEPS COMPUTER AND RACK
4510 ! *****
4520 OUTPUT 723;"@24T00140T"
4530 WAIT 200
4540 OUTPUT 723;"@00004T"
4550 SUBEXIT
4560 SUBEND
4570 ! *****
```

```
4580 ! *****
4590 DEF FNC821$(Sd$) ! TALKS TO 821 CONTROLLER
4600 Fnc821: !
4610 ! *****
4620 DIM Send$[25],A$[10]
4630 Input$=""
4640 Send$=Sd$
4650 Error=0
4660 IF LEN(Send$)<=2 THEN 4740
4670 R1=1
4680 Send$=Send$&CHR$(3)
4690 FOR J=1 TO LEN(Send$)
4700 A=BINEOR(A,NUM(Send$[J;1])) !A EXOR NUM(Send$[J;1])
4710 NEXT J
4720 Send$=CHR$(4)&"0000"&CHR$(2)&Send$&CHR$(A)
4730 GOTO 4760
4740 R1=10
4750 Send$=CHR$(4)&"0000"&Send$&CHR$(5)
4760 ON ERROR GOTO 4830
4770 A$=""
4780 STANDARD
4790 OUTPUT 10;Send$
4800 Receive: ENTER 10 USING "#, "&VAL$(R1)&"A";TRL(4),A$
4810 OFF ERROR
4820 GOTO 4940
4830 IF ERRN=167 THEN 4940
4840 IF ERRN<>163 THEN 5230
4850 IF Error>12 THEN 5230
4860 Error=Error+1
4870 BEEP
4880 DISP CHR$(129);"RETRY #";Error;CHR$(128)
4890 RESET 10
4900 WAIT WRITE 10,5;1
4910 WRITE BIN 10;64,64+32+16+8+2,32+16+4+2+1
4920 WAIT WRITE 10,5;0
4930 GOTO 4760
4940 Input$=A$
4950 IF NOT POS(Input$,CHR$(3)) THEN 4980
4960 P=POS(Input$,CHR$(3))
4970 RETURN Input$[2,P-1]
4980 IF NOT POS(Input$,CHR$(21)) THEN 5080
4990 P=POS(Input$,CHR$(21))
5000 BEEP
5010 WAIT 200
5020 BEEP
5030 CALL Rltime
5040 PRINTER IS 0
5050 PRINT "NAK -- "&Sd$
5060 PRINTER IS 16
```

```
5070 RETURN "NAK -- "&Sd$
5080 IF NOT POS(Input$,CHR$(6)) THEN 5120
5090 P=POS(Input$,CHR$(6))
5100 BEEP
5110 RETURN "ACK -- "&Sd$
5120 IF NOT POS(Input$,CHR$(4)) THEN 5210
5130 P=POS(Input$,CHR$(4))
5140 IF Error<12 THEN 4860
5150 CALL Rltime
5160 PRINTER IS 0
5170 PRINT "821 DOESN'T RECOGNIZE '&Input$[2,3]&' "
5180 PRINTER IS 16
5190 RETURN "BAD COMMAND '&Input$[2,3]&' "
5200 IF Error<12 THEN 4860
5210 RETURN "HUH??"
5220 PRINT #0;"UNRESOLVED ERROR IN TALKING TO 821:"
5230 PRINT #0;ERRMS
5240 RETURN "ER"&VAL$(ERRN)
5250 FNEND
5260 ! *****
```

```
5270  ! *****
5280 SUB Cs
5290 Cs:          ! CHECKS AND INCREMENTS CURRENT SEGMENT
5300  ! *****
5310 COM SHORT Tsnuz
5320 CALL Timer(999)
5330 Cs$=FNC821$("CS")
5340 Sp$=FNC821$("SP")
5350 PRINT Cs$,Sp$
5360 PRINTER IS 16
5370 INPUT "Increment CS? (Y/N)",G$
5380 IF G$<>"Y" THEN Exitcs
5390 CALL Rltime
5400 FIXED 0
5410 Dum$=FNC821$("CS"&VAL$(VAL(Cs$[4,7])+1))
5420 PRINTER IS 0
5430 PRINT "CS MANUALLY INCREMENTED"
5440 PRINTER IS 16
5450 Exitcs:      ! GOOD EXIT
5460 CALL Timer(Tsnuz)
5470 SUBEXIT
5480 SUBEND
5490  ! *****
```

```
5500 ! *****
5510 SUB Csnew(Co$,Cs$)
5520 Csnew:           ! INFORMS OF CHANGE IN CS
5530 ! *****
5540 IF Co$<>" THEN 5570
5550 Co$=Cs$
5560 SUBEXIT
5570 CALL Rltime
5580 PRINTER IS 0
5590 PRINT "CS CHANGED, WAS ";Co$;" NOW ";Cs$
5600 PRINTER IS 16
5610 Co$=Cs$
5620 SUBEXIT
5630 SUBEND
5640 ! *****
```

```
5650 ! *****
5660 SUB Dcr(SHORT V)
5670 Dcr: ! OUTPUTS CONTROL SIGNAL TO Dcr
5680 ! *****
5690 Vfmt: IMAGE #,2A,3Z,A
5700 IF V=999 THEN Oc
5710 IF V>7 THEN V=7
5720 IF V<0 THEN V=0
5730 Vi=OCTAL(V*511/7)
5740 OUTPUT 723;"H0500T" !CLOSES BIG RELAY
5750 OUTPUT 723 USING Vfmt;"H2",Vi,"T"
5760 SUBEXIT
5770 Oc: ! OPEN CIRCUIT
5780 OUTPUT 723;"H2000T"
5790 OUTPUT 723;"H0000T" !OPENS HONKER
5800 SUBEXIT
5810 SUBEND
5820 ! *****
```

```
5830 ! *****
5840 SUB Ddump(A)
5850 Ddump:      ! DUMPS DISK
5860 ! *****
5870 DISP "DISK DUMP"
5880 BEEP
5890 OPTION BASE 1
5900 COM SHORT Tsnuz,Ntc,Nhtc,Tc,Tb,Btc(*),Mtc(*),Rlypo(*),Trecord,Vrecord
5910 CALL Timer(999)
5920 Hd$=":A7,0,1"
5930 Tn$="TLMTEC"&Hd$
5940 Vn$="VLMTEC"&Hd$
5950 Aa=A
5960 IF A<>0 THEN 6130
5970 Menu:      ! DISC MENU
5980 IF Aa<>0 THEN Exdd
5990 ON ERROR GOTO Derror
6000 PRINT PAGE
6010 PRINT LIN(3)
6020 PRINT Tn$;" Current record is ";Trecord
6030 PRINT Vn$;" Current record is ";Vrecord
6040 PRINT LIN(3);"1. INITIALIZE FLOPPY 0"
6050 PRINT "2. INITIALIZE FLOPPY 1"
6060 PRINT "3. CATALOG SAVED DATA FILES"
6070 PRINT "4. SAVE DATA TO HARD DISK"
6080 PRINT "6. TRANSFER SAVED FILE TO TAPE CARTRIDGE :T14"
6090 PRINT "7. TRANSFER SAVED FILE TO FLOPPY CARTRIDGE"
6100 PRINT "8. EXIT DATA DUMP ROUTINE"
6110 A=0
6120 INPUT "ENTER MENU SELECTION",A
6130 IF (A>0) AND (A<9) THEN ON A GOTO IO,IO,Cat,Shh,Sf,Sht,Shf,Exdd
6140 BEEP
6150 GOTO 6120
6160 IO:      ! INITIALIZE
6170 ON ERROR GOTO Ierr
6180 Dev$=":A7,3,"&VAL$(A-1)
6190 PRINT LIN(3);"PURGING ";Dev$
6200 PURGE ALL Dev$
6210 GOTO Menu
6220 Ierr:    ! ERROR MEANS COULDN'T PURGE
6230 PRINT LIN(3);"INITIALIZING ";Dev$
6240 INITIALIZE Dev$
6250 GOTO Menu
6260 Cat:    ! CATALOGS FILES
6270 PRINT LIN(1),"TEMPERATURE DATA FILES:"
6280 CAT "T:A7,0,1"
6290 PRINT LIN(1),"IV DATA FILES:"
6300 CAT "V:A7,0,1"
6310 PRINT LIN(1),"FLOPPY FILES:"
```

```
6320 ON ERROR GOTO Cerr
6330 CAT "A7,3,0"
6340 CAT "A7,3,1"
6350 PRINT "HIT <cont>"
6360 PAUSE
6370 GOTO Menu
6380 Cerr: ! ERROR MEANS NO FLOPPY OR UNINITIALIZED
6390 GOTO Menu
6400 Shh: ! SAVE DATA FILES TO HARD DISK
6410 CALL Time(Time$)
6420 Ft$="T"&Time$[4,5]&Time$[9,10]
6430 Fv$="V"&Time$[4,5]&Time$[9,10]
6440 PRINT "SAVING FILES"
6450 RENAME Tn$ TO Ft$
6460 RENAME Vn$ TO Fv$
6470 Trecord=0
6480 Vrecord=0
6490 PRINT "CREATING ";Tn$
6500 CREATE Tn$,40,200
6510 PRINT "CREATING ";Vn$
6520 CREATE Vn$,150,444
6530 CALL Rltime
6540 PRINTER IS 0
6550 PRINT "DATA SAVED TO ";Ft$;" & ";Fv$;" :ON A7,0,1"
6560 PRINTER IS 16
6570 GOTO Menu
6580 Sf: ! COPIES FILES TO A FLOPPY
6590 CALL Time(Time$)
6600 Ft$="T"&Time$[4,5]&Time$[9,10]
6610 Fv$="V"&Time$[4,5]&Time$[9,10]
6620 PRINT "SAVING FILES"
6630 BACKUP Tn$ TO Ft$&" :A7,3,0"
6640 BACKUP Vn$ TO Fv$&" :A7,3,0"
6650 RENAME Tn$ TO Ft$
6660 RENAME Vn$ TO Fv$
6670 Trecord=0
6680 Vrecord=0
6690 PRINT "CREATING ";Tn$
6700 CREATE Tn$,450,200
6710 PRINT "CREATING ";Vn$
6720 CREATE Vn$,150,444
6730 GOTO Menu
6740 Shf: ! COPIES SAVED FILE TO FLOPPY
6750 CAT "T"&Hd$
6760 CAT "V"&Hd$
6770 G$=""
6780 INPUT "ENTER FILE NAME 'NONE' IF NONE",G$
6790 IF G$="" THEN 6780
6800 IF G$="NONE" THEN Menu
```

```
6810  BACKUP G$[1,6]&Hd$ TO G$[1,6]&":A7,3,0"  
6820  GOTO Menu  
6830  Sht:    ! COPIES SAVED FILE TO TAPE  
6840  CAT "T"&Hd$  
6850  CAT "V"&Hd$  
6860  G$=""  
6870  INPUT "ENTER FILE NAME 'NONE' IF NONE",G$  
6880  IF G$="" THEN 6870  
6890  IF G$="NONE" THEN Menu  
6900  COPY G$[1,6]&Hd$ TO G$[1,6]&":T14"  
6910  GOTO Menu  
6920  Exdd:  ! EXIT ROUTINE  
6930  CALL Timer(Tsnuz)  
6940  PRINT PAGE  
6950  OFF ERROR  
6960  SUBEXIT  
6970  Derror:    ! ERROR TRAPPING  
6980  BEEP  
6990  PRINT LIN(3), "ERROR DURING DATA TRANSFER"  
7000  PRINT "CORRECT PROBLEM AND TRY AGAIN!"  
7010  PRINT "HIT <CONT> TO RETURN TO MENU"  
7020  PRINT LIN(3),ERRM$  
7030  PAUSE  
7040  GOTO Menu  
7050  SUBEND  
7060  ! *****
```

```
7070 ! *****
7080 SUB Draw(Mto,Mvo,Fb)
7090 Draw: ! TEMPS ONSCREEN
7100 ! *****
7110 DISP "DRAW"
7120 OPTION BASE 1
7130 COM SHORT Tsnuz,Ntc,Nhtc,Tc,Tb,Btc(*),Mtc(*),Rlypo(*),Trecord,Vrecord
7140 COM Atc$(*),Ltc$(*),Lrly$(*),Relay$(*),Lvolt$(*
7150 COM SHORT Volt(*),St,Piv,Ivs,Hpower
7160 COM Iiv,Itemp
7170 E$=CHR$(27)
7180 H$=CHR$(228)
7190 V$=CHR$(231)
7200 CALL Time(Time$)
7210 PRINT USING "#,K";E$&"&a1rOC" !CURSOR TO TOP
7220 IMAGE 9X,DDD,X,A,40X,"|",3X,8A,2X,8A
7230 PRINT USING 7220;Btc(10),V$,Time$[1,8],Time$[9,16]
7240 Pa=Volt(5)*(-1)Fb+1)
7250 IMAGE 9X,DDD,X,A,40X,"| PUMP= ",DDD.D," AMPS"
7260 PRINT USING 7250;Btc(35),V$,Pa
7270 IMAGE 9X,DDD,X,A,X,DDD,9X,DDD,X,A,8X,A,X,DDD,9X,"| LOAD= ",DDD.D," AMPS"
7280 PRINT USING 7270;Btc(8),V$,Btc(9),Btc(22),CHR$(227),CHR$(227),
Btc(23),Volt(4)
7290 IMAGE 2X,DDD,5X,7A,14X,A,8X,A,13X,"| FEEDTHRU= ",DD.DDDD," VOLTS"
7300 PRINT USING 7290;Btc(32),CHR$(226)&RPT$(H$,2)&CHR$(251)&RPT$(H$,2)&
CHR$(229),V$,V$,Volt(3)
7310 IMAGE 2X,9A,4X,DDD,13X,A,8X,A,13X,"| TOP= ",DD.DDDD," VOLTS"
7320 PRINT USING 7310;CHR$(240)&RPT$(CHR$(236),7)&CHR$(246),
Btc(16),V$,V$,Volt(2)
7330 IMAGE 10X,A,,2X,DDD,A,14X,A,8X,A,13X,"| MID= ",DD.DDDD," VOLTS"
7340 PRINT USING 7330;V$,Btc(12),V$,V$,V$,Volt(1)
7340 PRINT USING 7330;V$,Btc(12),V$,V$,V$,Volt(1)
7350 IMAGE 2X,9A,DDD,X,DDD,2X,DDD,6X,12A,X,DDD,9X,"| STANDPIPE= ",
DD.DD," INCHES"
7350 IMAGE 2X,9A,DDD,X,DDD,2X,DDD,6X,12A,X,DDD,9X,"| STANDPIPE= ",
DD.DD," INCHES"
7370 IMAGE 2X,DDD,5X,A,2X,DDD,14A,X,A,8X,A,13X,"| HEATER= ",DDD.D," WATTS"
7380 PRINT USING 7370;Btc(33),V$,Btc(15),CHR$(225)&RPT$(H$,12)&
CHR$(253),V$,V$,Hpower
7390 IMAGE 10X,A,4X,DDD,2X,DDD,8X,A,8X,A,X,DDD,9X,"| POWER OUT= ",
DDD.D," WATTS"
7391 Po=Volt(4)*Volt(1)
7400 PRINT USING 7390;V$,Btc(13),Btc(21),V$,V$,Btc(19),Po
7410 IMAGE 10X,22A,8X,A,13X,"|"
7420 PRINT USING 7410;CHR$(250)&H$&CHR$(227)&H$&CHR$(227)&H$&CHR$(251)&
RPT$(H$,14)&CHR$(253),V$
7430 IMAGE 9X,DDD,A,X,A,DDD,21X,3A,12X,"| VRECORD= ",DDD
7440 PRINT USING 7430;Btc(6),V$,V$,Btc(7),CHR$(226)&CHR$(251)&CHR$(229),Vrecord
7450 IMAGE 12X,DDD,24X,A,X,A,12X,"| TRECORDER= ",DDD
```

```
7460 PRINT USING 7450;Btc(3),V$,V$,Trecord
7470 IMAGE 12X,DDD,24X,A,X,A,12X,"|"
7480 IF Mto<>999 THEN 7540
7490 IMAGE 9X,DDD,A,X,A,DDD,18X,DDD,A,X,A,12X,"| SHUTDOWN "
7500 PRINT USING 7490;Btc(1),V$,V$,Btc(2),Btc(24),V$,V$
7510 IMAGE 12X,A,X,A,24X,3A,2X,"|",X,DDD,5X,"|"
7520 PRINT USING 7510;V$,V$,CHR$(250)&CHR$(227)&CHR$(253),Btc(27)
7530 GOTO 7610
7540 Mn=VAL(Time$[12,13])+VAL(Time$[9,10])*60+VAL(Time$[4,5])*24+60+
VAL(Time$[1,2])*31+24*60-St
7550 Nt=Itemp-Mn+Mto
7560 Nv=Iiv-Mn+Mvo
7570 IMAGE 9X,DDD,A,X,A,DDD,18X,DDD,A,X,A,12X,"|"
7580 PRINT USING 7570;Btc(1),V$,V$,Btc(2),Btc(24),V$,V$
7590 IMAGE 12X,A,X,A,24X,3A,2X,"|",DDD,6X,"| NEXT V IN ",DDD," MINUTES"
7600 PRINT USING 7590;V$,V$,CHR$(250)&CHR$(227)&CHR$(253),Btc(27),Nv
7610 IMAGE 9X,DDD,A,X,A,DDD,22X,A,3X,"|",9X,"| NEXT T IN ",DDD," MINUTES"
7620 PRINT USING 7610;Btc(4),V$,V$,Btc(5),V$,Nt
7630 IMAGE 12X,3A,8X,DDD,14X,A,3X,"|",9X,"|"
7640 PRINT USING 7630;CHR$(250)&CHR$(227)&CHR$(253),Btc(18),CHR$(255)
7650 IMAGE 10X,DDD,A,8X,5A,3X,DDD,7X,A,3X,"|",9X,"|"
7660 PRINT USING 7650;Btc(28),V$,CHR$(234)&RPT$(CHR$(236),3)&CHR$(237),
Btc(31),CHR$(255)
7670 IMAGE 13X,A,DDD,5X,A,X,A,X,A,2X,6A,2X,DDD,A,3X,"|",9X,"|"
7680 PRINT USING 7670;V$,Btc(34),"|",CHR$(224),"|",CHR$(234)&RPT$(CHR$(236),4)&
CHR$(237),Btc(25),CHR$(255)
7690 IMAGE 13X,A,8X,5A,X,8A,4X,A,3X,"|",DDD,6X,"|"
7700 PRINT USING 7690;V$,CHR$(242)&CHR$(236)&CHR$(235)&CHR$(236)&CHR$(245),
CHR$(226)&CHR$(249)&RPT$(H$,4)&CHR$(249)&CHR$(229),V$,Btc(26)
7710 IMAGE #,10X,DDD,16A,X,DDD,2X,10A,9X,"|"
7720 PRINT USING 7710;Btc(29),CHR$(250)&RPT$(H$,10)&CHR$(249)&RPT$(H$,3)&
CHR$(253),Btc(30),CHR$(250)&RPT$(H$,4)&CHR$(251)&RPT$(CHR$(236),3)&CHR$(245)
7730 STANDARD
7740 SUBEXIT
7750 SUBEND
7760 ! *****
```

```
7770 ! *****
7780 SUB Dump(Mto,Mvo,Fb)
7790 Dump:          ! DUMPS SCREEN TO PRINTER FOR TEMPS
7800 ! *****
7810 COM SHORT Tsnuz,Ntc,Nhtc,Tc,Tb,Btc(*),Mtc(*),Rlypo(*),Trecord,Vrecord
7820 COM Atc$(*),Ltc$(*),Lrly$(*),Relay$(*),Lvolt$(*)
7830 DISP "DUMP TO PRINTER"
7840 PRINTER IS 0
7850 PRINT LIN(5)
7860 CALL Draw(Mto,Mvo,Fb)
7870 PRINT LIN(3)
7880 Cr=0
7890 FOR I=1 TO Ntc-3 STEP 4
7900 PRINT Ltc$(I),Ltc$(I+1),Ltc$(I+2),Ltc$(I+3)
7910 PRINT Btc(I),Btc(I+1),Btc(I+2),Btc(I+3)
7920 NEXT I
7930 FOR J=I TO Ntc
7940 PRINT Ltc$(J)
7950 PRINT Btc(J)
7960 NEXT J
7970 PRINT PAGE
7980 PRINTER IS 16
7990 SUBEXIT
8000 SUBEND
8010 ! *****
```

```
8020 ! *****
8030 SUB Ivdata
8040 Ivdata:      ! DOES IV CURVE & STORES IT
8050 ! *****
8060 DISP "IV CURVE DATA TAKING"
8070 OPTION BASE 1
8080 COM SHORT Tsnuz,Ntc,Nhtc,Tc,Tb,Btc(*),Mtc(*),Rlypo(*),Trecord,Vrecord
8090 COM Atc$(*),Ltc$(*),Lrly$(*),Relay$(*),Lvolt$(*
8100 COM SHORT Volt(*),St,Piv,Ivs,Hpower
8110 CALL Timer(MAX(Ivs*2,Tsnuz))
8120 SHORT V
8130 CHECK READ
8140 Mv=2 !MAXIMUM VOLTAGE IN CURVE
8150 CALL Tcrd
8160 CALL Time(Time$)
8170 ON ERROR GOTO Verror
8180 ASSIGN #1 TO "VLMTEC:A7,0,1"
8190 Vrecord=Vrecord+1
8200 PRINT #1,Vrecord;Vrecord,Time$,Btc(Tb),Btc(Tc),Hpower,Ivs,Piv
8201 Neg=0
8210 FOR I=0 TO 24
8211 MAT Volt=(0)
8220 V=(I-1)*Mv/23
8230 IF V<0 THEN V=999
8235 ! IF Neg=1 THEN 8270
8240 CALL Dcr(V)
8250 WAIT Ivs/25*1000
8260 CALL Voltrd
8261 IF Volt(1)>=0 THEN 8270
8262 Neg=1
8263 ! CALL Dcr(Piv)
8270 PRINT #1;Volt(1),Volt(2),Volt(3),Volt(4)
8280 NEXT I
8290 CALL Dcr(Piv)
8300 ASSIGN #1 TO *
8310 OFF ERROR
8320 IF Vrecord=150 THEN CALL Ddump(4)
8330 SUBEXIT
8340 Verror:      ! TRAPS VOLT STORAGE ERRORS
8350 PRINTER IS 0
8360 PRINT "IV CURVE STORAGE ERROR, TIME IS: "&Time$
8370 PRINT ERRMS$
8380 PRINT LIN(2);"DATA NOT STORED"
8390 PRINT LIN(5)
8400 CALL Dcr(Piv)
8410 PRINTER IS 16
8420 Vrecord=Vrecord-1
8430 ASSIGN #1 TO *
8440 SUBEXIT
8450 SUBEND
8460 ! *****
```

```
8470 ! *****
8480 SUB Ivp
8490 Ivp: ! SET IV PARAMETERS
8500 ! *****
8510 OPTION BASE 1
8520 COM SHORT Tsnuz,Ntc,Nhtc,Tc,Tb,Btc(*),Mtc(*),Rlypo(*),Trecord,Vrecord
8530 COM Atc$(*),Ltc$(*),Lrly$(*),Relay$(*),Lvolt$(*
8540 COM SHORT Volt(*),St,Piv,Ivs,Hpower
8550 COM Iiv,Itemp
8560 SHORT Ttc,Tth,Hp,Vr
8570 DIM V(4,25)
8580 CALL Timer(999)
8590 PRINT PAGE
8600 PRINT LIN(3);"IV CURVE DURATION: ";Ivs;" SECONDS"
8610 PRINT LIN(1);"HOLD VOLTAGE: ";Piv;" VOLTS (999 IS OPEN CIRCUIT)"
8620 PRINT LIN(1);"IV CURVE INTERVAL: ";Iiv;" MINUTES"
8630 PRINT LIN(1);"TEMPERATURE DATA INTERVAL: ";Itemp;" MINUTES"
8640 PRINT TAB(20);"1. CHANGE DURATION"
8650 PRINT TAB(20);"2. CHANGE VOLTAGE"
8660 PRINT TAB(20);"3. CHANGE IV CURVE INTERVAL"
8670 PRINT TAB(20);"4. CHANGE TEMPERATURE DATA INTERVAL"
8680 PRINT TAB(20);"5. DISPLAY LAST IV CURVE"
8690 PRINT TAB(20);"6. EXIT"
8700 INPUT "ENTER MENU CHOICE",A
8710 IF (A>0) AND (A<7) THEN 8740
8720 BEEP
8730 GOTO 8700
8740 ON A GOTO D,V,Vi,Ti,P,E
8750 D: ! DURATION
8760 INPUT "ENTER DURATION IN SECONDS: ",Ivs
8770 GOTO Ivp
8780 V: ! HOLD VOLTAGE
8790 INPUT "ENTER HOLD VOLTAGE, OR 999 FOR OPEN CIRCUIT",A
8800 IF A>=0 THEN 8830
8810 BEEP
8820 GOTO V
8830 IF A<>999 THEN 8870
8840 CALL Dcr(999)
8850 Piv=999
8860 GOTO Ivp
8870 IF A<=7 THEN 8900
8880 BEEP
8890 GOTO V
8900 Piv=A
8910 CALL Dcr(Piv)
8920 GOTO Ivp
8930 Vi: ! CHANGE IV INTERVAL
8940 INPUT "ENTER IV CURVE INTERVAL IN MINUTES",Iiv
8950 GOTO Ivp
```

```
8960 Ti:      ! CHANGE TEMPERATURE INTERVAL
8970 INPUT "ENTER TEMPERATURE DATA INTERVAL IN MINUTES",Itemp
8980 GOTO Ivp
8990 P:      ! DISPLAY LAST IV CURVE ON FILE
9000 IF Vrecord>0 THEN 9050
9010 BEEP
9020 PRINT "NO IV CURVES ON FILE!"
9030 WAIT 2000
9040 GOTO Ivp
9050 R=Vrecord
9060 PRINT "CURRENT RECORD IS ";R;", ENTER RECORD # TO USE OR <cont>:"
9070 INPUT R
9080 G$=""
9090 INPUT "ENTER 'H' FOR HARDCOPY, ELSE <cont>",G$
9100 ASSIGN #1 TO "VLMTEC:A7,0,1"
9110 READ #1,R;Vr,Time$,Tth,Ttc,Hp,Ivss,Pivv
9120 FOR I=1 TO 25
9130 FOR J=1 TO 4
9140 READ #1;V(J,I)
9150 NEXT J
9160 NEXT I
9170 ASSIGN #1 TO *
9180 PLOTTER IS 13,"GRAPHICS"
9190 GRAPHICS
9200 GCLEAR
9210 LIMIT 0,180,0,145
9220 LOCATE 30,120,30,95
9230 CLIP 30,120,30,95
9240 FRAME
9250 CSIZE 4
9260 SCALE 0,100,-1,1
9270 AXES 10,.05,0,0,10,5
9280 LINE TYPE 1 !SOLID
9290 PLOT V(4,1),V(3,1),-2
9300 FOR I=2 TO 25
9310 PLOT V(4,I),V(3,I),-1
9320 NEXT I
9330 LINE TYPE 4
9340 PLOT V(4,1),V(2,1),-2
9350 FOR I=2 TO 25
9360 PLOT V(4,I),V(2,I),-1
9370 NEXT I
9380 LINE TYPE 7
9390 PLOT V(4,1),V(1,1),-2
9400 FOR I=2 TO 25
9410 PLOT V(4,I),V(1,I),-1
9420 NEXT I
9430 LINE TYPE 1
9440 UNCLIP
```

```
9450 FIXED 0
9460 LORG 4
9470 FOR Xj=0 TO 300 STEP 100
9480 MOVE Xj,-.08
9490 LABEL Xj
9500 NEXT Xj
9510 LORG 8
9520 FIXED 2
9530 FOR Yj=0 TO 1.25 STEP .25
9540 MOVE -2,Yj
9550 LABEL Yj
9560 NEXT Yj
9570 SETGU
9580 CSIZE 6
9590 LORG 4
9600 MOVE 75,18
9610 LABEL "CURRENT (AMPS)"
9620 MOVE 75,10
9630 CSIZE 4
9640 LABEL "Time= ";Time$
9650 CSIZE 6
9660 DEG
9670 LDIR 90
9680 LORG 4
9690 MOVE 14,65
9700 LABEL "VOLTAGE"
9710 IF G$<>"H" THEN 9750
9720 DUMP GRAPHICS
9721 PRINTER IS 0
9730 PRINT CHR$(12)
9731 PRINTER IS 16
9740 GOTO 9760
9750 PAUSE
9760 EXIT GRAPHICS
9761 PRINTER IS 0
9762 FOR I=1 TO 25
9763 PRINT V(1,I),V(2,I),V(3,I),V(4,I)
9764 NEXT I
9765 PRINTER IS 16
9770 GOTO Ivp
9780 ! *****
9790 E: ! EXIT
9800 EXIT GRAPHICS
9810 STANDARD
9820 PRINT PAGE
9830 CALL Timer(Tsnuz)
9840 SUBEXIT
9850 SUBEND
9860 ! *****
```

```
9870 ! *****
9880 SUB M821
9890 M821:           ! MANUAL 821 MESSAGES
9900 ! *****
9910 OPTION BASE 1
9920 COM SHORT Tsnuz
9930 CALL Timer(999)
9940 Mm$=""
9950 INPUT "ENTER MESSAGE FOR 821, BLANK FOR RETURN",Mm$
9960 IF Mm$="" THEN Exitm821
9970 Mr$=FNC821$(Mm$)
9980 PRINTER IS 16
9990 PRINT Mr$
10000 GOTO M821
10010 Exitm821:     ! GOOD EXIT
10020 CALL Timer(Tsnuz)
10030 SUBEXIT
10040 SUBEND
10050 ! *****
```

```
10060 ! *****
10070 SUB Nmtc
10080 Nmtc:      ! ALLOWS INPUT OF NEW MAXIMUM Tc TEMPERATURES
10090 ! *****
10100 COM SHORT Tsnuz,Ntc,Nhtc,Tc,Tb,Btc(*),Mtc(*),Rlypo(*),Trecord,Vrecord
10110 COM Atc$(*),Ltc$(*)
10120 CALL Timer(999)
10130 PRINT "CHANGE TC TRIPOUT LEVELS (NOT PERMANANT)"
10140 FOR I=1 TO Ntc
10150 PRINT Ltc$(I);" CONNECTED TO COMPUTER LINE ";Atc$(I);", CURRENTLY: ";Mtc(I)
10160 INPUT "ENTER NEW MAXIMUM OR <cont> FOR UNCHANGED:",Mtc(I)
10170 NEXT I
10180 CALL Timer(Tsnuz)
10190 SUBEXIT
10200 SUBEND
10201 ! *****
```

```
10210 ! *****
10220 DEF FNPress(X)
10230 Press: ! CHECK PRESSURE AND RETURN STATUS OR VALUE
10240 ! *****
10250 OUTPUT 722;"F1R7M3A1HOT2T3"
10260 OUTPUT 709;"49E"
10270 OUTPUT 722;"T3"
10280 ENTER 722;Pir
10290 OUTPUT 709;"47E"
10300 OUTPUT 722;"T3"
10310 ENTER 722;Penh
10320 OUTPUT 709;"48E"
10330 OUTPUT 722;"T3"
10340 ENTER 722;Penl
10350 OUTPUT 709;"C"
10360 IF Pir>.5 THEN GOTO Leak
10370 IF Penh>8.0 THEN GOTO Leak
10380 IF X=1 THEN RETURN 0
10390 GOTO Pval
10400 Leak: RETURN -999
10410 Pval: IF X=2 THEN RETURN Penh
10420 IF X=3 THEN RETURN Penl
10430 RETURN 0
10440 FNEND
10450 ! *****
```

```
10460 ! *****
10470 SUB Reverse(Fb)
10480 Reverse:  ! REVERSES EM PUMP
10490 ! *****
10500 IF Fb=1 THEN GOTO 10540
10510 Fb=1
10520 OUTPUT 723;"K6500T"
10530 SUBEXIT
10540 Fb=0
10550 OUTPUT 723;"K6000T"
10560 SUBEXIT
10570 SUBEND
10580 ! *****
```

```
10590 ! *****
10600 SUB Rltime
10610 Rltime:      ! PRINTS CURRENT TIME ON PAPER
10620 ! *****
10630 CALL Time(Time$)
10640 IMAGE "Date ",8A,9X,"Time ",8A,9X
10650 PRINTER IS 0
10660 PRINT USING 10640;Time$[1,8],Time$[9,16]
10670 PRINTER IS 16
10680 SUBEXIT
10690 SUBEND
10700 ! *****
```

```
10710 ! *****
10720 SUB Rlyrd
10730 Rlyrd:          ! Reads and converts RELAYS
10740 ! *****
10750 OPTION BASE 1
10760 COM SHORT Tsnuz,Ntc,Nhtc,Tc,Tb,Btc(*),Mtc(*),Rlypo(*),Trecord,Vrecord
10770 COM Atc$(*),Ltc$(*),Lrly$(*),Relay$(*),Lvolt$(*
10780 OUTPUT 722;"F4R4M3A1HOT2T3"
10790 FOR I=1 TO 4
10800 OUTPUT 709;Relay$(I)
10810 OUTPUT 722;"T3"
10820 ENTER 722;Rlypo(I)
10830 Rlypo(I)=Rlypo(I) DIV 1000
10840 NEXT I
10850 OUTPUT 722;"F1R1M3A1HO"
10860 OUTPUT 709;"C"
10870 R$=FNC821$("SW")
10880 A$=R$[5,5]
10890 Rlypo(5)=0
10900 IF A$="0" THEN 10950
10910 Dum$=FNC821$("SW>0000")
10920 R$=FNC821$("SW")
10930 A$=R$[5,5]
10940 IF A$<>"0" THEN Rlypo(5)=1
10950 SUBEXIT
10960 SUBEND
10970 ! *****
```

```
10980 ! *****
10990 SUB Shutdown(Fb,Isd)
11000 Shutdown: ! EMERGENCY SHUTDOWN ROUTINE
11010 ! *****
11020 DISP "SHUTDOWN"
11030 OPTION BASE 1
11040 COM SHORT Tsnuz,Ntc,Nhtc,Tc,Tb,Btc(*),Mtc(*),Rlypo(*),Trecord,Vrecord
11050 COM Atc$(*),Ltc$(*),Lrly$(*),Relay$(*),Lvolt$(*
11060 COM SHORT Volt(*),St,Piv,Ivs,Hpower
11070 ON KEY #8,2 GOTO 11760
11080 ON KEY #5,2 GOSUB Rev
11090 ON KEY #0,2 GOSUB Ana
11100 ON KEY #9,2 GOTO Resume
11110 ON KEY #1,2 GOSUB Hardtog
11120 Safe=300 !SAFE TEMPERATURE FOR PUMP REVERSAL
11130 Somin=0
11140 Hc=1
11150 CALL Timer(999) !DISABLE ALARM
11160 OUTPUT 723;"K4000T" !TURN OFF MAIN HEAT
11170 CALL Dcr(999) !TURN OFF LOAD SUPPLY
11180 PRINTER IS 0
11190 PRINT "SHUTDOWN IS IN PROGRESS";LIN(3)
11200 CALL Rltime
11210 PRINTER IS 0
11220 IF Isd<100 THEN 11250
11230 PRINT "USER REQUESTED SHUTDOWN"
11240 GOTO 11270
11250 IF Isd<6 THEN PRINT CHR$(129);Lrly$(Isd),"RELAY TRIPPED";CHR$(128)
11260 IF Isd>5 THEN PRINT CHR$(129);"TEMPERATURE HIGH AT ";Ltc$(Isd-6);CHR$(128)
11270 FOR I=1 TO 5
11280 G$="OPEN"
11290 IF Rlypo(I)=0 THEN G$="CLOSED"
11300 PRINT Lrly$(I);" IS ";G$
11310 NEXT I
11320 CALL Tcrd
11330 FOR I=1 TO Ntc
11340 PRINT "TEMPERATURE AT ";Ltc$(I);" = ";Btc(I)
11350 NEXT I
11360 Sw$=FNC821$("SW")
11370 Os$=FNC821$("OS")
11380 Cs$=FNC821$("CS")
11390 Sp$=FNC821$("SP")
11400 PRINT "821 STATUS: ",Sw$,Os$,Cs$,Sp$
11410 Dum$=FNC821$("OS>0000")
11420 Dum$=FNC821$("SLO")
11430 IF Isd>6+Nhtc THEN Coldot
11440 PRINTER IS 16
```

```
11450 ! *****
11460 Moni: ! MONITORS SHUTDOWN PROGRESS
11470 ! *****
11480 CALL Tcrd
11490 Hot=0
11500 CALL Time(Time$)
11510 FOR I=1 TO Nhtc
11520 IF Btc(I)>Safe THEN Hot=1
11530 NEXT I
11540 IF Hot=0 THEN Final
11550 Min=INT(VAL(Time$[12,13])/2)
11560 IF (Min=Somin) OR (Hc=0) THEN 11270
11570 Somin=Min
11580 PRINTER IS 0
11590 CALL Draw(999,999,Fb)
11600 PRINTER IS 16
11610 GOTO Moni
11620 ! *****
11630 Final:      ! FINAL SHUTDOWN
11640 CALL Rltime
11650 PRINTER IS 0
11660 PRINT "FINAL SHUTDOWN"
11670 PRINTER IS 16
11680 Hc=0
11690 OUTPUT 723;"00140TK2000TK4000TK6000T"      !ALL HEAT OFF, PUMP REVERSED
11700 Fb=0
11710 CALL Timer(.1)
11720 BEEP
11730 CALL Beep
11740 WAIT 1000
11750 GOTO 11720
11760 OUTPUT 723;"QTOT"
11770 STOP
11780 ! *****
11790 Coldot:      ! TAKES CARE OF A COLD ZONE OVERTEMP
11800 OUTPUT 723;"00140TK2000T"
11810 CALL Rltime
11811 PRINTER IS 0
11820 PRINT "LOW TEMP TURNED OFF"
11830 PRINTER IS 16
11840 GOTO Moni
11850 ! *****
11860 Rev:      ! REVERSES PUMP
11870 CALL Reverse(Fb)
11880 RETURN
11890 ! *****
11900 Hardtog:      ! TOGGLES HARDCOPY
11910 Hc=(Hc+1) MOD 2
11920 RETURN
```

```
11930 ! *****
11940 Ana: ! ANAVAC
11950 CALL Anavac
11960 CALL Timer(999)
11970 RETURN
11980 Resume: ! RESUMES AFTER A SHUTDOWN
11990 Hc=0
12000 PRINTER IS 16
12010 SUBEXIT
12020 SUBEND
12030 ! *****
```

```
12040 ! *****
12050 SUB Start
12060 Start: ! This program is the STARTUP ROUTINE for the multi programmer
12070 ! *****
12080 OPTION BASE 1
12090 COM SHORT Tsnuz,Ntc,Nhtc,Tc,Tb,Btc(*),Mtc(*),Rlypo(*),Trecord,Vrecord
12100 COM Atc$(*),Ltc$(*),Lrly$(*),Relay$(*),Lvolt$(*
12110 COM SHORT Volt(*),St,Piv,Ivs,Hpower
12120 PRINTER IS 16
12130 PRINT CHR$(12)
12140 DISP "STARTUP"
12150 ! *****Setup RS232 line for 821
12160 RESET 10
12170 WAIT WRITE 10,5;1
12180 WRITE BIN 10;64,64+32+16+8+2,32+16+4+2+1
12190 WAIT WRITE 10,5;0
12200 SET TIMEOUT 10;1000
12210 OUTPUT 723;"@T00140T" ! Disable alarm if actuated
12220 ! *****
12230 Ntc=35      !NUMBER OF ACTIVE THERMOCOUPLES
12240 Nhtc=7     !NUMBER OF HOT ZONE THERMOCOUPLES
12250 Tb=1
12260 Tc=13
12270 ! *****
12280 DATA "29E",900,"BOILER 3"
12290 DATA "27E",900,"BOILER 4"
12300 DATA "23E",900,"BOLIER 5"
12310 DATA "21E",900,"BOILER 1"
12320 DATA "28E",900,"BOLIER 2"
12330 DATA "22E",900,"BOLIER 6"
12340 DATA "30E",900,"BOILER 7"
12350 DATA "24E",850,"FEEDTHRU HOT 1"
12360 DATA "25E",850,"FEEDTHRU HOT 2"
12370 DATA "26E",850,"FEEDTHRU TOP"
12380 DATA "31E",850,"COND RAD SHIELD"
12390 DATA "32E",850,"SUMP SHLD TOP"
12400 DATA "33E",850,"CONDENSER BOT"
12410 DATA "34E",850,"CONDENSER MID"
12420 DATA "35E",850,"SUMP SHLD BOTTOM"
12430 DATA "36E",850,"CONDENSER TOP"
12440 DATA "60E",850,"COND OUTLET"
12450 DATA "61E",450,"GAUGE"
12460 DATA "62E",450,"LOOP TO CAN"
12470 DATA "63E",450,"ELBOW ABOVE CAN"
12480 DATA "64E",850,"VACUUM LINE"
12490 DATA "65E",450,"VACUUM VALVE"
12500 DATA "66E",450,"LOOP VALVE"
12510 DATA "67E",450,"CANISTER"
12520 DATA "68E",450,"FLEX TUBE"
```

```
12530 DATA "69E",500,"STANDPIPE BOT"
12540 DATA "70E",500,"STANDPIPE TOP"
12550 DATA "71E",850,"BOILER INLET"
12560 DATA "72E",450,"INLET ELBOW"
12570 DATA "73E",850,"MAGNET"
12580 DATA "74E",450,"PUMP"
12590 DATA "75E",850,"AIR INLET"
12600 DATA "76E",850,"AIR OUTLET"
12610 DATA "77E",850,"INLET TUBE"
12611 DATA "78E",850,"FEEDTHRU MID"
12620 DATA "42E", "DIAL/POWER"
12630 DATA "40E", "821 OVERHEAT"
12640 DATA "41E", "810 OVERHEAT"
12650 DATA "02E", "FUME HOOD "
12660 DATA "44E", "821 ALARM"
12670 DATA "00E"      !INTERNAL VOLTAGE
12680 DATA "03E"      !INTERNAL VOLTAGE
12690 DATA "04E"      !FEEDTHRU VOLTAGE
12700 DATA "01E"      !LOAD PS CURRENT
12710 DATA "46E"      !EM PUMP CURRENT
12720 DATA "44E"      !STANDPIPE
12730 FOR I=1 TO Ntc
12740 READ Atc$(I),Mtc(I),Ltc$(I)
12750 NEXT I
12760 RESTORE 12620
12770 FOR I=1 TO 5
12780 READ Relay$(I),Lrly$(I)
12790 NEXT I
12800 RESTORE 12670
12810 FOR I=1 TO 6
12820 READ Lvolt$(I)
12830 NEXT I
12840 CHECK READ
12850 ! *****
12860 Temp2=0
12870 Trecord=0
12880 G$=""
12890 ASSIGN #1 TO "TLMTEC:A7,0,1",Temp1
12900 IF Temp1=1 THEN 13180
12910 PRINT "TEMPERATURE DATA FILE EXISTS. CHECKING FOR RECORDS"
12920 FOR I=1 TO 450 STEP 25
12930 ON ERROR GOTO 12980
12940 READ #1,I;Temp2
12950 IF Temp2=0 THEN 12980
12960 Trecord=Temp2
12970 NEXT I
12980 OFF ERROR
12990 IF I<26 THEN 13020
13000 I=I-25
```

```
13010 GOTO 13030
13020 I=1
13030 FOR J=I TO I+25
13040 ON ERROR GOTO 13090
13050 READ #1,J;Temp2
13060 IF Temp2=0 THEN 13090
13070 Trecord=Temp2
13080 NEXT J
13090 PRINT "CURRENT TEMPERATURE RECORD IS ";Trecord;". PURGE, APPEND, OR
SAVE? (P/A/S) "
13100 INPUT G$
13110 IF (G$<>"P") AND (G$<>"A") AND (G$<>"S") THEN 13090
13120 IF G$="A" THEN 13200
13130 IF G$="S" THEN 13160
13140 PURGE "TLMTEC:A7,0,1"
13150 GOTO 13180
13160 INPUT "ENTER SAVE FILENAME",G$
13170 RENAME "TLMTEC:A7,0,1" TO G$[1,6]
13180 PRINT "CREATING TLMTEC FILE"
13190 CREATE "TLMTEC:A7,0,1",450,200
13200 ASSIGN #1 TO "TLMTEC:A7,0,1"
13210 OFF ERROR
13220 ! *****
13230 Temp2=0
13240 Vrecord=0
13250 G$=""
13260 PRINT PAGE
13270 ASSIGN #2 TO "VLMTEC:A7,0,1",Temp1
13280 IF Temp1=1 THEN 13560
13290 PRINT "IV CURVE DATA FILE EXISTS. CHECKING FOR RECORDS"
13300 FOR I=1 TO 150 STEP 25
13310 ON ERROR GOTO 13360
13320 READ #2,I;Temp2
13330 IF Temp2=0 THEN 13360
13340 Vrecord=Temp2
13350 NEXT I
13360 OFF ERROR
13370 IF I<26 THEN 13400
13380 I=I-25
13390 GOTO 13410
13400 I=1
13410 FOR J=I TO I+25
13420 ON ERROR GOTO 13470
13430 READ #2,J;Temp2
13440 IF Temp2=0 THEN 13470
13450 Vrecord=Temp2
13460 NEXT J
13470 PRINT "CURRENT IV CURVE RECORD IS ";Vrecord;". PURGE, APPEND, OR
SAVE? (P/A/S) "
```

```
13480 INPUT G$
13490 IF (G$<>"P") AND (G$<>"A") AND (G$<>"S") THEN 13470
13500 IF G$="A" THEN 13580
13510 IF G$="S" THEN 13540
13520 PURGE "VLMTEC:A7,0,1"
13530 GOTO 13560
13540 INPUT "ENTER SAVE FILENAME",G$
13550 RENAME "VLMTEC:A7,0,1" TO G$[1,6]
13560 PRINT "CREATING IV STORAGE FILE"
13570 CREATE "VLMTEC:A7,0,1",150,444
13580 ASSIGN #2 TO "VLMTEC:A7,0,1"
13590 OFF ERROR
13600 ! *****
13610 PRINT CHR$(12)
13620 PRINT "The name of this program is LMTEC; it is a CONTROL/MONITOR
program";LIN(2)
13630 PRINT "intended to be used for the ENTIRE LMTEC;";LIN(2)
13640 PRINT "Hit CONT when ready to proceed, or hit STOP if you goofed"
13650 PAUSE
13660 CLEAR 722
13670 CLEAR 709
13680 CLEAR 723
13690 PRINT CHR$(12)
13700 ABORTIO 7
13710 PRINT "Verify the printer has adequate paper,then hit CONT.",LIN(4)
13720 PAUSE
13730 PRINT CHR$(12)
13740 ! Clear Relay Chassis
13750 OUTPUT 723;"00140TAT"
13760 PRINT "READY TO INITIALIZE MULTIPROGRAMMER"
13770 PRINT "THIS WILL CAUSE PUMP TO BE REVERSE"
13780 G$=""
13790 INPUT "SHOULD I ??? (<Y>/N)",G$
13800 IF G$="N" THEN 14280
13810 ! QUAD D/A card initilization
13820 OUTPUT 723;"00020T"
13830 OUTPUT 723;"H0000T"
13840 OUTPUT 723;"H2000T"
13850 OUTPUT 723;"H4000T"
13860 OUTPUT 723;"H6000T"
13870 OUTPUT 723;"I0000T"
13880 OUTPUT 723;"I2000T"
13890 OUTPUT 723;"I4000T"
13900 OUTPUT 723;"I6000T"
13910 OUTPUT 723;"J0000T"
13920 OUTPUT 723;"J2000T"
13930 OUTPUT 723;"J4000T"
13940 OUTPUT 723;"J6000T"
13950 OUTPUT 723;"K0000T"
```

```
13960 OUTPUT 723;"K2000T"  
13970 OUTPUT 723;"K4000T"  
13980 OUTPUT 723;"K6000T"  
13990 OUTPUT 723;"M0000T"  
14000 OUTPUT 723;"M2000T"  
14010 OUTPUT 723;"M4000T"  
14020 OUTPUT 723;"M6000T"  
14030 OUTPUT 723;"00000T"  
14040 STATUS 723;Status  
14050 !          CURRENT D/A card initialization  
14060 OUTPUT 723;"00100T"  
14070 OUTPUT 723;"B0000T"  
14080 OUTPUT 723;"C0000T"  
14090 OUTPUT 723;"D0000T"  
14100 OUTPUT 723;"E0000T"  
14110 OUTPUT 723;"F0000T"  
14120 OUTPUT 723;"G0000T"  
14130 OUTPUT 723;"H0000T"  
14140 OUTPUT 723;"L0000T"  
14150 OUTPUT 723;"00040T"  
14160 OUTPUT 723;"00000T"  
14170 OUTPUT 723;"00140T"  
14180 OUTPUT 723;"00000T"  
14190 OUTPUT 723;"A0000T"  
14200 ! *****  
14210 PRINT PAGE  
14220 PRINT "THIS IS A TEST OF THE ALARM"  
14230 PRINT "ONCE YOU HEAR THE ALARM, PRESS <cont>"  
14240 PRINT LIN(3),"IF IT DOES NOT SOUND, FIND THE PROBLEM"  
14250 CALL Timer(.1)  
14260 PAUSE  
14270 CALL Timer(999)  
14280 PRINT PAGE  
14290 CALL Time(Time$)  
14300 IMAGE "Current date= ",8A,9X,"Time= ",8A,9X  
14310 PRINT USING 14300;Time$[1,8],Time$[9,16]  
14320 PRINT "IF INCORRECT, ENTER NEW STRING MMDDHHMMSS, ELSE ENTER"  
14330 G$=""  
14340 INPUT G$  
14350 IF G$="" THEN Stexit  
14360 OUTPUT 9;"S"&G$  
14370 GOTO 14280  
14380 CALL Time(Time$)  
14390 Stexit: !  
14400 St=VAL(Time$[12,13])+VAL(Time$[9,10])*60+VAL(Time$[4,5])*24*60+  
VAL(Time$[1,2])*31*24*60  
14410 CALL Dcr(Piv)  
14420 SUBEXIT  
14430 SUBEND  
14440 ! *****
```

```
14450 ! *****
14460 SUB Stop
14470 Stop:           ! MANUAL SHUTDOWN
14480 ! *****
14490 CALL Timer(999)
14500 BEEP
14510 G$=""
14520 INPUT "SHUTDOWN REQUESTED--SHOULD I??? (Y/N) ",G$
14530 IF G$<>"Y" THEN 14290
14540 Isd=9999
14550 CALL Shutdown(Fb,999)
14560 SUBEXIT
14570 SUBEND
14580 ! *****
```

```
14590 ! *****
14600 SUB Tcrd
14610 Tcrd:           ! Reads and converts temperatures
14620 ! *****
14630 OPTION BASE 1
14640 COM SHORT Tsnuz,Ntc,Nhtc,Tc,Tb,Btc(*),Mtc(*),Rlypo(*),Trecord,Vrecord
14650 COM Atc$(*),Ltc$(*),Lrly$(*),Relay$(*),Lvolt$(*
14660 COM SHORT Volt(*),St,Piv,Ivs,Hpower
14670 COM Iiv,Itemp,INTEGER Gtc(*)
14680 SHORT Btcu
14690 OUTPUT 722;"F1R1M3A1HOT2T3"
14700 FOR T=1 TO Ntc
14710 OUTPUT 709;Atc$(T)
14720 OUTPUT 722;"T3"
14730 ENTER 722;Btc(T)
14740 NEXT T
14750 OUTPUT 722;"F4R4M3A1H1"
14760 OUTPUT 709;"20E"           ! Thermistor temp
14770 OUTPUT 722;"T3"
14780 ENTER 722;Rtherm
14790 Rtherm=5041.6/(LOG(Rtherm)+7.15)-314.052 !(Deg C)
14800 OUTPUT 709;"C"
14810 OUTPUT 722;"F1R3M3A1HO"
14820 FOR T=1 TO Ntc
14830 IF Gtc(T)=0 THEN 15000
14840 Btcu=Btc(T)
14850 IF Btcu>.050 THEN 14950
14860 IF Btcu<-.005 THEN 14950
14870 Btc(T)=FNTemp("K",Btcu,Rtherm)
14880 IF Btc(T)<Mtc(T) THEN 15010
14890 OUTPUT 722;"F4R7M3A1H1T2T3"
14900 OUTPUT 709;Atc$(T)
14910 OUTPUT 722;"T3"
14920 ENTER 722;Rthc
14930 OUTPUT 709;"C"
14940 IF Rthc<1000 THEN 15010
14950 CALL Rltime
14960 PRINTER IS 0
14970 PRINT "BROKEN TC MARKED ",Ltc$(T),Atc$(T)
14980 PRINTER IS 16
14990 Gtc(T)=0
15000 Btc(T)=0   !BROKEN Tc VALUE
15010 NEXT T
15020 OUTPUT 709;"C"
15030 OUTPUT 722;"F1R3M3A1HO"
15040 SUBEXIT
15050 SUBEND
15060 ! *****
```

```
15070 ! *****
15080 SUB Tdata
15090 Tdata:      ! TAKES AND STORES TEMPERATURE DATA
15100 ! *****
15110 DISP "TEMPERATURE READING AND STORAGE"
15120 OPTION BASE 1
15130 COM SHORT Tsnuz,Ntc,Nhtc,Tc,Tb,Btc(*),Mtc(*),Rlypo(*),Trecord,Vrecord
15140 COM Atc$(*),Ltc$(*),Lrly$(*),Relay$(*),Lvolt$(*)
15150 COM SHORT Volt(*),St,Piv,Ivs,Hpower
15160 CALL Tcrd
15170 CALL Time(Time$)
15180 CALL Voltrd
15190 CHECK READ
15200 ON ERROR GOTO Terror
15210 ASSIGN #1 TO "TLMTEC:A7,0,1"
15220 Trecord=Trecord+1
15230 PRINT #1,Trecord,Trecord,Time$,Ntc,Btc(*),Volt(*),Hpower
15240 OFF ERROR
15250 ASSIGN #1 TO *
15260 IF Trecord=450 THEN CALL Ddump(4)
15270 SUBEXIT
15280 Terror:      ! TRAPS TEMP STARAGE ERRORS
15290 PRINTER IS 0
15300 PRINT "TEMPERATURE STORAGE ERROR, TIME IS: "&Time$
15310 PRINT ERRMS
15320 PRINT LIN(2);"DATA NOT STORED"
15330 PRINT LIN(5)
15340 PRINTER IS 16
15350 Trecord=Trecord-1
15360 ASSIGN #1 TO *
15370 SUBEXIT
15380 SUBEND
15390 ! *****
```

```
15400 ! *****
15410 DEF FNTemp(Type$,SHORT Voltage,REAL Junct)
15420 Fntemp: ! This function calculates actual thermocouple temperature.
15430 ! *****
15440 OPTION BASE 1
15450 DIM Junct(4),Coeff(10)
15460     Junct(2)=3.9448872E1
15470     Junct(3)=2.4548362E-2
15480     Junct(4)=-9.0918433E-5
15490     Coeff(1)=.226584602
15500     Coeff(2)=24152.109
15510     Coeff(3)=67233.4248
15520     Coeff(4)=2210340.682
15530     Coeff(5)=-860963914.9
15540     Coeff(6)=4.83506E10
15550     Coeff(7)=-1.18452E12
15560     Coeff(8)=1.3869E13
15570     Coeff(9)=-6.33708E13
15580     Temp=FNPoly8(Coeff(*),Voltage+1E-6*FNPoly3(Junct(*),Junct))
15590 Rtn:RETURN Temp
15600 DEF FNPoly8(Co(*),Val)=(((((((Co(9)*Val+Co(8))*Val+Co(7))*Val+
Co(6))*Val+Co(5))*Val+Co(4))*Val+Co(3))*Val+Co(2))*Val+Co(1)
15610 DEF FNPoly3(Co(*),Value)=((Co(4)*Value+Co(3))*Value+Co(2))*Value
15620 FNEND
15630 ! *****
```

```
15640 ! *****
15650 SUB Timer(SHORT X)
15660 Timer:    ! SETS HANGUP TIMER; X IN SECONDS
15670 ! *****
15680 IF X=999 THEN Notime
15690 T=OCTAL(X*10)
15700 IF T>7777 THEN T=7777
15710 Tfmt:     IMAGE #,7A,4Z,7A
15720 OUTPUT 723 USING Tfmt;"00140TN",T,"T00004T"
15730 SUBEXIT
15740 Notime:   ! TURNS OFF TIMER
15750 OUTPUT 723;"00140T00000T"
15760 SUBEXIT
15770 SUBEND
15780 ! *****
```

```
15790 ! *****
15800 SUB Time(Time$)
15810 Time: ! RETURNS CURRENT TIME
15820 ! *****
15830 Year$="87"
15840 OUTPUT 9;"R"
15850 ENTER 9;Time$
15860 Time$=Time$[1,6]&Year$&Time$[7,14]
15870 SUBEXIT
15880 SUBEND
15890 ! *****
```

```
15900 ! *****
15910 DEF FN Trip(X)
15920 Trip:          ! PROTECTS FILAMENT
15930 ! *****
15940 Pc=FN Press(1)
15950 IF Pc<>1 THEN 15980
15960   OUTPUT 723;"A0000T"  !SET TO PROTECT FILAMENT
15970   RETURN 3
15980 IF X<>0 THEN 16010
15990 OUTPUT 723;"A0000T" !PROTECT FILAMENT
16000 GOTO Retn
16010 OUTPUT 723;"A0001T" !OVERRIDE
16020 Retn: RETURN 0
16030 FNEND
16040 ! *****
```

```
16050 ! *****
16060 SUB Voltrd
16070 Voltrd:           ! Reads and converts VOLTAGES OF LMTEC & POWER SUPPLIES
16080 ! *****
16090 OPTION BASE 1
16100 COM SHORT Tsnuz,Ntc,Nhtc,Tc,Tb,Btc(*),Mtc(*),Rlypo(*),Trecord,Vrecord
16110 COM Atc$(*),Ltc$(*),Lrly$(*),Relay$(*),Lvolt$(*)
16120 COM SHORT Volt(*),St,Piv,Ivs,Hpower
16130 OUTPUT 722;"F1R7M3A1HOT2T3"
16140 FOR I=1 TO 6
16150 OUTPUT 709;Lvolt$(I)
16160 OUTPUT 722;"T3"
16170 ENTER 722;Volt(I)
16180 NEXT I
16190 OUTPUT 722;"F1R1M3A1HO"
16200 OUTPUT 709;"C"
16210 Volt(4)=Volt(4)*300*1000/101.5      !CONVERT TO LOAD CURRENT
16220 Volt(5)=Volt(5)*100/.376          !CONVERT TO PUMP CURRENT
16230 Tavg=(Btc(26)+Btc(27))*0.5
16240 Amps=2
16250 F1=1+.000972*(Tavg-20)
16260 F2=1+.00429*(Tavg-98)
16270 R=Volt(6)/Amps
16280 Volt(6)=(10-766*R/F1)/(1-1/(1+7.38*F1/F2)) !Standpipe Height
16290 SUBEXIT
16300 SUBEND
```

APPENDIX G
BENCH TEST MODULE BAKEOUT

Blank Page

Bench Test Module Bakeout

The bench test module (BTM) was evacuated at elevated temperature before sodium was introduced into the system. This "bakeout" was necessary in order to eliminate most of the water expected to be evolved from the beta" alumina before sodium filling and other operations began. The bakeout was accomplished by thermally insulating the entire BTM and applying electrical power to the boiler heater. Temperature at the boiler was held at approximately 300 C for nearly 150 hours, and then was increased to 800 C at a rate of 2 degrees per minute. It was held at the upper temperature for several hours. Residual gas analysis was performed periodically using a quadrupole mass spectrometer.

Figures G1-G9 show representative residual gas spectra that were obtained before and during bakeout. An offset in the instrument mass calibration has not been corrected in these results. The peaks should be shifted +2 amu to be correct. The peak heights are roughly indicative of partial pressures.

Figure G1 shows the spectrum obtained initially before heating began. There is a strong peak at 18 atomic mass units (amu) characteristic of water, peaks at 28 and 32 amu characteristic of air, a peak at 40 associated with argon (which was used to purge the system), and a peak at 44 which indicates the presence of carbon dioxide. Figure G2 shows the spectrum obtained after 3 hours of heating with the boiler held steady at 300 C. The total pressure is considerably higher than when cold as expected. The strongest peak is now characteristic of hydrogen, most probably evolving from the stainless steel. The water peak is about the same height as earlier, and the argon peak is no longer evident. There is a small peak at 28 amu but none at 32, suggesting the presence of carbon monoxide. The next spectrum, taken after 52 hours of heating, is presented in Figure G3. All of the partial pressures are now greatly reduced, with hydrogen and water still most prominent. The signature for a small fraction of air is again present.

Results after 102 hours and 144 hours are shown in Figures G4 and G5 respectively. These results are very similar to those seen at 52 hours. At 144 hours, a spectrum was recorded for the vacuum system only, isolated from the bench test module. The result is displayed in Figure G6. It differs from the previous figure primarily in the reduction of the hydrogen peak. This indicates that after 144 hours of bakeout the BTM is producing mostly hydrogen, and that most of the other

peaks are attributable to the unbaked vacuum system. Figure G7 shows the spectrum obtained when the BTM boiler temperature was increased to 450 C. Strong peaks are evident for hydrogen, water, carbon monoxide, and carbon dioxide. This is consistent with the expected outgassing from stainless steel and from the decomposition of products of reaction of beta" alumina with the atmosphere, believed to have formed during storage and handling.

By 800 C, the evolution of all gases except hydrogen had slowed, as indicated in Figure G8. After 1.5 hours at 800 C, further reductions in all peaks were evident, as seen in Figure G9. After several hours at 800 C, the BTM was allowed to cool naturally overnight. The system was then opened inside an argon-purged glove bag and charged with sodium.

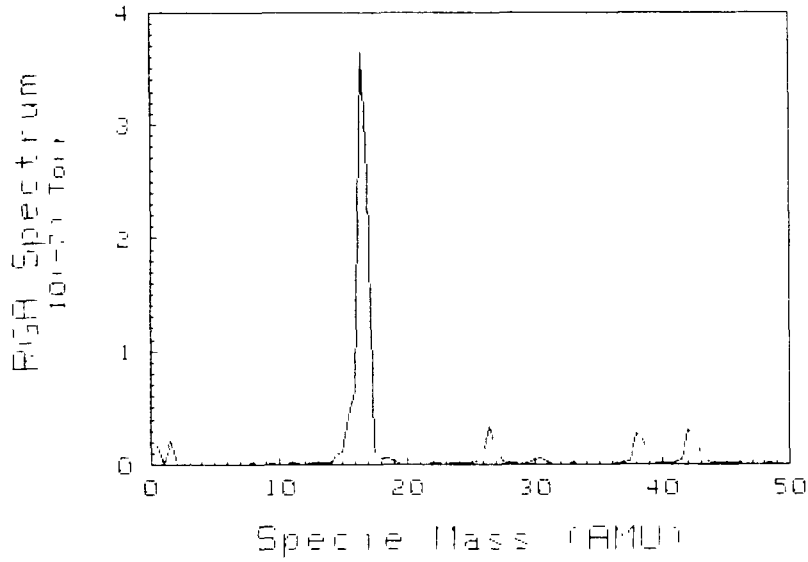


Figure G1. Residual Gas Analyzer Spectrum For Bench Test Module Before Heating Began.

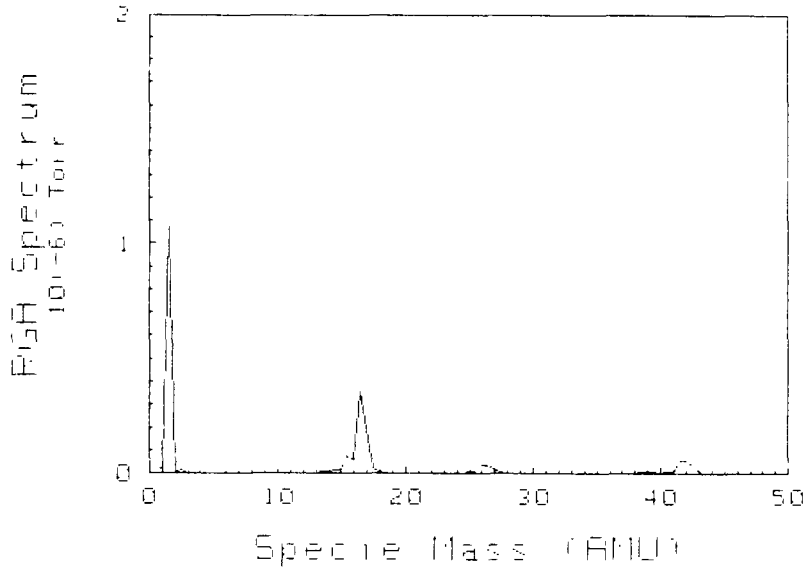


Figure G2. Residual Gas Analyzer Spectrum For Bench Test Module After 3 Hours At 300 C.

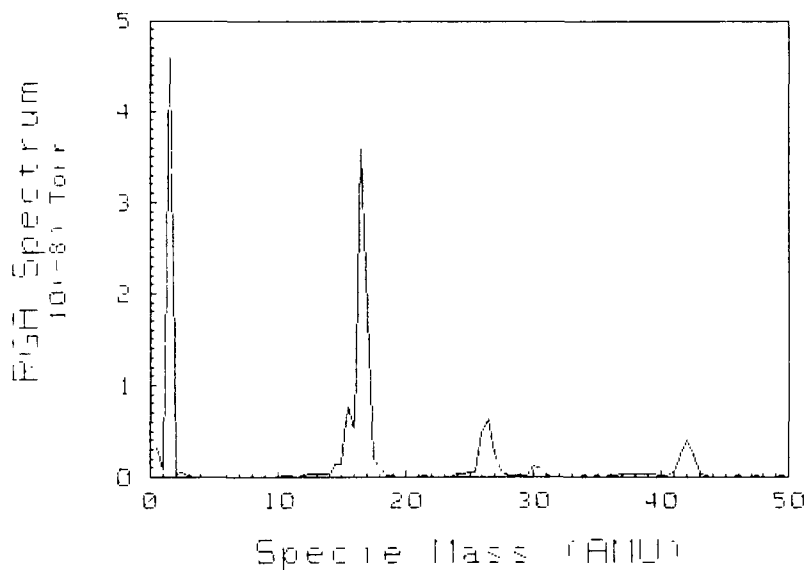


Figure G3. Residual Gas Analyzer Spectrum For Bench Test Module After 52 Hours At 300 C.

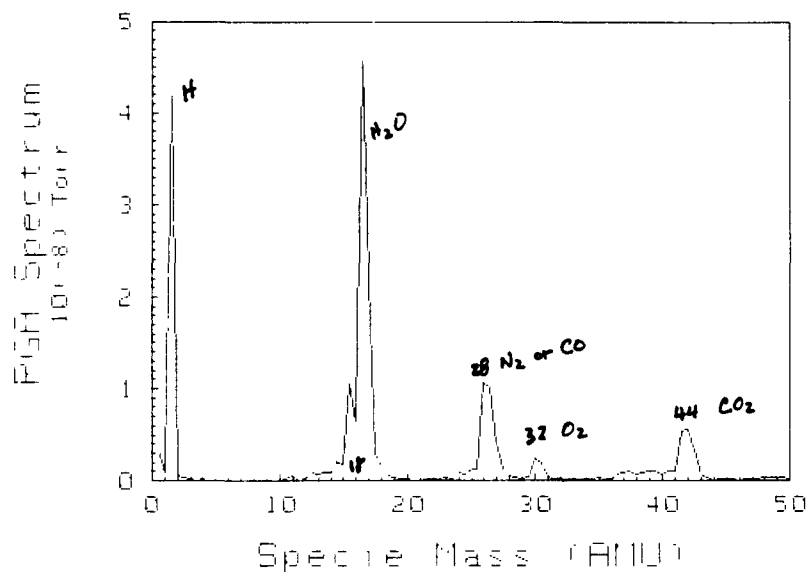


Figure G4. Residual Gas Analyzer Spectrum For Bench Test Module After 102 Hours At 300 C.

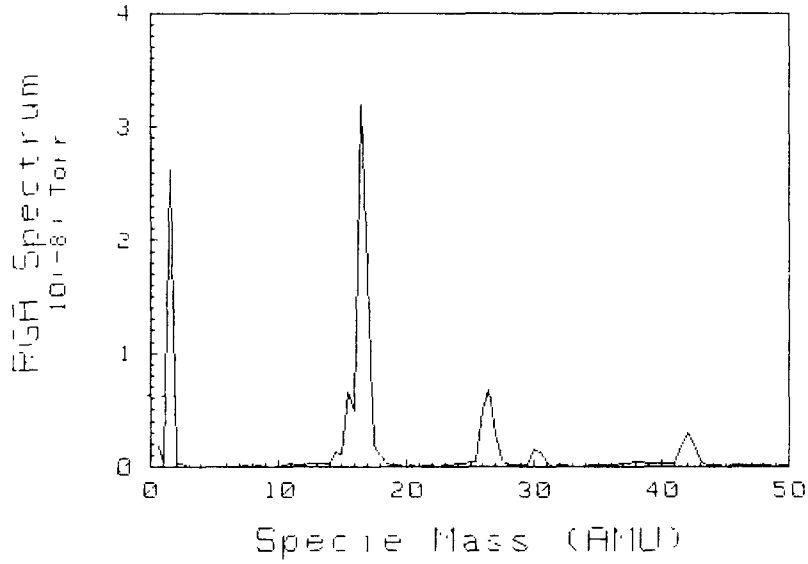


Figure G5. Residual Gas Analyzer Spectrum For Bench Test Module After 144 Hours At 300 C.

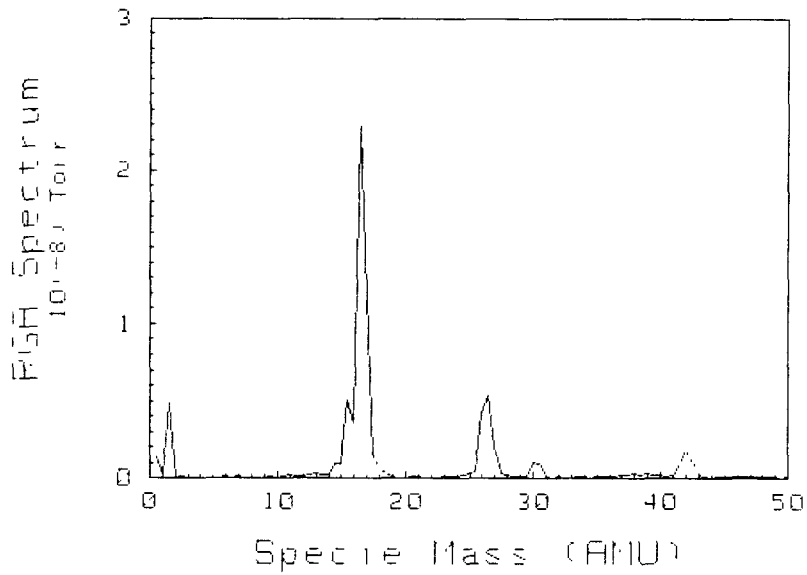


Figure G6. Residual Gas Analyzer Spectrum For Vacuum System Only At 144 Hours.

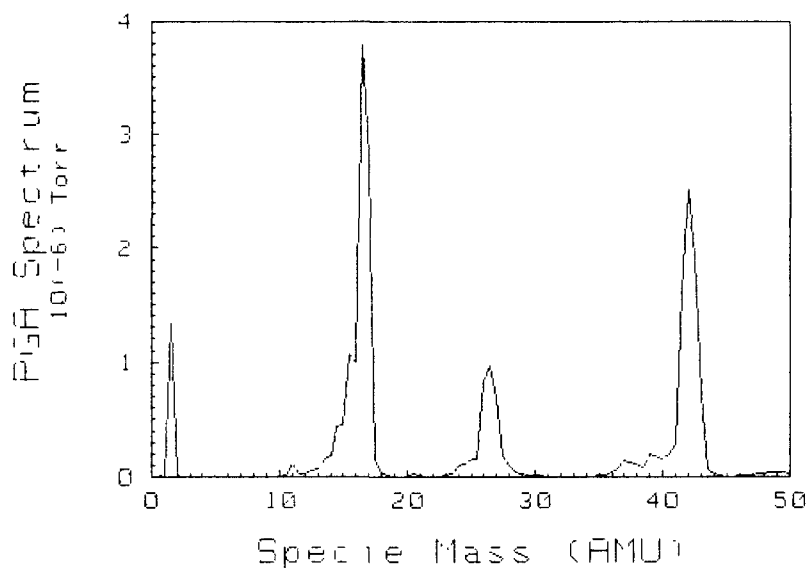


Figure G7. Residual Gas Analyzer Spectrum For Bench Test Module At 450 C, Ramping At 2 deg/min.

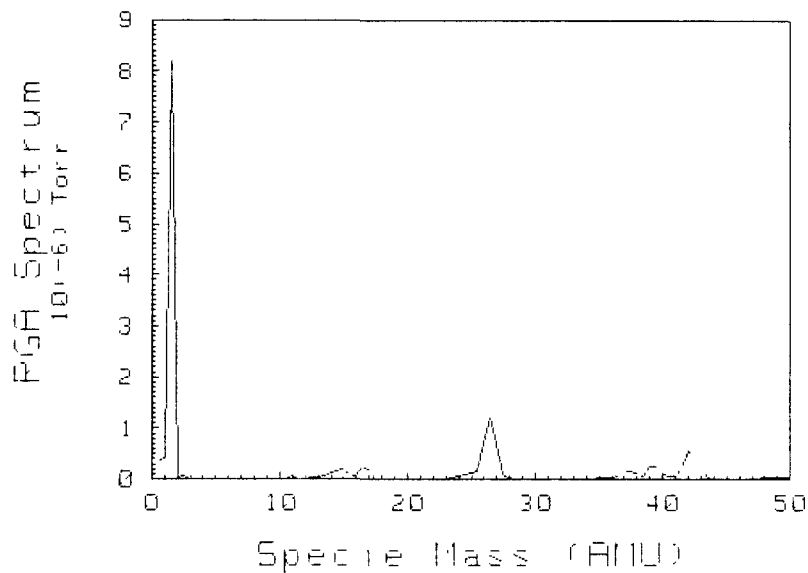


Figure G8. Residual Gas Analyzer Spectrum For Bench Test Module At Arrival At 800 C.

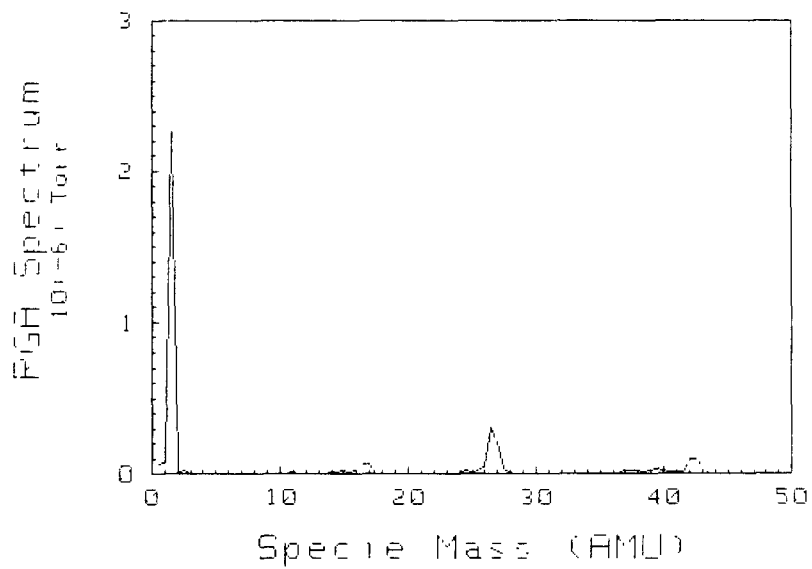


Figure G9. Residual Gas Analyzer Spectrum For Bench Test Module After 1.5 Hours At 800 C.

-210/-211-

APPENDIX H
BENCH TEST MODULE OPERATION

Bench Test Module Operation

The Bench Test Module was operated on March 26, 1987. The chronological sequence of events during the operation of the Bench Test Module are documented in this appendix. During The operation of the Bench Test Module the computer control and data acquisition system automatically recorded the status of the Bench Test Module at approximately ten minute intervals. The recorded information has been plotted against time by channel and included in this appendix.

BTM Operation
Sequence Of Events
March 26, 1987

Actual Time	Elapsed Time	Event
10:35	0:00	The BTM and sodium loop were heated to approximately 120 C.
11:39	1:04	Power was applied to the EM pump.
11:45	1:10	EM Pump operation was verified.
13:15	2:40	Additional heat was applied to the current bus at the bottom of the boiler to melt a sodium plug which was preventing the boiler from filling. The boiler thermocouples indicated a steady rate of fill. As the boiler filled with sodium an open circuit voltage of about 0.2 volts was noted. This voltage decreased to about 0.1 volts in less than 20 minutes.
13:35	3:00	The boiler was completely filled and a temperature increase ramp of about 2 C/min was started. The EM pump pressure was set at about 3 psia.
14:15	3:40	The boiler temperature was about 258 C. The open circuit voltage was 0.17 volts.
14:55	4:20	The boiler temperature was about 450 C. The pump pressure was set at about 3.5 psia.
16:15	5:40	Temperature control on the boiler was unsteady. Thermocouple no. 1 quit working. Boiler control was switched to the bottom thermocouple which was the most steady in the boiler.
17:19	6:44	The maximum boiler temperature was about 785 C (5.3 psia sodium saturated vapor pressure). Popping noises were coming from the BTM. Pump pressure was increased to 7 psia, and the noise stopped.

Actual Time	Elapsed Time	Event
17:25	6:50	The voltage probe at the top of the electrode was discovered to be connected wrong. The polarity was reversed to correct this. (Data plots are corrected for this.)
17:45	7:10	The maximum boiler temperature was about 814 C (7.6 psia sodium saturated vapor pressure). More noise was coming from the BTM (as above). The pump pressure was increased to about 10 psia, and the noise stopped.
18:24	7:49	A voltage/current curve was taken, to a maximum current of 300 amps. A peak power of 1.4 watts at 7 amps was recorded. The condenser temperature was about 450 C. Active air cooling of the condenser was started. The BTM circuit was closed and set for a 0.0 volt load.
18:33	7:58	A voltage current curve was taken, to a maximum current of 300 amps. The condenser temperature was about 300 C.
18:40	8:05	A voltage current curve was taken, to a maximum current of 300 amps. The condenser temperature was about 200 C. The plot routine for voltage/current curves was modified to show negative voltages.
18:45	8:10	The voltage/current data routine was modified to limit the maximum current to 100 amps.
18:50	8:15	The voltage/current curve data acquisition routine reduces voltage to zero between data points. The routine was modified to hold voltage until it is increased for the next point.
18:54	8:19	A voltage current curve was taken. The condenser temperature was about 200 C.
18:57	8:22	The condenser was opened to the vacuum system. The vacuum system pressure increased to about 2×10^{-4} torr. The condenser was valved closed after pumping down to a system pressure of about 2×10^{-7} torr.

Actual Time	Elapsed Time	Event
19:00	8:25	The delay parameter in the voltage/current routine was changed from 10 seconds to 0 seconds. A voltage current curve was taken.
19:01	8:26	The delay parameter in the voltage/current routine was changed from 0 seconds to 5 minutes. A voltage current curve was taken.
19:10	8:35	The delay parameter in the voltage/current routine was changed from 5 minutes to 10 seconds.
19:16	8:41	A voltage current curve was taken.
19:21	8:46	The BTM circuit was closed to record slow changes in operation The power dropped from 1.5 watts to 1.3 watts in about 2 minutes.
19:45	9:10	The running average in the main heater power routine was changed to 50 points (2 each cycle, 25 cycles).
19:53	9:18	A maximum open circuit voltage of 0.8971 volts at the middle of the electrode was recorded after several minutes at open circuit.
19:54	9:19	The BTM circuit was closed. A maximum power output of 1.8 watts at 7.6 amps was recorded.
20:08	9:33	The BTM circuit current was forced to 66.8 amps.
20:10	9:35	The BTM circuit current was forced to 136.2 amps.
20:11	9:36	The BTM circuit current was forced to 318.2 amps.
20:12	9:37	The voltage probes appear to be shorted. The BTM circuit is opened.
20:13	9:38	It was noticed that the main heater had stopped working.

Actual Time	Elapsed Time	Event
20:15	9:40	It was noticed that the boiler had lost pressure.
21:15	10:40	The pump was reversed to drain the boiler.

-218/-219-

Record No. 1

3/28/87 12:34:11

LMTEC BTM Voltage Current Data

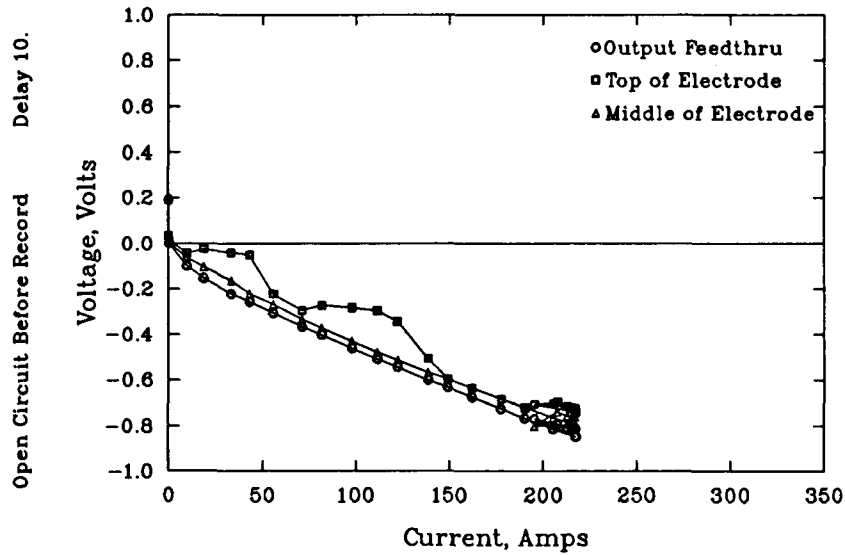


Boiler Temp. 162. °C Condenser Temp. 65. °C Main Heater Power 13. Watts

Record No. 2

3/26/87 14:17:51

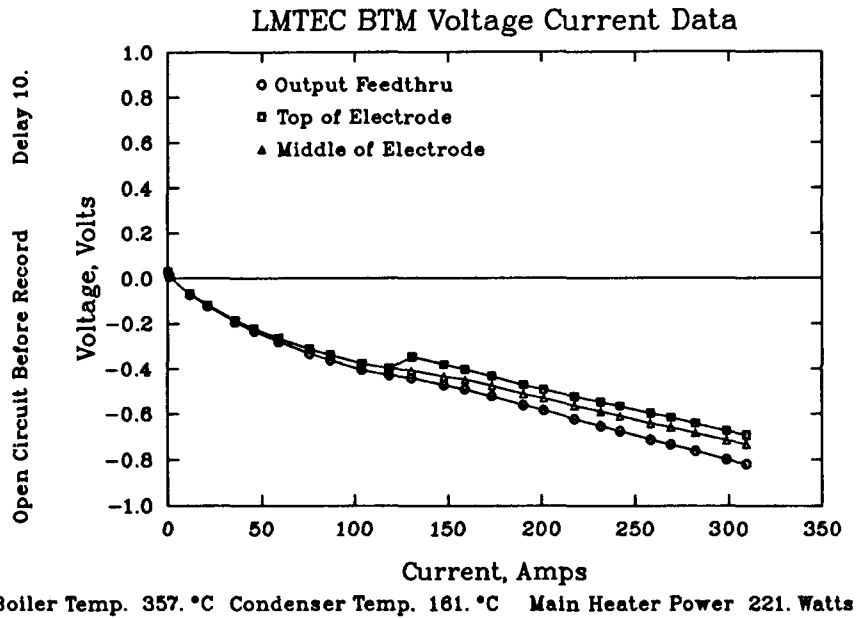
LMTEC BTM Voltage Current Data



Boiler Temp. 271. °C Condenser Temp. 132. °C Main Heater Power 159. Watts

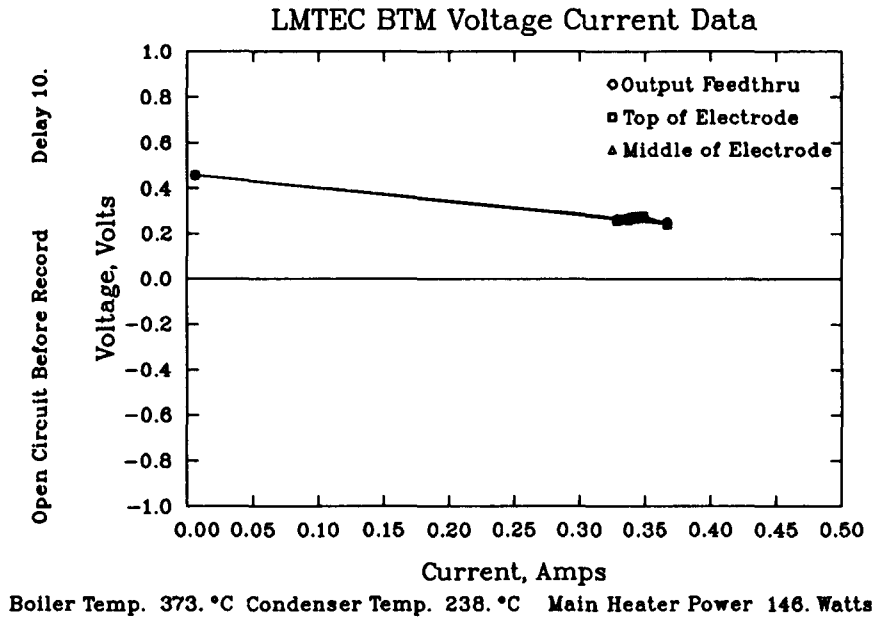
Record No. 3

3/26/87 14:35:18



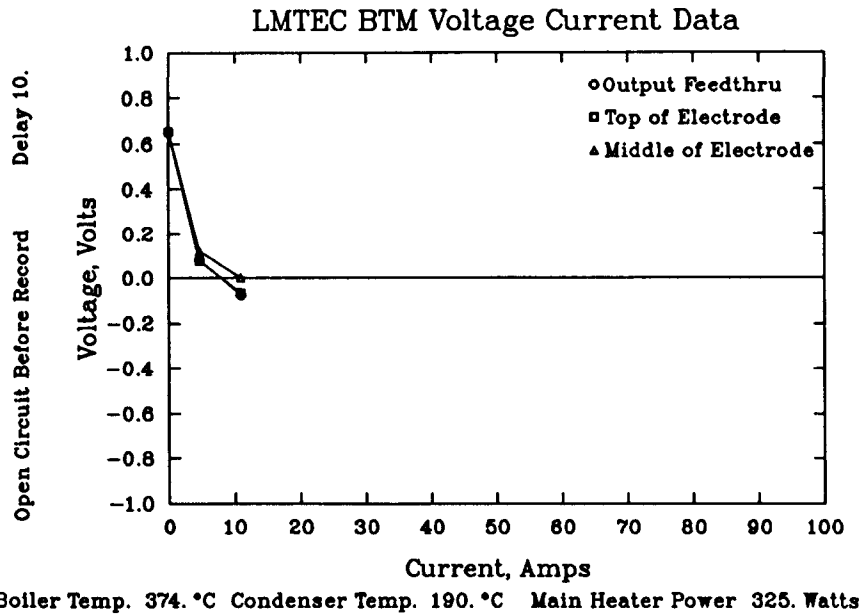
Record No. 4

3/26/87 15:53:57



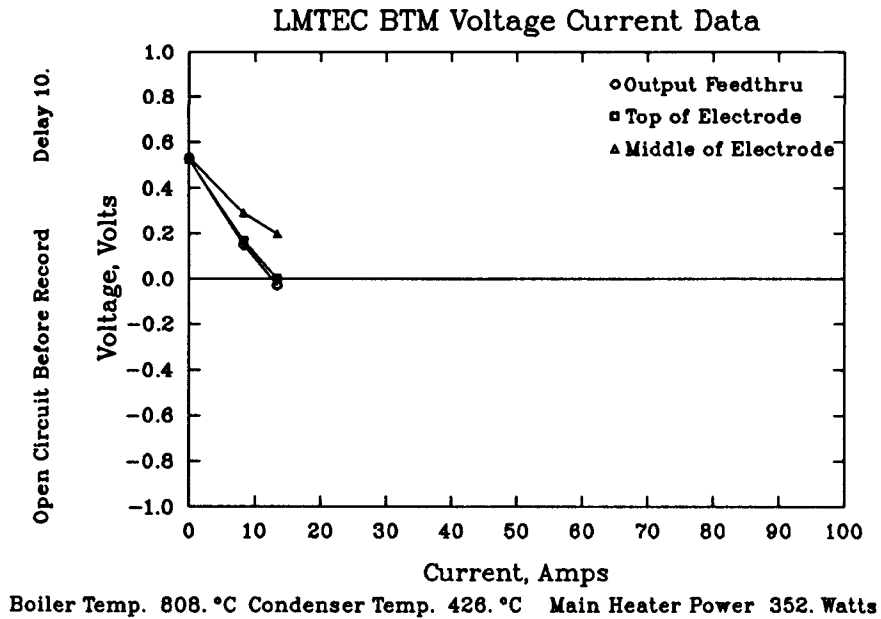
Record No. 5

3/26/87 16:47:17



Record No. 6

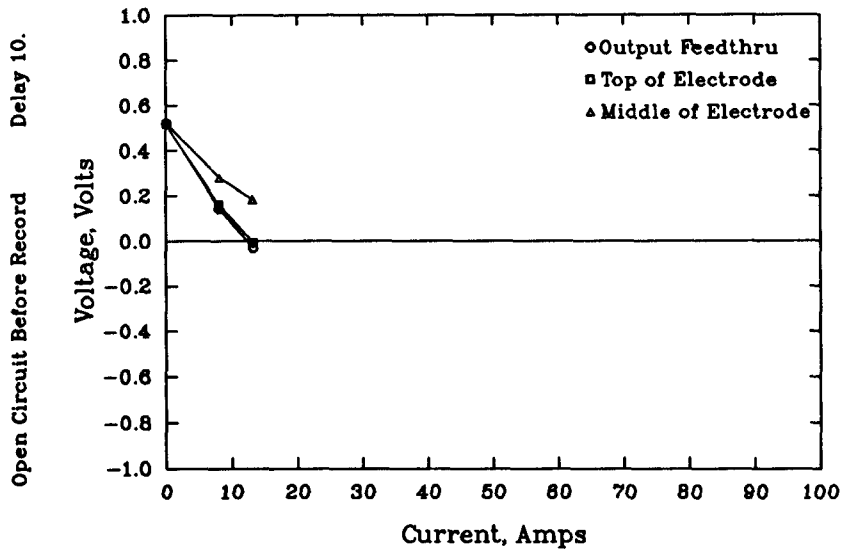
3/26/87 18:16:26



Record No. 7

3/26/87 18:16:52

LMTEC BTM Voltage Current Data

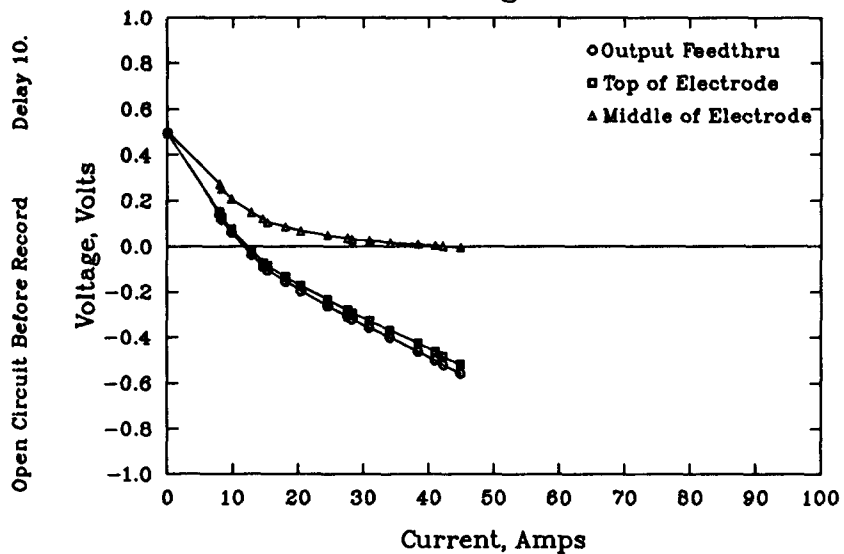


Boiler Temp. 808. °C Condenser Temp. 427. °C Main Heater Power 349. Watts

Record No. 8

3/26/87 18:24:33

LMTEC BTM Voltage Current Data

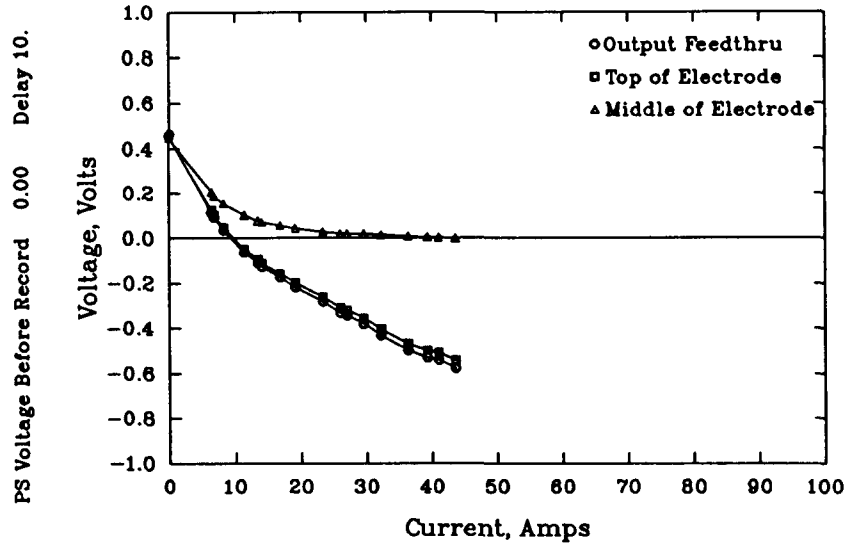


Boiler Temp. 802. °C Condenser Temp. 443. °C Main Heater Power 363. Watts

Record No. 9

3/26/87 18:30:24

LMTEC BTM Voltage Current Data

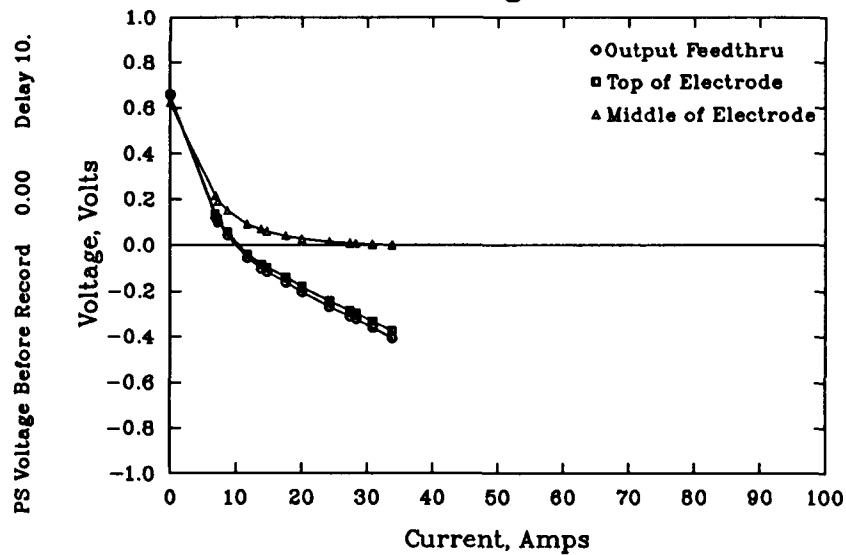


Boiler Temp. 801. °C Condenser Temp. 448. °C Main Heater Power 340. Watts

Record No. 10

3/26/87 18:33:42

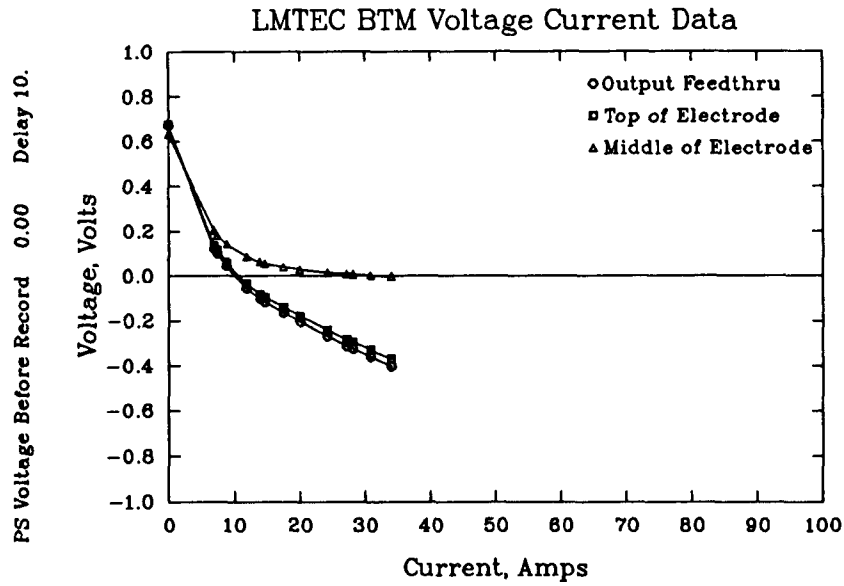
LMTEC BTM Voltage Current Data



Boiler Temp. 802. °C Condenser Temp. 303. °C Main Heater Power 292. Watts

Record No. 11

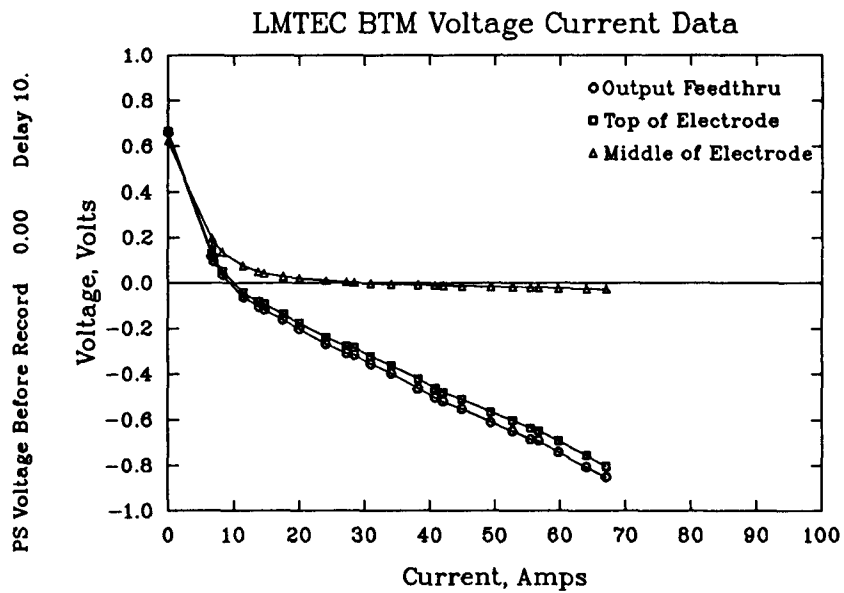
3/26/87 18:40:30



Boiler Temp. 803. °C Condenser Temp. 230. °C Main Heater Power 444. Watts

Record No. 12

3/26/87 18:50:18

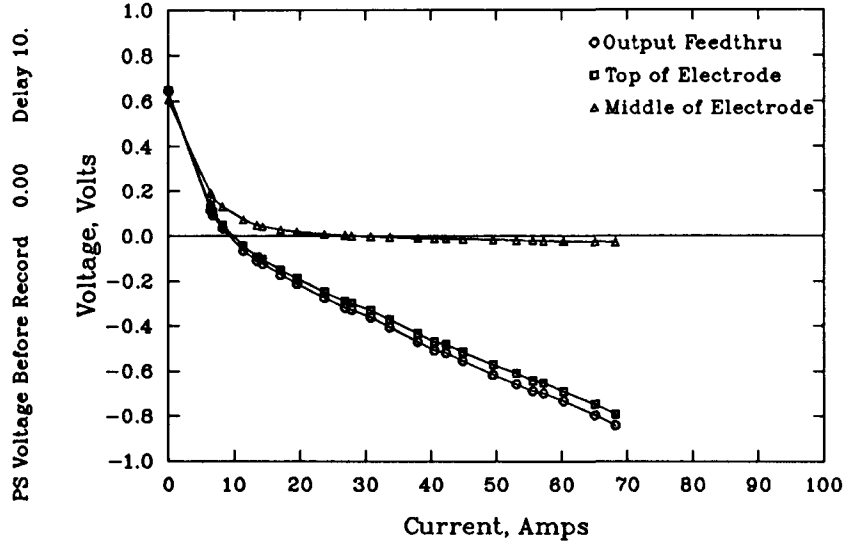


Boiler Temp. 801. °C Condenser Temp. 238. °C Main Heater Power 305. Watts

Record No. 13

3/26/87 18:54:50

LMTEC BTM Voltage Current Data

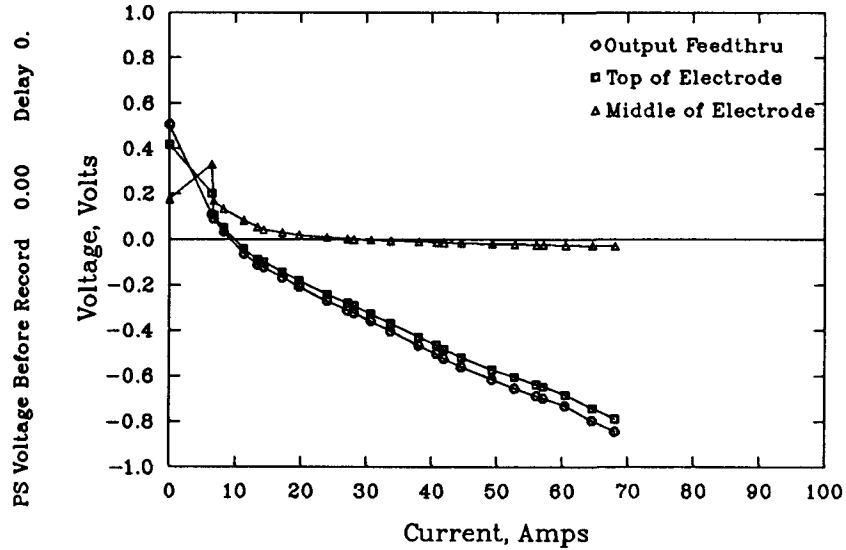


Boiler Temp. 802. °C Condenser Temp. 235. °C Main Heater Power 365. Watts

Record No. 14

3/26/87 19:01:18

LMTEC BTM Voltage Current Data

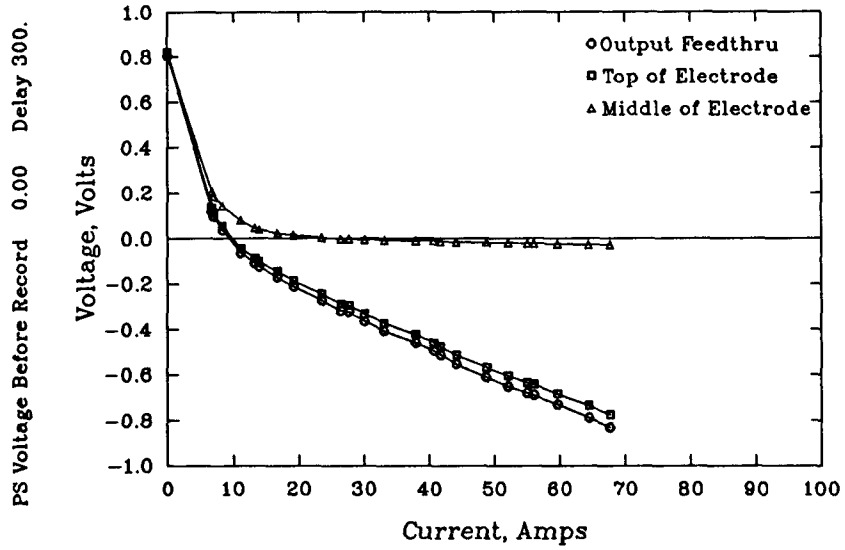


Boiler Temp. 804. °C Condenser Temp. 233. °C Main Heater Power 358. Watts

Record No. 15

3/26/87 19:2:40

LMTEC BTM Voltage Current Data

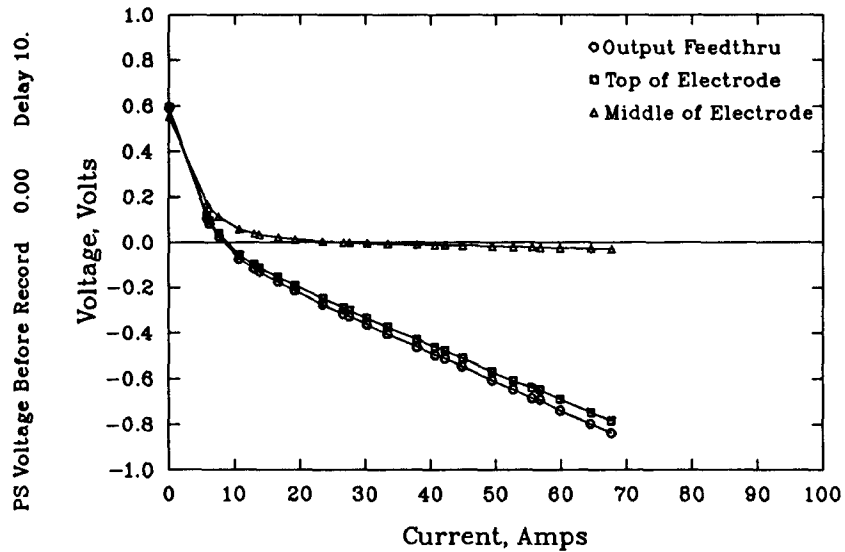


Boiler Temp. 804. °C Condenser Temp. 234. °C Main Heater Power 377. Watts

Record No. 16

3/26/87 19:10:19

LMTEC BTM Voltage Current Data

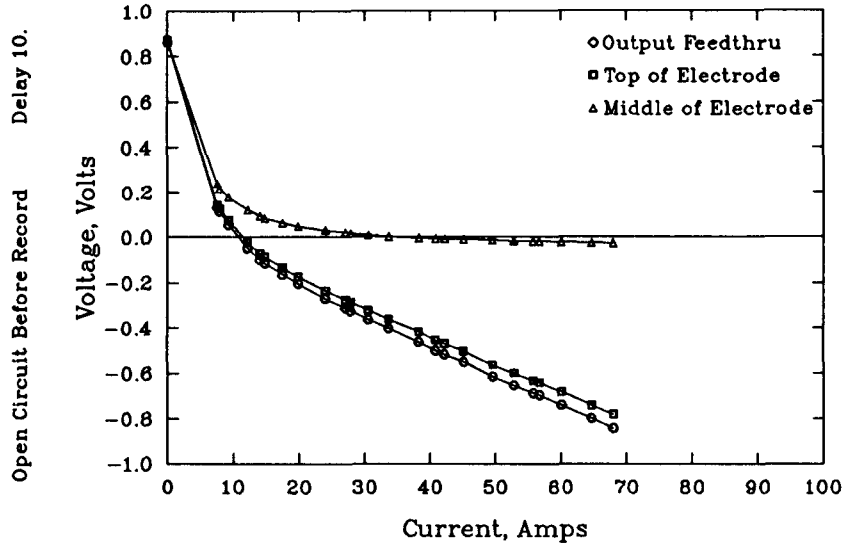


Boiler Temp. 802. °C Condenser Temp. 239. °C Main Heater Power 346. Watts

Record No. 17

3/26/87 19:18:21

LMTEC BTM Voltage Current Data

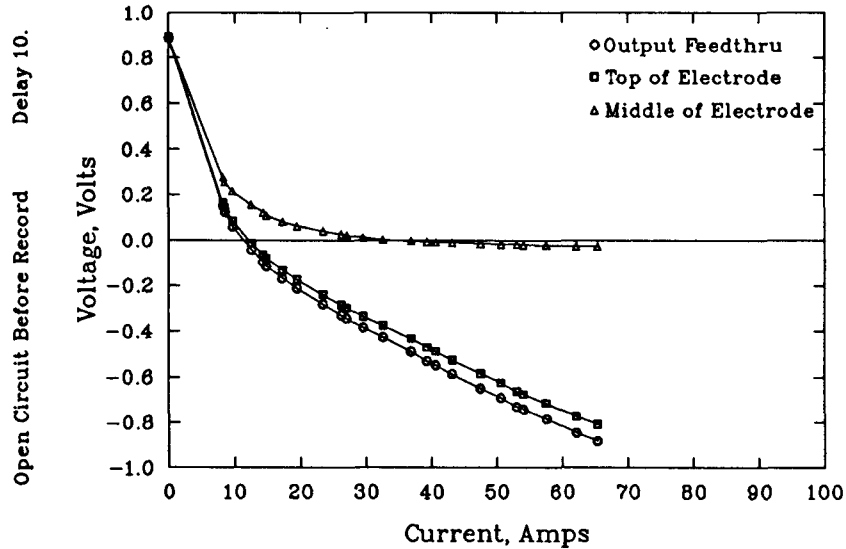


Boiler Temp. 801. °C Condenser Temp. 230. °C Main Heater Power 449. Watts

Record No. 18

3/26/87 19:30:21

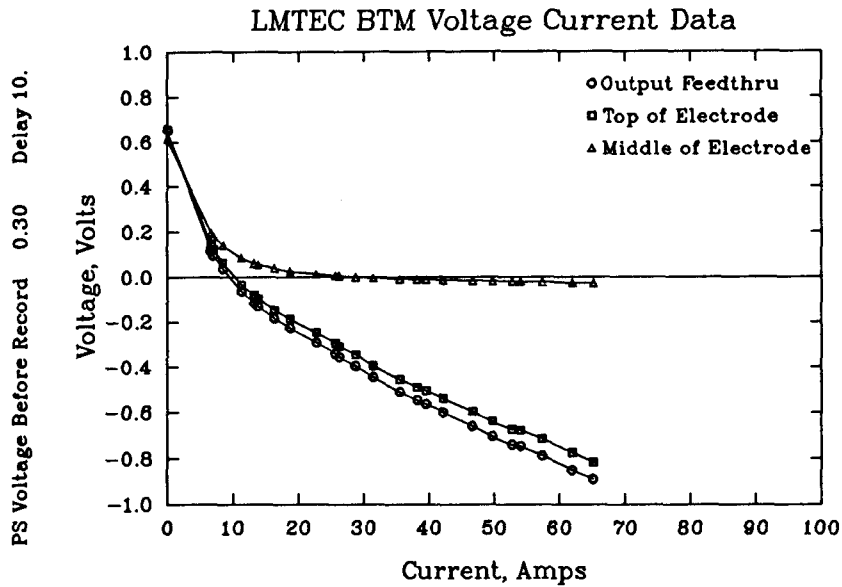
LMTEC BTM Voltage Current Data



Boiler Temp. 805. °C Condenser Temp. 225. °C Main Heater Power 453. Watts

Record No. 19

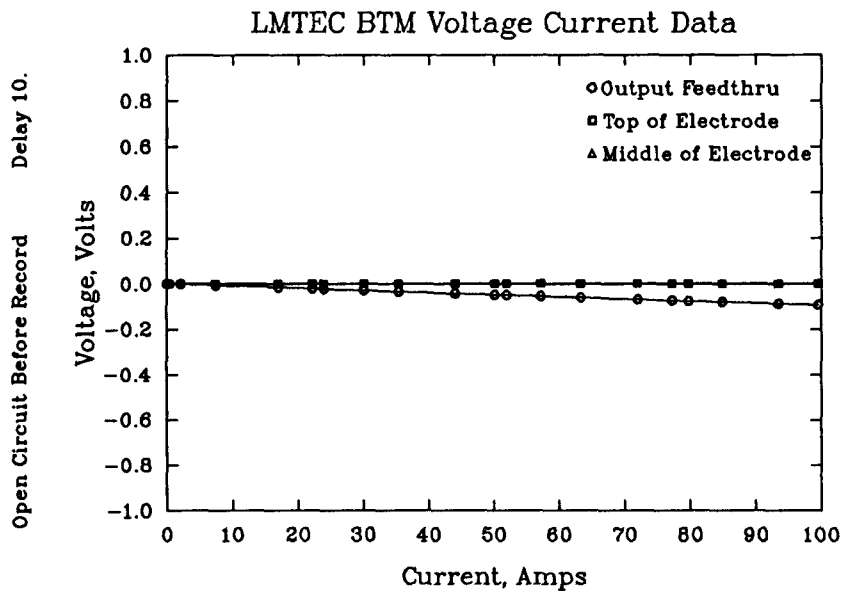
3/26/87 20:4:23



Boiler Temp. 801. °C Condenser Temp. 242. °C Main Heater Power 364. Watts

Record No. 20

3/26/87 20:24:26

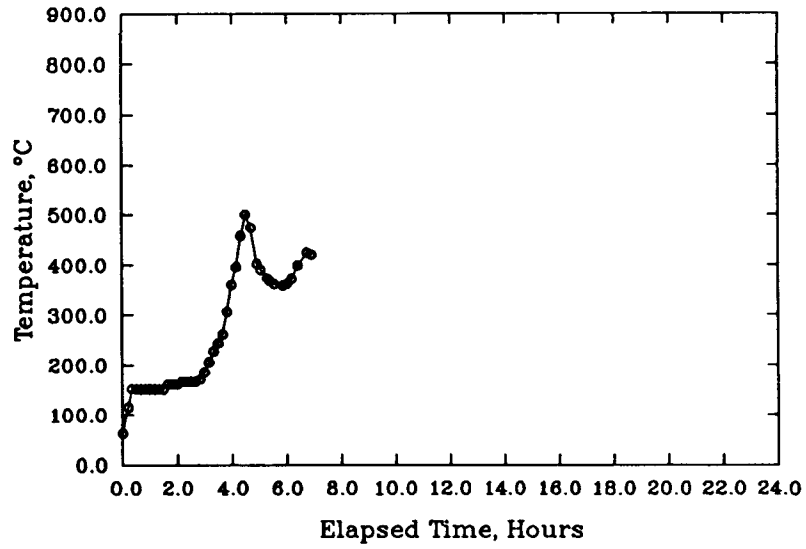


Boiler Temp. 437. °C Condenser Temp. 206. °C Main Heater Power 0. Watts

TC Index 1

3/26/87 10:35:39

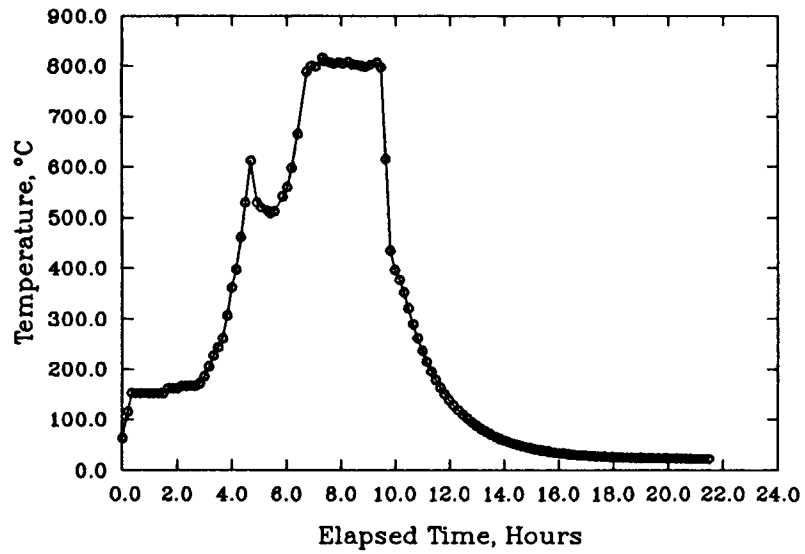
LMTEC BTM Boiler, No. 3



TC Index 2

3/26/87 10:35:39

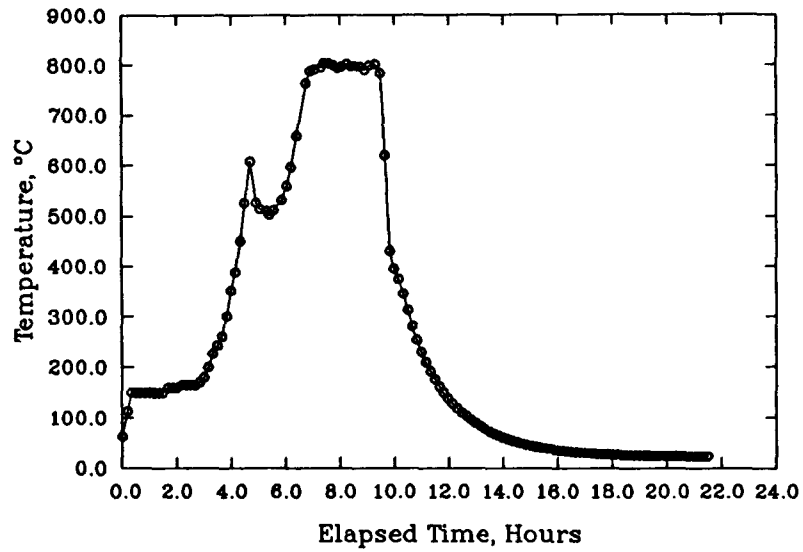
LMTEC BTM Boiler, No. 4



TC Index 3

3/26/87 10:35:39

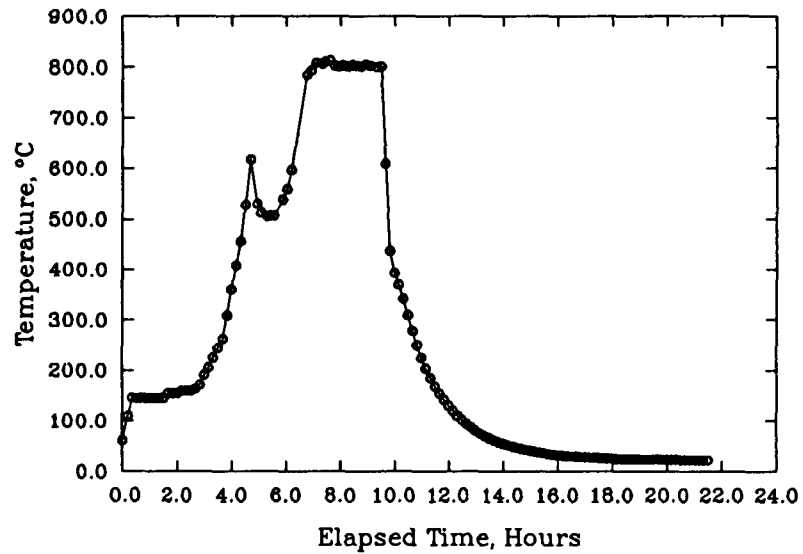
LMTEC BTM Boiler, No. 5



TC Index 4

3/26/87 10:35:39

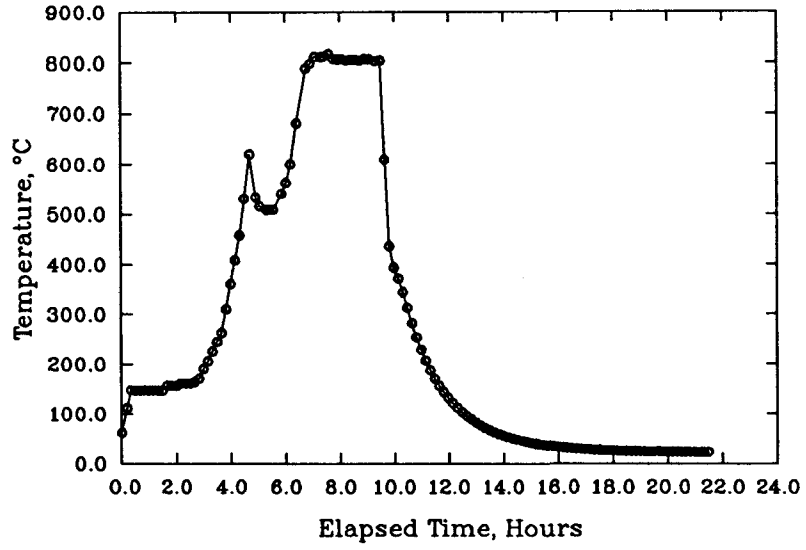
LMTEC BTM Boiler, No. 1



TC Index 5

3/26/87 10:35:39

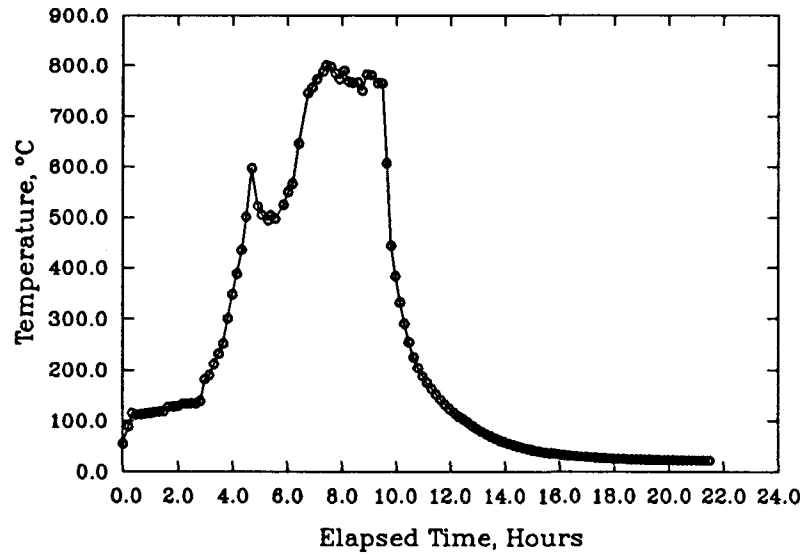
LMTEC BTM Boiler, No. 2



TC Index 6

3/26/87 10:35:39

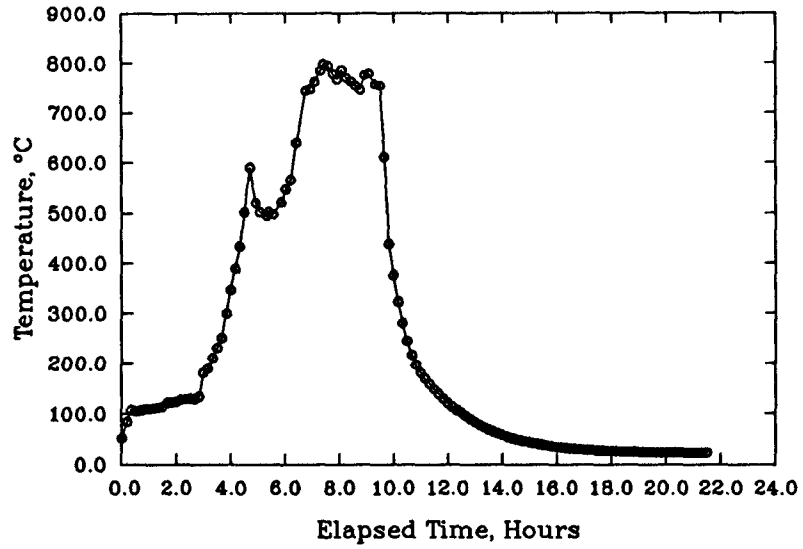
LMTEC BTM Boiler, No. 6



TC Index 7

3/26/87 10:35:39

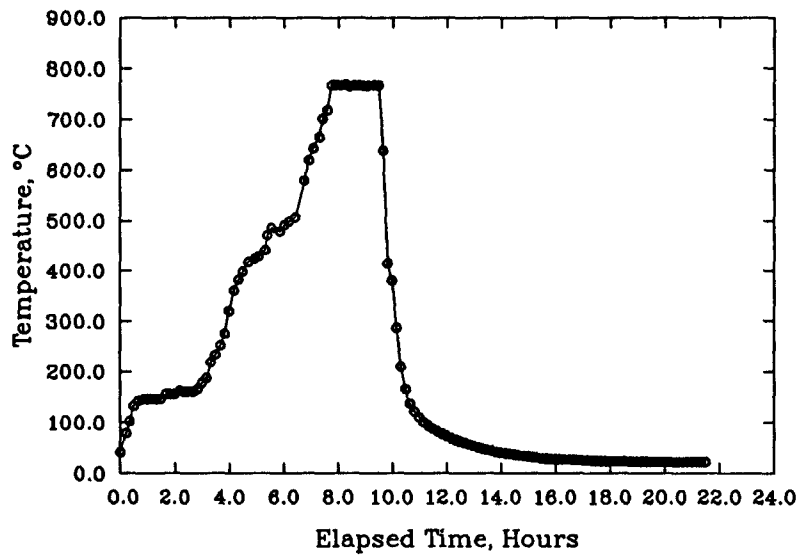
LMTEC BTM Boiler, No. 7



TC Index 8

3/26/87 10:35:39

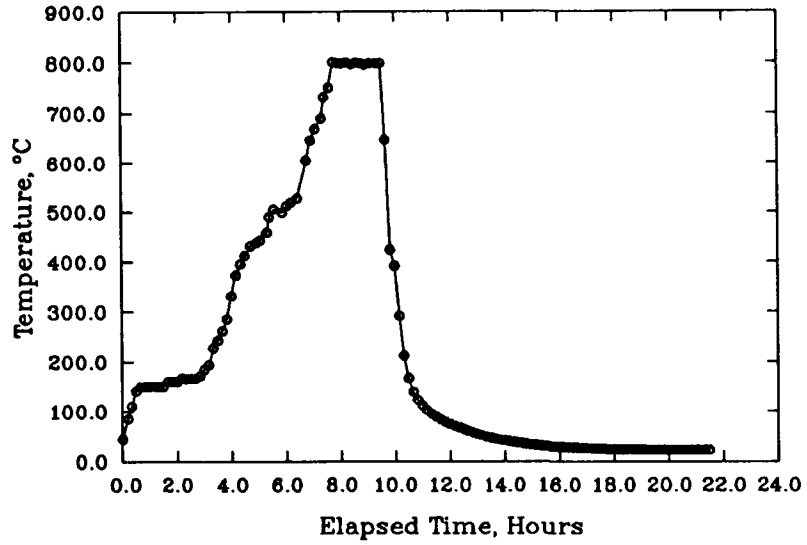
LMTEC BTM Feedthru - Bottom, 810



TC Index 9

3/26/87 10:35:39

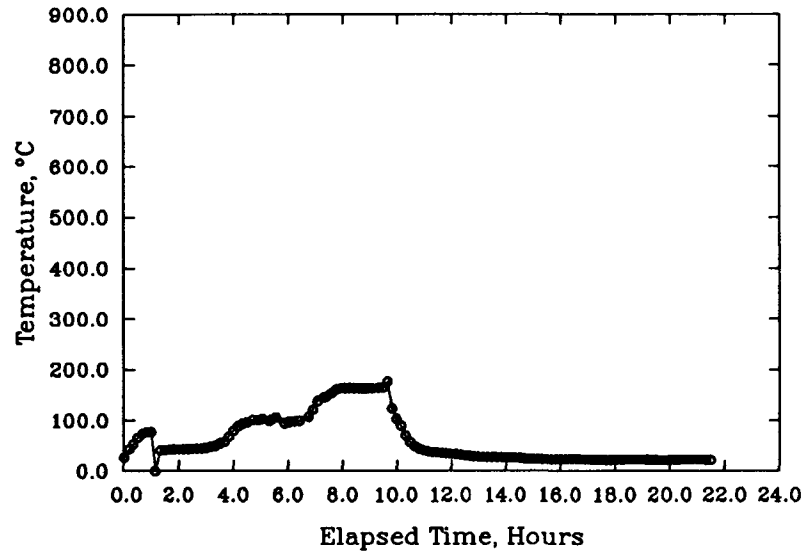
LMTEC BTM Feedthru - Bottom, OH



TC Index 10

3/26/87 10:35:39

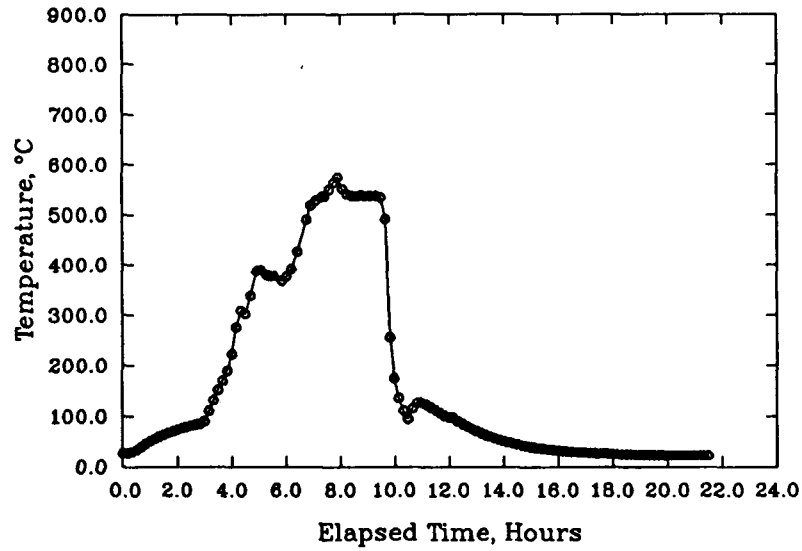
LMTEC BTM Feedthru - Top



TC Index 11

3/26/87 10:35:39

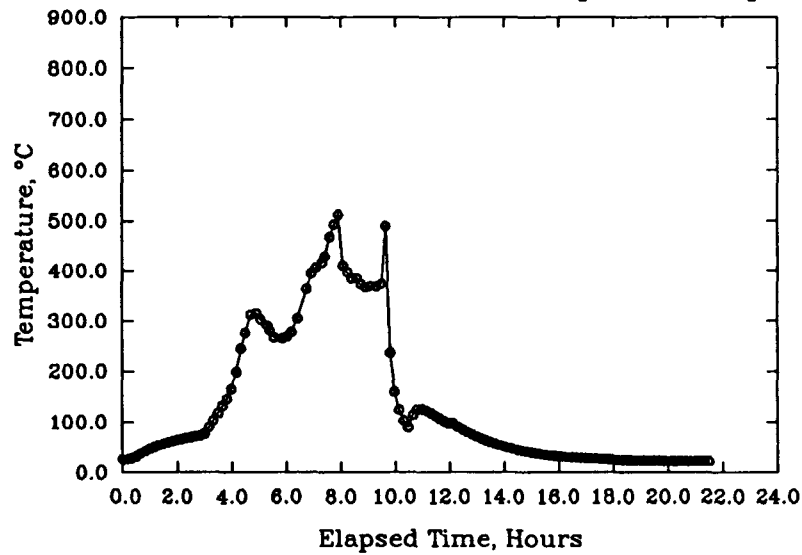
LMTEC BTM Condenser - Radiation Shield



TC Index 12

3/26/87 10:35:39

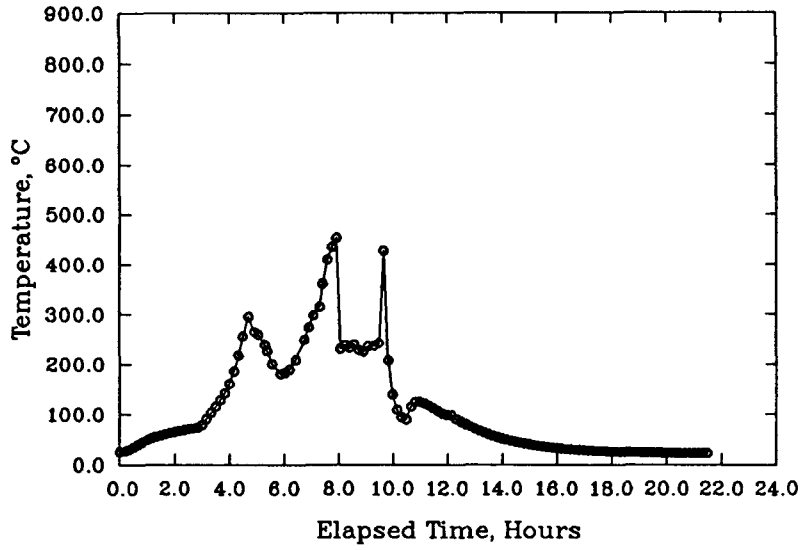
LMTEC BTM Condenser - Sump Shield, Top



TC Index 13

3/26/87 10:35:39

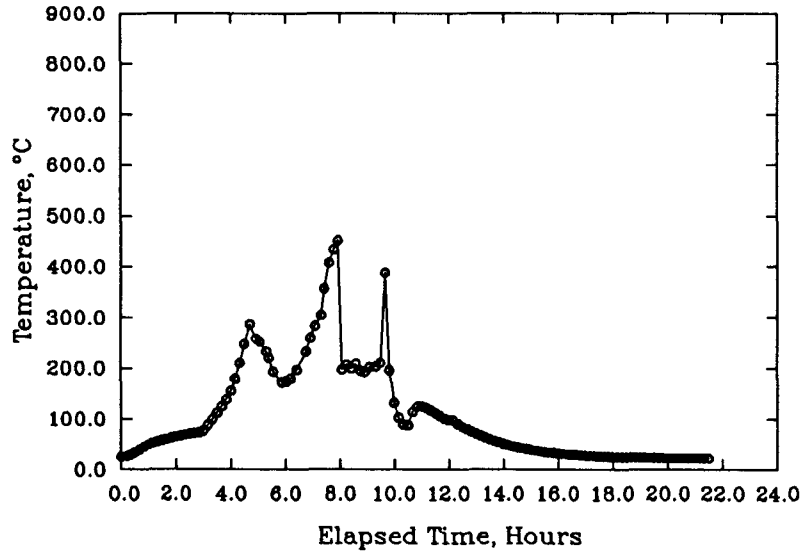
LMTEC BTM Condenser - Bottom



TC Index 14

3/26/87 10:35:39

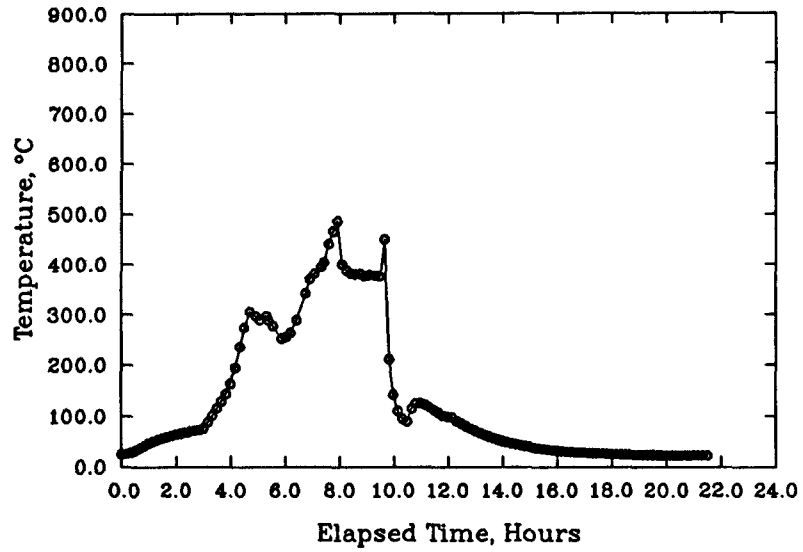
LMTEC BTM Condenser - Middle



TC Index 15

3/28/87 10:35:39

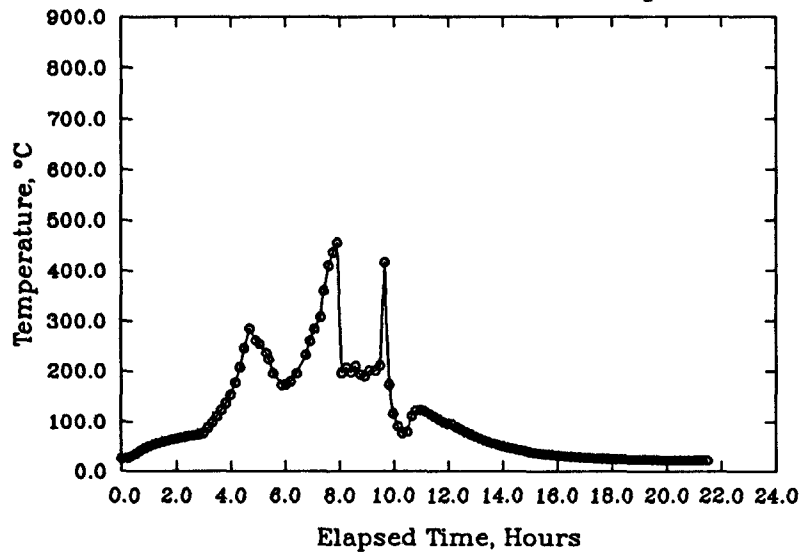
LMTEC BTM Condenser - Sump Shield, Bottom



TC Index 16

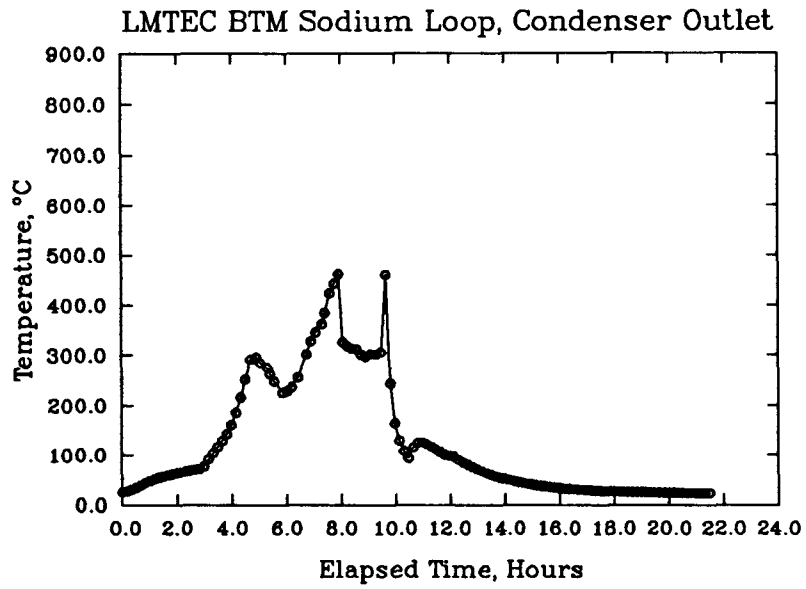
3/28/87 10:35:39

LMTEC BTM Condenser - Top



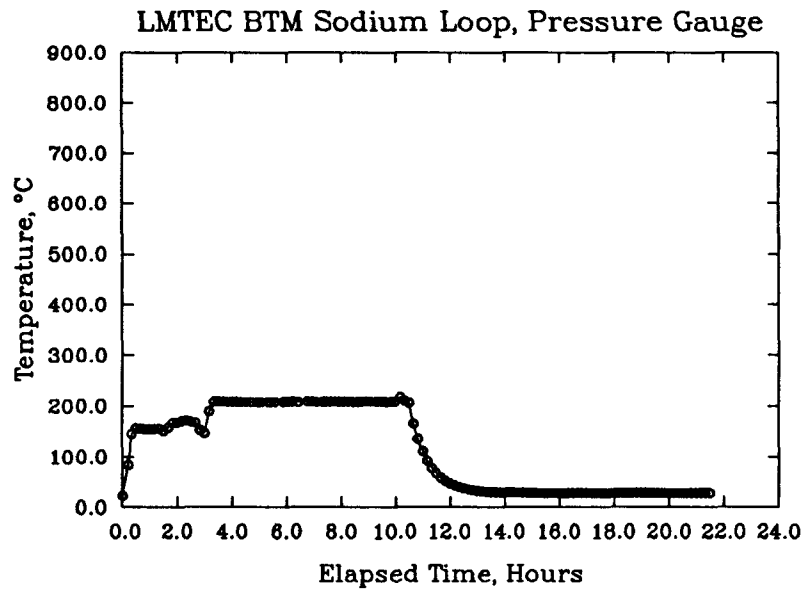
TC Index 17

3/28/87 10:35:39



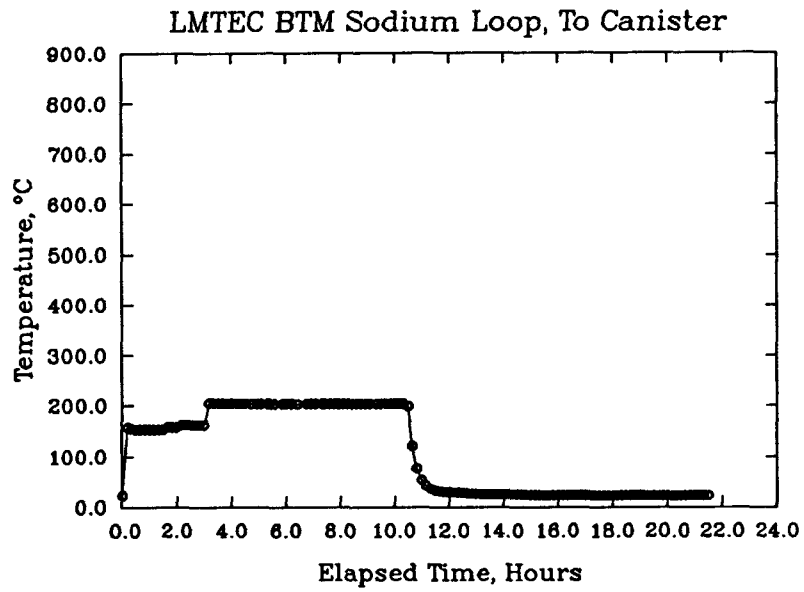
TC Index 18

3/28/87 10:35:39



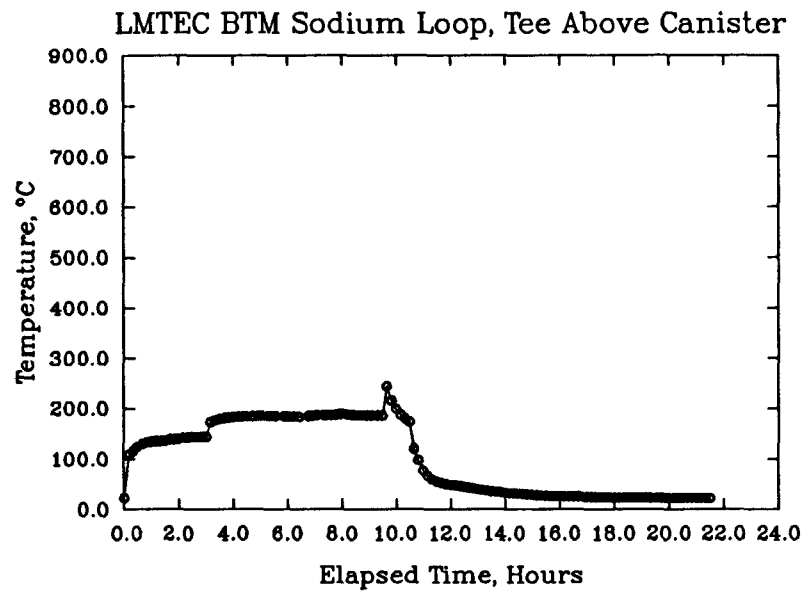
TC Index 19

3/26/87 10:35:39



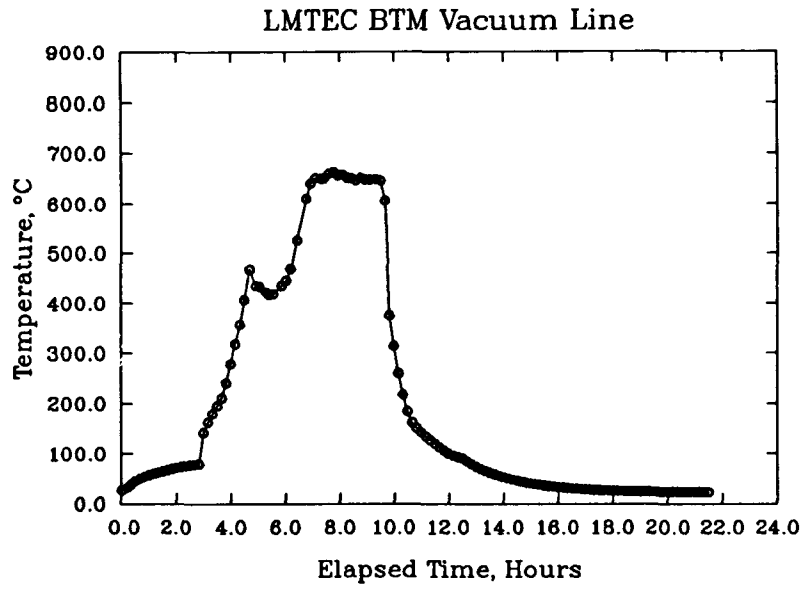
TC Index 20

3/26/87 10:35:39



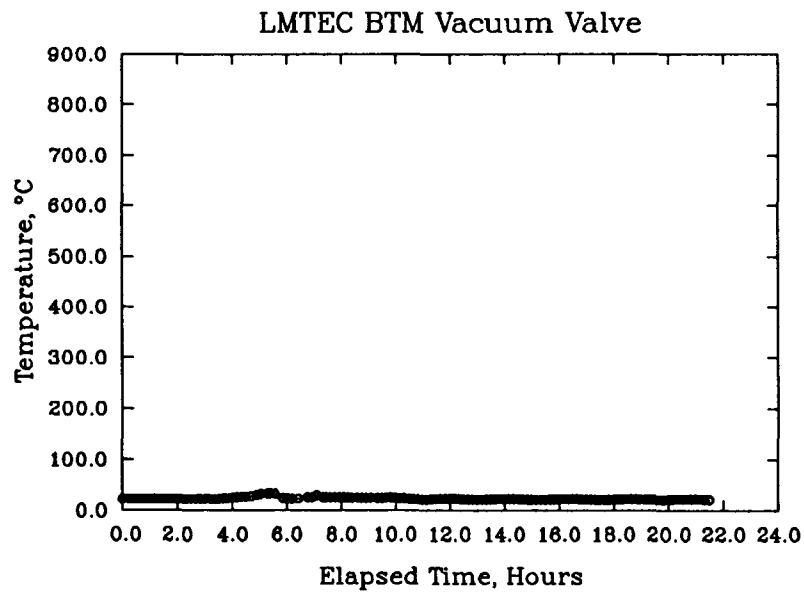
TC Index 21

3/26/87 10:35:39



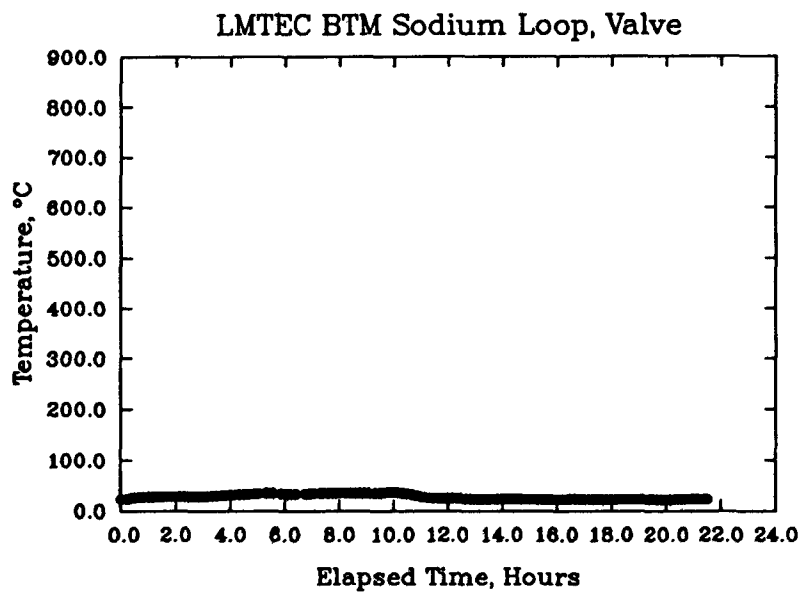
TC Index 22

3/26/87 10:35:39



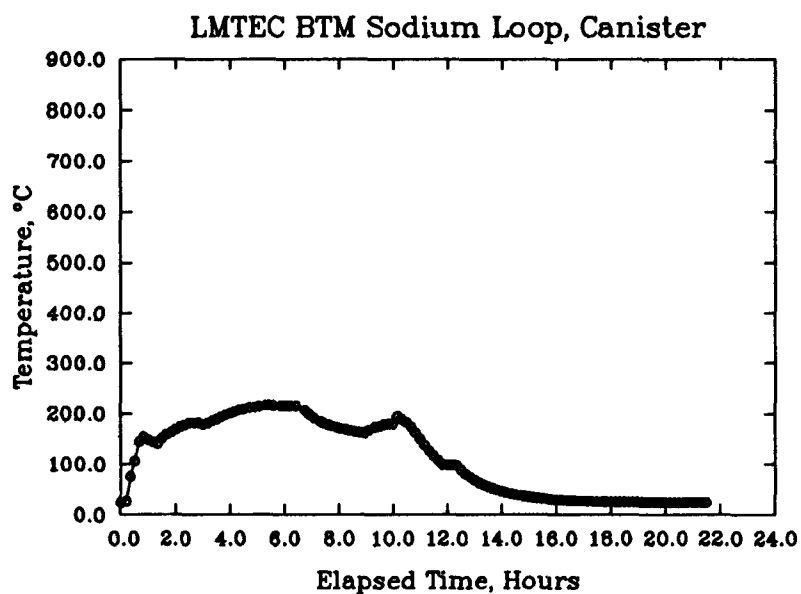
TC Index 23

3/26/87 10:35:39



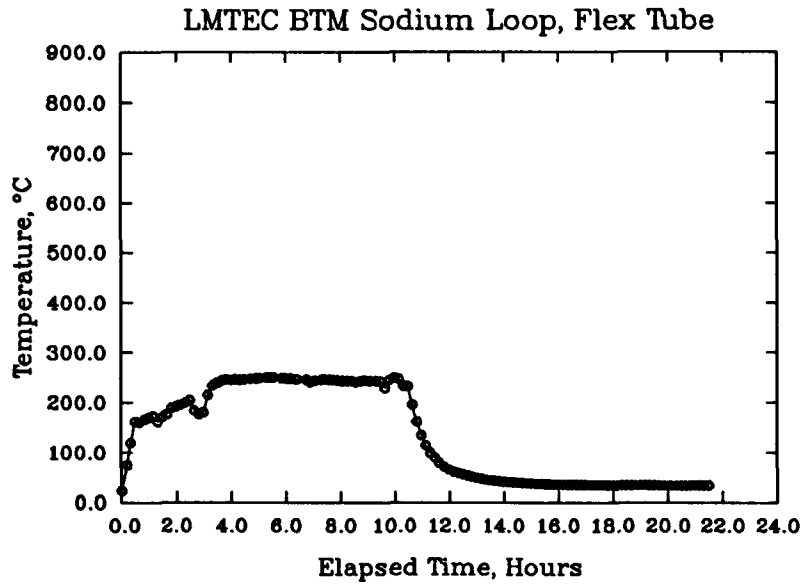
TC Index 24

3/26/87 10:35:39



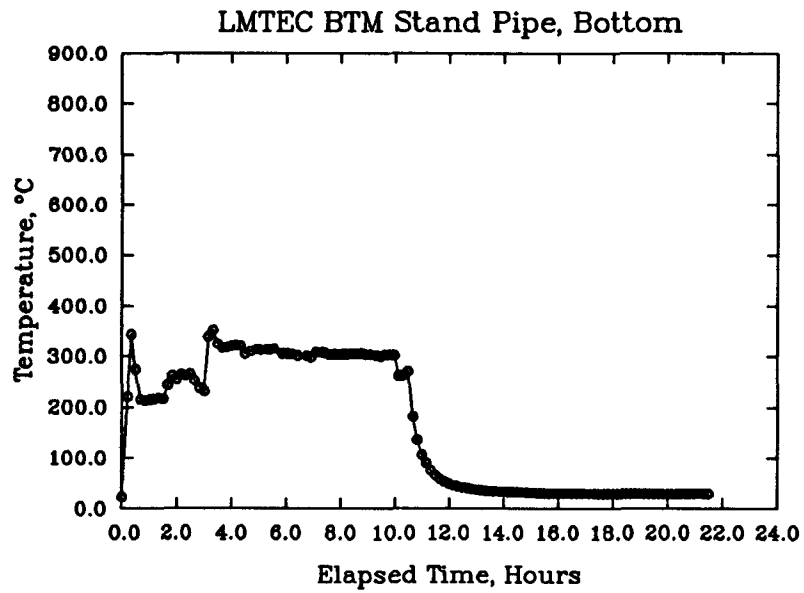
TC Index 25

3/26/87 10:35:39



TC Index 26

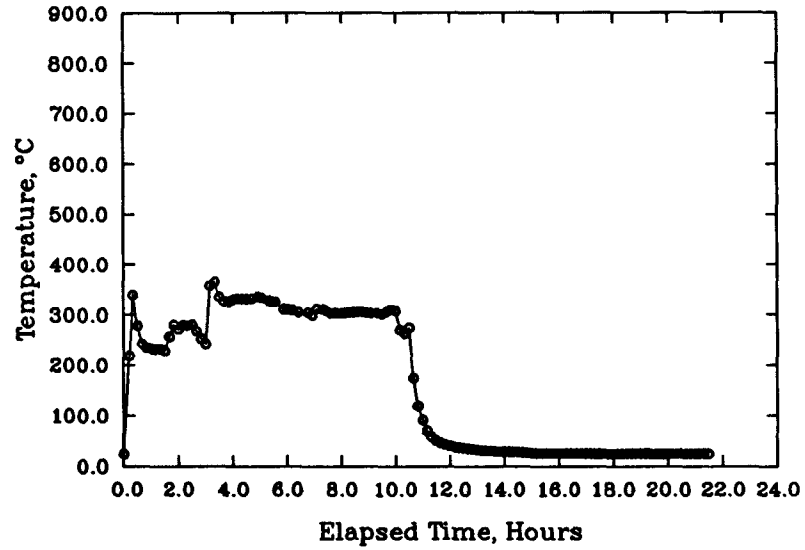
3/26/87 10:35:39



TC Index 27

3/26/87 10:35:39

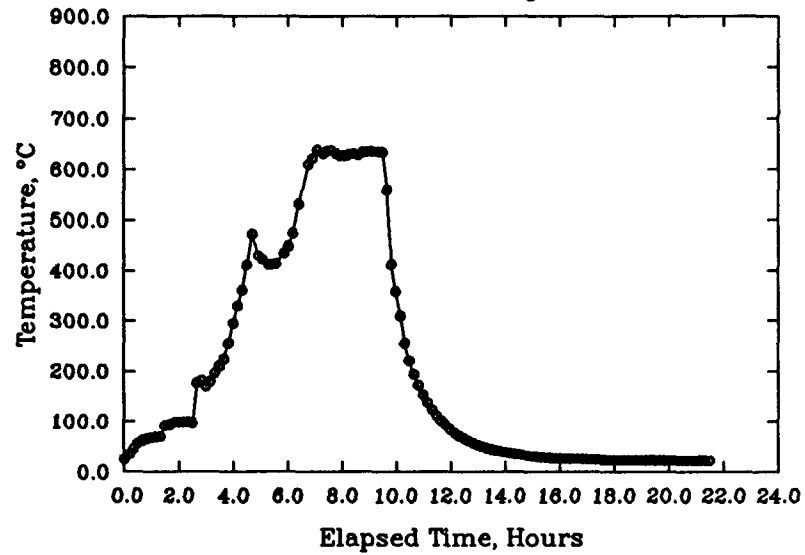
LMTEC BTM Stand Pipe, Top



TC Index 28

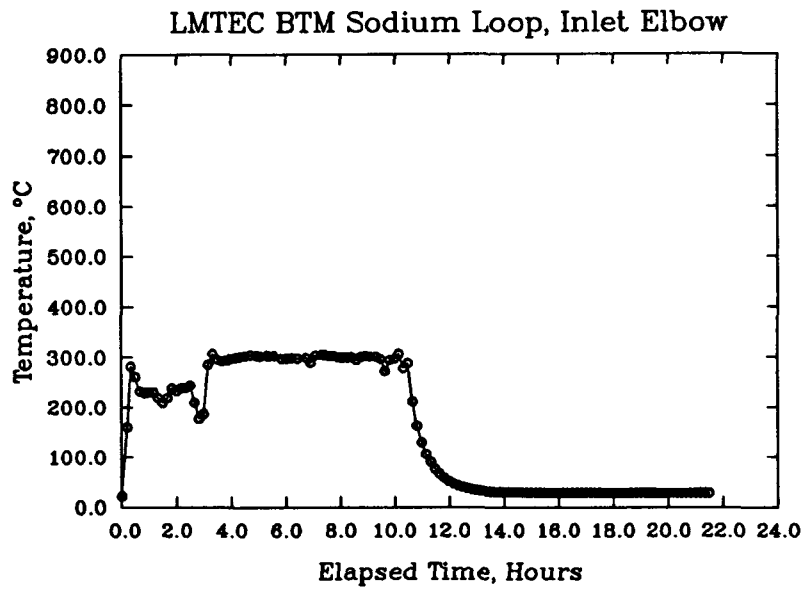
3/26/87 10:35:39

LMTEC BTM Sodium Loop, Boiler Inlet



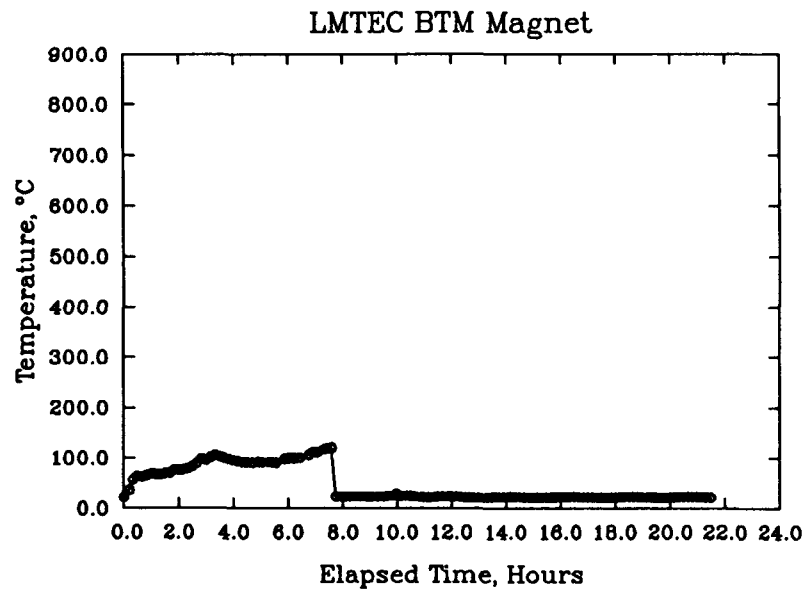
TC Index 29

3/26/87 10:35:39



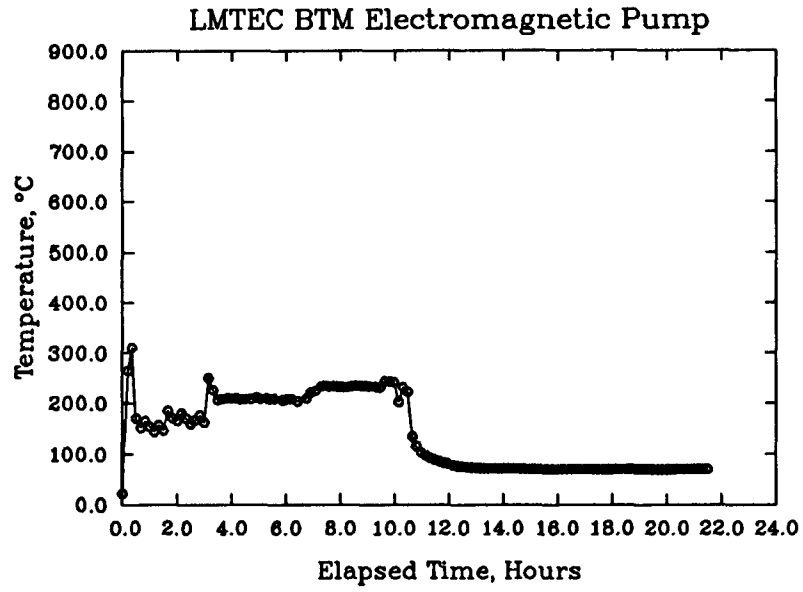
TC Index 30

3/26/87 10:35:39



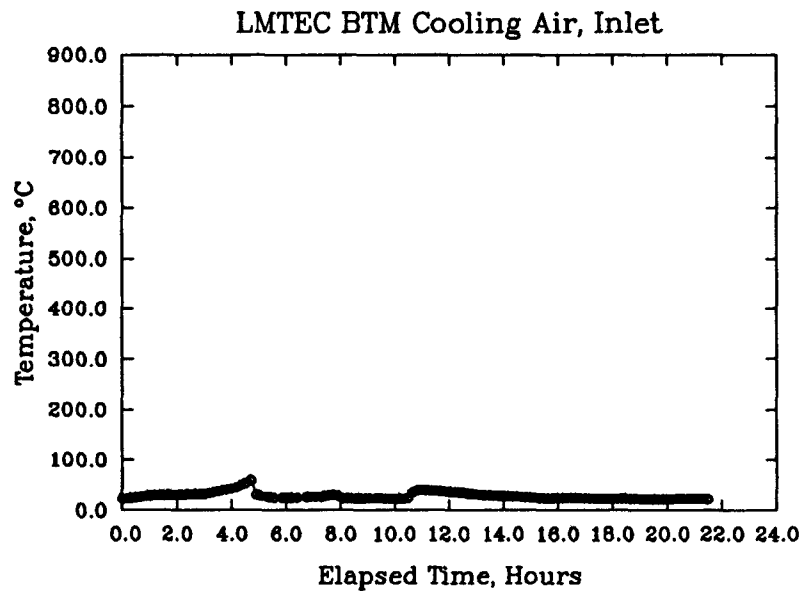
TC Index 31

3/26/87 10:35:39



TC Index 32

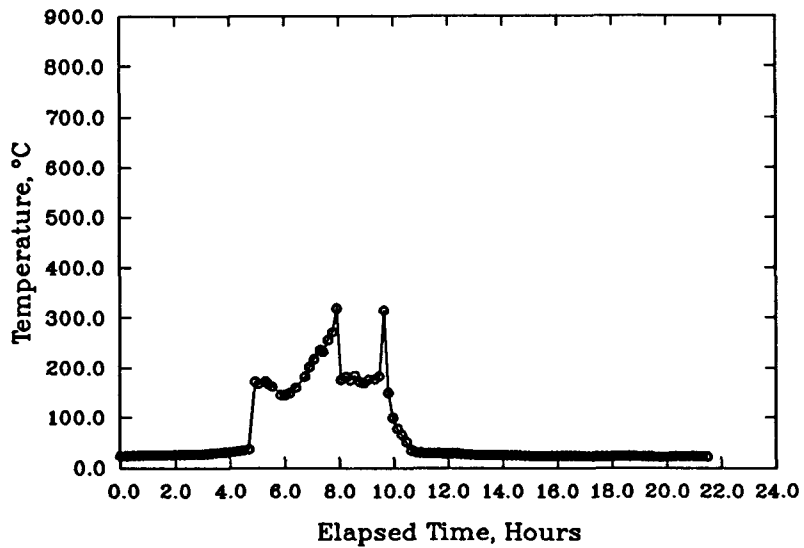
3/26/87 10:35:39



TC Index 33

3/26/87 10:35:39

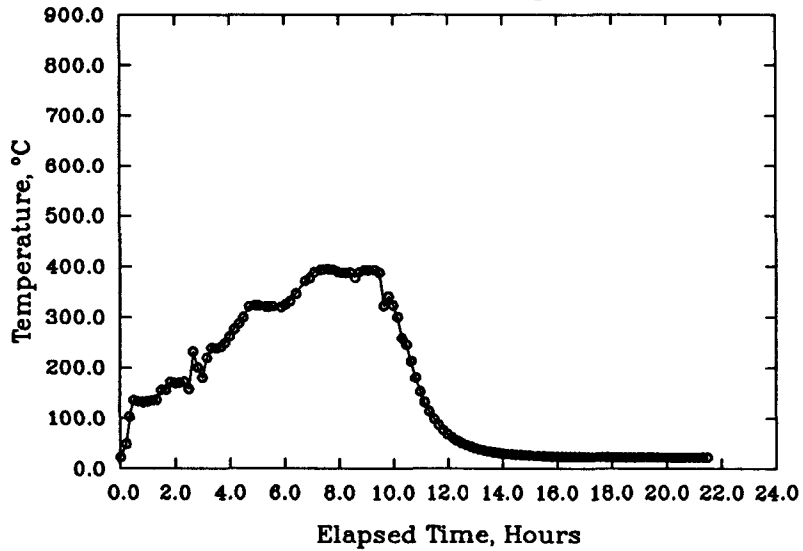
LMTEC BTM Cooling Air, Outlet



TC Index 34

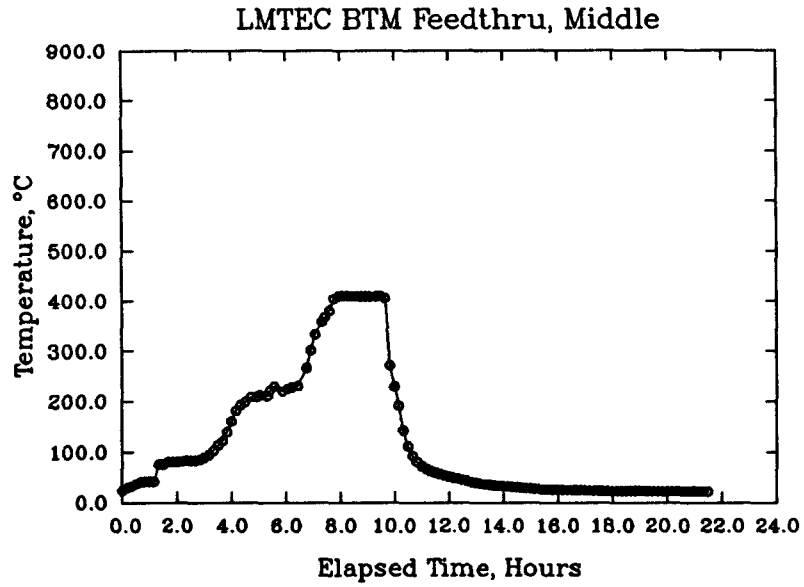
3/26/87 10:35:39

LMTEC BTM Sodium Loop, Inlet Tube



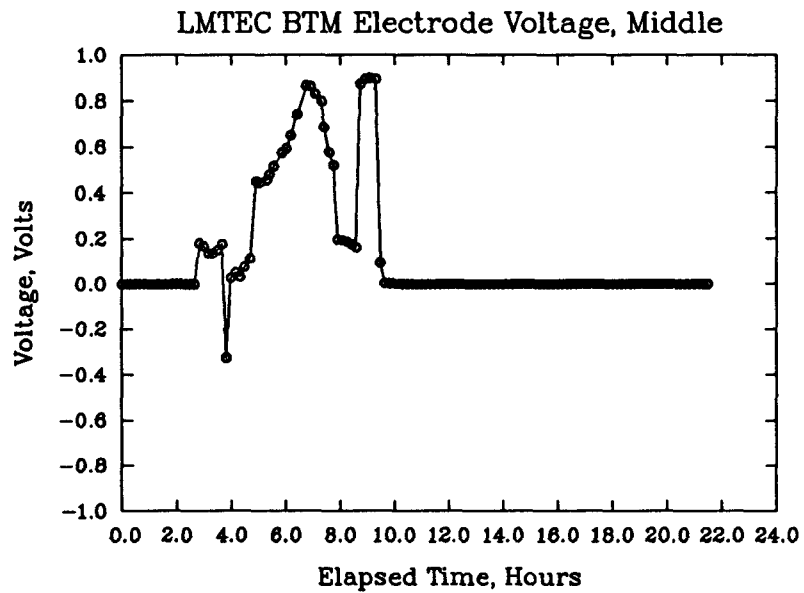
TC Index 35

3/26/87 10:35:39



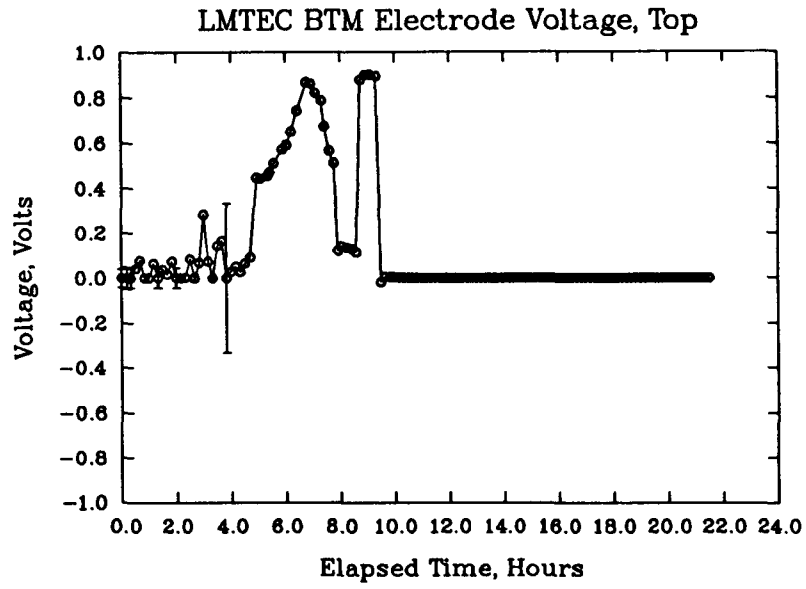
V Index 1

3/26/87 10:35:39



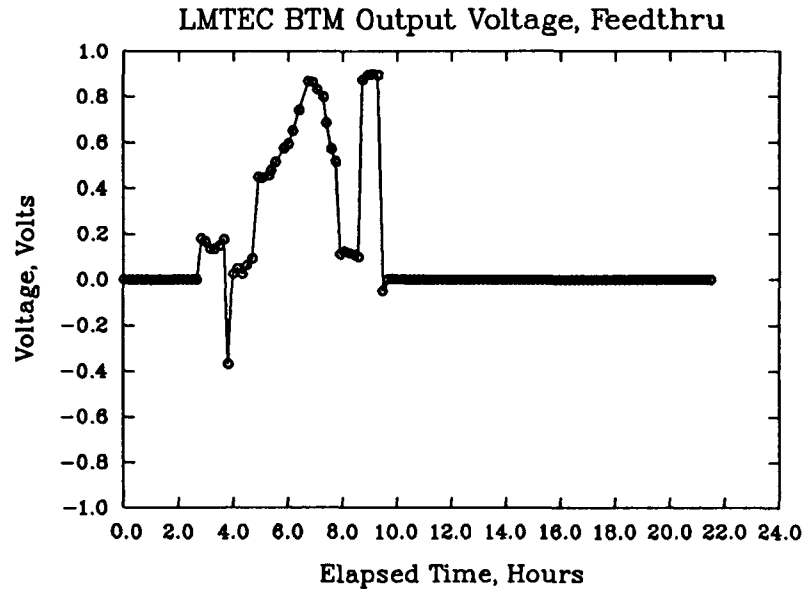
V Index 2

3/26/87 10:35:39



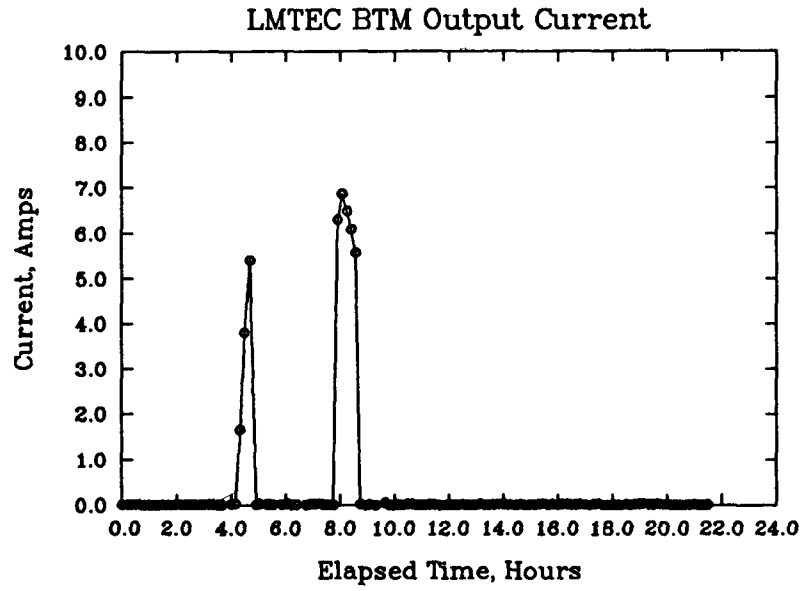
V Index 3

3/26/87 10:35:39



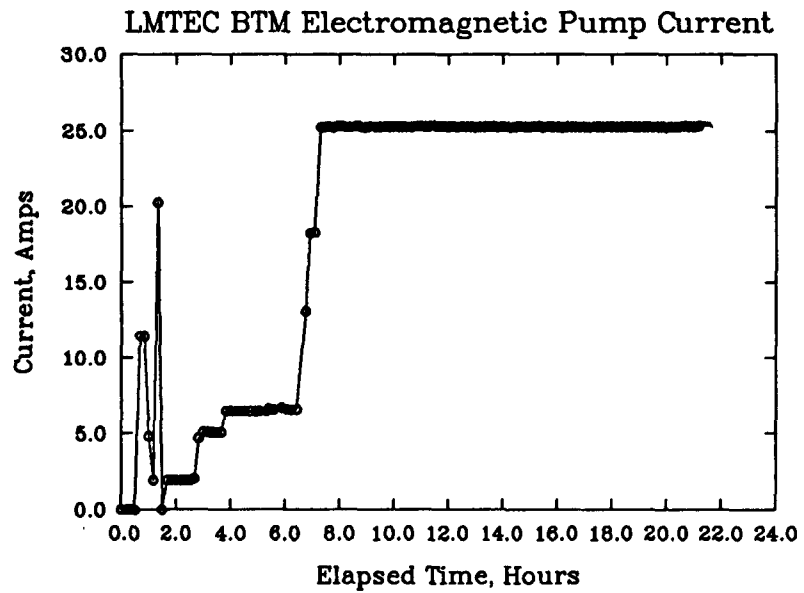
V Index 4

3/26/87 10:35:39



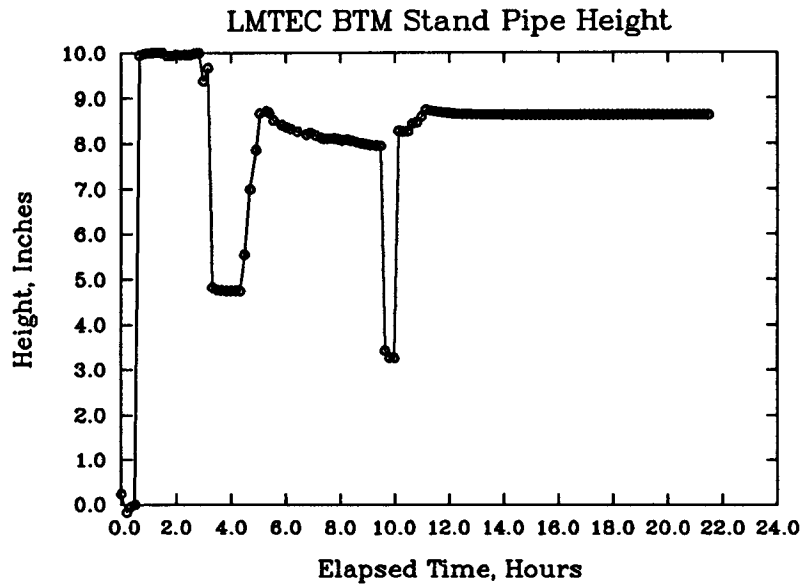
V Index 5

3/26/87 10:35:39



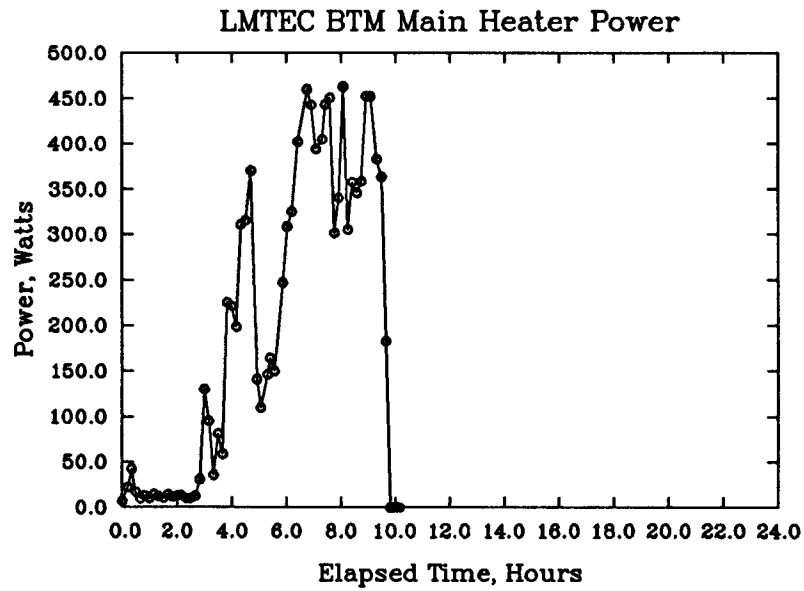
V Index 8

3/26/87 10:35:39



V Index 7

3/26/87 10:35:39



APPENDIX J
LMTEC PERFORMANCE MODEL

Blank Page

LMTEC Performance Model

A computer model of the Liquid Metal Thermal Electric Converter (LMTEC) was constructed for the purpose of making efficiency projections, guiding the design of the bench test modules, and aiding in the interpretation of experimental results. Efficiency projections obtained from the model have been reported on elsewhere ("Liquid Metal Thermal Electric Converter", L. L. Lukens, C. E. Andraka, J. B. Moreno, and J. P. Abbin; paper no. 879382, presented at and published in the proceedings of the 22nd Intersociety Energy Conversion Engineering Conference, August 10-14, 1987, Philadelphia, PA). In the post-test analysis of the LMTEC bench test module presented herein, a series of current-voltage characteristics were calculated with the model by varying the least-certain parameters in the model. The results were compared with the actual current-voltage characteristics to determine the most likely cause of the observed low output power.

A theoretical analysis of a "beta-alumina thermoelectric generator" was first presented by Weber (N. Weber, "A Thermoelectric Device Based on Beta-Alumina Solid Electrolyte", Energy Conversion, 14, 1, 1974). Thermodynamic limits were calculated for the maximum efficiency of devices using either sodium or potassium as the working fluid. A voltage-current relationship was derived and used in a model to calculate efficiency at maximum power for a device with an ideal porous electrode using sodium as the working fluid. Similar models have been subsequently presented by Hunt et al (T. K. Hunt and N. Weber, "Research and Development on a Sodium Heat Engine", final report under U.S. Department of Energy Contract No. DE-AC02-79ER10347, October 1982), and by Bankston et al (C. P. Bankston, T. Cole, R. Jones, and R. Ewell, Experimental and Systems Studies of the Alkali Metal Thermoelectric Converter for Aerospace Power", J. Energy, 7, 5, 1983).

The present work is an extension of these earlier models to include a systematic exploration of the effects of electrode degradation, electrode sheet resistance, vapor-flow induced pressure variation along the electrode surface, and alternative working fluids. All of these extensions are of great importance to the development of the LMTEC for solar application. The effect of electrode degradation and sheet resistance is of interest because it is currently a significant limitation on the performance of state-of-the-art LMTEC's. The effect of vapor-flow pressure variation has generally been neglected in previous analyses but can be important in both existing and proposed configurations.

Finally, the benefit of using working fluids other than sodium may be significant in solar and other applications and has not been previously explored in depth.

The basic phenomenological equations for the LMTEC can be found in Hunt and Weber's report. The effect of electrode degradation and vapor-flow pressure loss can be accounted for by adding additional back-pressure loss terms in the voltage-current relationship. These additional pressure losses correspond respectively to the transport of working-fluid vapor through the porous electrode and from the electrode to the condenser.

In some electrodes the transport of working fluid is believed to occur by a combination of efficient ionic conduction and relatively ineffective Knudsen flow. Electrode degradation is thought to occur as a result of the eventual loss of ionic conductivity in the electrode, according to Bankston et al. In the present work transport across the electrode is modeled by a Knudsen-flow pressure-loss term. Accordingly, it is a term proportional to the specific current times the square root of the product of the electrode temperature and the working-fluid atomic mass. The constant of proportionality was chosen so that the theoretical voltage-current relationship matched that of a good-performance degraded electrode as supplied by Hunt (T. K. Hunt, private communication and Bankston et al).

The transport of working-fluid vapor from the electrode to the condenser may occur in any flow regime from free molecular to continuum, depending on the fluid vapor pressure at the condenser and on the LMTEC dimensions and configuration. For the tubular Beta" alumina solid electrolyte (BASE) configuration with internal electrode that has been identified for solar application, most of the pressure loss should occur in the annular flow between the tube and its internal bus. An exact model of this flow is not currently feasible. For present purposes the pressure loss is modeled starting with an expression for the pressure gradient in an annulus. The expression varies smoothly with Knudsen number from an approximation for free molecular flow to the result for continuum laminar annular flow. This result is used to express the differential pressure drop along a differential length of the BASE tube. A differential mass addition to the flow is included, consistent with the local electrode specific current. The boundary condition at the mouth of the tube is taken to be the choked-flow pressure or the pressure in equilibrium with the condenser at zero current, whichever is greater.

As implied in the previous paragraph, the model for the tubular solid electrolyte with internal electrode is divided into differential axial segments. The overall scheme is illustrated in Figure J1. Each axial segment corresponds to the axial length of electrode served by one segment of the central bus and its set of current-collection fingers. The electrode is further divided into azimuthal segments corresponding to the area of electrode served by a single current-collection finger. Each such segment is further divided into differential azimuthal segments in order to account for voltage drops caused by current flowing in the electrode sheet to the fingers. Each differential azimuthal segment is modeled as a discrete LMTEC cell with its own specific current and its own cell potential, again as shown in Figure J1. Each cell potential is dependent on its own specific current and the local axially-varying sodium vapor pressure, as well as on the common boiler temperature and pressure. It is in series with the solid-electrolyte ionic resistance, and the series pair is shunted by the electronic resistance. Locally the differential segments are coupled by the electrode sheet resistance, and globally by the finger and bus resistances. The coupled network is incorporated into the overall circuit exactly as in the experiment.

Mathematically, the model described above takes the form of a large system of coupled nonlinear equations. In matrix form they are represented by a sparse matrix involving the linear terms and by a nonlinear nonhomogeneous term. The system is unstable to Picard iteration. Solutions have been obtained by implicit iteration, evaluating the nonhomogeneous term at the new iterate by locally linearizing about the old iterate. By capitalizing on the regular structure and sparseness of the matrix, significant savings have been realized in computational time and computer memory requirements.

A representative experimental current-voltage characteristic for the LMTEC BTM is shown in Figure J2. The boiler temperature in this case was 800 C and the condenser temperature was 230 C. The BTM electrical load consisted of a high-wattage resistor in series with a power supply. The first closed-circuit point corresponds to zero volts set at the power supply. Succeeding points correspond to incremental increases in the power-supply voltage which effectively decrease the BTM load.

The experimentally-produced voltages are seen to drop off very quickly with increasing current; the voltages on the bus at the feedthru and at the top of the electrode are much lower than on the electrode mid-way down the tube. In

contrast, the computer-model calculated characteristic is displayed in Figure J3. This result was produced assuming a "nominal" electrode (equivalent to the best degraded electrodes). With this assumption, the electrode/electrolyte interfacial pressure was calculated to be approximately two-thirds of a torr at 40 amps total current, varying only slightly along the length of the tube. The model calculation also assumed best estimates made before the test for vapor-flow pressure loss in the electrolyte-tube/bus annulus and for circuit electrical resistances. Compared with experiment, the computed result shows a much more desirable flat characteristic with considerably less difference between bus and electrode voltages.

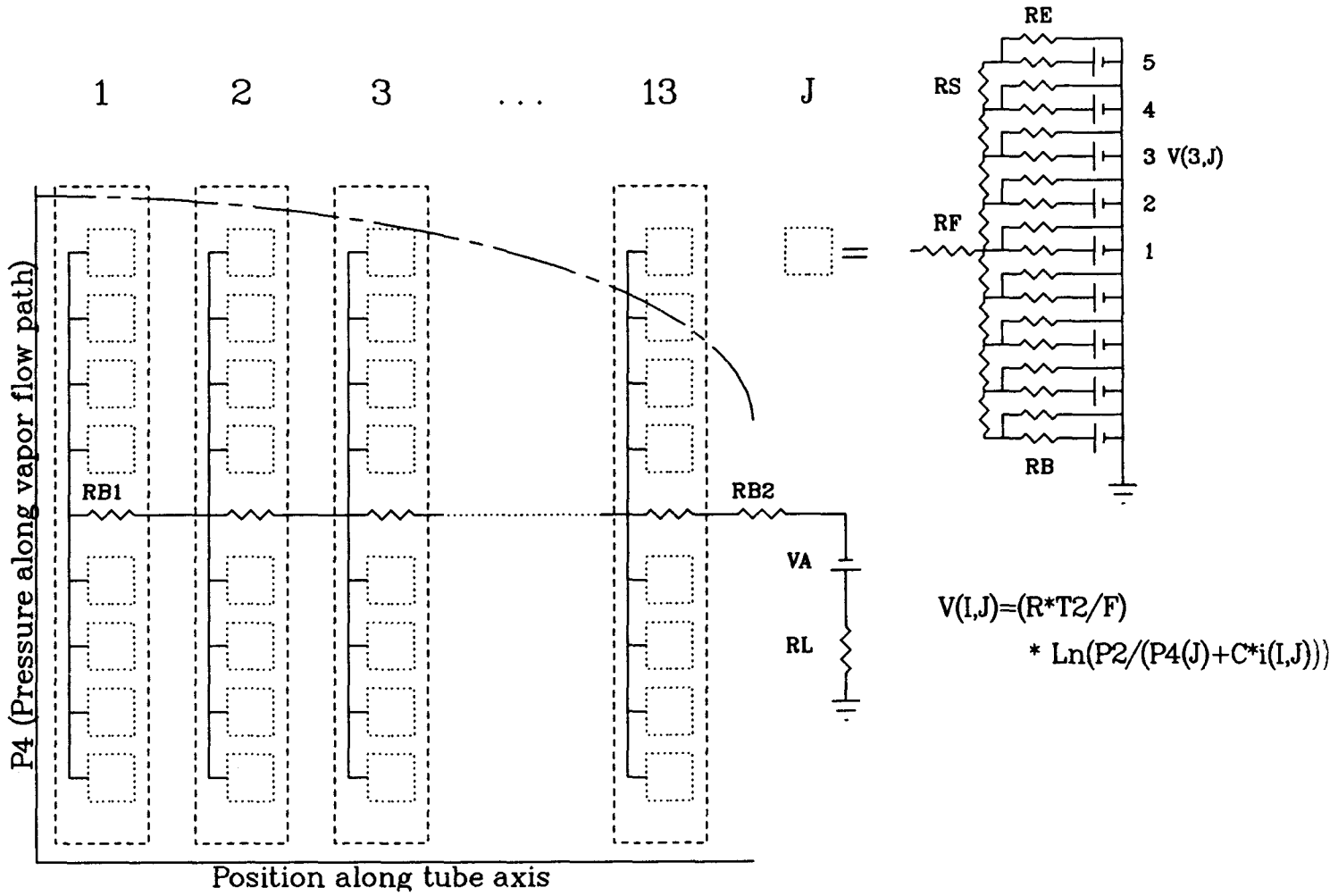
The voltage difference between the bus and the electrode can only be a result of high contact resistance between the current-distribution fingers and the electrode. The other possibilities - finger resistance, electrode sheet resistance, etc - are known with good confidence. A contact resistance of 1.3 ohms brings the calculated voltage between the middle electrode and the bus at the feedthru into good agreement with experiment. This resistance is also in agreement with values measured after the experiment (see Appendix H).

The small observed voltage difference between the top of the electrode and the bus at the feedthru is believed to be a result of shorting of the voltage probe to the bus. The small observed voltage difference is consistent with the measured resistance along the bus between these two points as is evident in all of the model results.

The rapid and nonlinear decrease in voltage as current increases from open circuit could only be modeled by assuming a very large electrode vapor-flow resistance (FigureJ4) or by multiplying the pressure gradient in the annulus by a large constant (FigureJ5). In either case the necessary increase is approximately a factor of 1000 over nominal values. In the latter case the model demonstrated that the electrode voltage would vary significantly with axial position, as can be seen in Figure J5. Unfortunately, the failure of two out of three electrode-voltage probes made it impossible to detect such an axial variation. Nevertheless, it seems extremely unlikely that the annular-pressure-drop calculation could be in error by a factor of 1000. Conversely, it appears very likely that the tungsten electrode that was used in the BTM could have been 1000 times more resistive to vapor flow than expected. At the time that the BTM was assembled, there was no way to pre-evaluate the electrode. Since the test however, a simple

test has been devised (see Appendix K). The results obtained by this independent method, with a CVD tungsten-coated tube similar to the one used in the BTM, are consistent with the inference from the model that the electrode was 1000 times more resistant to vapor flow than desired.

Figure J1. LMTEC Model Network



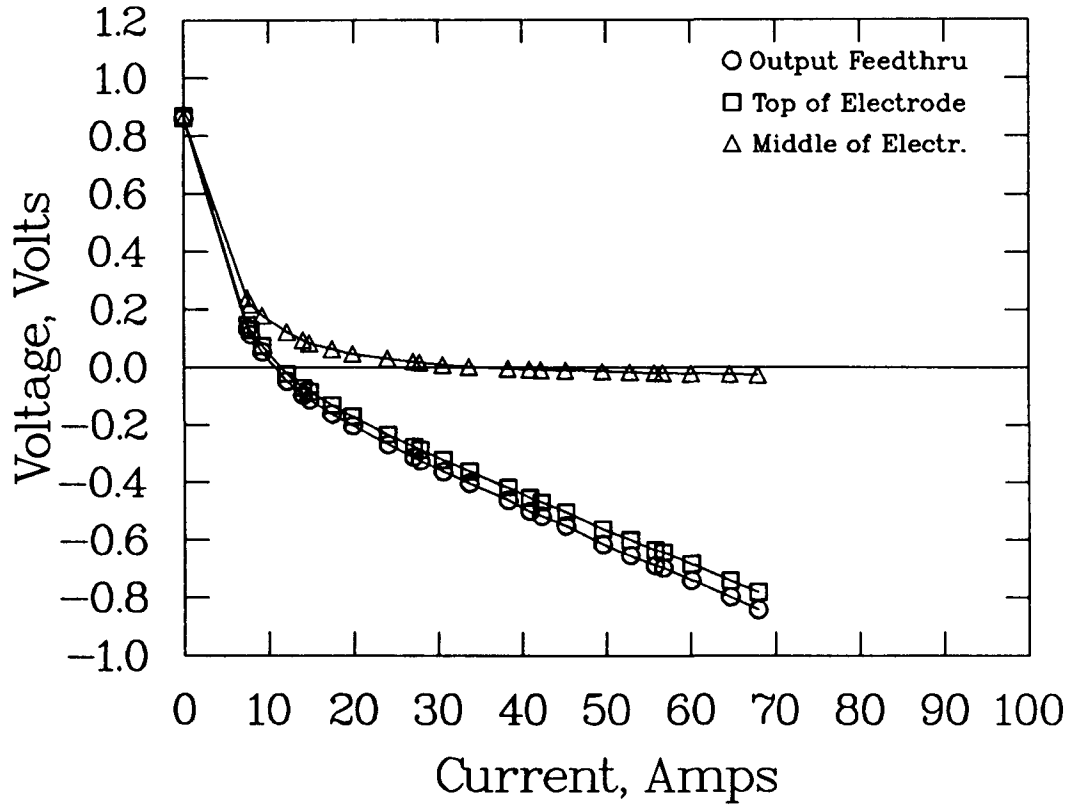


Figure J2. LMTEC BTM Experimental V-I Characteristics.

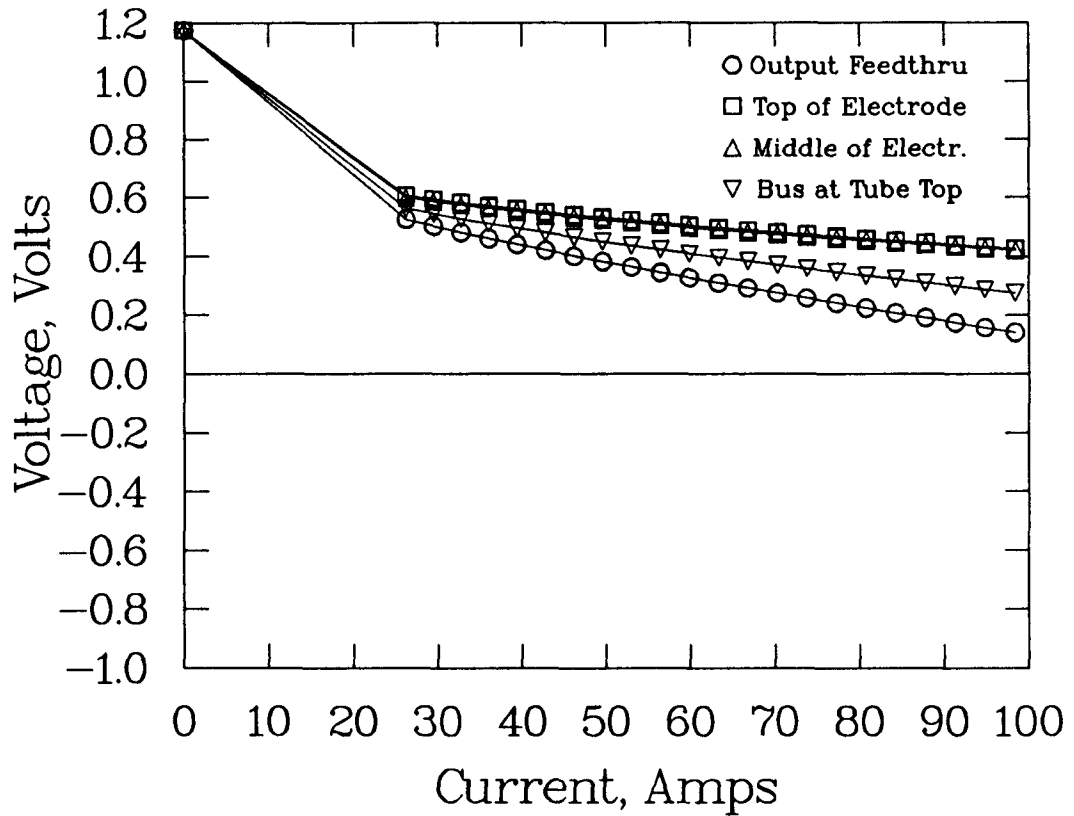


Figure J3. V-I Curves Calculated Using Initial Estimates For Electrical Resistances And Electrode Flow Resistance.

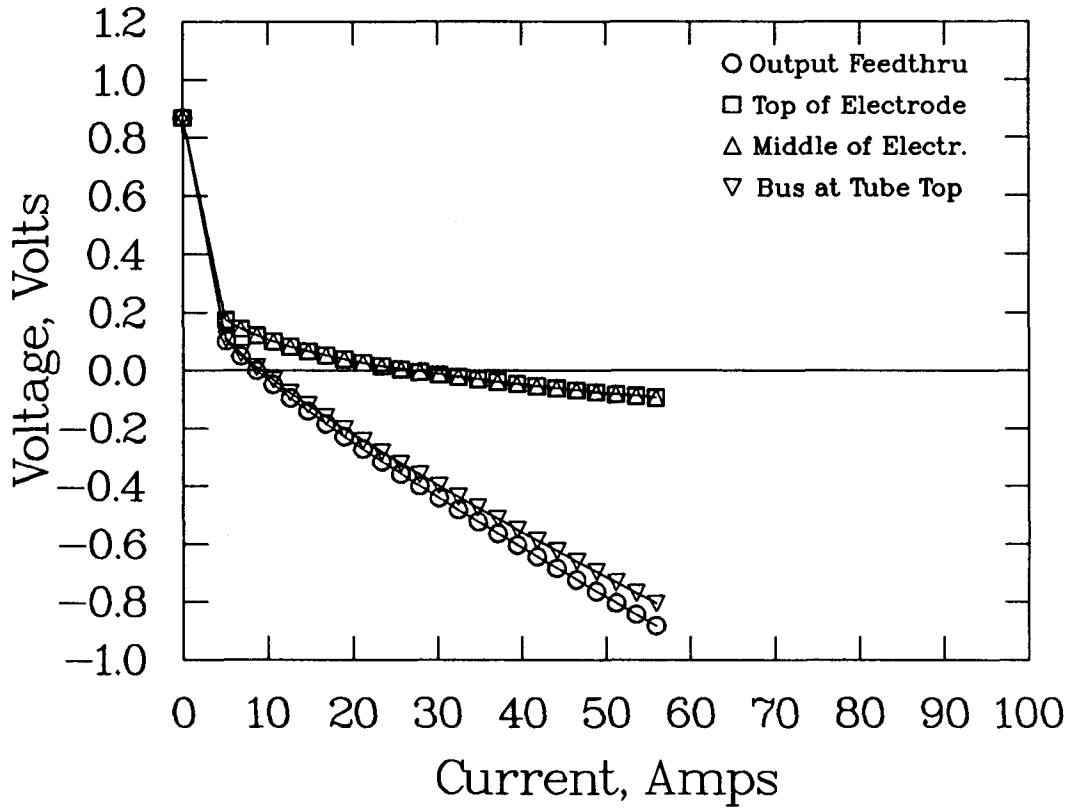


Figure J4. V-I Curves Calculated Using 1.3 ohm Finger To Electrode Resistance And 1000 x Nominal Electrode Flow Resistance.

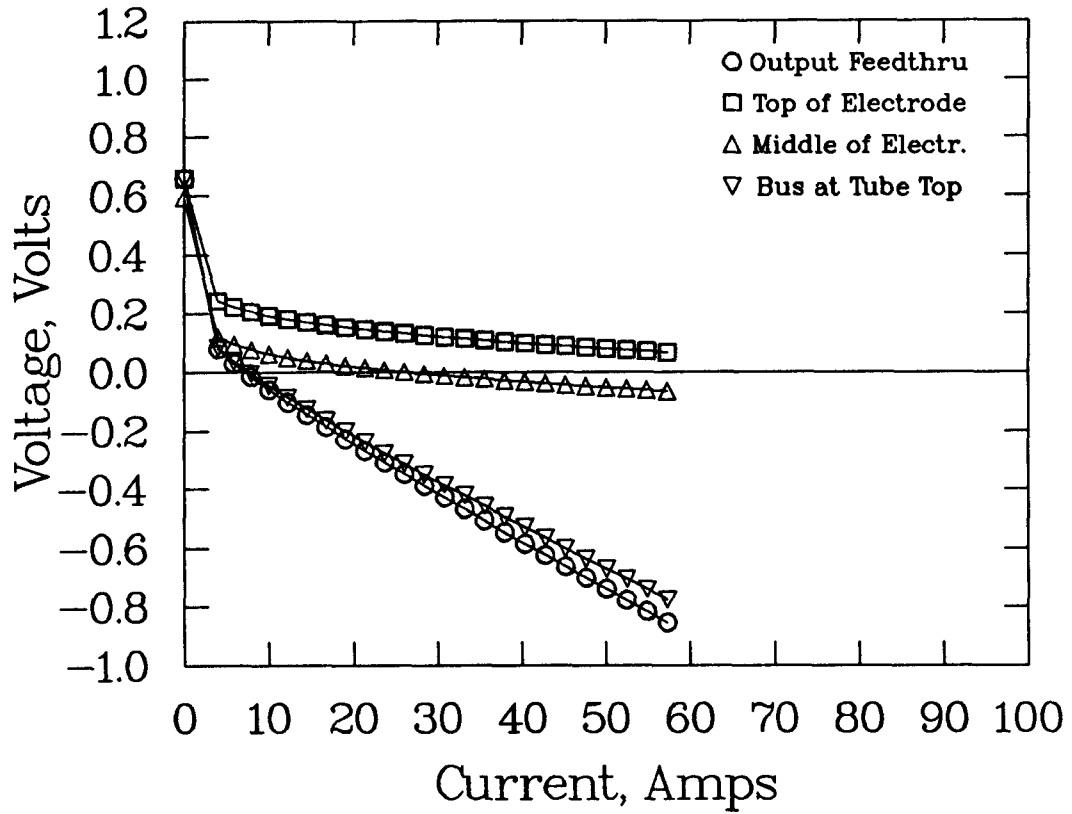


Figure J5. V-I Curves Calculated Using 1.3 ohm Finger To Electrode Resistance And 1000 x Nominal Annulus Flow Resistance.

APPENDIX K
BENCH TEST MODULE POSTMORTEM

Blank Page

Bench Test Module Postmortem

An extensive postmortem of the Bench Test Module (BTM) was conducted. The primary goals of the postmortem were to explain the much lower than expected maximum power and the unexpected loss of boiler pressure which ended the operation of the BTM. The cause of the low power output and the loss of boiler pressure were covered in the body of the the report. A memo documenting the electrode permeability test which verified the cause of the low power output is included. This appendix includes a section on postmortem notes which details the the disassembly of the BTM.

The computer modeling effort which helped explain the low power output of the BTM also indicated the possibility of high contact resistance between the buss and the electrode. This high resistance could have been in the contact of the fingers with the electrode or the buss to the fingers. An experiment has been conducted to measure contact resistance at up to 800 C. The contact resistance between the fingers and the electrode was 1 to 3 ohms. This agrees with the inferences made using the model. The resistance between the finger assembly and the buss was negligible on the same scale. A memo documenting this experiment is included.

Postmortem Notes

The following observations were made from the LMTEC BTM data sets printed out at 20h 10m 2s and at 20h 11m 19s on March 26, 1987. During this time period;

The electrode voltages changed to approximately 0 volts.

The feedthru voltage changed from -1.536 to -.406 volts.

The current being driven through the LMTEC changed from 136 to 318 amps. This current was applied by an external power supply as part of a planned test. It was not generated by the LMTEC BTM.

The main heater power changed from 355 to 318 Watts.

The height of sodium in the stand pipe changed from 8 to 4 inches.

The boiler inlet and the boiler temperatures decreased.

The condenser and condenser outlet temperatures increased.

The following observations were made after the LMTEC BTM had been shut down and cooled to room temperature:

The main feedthru is shorted to the LMTEC body with a resistance of approximately 0 ohms.

The instrumentation feedthru to the top of the electrode is shorted to the LMTEC body with a resistance of Approximately .8 ohms.

The instrumentation feedthru to the middle of the electrode is shorted to the LMTEC body with a resistance of Approximately 0 ohms.

When the insulation was removed from the LMTEC BTM a white and green substance was observed in area where the thermocouples are brazed into the boiler. The substance appeared to be the product of a corrosive reaction.

In preparing the boiler section for Xray photography the BTM boiler thermocouples had to be bent to one side to allow proper placement of the film. While attempting to bend the thermocouples 5 out of 7 broke off flush with the boiler surface.

An attempt to pressurize the condenser section (the low temperature zone) of the LMTEC BTM had no effect on the pressure gauge between the electromagnetic pump (EM pump) and the boiler. (This pressure gauge is located on the sodium feed line between the EM pump and the high temperature zone, a schematic of the LMTEC BTM, see Figure 2, in the main body of the report, shows the sodium line, the EM pump and the boiler.) The condenser was pressurized by heating the sodium line to the condenser outlet to melt any sodium which might be plugging the line and back pressuring the line with argon. When the sodium plug melted there was an unexplained rise in pressure in the argon supply line.

The pressure gauge inlet was heated to melt any sodium that might be present. The pressure gauge then changed from reading a good vacuum to reading atmospheric pressure. This verified that the pressure gauge was blocked by a sodium plug. The sodium line to the condenser outlet was reheated to melt any sodium which might be plugging the line while the pressure gauge was still above the melting point of sodium. The condenser was then pressurized with argon and the gauge between the EM pump and the boiler indicated the pressure rise. This confirmed that there was a breach between the boiler and condenser sections of the LMTEC BTM.

With the LMTEC BTM pressurized with argon the locations where the boiler thermocouples had broken off were checked and large leaks to the atmosphere were detected. The inside of the LMTEC has therefore been exposed to air since it has cooled down.

The following observations were made from Xray photographs of the LMTEC BTM:

There is no apparent damage to the Beta" alumina tube or the Beta" alumina to stainless steel joint assembly.

There is no evidence of sodium inside the Beta" alumina tube.

There is evidence of a small amount of sodium on the shelf of the boiler where the boiler diameter changes from 1.5 to 3 inches. There is also evidence that the annular disk between the bulkhead and the bottom of the radiation shield is nearly full of sodium.

The BTM was removed from the fume hood. The boiler inlet tube and the condenser outlet tube were cut off so that the BTM would fit in the glove box air lock. The boiler inlet tube was clear of sodium. The condenser outlet tube was also clear of sodium.

When the mini-conflat fittings that connected the BTM to the vacuum system were disassembled a large amount of sodium was discovered. The vacuum line coming from the top of the boiler was full of sodium at the mini-conflat fitting. The sodium contamination was seen as far away as the main valve on the vacuum system.

Inside the air lock the VCR fittings in the sodium loop were disassembled.

The canister weighed 638 gm compared to 735 gm when installed in the BTM sodium loop.

The bottom of the boiler was cut off as close as possible to the copper bus bar using a modified tubing cutter. The cut was slightly below the bottom of the Beta" alumina tube. No cracks were visible on the bottom of the Beta" alumina tube. There was a light coating and a few drops of sodium on the bottom of Beta" alumina tube. The baffle plate and tantalum wire in the bottom of the boiler were covered with sodium. There was a small path through the sodium to the boiler inlet tube.

The remainder of the boiler was cut off in the three inch section just above the weld joint at the transition from the smaller diameter to the three inch diameter. A Dremel tool with an abrasive cutoff wheel was used to make the cut. A large circumferential crack was visible approximately 3/4 inch below the molybdenum to Beta" alumina braze joint in the Beta" alumina. An extensive network of smaller cracks was visible throughout the bottom half of the Beta" alumina tube. There was circumferential build up of material, "fluff," that was yellow, black and white in color about 1 inch below the molybdenum to Beta" alumina braze joint on the Beta" alumina. In scraping off a small sample of the material it was apparent that it was mostly solid sodium. The outside molybdenum sleeve and the Beta" alumina tube adjacent to it had a heavier coating than the remainder of the Beta" alumina tube. The area where the molybdenum backup ring joins the molybdenum sleeve and where the molybdenum sleeve joins the stainless steel bulkhead were filled with fillets of sodium. The middle section of the inside of the boiler was very clean.

An opening was cut in the condenser section using a Dremel tool with an abrasive cutoff wheel. The copper bus was clean and shiny with the exception of a very light white film. The alumina insulation on the main power feedthru appeared to be copper colored. There was a high level mark from the sodium about 3/4 inch above the bottom of the condenser sump. An examination of the inside of the engine above the bulkhead was made with a bore scope. There was no evidence of any shorting of the bus or the voltage probe wires in this area. The thermocouple brazed into the section of the condenser wall that was removed broke off easily with one or two flexes.

The copper bus was cut where it joins the main power feedthru using a jewelers saw. This was accomplished by making a second opening in the condenser opposite the initial opening and threading the blade of the jewelers saw through the two openings. When the bus separated the major crack in the Beta" alumina tube opened up.

The top of the condenser was cut off using a Dremel tool with an abrasive cutoff wheel. The bus was shorted to the body by a film of sodium on the Beta" alumina connecting the top molybdenum fingers to the molybdenum sleeve. The main power feedthru was not shorted (it was checked through the 200 k ohm scale). The voltage probe feedthru to the top of the electrode was shorted to the lid with a resistance of 4.2 ohms. The voltage probe feedthru to the middle of the electrode was not shorted (it was checked through the 200 k ohm scale). A short was detectable if the nickel wire was pushed hard to the side on the voltage probe feedthru to the middle of the electrode. The voltage probe wire to the middle of the electrode was not shorted to the bus. The voltage probe wire to the top of the electrode was shorted to the bus by a film of sodium on the Beta" alumina.

The bus was pulled out of the Beta" alumina tube leaving the section of the Beta" alumina tube below the major crack separated from the rest of the tube. Very little sodium was seen inside the Beta" alumina tube except near the open end of the tube and in the bottom of the tube where a film was present. The bus and molybdenum fingers appeared very clean and shiny except for the top molybdenum fingers which had some sodium on them.

The top of the bulkhead was clean and shiny. The annular gap between the bottom of the radiation shield and the top of the bulkhead was full of sodium. The inside diameter of the radiation shield was coated with sodium frost in the area

between the bottom of the sump and the high sodium mark in the sump. The bottom of the sump was full of sodium, covering most of the tantalum wire in the sump. The condenser wall was coated with sodium to the top of the engine. The sump wall opposite the condenser wall was clean above the high sodium mark.

The sheet resistance of the tungsten coating in the section of the Beta" alumina tube which separated from engine was measured. It was found to be about three times higher than was measured in a previous sample (9/3/86). This increase may be due in part to the extensive cracking of the Beta" alumina.

The resistance of the bus from the bottom nut on the bus to the end cut from the main feedthru was measured. The resistance was 0.44 milliohms, about 5.5 times larger than would be expected for a pure copper rod 3/8 inch in diameter 14 inches long. The increased resistance is probably the contact resistance between the bus nuts and the bus.

The resistance from one molybdenum finger through the bus to another molybdenum finger about one inch away axially was measured. The resistance was 10. milliohms, about two times higher than the calculated resistance with no contact resistance along the path. The increased resistance is probably the material interface contact resistances along the path.

date: July 23, 1987

to: DISTRIBUTION

from:  J. B. Moreno, 2541

subject: Glove Box Test of Electrode Permeability

A possible method to assess LMTEC-electrode permeability has been conceived and tested.

The results indicate that the CVD tungsten electrode used in Bench Test Module #1 (BTM-1) is approximately 1000 times less permeable than a nominal electrode. This is consistent with inferences that had previously been made by comparing model predictions to BTM-1 test results.

An attempt to evaluate the Leonard Reed molybdenum electrode was not successful for reasons that were anticipated. A more generally applicable extension of the testing method has been formulated and may make it possible to evaluate the molybdenum electrode.

Details are presented in the attached appendix. Comments and criticism are invited.

Attachments

DISTRIBUTION:
1842 Bill Hammett
2523 Frank Delnick
2541 Joe Abbin
2541 Chuck Andraka
~~2541 Larry Dukens~~

APPENDIX

The method used to evaluate the tungsten electrode is based upon the idea of arranging a coated beta" tube so that a voltage-driven ionic current through the tube is limited by the vapor-pressure driven flow of neutrals through the electrode. This was accomplished by filling a tube with sodium and immersing it in a sodium pool at 350°C. The particular arrangement used gave an estimated 24 cm² of active electrode area.

If a voltage is applied so as to drive sodium from the uncoated to the coated side of the tube, the usual ohmic voltage-current relationship will be observed. The electrode will have a negligible effect because a very small additional voltage is all that is necessary to produce the pressure increment corresponding to neutral-sodium flow resistance in the electrode (see the memo of May 28, 1987 from Moreno to Distribution, "Clarification of LMTEC Voltage Dependence on Pressures; Impact on Electrode Permeability Measurement"). On the other hand, if the voltage polarity is reversed, then the flow of neutral sodium through the electrode can be driven only by a pressure associated with the liquid sodium.

More specifically, if the electrode is not wetted by sodium, then flow in the pores is gaseous, and is driven only by the saturated vapor pressure of sodium. This vapor pressure is only 10⁻⁴ atmospheres at 350°C. It is easy to show under this condition for a nominal electrode or worse, that the evaporation rate from the liquid sodium surface at the mouth of a pore will not be a limitation. Rather, the combination of pore size and abundance, and vapor pressure, will limit the flow of neutral atoms through the electrode and therefore the ionic current that can be produced by the applied voltage. This current limit is thus a measure of electrode permeability.

On the other hand, if electrode wetting does occur, then sodium will enter the pores and liquid flow will occur driven by the static pressure applied to the sodium. In this case it can be shown that flow resistance will not limit the ionic current that can be driven by an applied voltage. Then the present method will not be useful.

Figures 1-3 (attached) show data taken under the stated conditions for both voltage polarities. The time sequence of the data is indicated by the numbers

adjacent to the points. In Figure 1 the slope of the current-voltage curve when sodium exits through the electrode yields an ionic resistivity of 8.1 ohm-cm. At higher voltages (Figure 3) the data indicate 5.6 ohm-cm, and data taken earlier with a similar tube yielded 4.3 ohm-cm. Weber et al report 2.8 ohm-cm at 350 °C. The significance of these various differences is not yet clear. The current-voltage data for the opposite polarity (Figure 1) show the expected current plateau. For a nominal electrode this plateau would occur at 910 mA. Thus the present electrode appears to be about three orders of magnitude less permeable than a nominal electrode.

Figure 2 shows data taken at higher applied voltages. These data indicate a slight increase in current as voltage is increased and further increases at a given voltage as time passes. However it should be understood that the unlimited ionic current at (for example) 0.5 volts would be on the order of 35 Amps! Moreover, the evaporation rate limit is 17.5 Amps. Figure 3 shows the data on yet another voltage scale, continuing the trends noted for Figure 2.

Tentatively the data in Figures 1-3 are being interpreted as follows: at early times, little wetting of the tungsten has occurred and the vapor-pressure flow limit applies. As time passes, electrode wetting progresses until all of the electrode is finally wet. Because wetting of a pore removes that pore from the flow-limiting category, an ohmic current-voltage curve of progressively larger slope is added to the original current plateau. Consistent with this interpretation, the tungsten electrode was found to be partially wet with sodium at the end of the test.

Figures 4 and 5 show data taken with the molybdenum-coated tube, again near 350°C. Very little effect of voltage polarity can be seen. This suggests that the molybdenum electrode was promptly wet by sodium. Consistent with this, it was observed that the molybdenum was completely wet by a tenacious coating of liquid sodium at the end of this very brief experiment. The slope of the current-voltage curve yields an ionic resistivity of 5.4 ohm-cm, which falls in the range of values mentioned earlier. The slight voltage offset at zero current is tentatively attributed to electrode chemistry.

An extension of the testing method may make it possible to avoid the problem of wetting. The extension would require that the test be carried out in a vacuum chamber. The beta" tube would be immersed in a sodium

pool as before, but would not be filled with sodium. Instead, sodium would be delivered to the electrode by vapor flow from the pool. An internal bus with voltage probes as in BTM-1 would be necessary. The heat source would be inside the tube, possibly incorporated into the bus. With this arrangement, wetting of the electrode should be avoidable, so that the molybdenum electrode could be evaluated. While considerably more complicated than the original test, this method would still be very much simpler than building a LMTEC bench test module.

ULTRAMET W-COATED TUBE

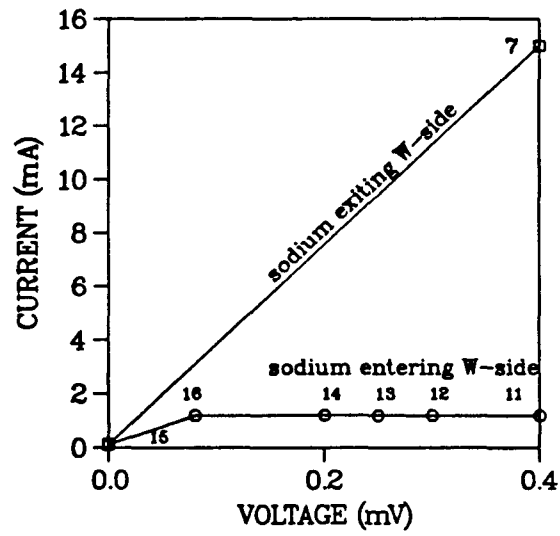


FIGURE 1

ULTRAMET W-COATED TUBE

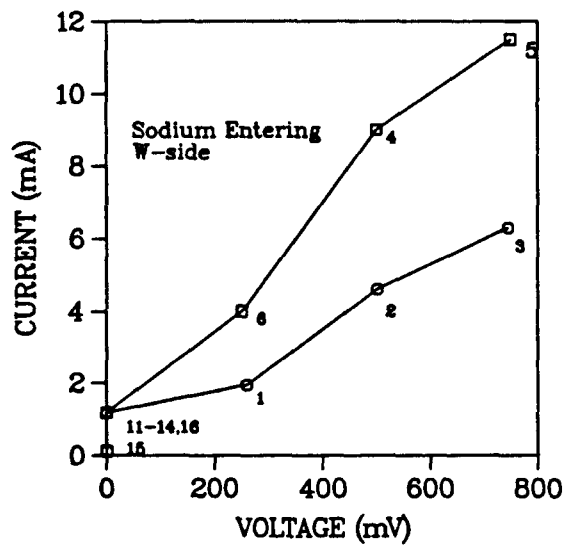


FIGURE 2

ULTRAMET W-COATED TUBE

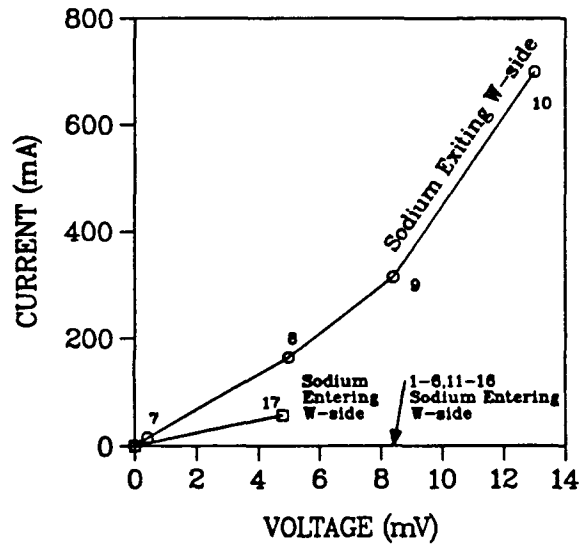


FIGURE 3

REED'S Mo-COATED TUBE

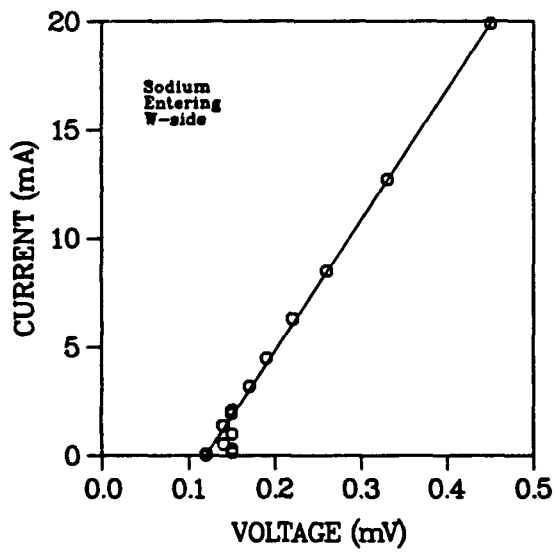


FIGURE 4

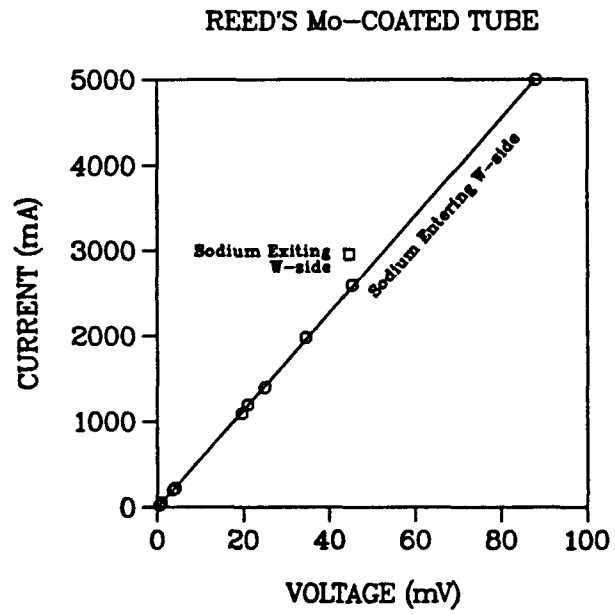


FIGURE 5

Sandia National Laboratories

date: July 6, 1987

Albuquerque, New Mexico 87185

to: J.P. Abbin



from: C. E. Andraka, 2541

subject: Contact resistance experiment

An experiment was conducted to determine where the high resistance in LMTEC occurred. The resistance was identified by Jim Moreno's analytic model. The possibilities included contact resistance between the fingers and the electrode and contact resistance between the fingers and the buss.

A previous experiment had been performed before LMTEC, which indicated that contact resistance was low and did not change with time. However, at that time, no electrode was available. A thin moly foil was wrapped inside a Beta" tube to simulate an electrode.

The test setup is illustrated in figure 1. Two separate assemblies were aligned and spaced by an alumina tube. Each assembly has one spider set and one electrode voltage probe. The current source is connected to one buss (#7), and ground connected to the other (#2). All voltages were measured relative to the external connection to ground (#2). This is a typical 4-wire resistance measurement. The current must flow from the buss, through the fingers, through the electrode, and into the second set of fingers and buss. The isolated voltage probe sense the voltage of the electrode near the interface with the finger, so the resistance of the contact may be measured.

This experiment is designed to locate a resistance on the order of 2 ohms. The resistance of the buss and of the finger, as shown by measurement and calculation, is negligible compared to the expected 1-2 ohm contact resistance. The sheet resistance should be on the order of 0.042 ohms/square at room temperature, and may be corrected for temperature. It may be measured between probes 3 and 6.

The resulting data is shown in Table 1. Unfortunately, one probe (#3) was floating at the beginning of the test, and therefore was useless. It was determined that any repair attempt would endanger the remaining probes. Contact data should still be available from the other probe/finger pair.

As can be seen, the resistance of the remaining contact at temperature was approximately 0.406 ohms, or 3.2 Ohms per contact. Subtracting the calculated sheet resistance and the known contact resistance from the total resistance between

buss assemblies, we find that the contact of the other set of fingers is about 0.16 ohms, or 1.27 ohms per contact. This discrepancy may be due to poor or no contact of several of the legs of the first spider. Both spiders closely followed the buss voltages, indicating a very small buss-to-spider contact resistance compared to the finger-to-electrode contact. These results confirm the resistance predictions of Jim's model, and indicate a development need if "electrode power" is not good enough, i.e. if power delivered to the engine external must be maximized. A brazed contact may help, as might a change of electrode material.

The second probe (#6) started to closely follow the buss voltage soon after 800 °C was reached. Table 2 shows measurements made lead-to-lead with a DVM. Contact #3 can be explained as a high contact resistance between the stainless sense wire and the moly voltage probe or between the probe and the electrode. A brazed sense wire is recommended to alleviate this problem. Probe 6 suddenly jumps to 5.5 k-ohm at the same time it locks on to the buss voltage. This could indicate a high resistance short to the buss and a loss of contact with the electrode. Better insulators and a more intimate electrode contact are recommended for future probes. Since both probes failed, the probe should be re-designed and tested before the next BTM is assembled.

Disassembly of the test apparatus and visual inspection indicate that the probe #3 failure was probably due to poor contact to the electrode, rather than the sense wire connection. Probe 6 may have a short to the buss due to broken alumina insulators. There was no indication that different sense wires touched each other.

Figure 2 illustrates one possible voltage probe design. Several moly fingers are formed into loops and wired and brazed to the central insulator. The wrapping wire doubles as the probe hook-up. This design allows several probe contacts while removing a minimum of active area from service.

In summary, this test showed:

1. Contact resistances on the order of 1-2 ohms exist between the fingers and the electrode.
2. Negligible contact resistance exists between the spider and the buss compared to the spider-to-electrode contact resistance.
3. Contact to the electrode may be unreliable, on both the probes and the spiders.
4. The present voltage probe design is unreliable and must be re-designed and tested.

Copies to:
2541 J.B. Moreno
2541 L.L. Lukens
2541 C.E. Andraka

22-141 50 SHEETS
22-142 100 SHEETS
22-144 200 SHEETS
AMMCO

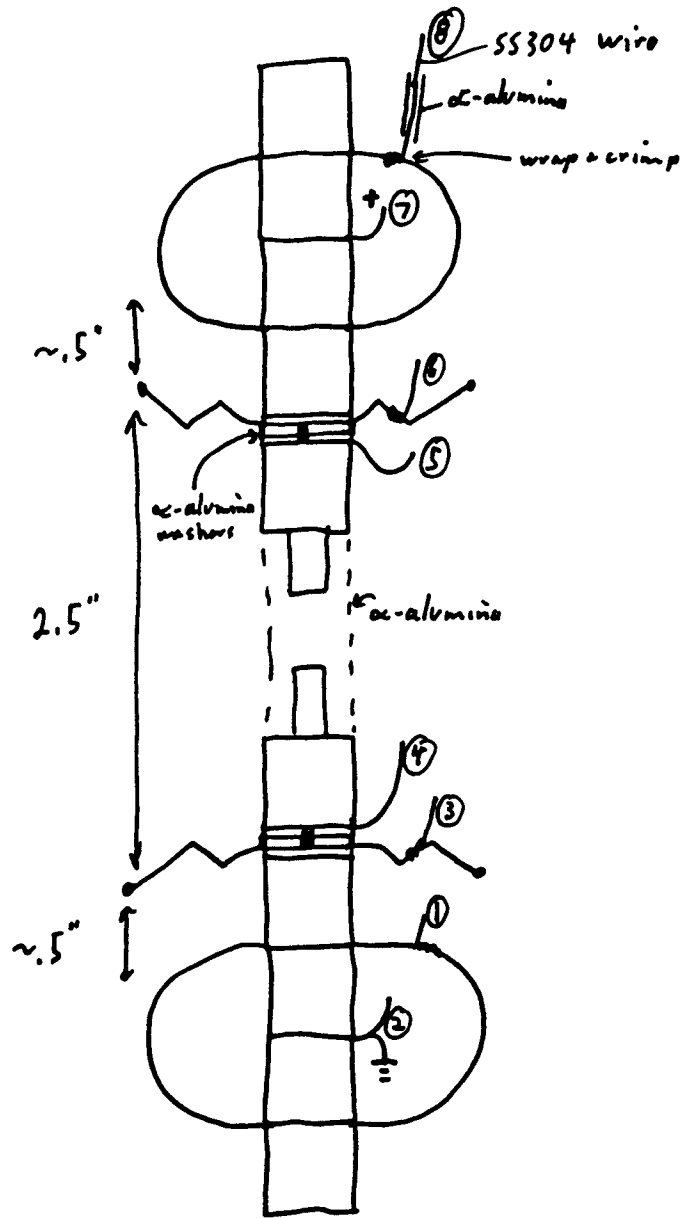


fig 1 Contact Resistance Setup

Table 1. Contact Resistance Test: Run #1

Time	Temperature	R_{6-8}	R_{1-8}	R_{5-8}	$R_{sum, 1-8}$ (calculated)	Comments
0	35°C	0.027 Ω	0.182	0.001	0.046	probe 3 floating, lower than all other voltages. Attempted repair may cause more damage. ~1.5V compared to 1.95V for others
10:27	250°C	0.113	0.2	0.002	0.070	$R_{5-8} = R_{1-4}$ float around 0 Ω
10:30	400°C	0.134	0.254	$\pm 0.015 \Omega$	0.097	
10:33	600°C	0.238	0.401	0.008	0.109	
10:35	740°C	0.320	0.575	0.002	0.125	
10:37	800°C	0.373	0.654	0.001	0.13	
10:39	800°C	0.418	0.737	0.022	0.13	
10:40	800°C	0.406	0.6952	0.0036	0.13	Current raised from 1A to 25A
11:20	800°C	± 0.0072	0.8508	0.006	0.13	Loss of lower probe - looked to loss
11:38	800°C	± 0.0064	0.7964	0.004	0.13	
12:20	800°C	0.0004	0.6664	0.0016	0.13	
13:20	800°C	0.0004	0.6444	0.009	0.13	Start cooling
14:09	535°C	0.0008	0.4972	0.0008	0.107	
14:20	450°C	0.280	0.4872	0.0016	0.093	recover probe, #3 still float

22-141 50 SHEETS
22-142 100 SHEETS
22-144 200 SHEETS



Lead-to-Lead resistance measurements

Table 2

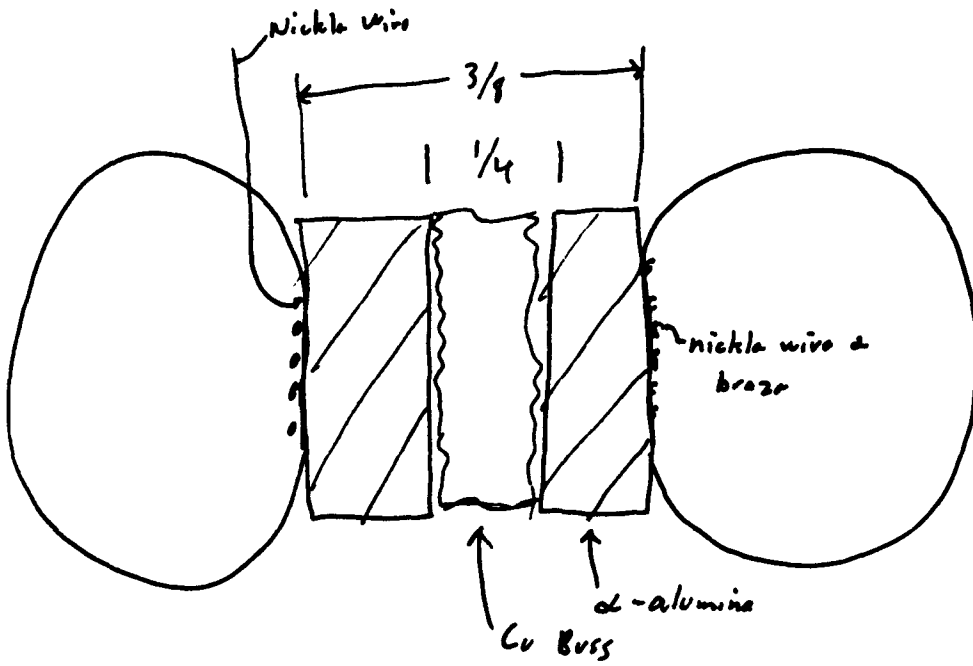
	DVM resistance										
	3-1	3-2	3-4	6-7	6-5	6-8	1-8	1-2	7-8	DVM leads	to ground
Room Temp	0.C.	0.C.	0.C.	29.3	29.1	30.4	31.9	33.0	29.2	0.3	0.C.
800'L	0.3M Ω	0.3M Ω	0.3M Ω	5.49k	5.5k	5.5k	32.3	32.7	-	0.3	0.C.

- 0.C. is on 20 M Ω scale
- all measurements in Ω unless noted



Figure 2

Probe Design



22-141 50 SHEETS
22-142 100 SHEETS
22-144 200 SHEETS
AARCO

APPENDIX L
SAFE HANDLING OF SODIUM

Blank Page

-288-/-289-

SOP NUMBER: 08000 8604
Original Issue
Organization: 2541

SAFE OPERATING PROCEDURE
FOR SODIUM HANDLING

Electromechanical Subsystems Dept., 2540

ESD Division I, 2541

ESD Division I, 2541

Industrial Hygiene Division, 3311

Safety Engineering Division, 3441

Fire Protection Division, 7862

SAFE OPERATING PROCEDURE
FOR SODIUM HANDLING
ESD Division I, 2541

Introduction

Division 2541 is researching a heat engine referred to as a Liquid Metal Thermal Electric Converter (LMTEC) which uses sodium as the working fluid. The research is part of the DOE Solar Thermal Technology Program. The research involves experiments with a prototype bench test module of the LMTEC. Operations involving the preparation of sodium and the testing of components such as the pump for the bench test module will be necessary as a part of this activity. These procedures cover all operations involving sodium performed in room 2019 in building 807.

A glove box has been purchased for use in these sodium handling operations. The glove box located in room 2019 in building 807 is a hermetically sealed system that maintains a moisture and oxygen free atmosphere. It has a one piece stainless steel tub shaped bottom.

All personnel working under this procedure must signify their knowledge of these procedures with their signature on the authorized personnel list attached.

Any change of these procedures must be approved by the Safety Standards Division, Fire Protection Division, and Industrial Hygiene Division Before they are adopted.

Hazards

Sodium is a flammable metal which reacts violently with water and chlorinated hydrocarbons. Sodium when exposed to air may ignite spontaneously at a temperature as low as 240 deg. F depending on such conditions as humidity, dispersion, etc. Burning sodium will react violently with almost all common fire extinguishing materials. Sodium fires produce a dense white smoke which contains highly alkaline materials; sodium monoxide (Na_2O), and sodium hydroxide (NaOH) which can cause irritation and rapid tissue destruction through chemical and thermal burns.

The glove box will provide a safe environment for working with sodium in its solid or molten state. If the glove box should breach while the sodium is in a molten state a sodium fire will occur.

Handling Precautions

The glove box and any cabinets shall be clearly marked as containing sodium when sodium is present. No more than 120 grams of sodium shall be exposed to the glove box atmosphere at any time. No more than 250 grams of sodium shall be placed in the glove box at any time. No more than 500 grams of sodium shall be in the laboratory, including the glove box, at any time.

When handling sodium containers outside the glove box protective gloves and a face shield will be worn. The gloves should be rubber or pvc and should be loose fitting so they can be easily thrown off if contaminated.

Containers of sodium shall not be opened outside the glove box.

Operations in which the sodium is heated to above its melting temperature shall be attended at all times.

Sodium will be disposed of by placing it in a air tight metal container and contacting the Environmental Protection and Hazardous Waste Management Division, 3314, for pickup and disposal.

Emergency Procedures

In the event of the breach of the glove box and apparent fire as evidenced by smoke and/or flame any experiments in progress should be terminated. The fire alarm pull station should be activated to evacuate the building, and the fire department alerted to the possibility of a fire in the lab. The inventory control of sodium and construction of the glove box should eliminate the need for attempts to extinguish a fire by laboratory personnel.

Should it be necessary to fight the fire a sodium approved fire extinguisher, MET-L-X, will be available. All Personnel should avoid any contact with smoke from a sodium fire.

In case of contact with sodium any sodium clinging to the skin or clothing should be brushed off. Affected areas should be washed with large amounts of water. A safety shower is located in the laboratory on the north wall. All clothing should be removed as soon as possible in case sodium is trapped in it. Water dilutes the caustic reaction products and will limit skin or wound damage.

SAFE OPERATING PROCEDURE
FOR SODIUM HANDLING
ESD Division I, 2541

Authorized Personnel

The following personnel have read and understood this Safe Operating Procedure and will work within its restraints.

name	org.	date
------	------	------

name	org.	date
------	------	------

name	org.	date
------	------	------

name	org.	date
------	------	------

name	org.	date
------	------	------

name	org.	date
------	------	------

name	org.	date
------	------	------

SOP NUMBER: 08001 8701
Addendum No. 1 to 08000 8604
Organization: 2541

SAFE OPERATING PROCEDURE
FOR SODIUM HANDLING

Electromechanical Subsystems Dept., 2540

ESD Division I, 2541

ESD Division I, 2541

Industrial Hygiene Division, 3311

J. R Doyle, Safety Engineering Division, 3441

J. E. Dotts, Safety Engineering Division, 3441

Fire Protection Division, 7862

SAFE OPERATING PROCEDURE
FOR SODIUM HANDLING
ADDENDUM NO. 1
ESD Division I, 2541

Introduction

The purpose of this addendum is to add to the existing sodium handling SOP (No. 08000 8604) certain provisions for cleaning residual sodium from hardware used in tests. The hardware consists of small vacuum vessels (1 to 2 liter) and associated tubing, fittings, valves and pressure gauges.

Cleanup of residual sodium from this hardware is required primarily so that the parts can be inspected for material performance after testing. Cleanup is also necessary so that the parts do not remain indefinitely hazardous. And finally, cleanup also enables the economy of reusing expensive hardware.

The existing SOP permits sodium handling only within a glovebox in room 2019 of building 807. Within this glovebox and under the existing SOP, hardware can be heated to melt and drain out the majority of contained sodium. However, the next step in conventional sodium cleanup technique is not compatible with operation within the glovebox. Alcohol (methyl, ethyl, propyl or butyl) is usually used for cleaning small or irregularly shaped pieces of equipment (Liquid Metals Handbook, Government Printing Office, Washington, D. C., 1955). The glovebox is not designed to cope with the alcohol vapors, water absorbed in the alcohol and hydrogen liberated during sodium cleanup. This Addendum is intended to present a safe operating procedure for alcohol cleanup of small hardware parts using the fume hood adjacent to the glovebox in room 2019.

All personnel working under this procedure must signify their knowledge of the procedure with their signature on the authorized personnel list attached.

Any change of this procedure must be approved by the Safety Standards Division, Fire Protection Division, and Industrial Hygiene Division before it is adopted.

Hazards

Sodium is a flammable metal which reacts violently with water and chlorinated hydrocarbons. Sodium when exposed to air may ignite spontaneously at a temperature as low as 240 deg. F depending on such conditions as humidity, dispersion, etc. Burning sodium will react violently with almost all common fire extinguishing materials. Sodium fires produce a dense white smoke which contains highly alkaline materials; sodium monoxide (Na_2O), and sodium hydroxide (NaOH) which can cause irritation and rapid tissue destruction through chemical and thermal burns.

Sodium reacts with the alcohols as well as with water to release heat, caustic products and hydrogen. One gram of sodium will produce 0.044 gram of hydrogen; in air this can be the explosive equivalent of 1.11 grams of TNT. However, the reaction with the larger molecular weight alcohols is mild. The heat and the hydrogen is liberated slowly. Using 2-propanol the cleanup of grams of sodium can require days.

The alcohols are flammable.

Handling Precautions

Alcohol cleanup of sodium shall be carried out in the fume hood adjacent to the glovebox in room 2019 of building 807. The operation should be conducted within a stainless steel pan so that if necessary a fire can be allowed to burn itself out. The fume hood shall be clearly marked as containing sodium and alcohol when cleanup is in progress.

Parts shall be drained of sodium as completely as possible in the glovebox.

Estimates shall be made of sodium quantity remaining in each part after drainage. A written log will be maintained.

After drainage the larger parts should be loosely capped; the smaller parts should be placed in a covered metal beaker. In this condition the sodium-coated surfaces are covered with glove-box argon and ready for transfer to the fume hood. Parts should be oriented to the extent possible so that when alcohol is added it can reach all sodium-coated surfaces. It should also be possible for all gas contained or produced within the part to be easily vented to avoid overpressure.

During transfer of parts from the glove-box air lock to the fume hood and during the subsequent cleaning procedure, rubber gloves and splashproof cup-type goggles under a face shield must be worn.

Each batch of parts transferred to the fume hood for alcohol cleanup must total no more than 5 grams (estimated) of residual sodium. Cleanup must be completed for a batch before the next batch is moved into the hood.

In the fume hood, a slight inert-gas bleed should be established into the part or beaker of parts and maintained until the parts are later covered with a fire suppression lid for unattended storage (see below).

Transfer of alcohol from its commercial bottle to a metal beaker should be done in the adjacent fume hood. Use 2-propanol initially. Only the minimum quantity of alcohol that is practical should be used in order to minimize fire potential.

The part or beaker of parts should be filled in 10% increments. Watch for boiling and spattering. Monitor rate of hydrogen liberation and agitate periodically.

When unattended, the part or beaker of parts should be covered with a metal cap or plate so that evolved gas can readily escape but any fire would be suppressed.

After one or more days, drain and re-fill with 2-propanol cut with 20% methyl or ethyl alcohol, continuing to observe all precautions. After an additional one or more days, drain and refill with 2-propanol cut 20% with water. Repeat this step until no further hydrogen liberation is observed even with agitation. Drain and refill with 2-propanol cut 50% with water. Repeat this step until no hydrogen liberation is observed. Drain and fill with water. Soak and drain.

The products of reaction from sodium cleanup shall be stored in a flammable liquid waste container approved by the Industrial Hygiene Division and the fire protection engineers. This shall be disposed of by contacting the Environmental Protection and Hazardous Waste Management Division, 3314, for pickup and disposal.

Emergency Procedures

In the event of an apparent fire as evidenced by smoke and/or flame any cleaning procedure in progress should be terminated. The fire alarm pull station should be activated to evacuate the building, and the fire department alerted by dialing 117.

All personnel should avoid any contact with smoke from a sodium fire. The smoke is caustic. Eyes and lungs are particularly at risk.

If the fire is small, it should be attacked using a sodium approved fire extinguisher, NaX (filled with the sodium-specific powder soda ash) which shall be kept available. If alcohol as well as sodium is involved in the fire, extinguishment with NaX may be difficult as NaX will not work on alcohol. The metal lids used for unattended storage (see the handling precautions section) should be kept on hand and may be used if the fire can be safely approached.

In case of contact with sodium any sodium clinging to the skin or clothing should be brushed off. All clothing should be removed as soon as possible in case sodium is trapped in it. Affected areas should be washed with large amounts of water, but only if it is certain that metallic sodium is not present. A safety shower is located in the laboratory on the north wall. Water dilutes the caustic reaction products and will limit skin or wound damage. Medical attention should be obtained.

SAFE OPERATING PROCEDURE
ADDENDUM NO. 1 TO SOP 08000 8604
ESD Division I, 2541

Authorized Personnel

The following personnel have read and understood this Safe Operating Procedure and will work within its restraints.

name	org.	date
------	------	------

name	org.	date
------	------	------

name	org.	date
------	------	------

name	org.	date
------	------	------

name	org.	date
------	------	------

name	org.	date
------	------	------

name	org.	date
------	------	------

Sandia National Laboratories

Albuquerque, New Mexico 87185

date: December 23, 1986

to: DISTRIBUTION

from: J. B. Moreno and C. E. Andraka -2541

subject: Sodium Fire Exercise

On December 19, 1986, Division 2541 successfully staged a sodium fire exercise in Area III adjacent to Building 6730. A short video tape of the exercise was made and is available to anyone interested. A detailed chronology of the fire is attached to this memo.

The purpose of the exercise was to provide the Division with experience in sodium fire behavior and extinguishment. Of particular interest was the nature and rate of production of sodium oxide smoke. The information obtained from this exercise will be used in preparing an S.O.P. for planned experimental operation of a sodium liquid metal thermal electric converter (LMTEC) presently being assembled. The LMTEC will be a sealed metallic loop containing approximately 1/4 pound of sodium circulating between a heat addition section at 800°C and a heat removal section at up to 400°C. Current plans call for this device to be operated in a fume hood in Building 807 beginning in the Spring of 1987.

Prior approval for the sodium fire exercise had been obtained from Jim Dotts of Safety Engineering Division 3315. On his instruction we consulted with Julie Hawkins of Environmental Protection and Hazardous Waste Management Division 3314. We also consulted with Vern Duke of Operations Engineering Division 7862.

What we learned:

1. The smoke from 1/4 pound of sodium in a 4"x4" pool was about equivalent to a small campfire.
2. The fire was quiet and slow to propagate across the pool. A crust of sodium oxide floats on the surface of the pool. Sodium wicks through the crust. Where sodium burns on the surface of the crust, the crust is incandescent.
3. Growth of the incandescent crust on the surface of the pool can result in an enlarged area of involvement.
4. The NA-X extinguisher scattered burning sodium into a wider area.
5. Unless the fire can be attacked from opposite sides, shielding can prevent achievement of adequate depths of sprayed-on NA-X powder. Spooning or shoveling the powder on works well and is less messy.
6. Vertical surfaces of oxide crust can form and wick sodium. Sodium burning on these vertical surfaces can not be controlled with NA-X powder. The crusts must be dislodged and buried in powder.
7. Re-ignition may occur where the depth of NA-X powder is deficient.

DISTRIBUTION:

2540 Gary Beeler
2541 Joe Abbin
2541 Chuck Andraka
2541 Larry Lukens
3311 Bill Stocum
3314 Sharon Felicetti
3314 Julie Hawkins
3315 Jim Dotts
3315 Paul Fleming
6227 Jim Leonard
6227 Jesus Martinez
6227 Rich Diver
7862 Vern Duke

Sodium-Fire Chronology:

A 1/4-pound cylinder of sodium was heated (using Sterno) in a 1"-deep, 4"x4" stainless steel pan. The sodium was covered with a thick oxide shell at the beginning of the test. The pan was instrumented with a single thermocouple directly under the sodium inside the pan.

About 5 minutes after the start of heating, fluctuating temperature readings on the order of 400°C were attained. At 8 minutes some wisps of smoke were visible. At 9 minutes the oxide shell was tapped with a steel bar. The shell fractured and the molten sodium within flowed out to fill the pan to a depth of about 1/3 inch. About 1 cc slopped over the edge of the pan. Almost immediately some very slight traces of flame and smoke were observed inside the pan.

At 10 minutes orange incandescence was observed in one corner of the pan. Because they appeared to be hindering the spread of the fire, the oxide shell remnants were slightly stirred into the sodium pool at 11 minutes. The number of incandescent spots multiplied, appearing as raised glowing bumps on a generally level surface. The bumps appeared to be oxide layers that continually thickened as time progressed. Light to moderate white smoke was produced. At 12 minutes the shell remnants were further stirred into the sodium. At 13 minutes half of the pan was covered with glowing bumps. Brightness varied strongly with wind gusts.

During this time heating continued and temperatures of approximately 320°C were observed. At 13.5 minutes a glowing oxide bump on one side of the pan began to rapidly enlarge. It quickly "grew" over the side of the pan and down towards the ground, all the while incandescing. At 14 minutes into the test 75% of the pan surface was involved. At 14.5 minutes the entire pan was full of incandescent patches nearly touching each other. The smoke was moderately thick at the surface, and overall was equivalent to a small campfire.

At about 15 minutes into the test, an attempt was made to put out the fire with an NA-X extinguisher. Initially the nozzle of the extinguisher seemed to be plugged. After some agitation of the nozzle and the powder reservoir, the extinguisher worked. Powder was applied to a depth of about 1/2 inch. The gas blast from the extinguisher blew some sodium out of the pan and onto the ground several feet away, where it continued to burn until covered with powder. On the side of the pan nearest to the extinguisher, the pan's side shielded the sodium from the powder spray, and the powder depth was only about 1/4 inch. Nevertheless by 15.5 minutes smoke had stopped even in the shielded area. At 16 minutes smoke wisps were observed in the shielded area. An alternative to spraying on more powder that was tried was to spoon oversprayed powder onto the deficient areas. This ended the fire within the pan.

At 16.45 minutes the crust that had grown over the side of the pan re-ignited, producing smoke and incandescence. However, the crust quickly fell off the side of the pan in several pieces and no further fire was observed. An area of approximately 25 square feet surrounding the pan was left covered with NA-X powder and a small amount of spattered sodium. The area is now free of hazardous material.

SOP NUMBER: 02800 8701
Original Issue
Organization: 2541

SAFE OPERATING PROCEDURE
FOR CLOSED LOOP SODIUM EXPERIMENTS

Electromechanical Subsystems Dept., 2540

ESD Division I, 2541

ESD Division I, 2541

Industrial Hygiene Division, 3311

Safety Engineering Division, 3441

Fire Protection Division, 7862

SAFE OPERATING PROCEDURE
FOR CLOSED LOOP SODIUM EXPERIMENTS
ESD Division I, 2541

Reference

SOP Number: 08000 8604
Safe Operating Procedure For Sodium Handling

SOP Number: 08300 8503
Safe Operating Procedures Storage Battery Division 2525

Introduction

Division 2541 is researching a heat engine referred to as a Liquid Metal Thermal Electric Converter (LMTEC) which uses sodium as the working fluid. The research is part of the DOE Solar Thermal Technology Program. The research involves experiments with a prototype bench test module of the LMTEC. Operations involving the preparation of sodium and the testing of components such as the pump for the bench test module will be necessary as a part of this activity. These procedures cover all operations involving sodium performed in room 2131 in building 807.

All personnel working under this procedure must signify their knowledge of these procedures with their signature on the authorized personnel list attached.

Any change of these procedures must be approved by the Safety Standards Division, Fire Protection Division, and Industrial Hygiene Division before they are adopted.

Hazards

Sodium is a flammable metal which reacts violently with water and chlorinated hydrocarbons. Sodium when exposed to air may ignite spontaneously at a temperature as low as 115 C depending on such conditions as humidity, dispersion, etc. Burning sodium will react violently with almost all common fire extinguishing materials. Sodium fires produce a dense white smoke which contains highly alkaline materials; sodium monoxide (Na_2O), and sodium hydroxide (NaOH) which can cause irritation and rapid tissue destruction through chemical and thermal burns.

Handling Precautions

Experiments in which the sodium is heated to above its melting temperature shall be conducted inside the fume hood, building 807/room 2131, with the fume hood operating normally. The fume hoods draft shall be actively monitored, and experiments shall be terminated if the fume hood ceases to operate normally.

The fume hood and any cabinets shall be clearly marked as containing sodium when sodium or any apparatus containing sodium is present. No more than 120 grams of sodium shall be used in any experiment performed in the fume hood in room 2131 building 807.

When handling sodium containers or working on any apparatus containing sodium protective gloves and a face shield will be worn. The gloves should be rubber or pvc and should be loose fitting so they can be easily thrown off if contaminated.

When experiments in which the sodium is heated to above its melting temperature are in progress, protective gloves and a face shield will be worn by persons attending the experiment or the protective shield of the fume hood will be closed.

A steel tray large enough to catch and hold at least ten times the volume of sodium used in any experiment will be placed in the fume hood under the experimental apparatus.

Experiments designed for use in the fume hood will be closed loop sealed systems with welded, brazed, or vacuum fittings used to seal the system. The experiments will be evacuated before heating sodium to above its melting point. The experiments will be controlled so that the temperature of the sodium cannot exceed 850 C. These precautions will maintain a subatmospheric pressure inside the experimental apparatus.

Sodium will be disposed of by placing it in a air tight metal container and contacting the Environmental Protection and Hazardous Waste Management Division, 3314, for pickup and disposal.

Unattended Operation

A computer control and data acquisition system has been assembled to allow safe unattended operation of closed loop sodium experiments.

Several closed loop experiments may be performed with this equipment. Some experiments will have a closed loop in which all temperatures are limited to below 600°C, as shown in Fig. 1. Other experiments will include a high temperature furnace region, as shown in Fig. 2.

Independent temperature controllers will regulate temperatures for each portion of the closed loop. Temperatures will be limited such that the sodium vapor pressure will always be subatmospheric. All controllers have upscale thermocouple break protection (heater shuts off on thermocouple breakage), and each heater is fuse-protected.

The main furnace controller has two over-temperature limit controllers, each with manual reset and thermocouple break protection. The over-temperature controllers will be checked for proper function by simulating thermocouple input to the controller prior to any experiment. The guard heater, which operates at the furnace temperature, also has an over-temperature limit controller. These controllers and backups will control any temperature above 600°C in any test. In the event the main controller thermocouple shorts and indicates a low or ambient temperature, power will be added to the heaters, and the over-temperature controllers will cause a system shutdown.

Trace heating is used on all low temperature sodium plumbing in closed loop sodium experiments to keep sodium from freezing. Trace heating is accomplished with low-power electrical heaters, each controlled by a proportioning on-off controller with thermocouple break protection. The maximum temperature setting is hardware limited to 600°C. Trace heater power is limited by a variac connected to the controller output, and an inline fuse.

The overtemperature controllers, main heater failure sensor, and a panic button are hardware connected to the main and guard heaters through relays. Therefore, any of these can trigger an immediate, positive removal of power from the main heaters. After any such shutdown, a manual reset is required to return power to the heaters.

A computer control and data acquisition system monitors temperatures throughout the system. The computer also can positively remove power from the heaters in the event of an overtemperature or other failure.

The computer control system shall monitor the operation of the fume hood and will terminate any experiment involving molten sodium if the fume hood ceases to function normally.

If the computer senses that the main heaters have been disabled, an orderly shutdown procedure is performed. The sodium pump remains on until the hot zone is reduced below 200°C. The cell is set to open circuit, thereby stopping the flow of sodium through the cell. At 200°C, the pump power is reversed to move the sodium inventory to the storage reservoir. This procedure prevents hot sodium from contacting low temperature seals in the return loop. Trace heating will remain active to prevent sodium freezing, unless an overtemperature is recorded in the return lines. The computer can remove power from the main heaters and/or the trace heaters, as required.

Emergency Procedures

In the event of the breach of an experiment or apparent fire as evidenced by smoke and/or flame any experiments in progress should be terminated by pressing the red panic button on the controller panel. The fire alarm pull station should be activated to evacuate the building, and the fire department alerted to the possibility of a fire in the lab. The inventory control of sodium, the construction of the fume hood, and the steel catch tray should prevent the spread of the fire.

If the fire is small it may be attacked using a sodium approved fire extinguisher, MET-L-X, which is available in the hall outside the adjacent laboratory, Room 2019. All Personnel should avoid any contact with smoke from a sodium fire.

SAFE OPERATING PROCEDURE
FOR CLOSED LOOP SODIUM EXPERIMENTS
ESD Division I, 2541

Authorized Personnel

The following personnel have read and understood this Safe Operating Procedure and will work within its restraints.

name	org.	date
------	------	------

name	org.	date
------	------	------

name	org.	date
------	------	------

name	org.	date
------	------	------

name	org.	date
------	------	------

name	org.	date
------	------	------

name	org.	date
------	------	------

DISTRIBUTION:

DOE/TIC-4500(Rev.74)UC-236 (10)

AAI Corporation
P.O. Box 6787
Baltimore, MD 21204

Acurex Aerotherm
555 Clyde Avenue
Mountain View, CA 94039
Attn: H. Morse

Alabama A&M University (2)
Department of Physics
P.O. Box 271
Normal, AL 35762
Attn: M. D. Aggarwal
A. Tan

Alpha Solarco
600 Vine St.
Cincinnati, OH 45202

Applied Concepts
405 Stoney Creek Blvd.
P.O. Box 490
Edinburg, VA 22824
Attn: J. S. Hauger

Applied Concepts
2501 S. Larimer County Rd. 21
Berthound, CO 80513
Attn: S. Pond

Arizona Public Service Co. (2)
P.O. Box 21666
Phoenix, AZ 85036
Attn: J. McGuirk
E. Weber

Australian National University
Department of Engineering Physics
P.O. Box 4
Canberra ACT 2600, AUSTRALIA
Attn: Prof. Stephen Kaneff

B&E Technical Services Inc.
Attn: William R. Lang
6314 S. Piccadilly St.
Aurora, CO 80016

Barber-Nichols Engineering
6325 West 55th Ave.
Arvada, CO 80002
Attn: R. Barber

BDM Corporation
1801 Randolph Street
Albuquerque, NM 87106
Attn: W. E. Schwinkendorf

Battelle Memorial Institute
Pacific Northwest Laboratory
4000 NE 41st St.
Seattle, WA 98105
Attn: K. Drumheller

Battelle Memorial Institute
Pacific Northwest Laboratory
P.O. Box 999
Richland, WA 99352
Attn: T. Williams

Bechtel Group, Inc.
P.O. Box 3965
50 Beale Street
San Francisco, CA 94119
Attn: P. DeLaquil

Black & Veatch
P.O. Box 8405
Kansas City, MO 64114
Attn: J. C. Grosskreutz

Boeing Engineering & Construction
P.O. Box 3999
Seattle, WA 98124
Attn: R. Gillette

Budd Company (The)
Fort Washington, PA 19034
Attn: W. W. Dickhart

Budd Company (The)
Plastic R&D Center
356 Executive Drive
Troy, MI 48084
Attn: K. A. Iseler

Burns & Roe (2)
800 Kinderkamack Road
Oradell, NJ 07649
Attn: G. Fontana
R. Cherdack

California Energy Commission
1516 - 9th Street
Sacramento, CA 95814
Attn: Alec Jenkins

Cal Poly State University
San Luis Obispo, CA 93407
Attn: E. J. Carnegie

California Institute of Technology
Aeronautics Library
MS 205-45
Pasadena, CA 91125
Attn: Jean Anderson

California Polytechnic University
Dept. of Mechanical Engineering
Pomona, CA 91768
Attn: W. B. Stine

Chicago Bridge and Iron
800 Jorie Blvd.
Oak Brook, IL 60521
Attn: J. M. Shah

Colorado State University
Ft. Collins, CO 80523
Attn: T. G. Lenz

Columbia Gas System Service Corp.
1600 Dublin Road
Columbus, OH 43215
Attn: J. Philip Dechow

Datron Systems, Inc.
200 West Los Angeles Ave.
Simi Valley, CA 93065-1650

DFVLR (2)
Institute for Technical Thermodynamics
Attn: W. Schiel
R. Kohne
Pfaffenwaldring 38-40
7000 Stuttgart 80
FEDERAL REPUBLIC OF GERMANY

DSET
Box 1850
Black Canyon Stage I
Phoenix, AZ 85029
Attn: G. A. Zerlaut

Donnelly Corporation
49 West Third Street
Holland, MI 49423
Attn: M. DeVries

Eder Solar
512 S. Hobart Bl. #104
Los Angeles, CA 90020
Attn: Harvey Eder

Electric Power Research Inst. (2)
3412 Hillview Avenue
Palo Alto, CA 94303
Attn: E. A. Demeo
J. E. Cummings

Energy Technology Engr. Ctr.
Rockwell International Corp.
P.O. Box 1449
Canoga Park, CA 91304
Attn: W. L. Bigelow

ENTECH, Inc. (3)
P.O. Box 612246
DFW Airport, TX 75261
Attn: R. R. Walters
W. Hesse
M. O'Neill

Eurodrive, Inc.
30599 San Antonio Rd.
Hayward, CA 94544

Florida Solar Energy Center
300 State Road 401
Cape Canaveral, FL 32920
Attn: Library

Ford Motor Company
Glass Div., Technical Center
25500 West Outer Drive
Lincoln Park, MI 48246
Attn: V. L. Lindberg

Foster Wheeler Solar Dev. Corp. (2)
12 Peach Tree Hill Road
Livingston, NJ 07039
Attn: M. D. Garber
R. J. Zoschak

Garrett Turbine Engine Co.
111 South 34th Street
P.O. Box 5217
Phoenix, AZ 85010
Attn: Ed Strain

Georgia Power Co. (2)
7 Solar Circle
Shenandoah, GA 30264
Attn: E. Ney
E. Ellingston

Heery Energy Consultants, Inc.
Project Energy Manager
880 West Peachtree St. NW
Atlanta, GA 30309
Attn: Glenn Bellamy

Highland Plating
10001 N. Orange Drive
Los Angeles, CA 90038
Attn: M. Faith

Industrial Solar Technologies
5775 West 52nd Ave.
Denver, CO 80212
Attn: Randy Gee

Institute of Gas Technology
Attn: Library
34245 State Street
Chicago, IL 60616

Jet Propulsion Laboratory
4800 Oak Grove Drive
Pasadena, CA 91109
Attn: M. Alper

Kearney & Associates
14022 Condessa Drive
Del Mar, CA 92014
Attn: David W. Kearney

LaCour Kiln Service
P.O. Box 247
Canton, MS 39046
Attn: J. A. LaCour

LaJet Energy Co. (2)
P.O. Box 3599
Abilene, TX 79604
Attn: Monte McGlaun
Carl Williams

L'Garde, Inc.
1555 Placentia Avenue
Newport Beach, CA 92663
Attn: Mitchell Thomas

Lawrence Berkeley Laboratory
Applied Science Division
University of California
Berkeley, CA 94720
Attn: Arlon J. Hunt

Lewis Resarch Center
Mail Stop 301-2
Cleveland, Ohio 44135
Attn: Jack G. Slaby

John Lucas
865 Canterbury Road
San Marino, CA 91108

Luz International Limited
924 Westwood Blvd.
Los Angeles, CA 90024
Attn: Dr. D. W. Kearney

Martin Marietta Corp. (2)
12250 So. Hwy. 75
Littleton, CO 80125
Attn: Tom Tracey
H. Wroten

McCarter Corporation
200 E. Washington St.
P.O. Box 351
Norristown, PA 19404
Attn: R. A. Powell

McDonnell-Douglas Astronautics
Company (3)
5301 Bolsa Avenue
Huntington Beach, CA 92647
Attn: R. L. Gervais
J. Rogan
D. Steinmeyer

Mechanical Technology, Inc. (2)
968 Albany Shaker Road
Latham, NY 12110
Attn: G. R. Dochat
J. Wagner

Meridian Corporation
4300 King St.
Suite 400
Alexandria, VA 22302-1508
Attn: D. Kumar

Midwest Research Institute (2)
425 Volker Blvd.
Kansas City, MO 64110
Attn: R. L. Martin
J. Williamson

NASA Lewis Research Center
21000 Brook Park Road
Cleveland, OH 44135
Attn: R. Beremand, MS 301-2
J. Savino, MS 301-5
T. McCoy, MS 301-5
R. Puthoff
R. Corrigan

New Mexico Solar Energy Institute
New Mexico State University
Box 3S0L
Las Cruces, NM 88003

Parsons of California
P.O. Box 6189
Stockton, CA 95206
Attn: D. R. Biddle

PG&E
3400 Crow Canyon Rd.
San Ramon, CA 94583
Attn: J. Iannucci
G. Braun

Power Kinetics, Inc.
415 River Street
Troy, NY 12180-2822
Attn: W. E. Rogers

Renewable Energy Institute
1001 Connecticut Avenue NW
Suite 719
Washington, DC 20036
Attn: Kevin Porter

Research Systems, Inc.
Suburban Trust Bldg.,
Suite 203
5410 Indian Head Hwy.
Oxon Hill, MD 20745
Attn: T. A. Chubb

Rockwell International
Energy Systems Group
8900 De Soto Avenue
Canoga Park, CA 91304
Attn: T. Springer

Rockwell International
Space Station Systems Division
12214 Lakewood Blvd.
Downey, CA 90241
Attn: I. M. Chen

Sanders Associates
144 D.W. Highway South
C.S. 2034
Nashua, NH 03061-2034
Attn: J. Kesseli

Science Applications
International Corp.
10401 Roselle Street
San Diego, CA 92121
Attn: Barry Butler

Solactor Corporation
2065 Keystone Blvd.
Miami, FL 33181
Attn: Joseph Womack

Solar Energy Industries Association (2)
Suite 610
1730 North Lynn St.
Arlington, VA 22209-2009
Attn: C. LaPorta
S. Sklar

Solar Energy Research Inst. (4)
1617 Cole Blvd.
Golden, CO 80401
Attn: B. P. Gupta
J. Thornton
M. Murphy
D. Hawkins

Solar Kinetics, Inc.
P.O. Box 540636
Dallas, TX 75354-0636
Attn: J. A. Hutchison

Solar Steam
P.O. Box 32
Fox Island, WA 98333
Attn: D. E. Wood

Southern California Edison (3)
P.O. Box 800
Rosemead, CA 92807
Attn: J. N. Reeves
P. Skvarna

SLEMCO
19655 Redberry Dr.
Los Gatos, CA 95030
Attn: A. J. Slemmons

Stearns-Catalytic Corp.
Box 5888
Denver, CO 80217
Attn: T. E. Olson

Stirling Thermal Motors
2841 Boardwalk
Ann Arbor, MI 48104
Attn: Ben Ziph

Sun Exploration and Production Co.
P.O. Box 2880
Dallas, TX 75221-2880
Attn: R. I. Benner

Sun Power, Inc.
6 Byard St.
Athens, OH 45701
Attn: Mac Thayer

Sundstrand ATG
P.O. Box 7002
Rockford, IL 61125
Attn: D. Chaudoir

Suntec Systems, Inc. (2)
Suite B-4
Loring Park Office Bldg.
430 Oak Grove St.
Minneapolis, MN 55403
Attn: Harrison Randolph
J. H. Davison

Swedlow, Inc.
12122 Western Avenue
Garden Grove, CA 92645
Attn: E. Nixon

3M-Energy Control Products (2)
207-1W 3M Center
St. Paul, MN 55144
Attn: B. Benson
J. L. Roche

Texas Tech University
Dept. of Electrical Engineering
P.O. Box 4439
Lubbock, TX 79409
Attn: E. A. O'Hair

TRW (3)
Space & Technology Group
One Space Park
Redondo Beach, CA 90278
Attn: G. M. Reppucci
A. D. Schoenfeld
J. S. Archer

U.S. Department of Energy (3)
Albuquerque Operations Office
P.O. Box 5400
Albuquerque, NM 87185
Attn: C. Garcia
D. Graves
N. Lackey

U.S. Department of Energy
Office of Solar Heat Technologies
Forrestal Building
Washington, DC 20585
Attn: Fred Morse

U.S. Department of Energy
Office of Solar Heat Technologies
Forrestal Building
Washington, DC 20585
Attn: C. Carwile

U.S. Department of Energy
Division of Solar Thermal Tech.
Forrestal Building
Washington, DC 20585
Attn: Howard S. Coleman
R. Shivers
S. Gronich
M. Scheve
F. Wilkins

U.S. Department of Energy
San Francisco Operations Ofc.
1333 Broadway
Oakland, CA 94612
Attn: R. W. Hughey

U.S. Robotics
8100 N. McCormack Blvd.
Skokie, IL 60076
Attn: Paul Collard

University of Houston (2)
Energy Laboratory; SPA
Houston, TX 77004
Attn: Lorin Vant-Hull
A. F. Hildebrandt

University of New Mexico (2)
Department of Mechanical Engr.
Albuquerque, NM 87131
Attn: M. W. Wilden
W. A. Gross

Viking Solar Systems, Inc.
1850 Earlmont Ave.
La Canada, CA 91011
Attn: George Goranson

WG Associates
6607 Stonebrook Circle
Dallas, TX 75240
Attn: Vern Goldberg

0400 R. P. Stromberg
1510 J. W. Nunziato
1513 D. W. Larson
1820 R. E. Whan
1824 J. N. Sweet
1840 R. J. Eagan
1841 R. B. Diegle
1842 R. E. Loehman
1846 D. H. Doughty
2520 N. J. Magnani
2525 R. P. Clark
2540 G. N. Beeler
2541 J. P. Abbin
2541 C. E. Andraka(5)
2541 L. L. Lukens (2)
2541 J. B. Moreno (20)
3141 S. A. Landenberger (5)
3151 W. L. Garner (3)
3154 C. H. Dalin (8) for DOE/OSTI
3160 J. E. Mitchell
4031 R. P. Stromberg (3)
6000 D. L. Hartley
6200 V. L. Dugan
6220 D. G. Schueler
6221 E. C. Boes
6222 J. V. Otts
6223 G. J. Jones
6224 D. E. Arvizu
6225 H. M. Dodd
6226 J. T. Holmes
6227 R. B. Diver
6227 J. A. Leonard (20)
6227 J. I. Martinez
6250 B. W. Marshall
6254 B. Granoff
7470 J. L. Ledman
7471 D. L. Stewart
8470 R. L. Rinne
8471 A. C. Skinrood
8524 P. W. Dean